ScienceInnovation
INTERNATIONAL SCIENTIFIC JOURNAL

ISSN:
2181-3337

INTERNATIONAL SCIENTIFIC JOURNAL

SCIENCE AND INNOVATION

VOLUME 5 / ISSUE 6

D:
BIOLOGY
AGRICULTURE
MEDICINE
PHARMACETICS
VETERINARY

JUNE 2026

International Scientific Journal
SCIENCE AND INNOVATION
Series D
Volume 5 Issue 6
June 2026

Tashkent 2026

ISSN: 2181-3337

International Scientific Journal SCIENCE AND INNOVATION. Series D volume 5 issue 6 – 138 p.

The collection contains scientific articles accepted for issue 6 for 2026 of the international scientific journal "Science and Innovation".

In this scientific journal, in the form of scientific articles, the results of scientific research conducted by professors and teachers of the Republic of Uzbekistan and international higher educational institutions, independent researchers, doctoral students, undergraduates were published. In addition to higher educational institutions, the journal also includes scientific articles by employees working in other research institutes, production organizations and enterprises of our region and republic.

The materials of the journal can be used by professors, teachers, independent researchers, doctoral students, undergraduates, students, teachers of lyceums and schools, scientists and everyone who is interested in science.

This issue of the journal is indexed in the international scientific databases Index Copernicus, eLibrary.ru, OpenAire, EuroPub, ZENODO and Google Scholar.

All articles were placed in the electronic scientific database of the journal (scientists.uz).

© Science and Innovation

© Authors

Editorial team			
Baxtiyor Rustamov	Chief Editor	**Gulirano Raxmatullayeva**	Deputy Chief Editor
Mahliyo Sotivoldiyeva	Reception Manager	**Feruza Ollomurodova**	Reception Manager
Farangiz Sagdullayeva	Technical Editor	**Dilnoza Narzullayeva**	Manager
Zulayxo Xakimova	Editor	**Sevara O'rinboyeva**	Manager
Kozim Ergashov	Editor	**Humoyun Qodirov**	Technical Editor
Feruzabonu Mannonova	Translator	**Mansur Suyunqulov**	Technical Editor
Jahongir Bekmuradov	Translator	**Samandar Rasulov**	Motion Designer
Asila Xaydaralieva	Editor	**Zafarbek Madaminov**	Motion Designer

Scientific editorial board	
Khashim Yakhyayev	Doctor of Agricultural Sciences, professor, Leading scientific researcher of the laboratory for pest control of landscape and forest trees at Scientific research institute for plant quarantine and protection.
Azimjon Anorbaev	Doctor of Agricultural Sciences, professor, Director a.i. of the Scientific Research Institute of Plant Quarantine and Protection.
Ajimurat Jumamuratov	Doctor of agricultural sciences, Professor of Nukus State Pedagogical Institute named after Ajiniyaz.
Murodjon Isagaliyev	Doctor of Biological sciences, Associate Professor, Dean of the Faculty of Animal Husbandry of Fergana State University.
Avazbek Turdaliyev	Doctor of Biological sciences, Associate Professor, Head of the Department of Zootechnics and Agronomy pf Fergana State University.
Zafarjon Jabbarov	Doctor of Biological Sciences, Head of the Department of Soil Science of the National University of Uzbekistan named after Mirzo Ulugbek, Professor.
Gulnora Djalilova	Doctor of Biological Sciences, Associate Professor a.i. of the Department of Soil Science of National University of Uzbekistan named after Mirzo Ulugbek.
Mokhidil Yusupova	Philosofy Doctor on Biological sciences, Head a.i. of the Department of "Effective Use of Residential Estates" of Fergana State University.
Dilmurod Darmonov	Philosofy Doctor on Biological sciences, Dean of the Faculty of Viticulture, Fruit Growing and Vegetable Growing of Fergana State University.
Ulugbek Mirzayev	Candidate of Biological Sciences, Associate Professor, Head of the Department of Soil Science of Fergana State University.
Bakhtiyor Ruziyev	Candidate of Biological Sciences, Associate Professor of the Department of Zoology of Karshi State University.
Akmal Yuldashev	Philosofy Doctor on Biological Sciences, Dean of the Faculty of Teaching Methodology of Exact and Natural Sciences of Pedagogical Institute of Andijan State University.
Khusanjon Idrisov	Philosofy Doctor on Agricultural Sciences, Head of the Department of Fruit and Vegetable Growing of Fergana State University.
Sherzod Teshabayev	Philosofy Doctor on agricultural sciences, Head of the Department of Agriculture and Forest Reclamation of Andijan Institute of Agriculture and Agrotechnologies.
Shavkat Eshpulatov	Candidate of agricultural sciences, Head of the Department of EIAT of Ferghana State University.
Madinakhon Rakhmonova	Philosofy Doctor on Agricultural sciences, Head of the Department "Quarantine of plants and agricultural products" of the Andijan Institute of Agriculture and Agrotechnologies.
Bobomurod Kuldashov	Philosofy Doctor on Agricultural sciences, Head of the department "Agrotechnology, automation and management of production " of Samarkand State University of Veterinary Medicine, Animal Husbandry and Biotechnology.
Khasanboy Askarov	Philosofy Doctor on Agricultural sciences, Head of the Department "Technology of production, storage and preliminary processing of agricultural products" of Fergana Polytechnic Institute.
Sevara Nazarova	Philosofy Doctor on Agricultural sciences, Associate Professor of the Department of Soil Science of Bukhara State University.
Gayratbek Rakhmatullayev	Philosofy Doctor on Agricultural sciences, Head of the Department "Genetics, selection and seed production of agricultural crops" of Andijan Institute of Agriculture and Agrotechnologies, Associate professor a.i..
Dilfuza Jalolova	Candidate of Medical Sciences, Associate Professor of Samarkand State Medical University.
Shakhnoza Abzalova	Candidate of medical sciences, Head of the Department of Scientific Research, Innovation and Scientific Pedagogical Personnel Training of the Tashkent State Medical University, Associate Professor
Khusnidakhon Abdukhakimova	Philosofy Doctor on Biological sciences, Assistant professor of the Department of Soil Science of Fergana State University

ENDOPHYTIC FUNGI FROM *PERSICARIA HYDROPIPER* PRODUCE METABOLITES WITH SELECTIVE ANTIBACTERIAL AND CELL-PROLIFERATIVE ACTIVITIES

A. Abdurashidov[1], F. Kholiyorova[2], N. Tosheva[1], R. Sayidova[2], E. Yusupova[1]
S.Yu. Yunusov Institute of the Chemistry of Plant Substances, Academy of Sciences of the Republic of Uzbekistan, 77 Mirzo Ulugbek Str., Tashkent 100170, Uzbekistan[1]
Tashkent Institute of Irrigation and Agricultural Mechanization Engineers, National Research University, Tashkent, Uzbekistan[2]
https://doi.org/10.5281/zenodo.20697096

Abstract. *Six endophytic fungal isolates were obtained from healthy tissues of Persicaria hydropiper L., and the root-derived isolate 8i3k was selected for detailed biological investigation. The crude ethyl acetate extract exhibited selective antibacterial activity against Gram-positive bacteria, with inhibition zones of 17.0 ±0.2 mm against Bacillus subtilis and 12.0 ±0.1 mm against Staphylococcus aureus, and no activity against Gram-negative bacteria or Candida albicans. Minimum inhibitory concentrations were determined as 312.5 µg/mL (B. subtilis) and 1250 µg/mL (Escherichia coli) by broth microdilution. MTT cytotoxicity evaluation at 100 µg/mL revealed a pro-proliferative rather than cytotoxic effect, with cell viability reaching 132.1 ± 6.9% in HEp-2 and 117.5 ± 6.0% in A549 cells. These findings demonstrate that isolate 8i3k produces secondary metabolites with selective antibacterial and cell-stimulatory activities, potentially linked to the traditional wound-healing properties of the host plant. Further compound purification and molecular identification of the isolate are warranted.*

Keywords: *endophytic fungi; Persicaria hydropiper; secondary metabolites; antimicrobial activity; cell proliferation; MTT assay; natural products.*

1. Introduction

Medicinal plants represent an important reservoir of natural compounds with diverse and biologically significant activities. Nevertheless, the accumulation of these metabolites in plant tissues is often limited, making large-scale extraction challenging. In this context, endophytic microorganisms associated with medicinal plants have gained increasing scientific attention. Medicinal plants possess a distinct microbiome, and their endophytes are known to produce unique, structurally diverse, and biologically active secondary metabolites. Consequently, endophytes of medicinal plants are considered promising sources of novel bioactive compounds for pharmaceutical and agricultural applications and provide valuable opportunities for the discovery of new microorganisms with significant biotechnological potential. Therefore, the isolation of endophytic fungi associated with the medicinal plant *Persicaria hydropiper* and the evaluation of the biological activities of secondary metabolites produced by these fungal isolates are of significant scientific and practical importance.

Endophytic fungi are recognized as important components of plant-associated microbiomes, contributing to plant growth, metabolic regulation, and defense against pathogens, herbivores, insects, and other environmental challenges. Their ability to synthesize diverse secondary metabolites with potential biological activities has stimulated increasing global interest in their study and utilization, particularly in pharmaceutical and agricultural biotechnology.

Comprehensive studies have demonstrated that endophytic fungi are promising reservoirs of biologically active compounds with significant therapeutic and protective potential for both human health and plant protection under adverse environmental conditions. Secondary metabolites obtained from endophytes exhibit a broad spectrum of biological activities, including antimicrobial, antioxidant, and cytotoxic properties. In particular, the screening of antimicrobial compounds from endophytic fungi offers a promising approach to overcoming the growing global challenge of drug-resistant pathogenic microorganisms in medical and agricultural contexts.

Infectious diseases continue to represent one of the most serious global health challenges [1–3]. In 2019, 13.66 million people died globally because of infection-related causes. Most of these infection-related deaths (4.95 million) are associated with antibiotic-resistant pathogens [4]. Projections indicate that by 2050, deaths caused by antibiotic-resistant bacteria may rise substantially compared with present-day mortality rates [5]. Furthermore, various alternative strategies are increasingly being employed in the search for novel antibacterial compounds. These strategies include the exploration of uncultured microorganisms [6], *in silico* screening of chemical compound libraries through deep machine learning approaches [7], and the investigation of insect [8] and animal microbiota [9] as promising reservoirs of new antibacterial substances. Endophytic microorganisms are increasingly recognized as a promising source of new antibiotics. Their high species diversity and adaptability to diverse environmental conditions make them valuable reservoirs of biologically active metabolites [10,11]. In addition, endophyte-derived secondary metabolites have been reported to possess a wide range of biological properties, including antibacterial, antifungal, anticancer, antiviral, antioxidant, anti-inflammatory, immunomodulatory, and hepatoprotective activities [12–14]. Endophytes represent a taxonomically diverse group of microorganisms that colonize the internal tissues of plants and maintain symbiotic relationships with their hosts without inducing apparent disease symptoms. They constitute the plant endosphere, comprising the endorhizosphere and endophyllosphere, and are recognized as an integral component of the plant microbiome alongside the phyllosphere and rhizosphere. Owing to their broad biological activities and promising pharmacological potential, endophytic microorganisms, including fungi, bacteria, and archaea [15], have long attracted the interest of researchers in biology and pharmacology [16–18].

2. Materials and methods

2.1. Plant material and isolation of endophytic fungi

Healthy tissues (leaves, stems, flowers, fruits, and roots) of *Persicaria hydropiper* L. were collected from the Academician F.N. Rusanov Tashkent Botanical Garden on May 18, 2025. Samples were processed within 24 hours. Tissue segments (~0.5 cm in diameter) were surface-sterilized by sequential immersion in 70% ethanol for 1 min and 2% sodium hypochlorite for 3 min, followed by rinsing with sterile distilled water for 2 min. The sterilized segments were placed on Potato Dextrose Agar (PDA) supplemented with chloramphenicol (100 mg/L) and incubated at 26 °C for 7 days. Pure fungal cultures were obtained by subculturing actively growing mycelial tips onto fresh PDA plates and maintained in 15% glycerol at −20 °C for long-term storage.

2.2. Cultivation and extraction of secondary metabolites

Fungal isolates were initially grown on PDA at 26 °C for 7 days. Mycelial agar plugs (approximately 5 mm in diameter) were inoculated into Erlenmeyer flasks containing Potato Dextrose Broth (PDB). The cultures were incubated on an orbital shaker at 120 rpm and 26 °C for 21 days. Following incubation, the culture broth was extracted with an equal volume of ethyl

acetate. The organic phase was separated and concentrated using a rotary evaporator at 40 °C to yield the dry crude extract.

2.3. Antimicrobial activity assay

The test microorganisms included *Bacillus subtilis* (RKMUz-5), *Staphylococcus aureus* (ATCC 25923), *Pseudomonas aeruginosa* (ATCC 27879), *Escherichia coli* (RKMUz-221), and *Candida albicans* (RKMUz-247). Antimicrobial activity was evaluated using the agar disk diffusion method. Standardized bacterial suspensions were inoculated into Nutrient Agar, while *C. albicans* (1×10^6 CFU/mL) was inoculated into Mueller-Hinton agar. Sterile filter paper discs (6 mm) were impregnated with 20 µL of each extract. Ampicillin, gentamicin, and fluconazole were used as positive controls. Discs were placed on the inoculated plates and pre-incubated at 4 °C for 3 h, followed by incubation at 37 °C for 24 h for bacteria, and 29 °C for 48 h for fungi. The zones of inhibition were measured in millimeters, and all tests were performed in triplicate.

2.4. Determination of Minimum Inhibitory Concentration (MIC)

The minimum inhibitory concentration (MIC) of the crude ethyl acetate extract of isolate 8i3k was determined using the broth microdilution method in 96-well microtiter plates. Briefly, 2 mg of the crude extract was accurately weighed, and a stock solution was prepared in DMSO at an initial concentration of 5000 µg/mL. Mueller-Hinton Broth (MHB) was prepared and sterilized by autoclaving at 121 °C for 15 min; all equipment and consumables were sterilized prior to use.

Bacterial inocula of *Bacillus subtilis* (RKMUz-5) and *Escherichia coli* (RKMUz-221) were prepared by suspending a single colony of each organism in 2 mL of sterile physiological saline. The turbidity of each suspension was adjusted to be equivalent to the 0.5 McFarland standard. Working inocula were subsequently prepared by adding 50 µL of each standardized bacterial suspension to 5 mL of MHB (1:100 dilution ratio).

For the microdilution assay, 50 µL of MHB was dispensed into each well of columns 1–11. A 50 µL aliquot of the stock solution (5000 µg/mL) was added to the wells of column 1, yielding an initial extract concentration of 2500 µg/mL. Two-fold serial dilutions were performed sequentially from column 1 through column 10 by transferring 50 µL from each well to the next; the excess 50 µL was discarded from column 10 to maintain uniform volumes throughout the dilution series. This procedure generated a concentration gradient of 2500, 1250, 625, 312.5, 156.25, 78.13, 39.06, 19.53, 9.77, and 4.88 µg/mL in columns 1 through 10, respectively. Subsequently, 50 µL of the standardized bacterial inoculum was added to each well of columns 1–10. The assay was performed in three technical replicates per bacterial strain.

Column 11 served as the growth control (positive control), containing bacterial inoculum in MHB without the test extract. Column 12 served as the sterility control (negative control), containing only sterile MHB without bacteria or extract. Following inoculation, the microtiter plates were incubated at 37 °C for 18 h. Optical density was subsequently measured using a microplate reader, and the MIC was defined as the lowest concentration of the extract that completely inhibited visible bacterial growth.

2.5. Cytotoxicity Assay

The cytotoxic potential of the crude ethyl acetate extract of isolate 8i3k was evaluated at a single concentration of 100 µg/mL against two human cancer cell lines: HEp-2 (human laryngeal carcinoma) and A549 (lung adenocarcinoma), using the MTT assay. Cells were seeded in 96-well plates at a density of 2.5×10^3 cells/well in RPMI-1640 medium supplemented with 10% fetal bovine serum (FBS) and 1% antibiotic-antimycotic solution, and incubated at 37 °C in a 5% CO_2 atmosphere for 24 h. Following the initial incubation, the medium was replaced with extract-

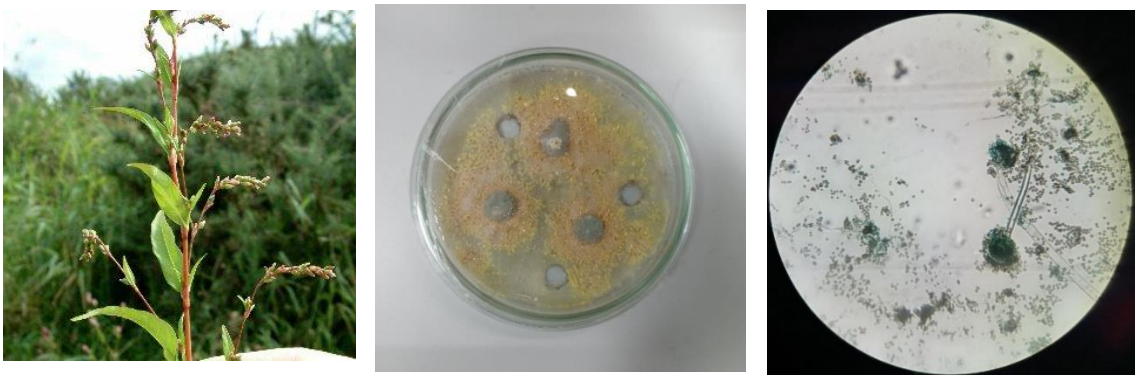
supplemented medium containing the 8i3k crude extract at 100 µg/mL (prepared from a stock solution in DMSO; final DMSO concentration ≤ 0.1%), and cells were incubated for an additional 24 h. Subsequently, 20 µL of MTT solution (5 mg/mL in phosphate-buffered saline) was added to each well and incubated for 4 h at 37 °C. The resulting formazan crystals were dissolved in 50 µL of DMSO, and absorbance was measured at 630 nm using a microplate reader. Cisplatin served as the positive (cytotoxic) control, and untreated cells served as the negative control. Cell viability was expressed as a percentage relative to untreated controls. All experiments were performed in triplicate, and statistical analysis was conducted using Origin 2024 software.

3. Results

3.1. Isolation and Morphological Characterization of Endophytic Fungi

Persicaria hydropiper L., commonly known as water pepper, is a medicinal plant belonging to the Polygonaceae family (Figure 1A). A total of six endophytic fungal isolates were successfully obtained from various healthy tissues of this plant: two isolates from flowers, one from leaves, and three from roots. Among these, the root-derived isolate designated as 8i3k was selected for detailed investigation based on its distinct morphology and subsequently confirmed antibacterial activity.

Morphological evaluation on Potato Dextrose Agar (PDA) after 18–21 days of incubation revealed that isolate 8i3k initially produced pale lemon-colored colonies, which transitioned to orange after several days, eventually developing a distinctive purple pigmentation in older cultures (Figure 1B). The isolate demonstrated limited aerial mycelial development, forming a very thin growth layer on the solid medium surface. Microscopic examination revealed non-septate hyphae (Figure 1C), a morphological trait characteristic of certain early-diverging fungal lineages.



A ***B*** ***C***

Figure 1. Morphological appearance of the medicinal plant Persicaria hydropiper L.(A), Macroscopic morphology of the root-derived endophytic fungal isolate 8i3k cultured on Potato Dextrose Agar (PDA) medium(B), Microscopic characteristics of endophytic isolate 8i3k under a compound light microscope, demonstrating non-septate hyphae(C).

3.2. Antimicrobial Activity and Minimum Inhibitory Concentration (MIC)

3.2.1. Disk Diffusion Assay

The crude ethyl acetate extract of isolate 8i3k was evaluated for antimicrobial activity using the agar disk diffusion method against a panel of pathogenic microorganisms. The results demonstrated selective antibacterial activity against Gram-positive bacteria, producing distinct inhibition zones of 17 mm against *Bacillus subtilis* (RKMUz-5) and 12 mm against *Staphylococcus aureus* (ATCC 25923). In contrast, no inhibitory activity (inhibition zone < 6 mm) was observed against the Gram-negative bacteria *Escherichia coli* (RKMUz-221) and

Pseudomonas aeruginosa (ATCC 27879), or against the yeast *Candida albicans* (RKMUz-247) under the tested conditions. Ampicillin, gentamicin, and fluconazole served as reference controls and produced inhibition zones consistent with established breakpoints (Table 1).

Isolated fungal isolates	Inhibition zone (mm, ± SE, P≤0.05)				
	Gram-positive bacteria		Gram-negative bacteria		*Candida albicans*
	Bacillus subtilis	*Staphylococcus aureus*	*Escherichia coli*	*Pseudomonas aeruginosa*	
8i3k	17.0 ±0.2	12.0 ±0.1	N/A	N/A	N/A
Ampicillin* (10 µg/disk)	23.01 ±0.2	22.02 ±0.3	Not tested	Not tested	Not tested
Gentamicin* (10 µg/disc)	Not tested	Not tested	19.04 ±0.3	26.05 ±0.1	Not tested
Fluconazole* (25 µg/disc)	Not tested	Not tested	Not tested	Not tested	26.01 ±0.3

Table 1. Antimicrobial activity of the crude ethyl acetate extract from endophytic isolate 8i3k (inhibition zone diameter, mm, mean ± SE, P ≤ 0.05). Ampicillin (10 µg/disc): positive control for Gram-positive bacteria; Gentamicin (10 µg/disc): positive control for Gram-negative bacteria; Fluconazole: positive control for yeast. N/A: no activity detected (zone < 6 mm); —: not tested.

3.2.2. Minimum Inhibitory Concentration (MIC)

Following confirmation of antibacterial activity by disk diffusion, the MIC of the 8i3k crude extract was determined against Bacillus subtilis (RKMUz-5) and Escherichia coli (RKMUz-221) using the broth microdilution method in Mueller-Hinton Broth. A stock solution (5000 µg/mL) was prepared, and the extract was introduced into column 1 of the microtiter plate at an initial concentration of 2500 µg/mL, followed by two-fold serial dilutions across columns 1 through 10, yielding a concentration gradient ranging from 4.88 to 2500 µg/mL. Columns 11 and 12 were reserved for growth and sterility controls, respectively.

The 8i3k extract demonstrated differential antibacterial potency against the two test organisms. Against Bacillus subtilis (RKMUz-5), complete growth inhibition was observed at a MIC of 312.5 µg/mL, indicating strong activity consistent with the pronounced inhibition zone recorded in the disk diffusion assay. Against Escherichia coli (RKMUz-221), the MIC was determined to be 1250 µg/mL, reflecting a markedly reduced susceptibility of this Gram-negative organism to the crude extract under the tested conditions. This difference in MIC values between the two species further corroborates the selective Gram-positive antibacterial activity observed in the disk diffusion assay. The positive growth control (column 11) confirmed bacterial viability throughout the assay, and the sterility control (column 12) remained turbidity-free, validating the experimental conditions. The MIC values are summarized in Table 2.

Table 2. Minimum Inhibitory Concentration (MIC) of the crude ethyl acetate extract from endophytic isolate 8i3k against *Bacillus subtilis* and *Escherichia coli*, determined by broth microdilution in Mueller-Hinton Broth (MHB; 37 °C, 18 h, n = 3).

3.3. Cytotoxic Activity of Isolate 8i3k

The cytotoxic potential of the crude ethyl acetate extract of isolate 8i3k was assessed at a concentration of 100 µg/mL against HEp-2 and A549 human cancer cell lines using the MTT assay. The results are summarized in Table 3.

Microorganism	Strain	Concentration range tested (µg/mL)	MIC (µg/mL)
Bacillus subtilis	RKMUz-5	4.88 – 2500	312.5
Escherichia coli	RKMUz-221	4.88 – 2500	1250

At the tested concentration, the 8i3k extract did not exhibit cytotoxic activity against either cell line. Instead, it produced a pronounced pro-proliferative effect, increasing cell viability to 117.5 ± 6.0% in A549 cells and 132.1 ± 6.9% in HEp-2 cells relative to the untreated control (100%). Cisplatin, used as a positive cytotoxic control, reduced viability to 48.3 ± 3.4% and 57.1 ± 3.0% in A549 and HEp-2 cells, respectively, confirming the validity of the assay conditions. These findings indicate that the secondary metabolites present in the crude extract of isolate 8i3k stimulate mammalian cell proliferation rather than inhibiting it under the tested conditions.

Cell Line / Sample, µg/mL	Number of viable cells, %	
	A549	HEp-2
8i3k	117,5±6,0	132,1±6,9
Cisplatin (positive control)	48,3±3,4	57,1±3,0
Control (untreated)	100	100

Table 3. Effect of crude fungal extract (100 µg/mL) on viability of HEp-2 and A549 cancer cell lines (MTT assay, mean ± SE, $n = 3$).

4. Discussion

The selective antibacterial activity of the 8i3k extract against Gram-positive bacteria is consistent with findings commonly reported for ethyl acetate extracts of endophytic fungi [11, 12, 13]. The lack of activity against Gram-negative organisms likely reflects the permeability barrier imposed by their outer membrane, which limits the uptake of hydrophobic compounds enriched in organic solvent extracts [11, 18]. The MIC of 312.5 µg/mL against *B. subtilis* compares favorably with values reported for crude endophyte-derived extracts in related studies [12, 13], indicating the presence of bioactive metabolites worthy of further isolation. Given the growing global burden of antimicrobial resistance, with 4.95 million deaths linked to resistant pathogens in 2019 alone [4], endophytic fungi represent a valuable and underexplored source of novel antibacterial leads [10, 11].

Rather than cytotoxicity, the 8i3k extract produced a pronounced pro-proliferative effect on both tested cancer cell lines, which contrasts with the cytotoxic properties frequently reported for endophyte-derived secondary metabolites [12, 13]. This stimulatory activity may be linked to the traditional wound-healing and regenerative properties of *P. hydropiper* [14]. It has been proposed that endophytes contribute to host plant bioactivities through the biosynthesis of functionally related metabolites [10, 14, 17], and the observed cell-stimulatory effect is consistent with this hypothesis, since active cell proliferation is a central component of tissue repair. The absence of cytotoxicity at the tested concentration further indicates low mammalian toxicity, which is favorable for potential therapeutic development.

Several limitations should be acknowledged. Biological activities were assessed using crude extracts at a single concentration, precluding dose-response analysis and IC_{50} determination. The molecular identity of isolate 8i3k remains unestablished, limiting comparison with related taxa and known metabolite profiles. Future work should focus on ITS-based molecular identification, compound isolation, and structural characterization by LC-MS and NMR spectroscopy.

5. Conclusion

This study demonstrates that the root-derived endophytic fungal isolate 8i3k from *Persicaria hydropiper* produces secondary metabolites with selective Gram-positive antibacterial activity and a notable pro-proliferative effect on human cancer cell lines. The low mammalian cytotoxicity and cell-stimulatory properties of the extract suggest a possible microbiological contribution to the traditional wound-healing properties of the host plant, and highlight the biotechnological potential of endophytic fungi associated with *P. hydropiper*. Compound purification, structural elucidation, and molecular identification of the isolate are the priority for future investigations.

REFERENCES

1. Baker, R.E.; Mahmud, A.S.; Miller, I.F.; Rajeev, M.; Rasambainarivo, F.; Rice, B.L.; Takahashi, S.; Tatem, A.J.; Wagner, C.E.; Wang, L.-F.; et al. Infectious disease in an era of global change. *Nat. Rev. Microbiol.* 2022, *20*, 193–205.
2. Bloom, D.E.; Cadarette, D. Infectious disease threats in the twenty-first century: Strengthening the global response. *Front. Immunol.* 2019, *10*, 549.
3. Zhang, X.-X.; Jin, Y.-Z.; Lu, Y.-H.; Huang, L.-L.; Wu, C.-X.; Lv, S.; Chen, Z.; Xiang, H.; Zhou, X.-N. Infectious disease control: From health security strengthening to health systems improvement at global level. *Glob. Health Res. Policy* 2023, *8*, 38.
4. Murray, C.J.L.; Ikuta, K.S.; Sharara, F.; Swetschinski, L.; Robles Aguilar, G.; Gray, A.; Han, C.; Bisignano, C.; Rao, P.; Wool, E.; et al. Global burden of bacterial antimicrobial resistance in 2019: A systematic analysis. *Lancet* 2022, *399*, 629–655.
5. O'Neill, J. *Tackling Drug-Resistant Infections Globally: Final Report and Recommendations*; Review on Antimicrobial Resistance; Government of the United Kingdom: London, UK, 2016.
6. Ling, L.L.; Schneider, T.; Peoples, A.J.; Spoering, A.L.; Engels, I.; Conlon, B.P.; Mueller, A.; Schäberle, T.F.; Hughes, D.E.; Epstein, S.; et al. A new antibiotic kills pathogens without detectable resistance. *Nature* 2015, *517*, 455–459.
7. Stokes, J.M.; Yang, K.; Swanson, K.; Jin, W.; Cubillos-Ruiz, A.; Donghia, N.M.; MacNair, C.R.; French, S.; Carfrae, L.A.; Bloom-Ackermann, Z.; et al. A deep learning approach to antibiotic discovery. *Cell* 2020, *180*, 688–702.e13.
8. Imai, Y.; Meyer, K.J.; Iinishi, A.; Favre-Godal, Q.; Green, R.; Manuse, S.; Caboni, M.; Mori, M.; Niles, S.; Ghiglieri, M.; et al. A new antibiotic selectively kills Gram-negative pathogens. *Nature* 2019, *576*, 459–464.
9. Terekhov, S.S.; Smirnov, I.V.; Malakhova, M.V.; Samoilov, A.E.; Manolov, A.I.; Nazarov, A.S.; Danilov, D.V.; Dubiley, S.A.; Osterman, I.A.; Rubtsova, M.P.; et al. Ultrahigh-throughput functional profiling of microbiota communities. *Proc. Natl. Acad. Sci. USA* 2018, *115*, 9551–9556.

10. Gouda, S.; Das, G.; Sen, S.K.; Shin, H.-S.; Patra, J.K. Endophytes: A treasure house of bioactive compounds of medicinal importance. *Front. Microbiol.* 2016, *7*, 1538.
11. Tiwari, P.; Bae, H. Endophytic fungi: Key insights, emerging prospects, and challenges in natural product drug discovery. *Microorganisms* 2022, *10*, 360.
12. Singh, V.K.; Kumar, A. Secondary metabolites from endophytic fungi: Production, methods of analysis, and diverse pharmaceutical potential. *Symbiosis* 2023, *90*, 111–125.
13. Gupta, A.; Meshram, V.; Gupta, M.; Goyal, S.; Qureshi, K.A.; Jaremko, M.; Shukla, K.K. Fungal endophytes: Microfactories of novel bioactive compounds with therapeutic interventions; a comprehensive review on the biotechnological developments in the field of fungal endophytic biology over the last decade. *Biomolecules* 2023, *13*, 1038.
14. Eshboev, F.; Egamberdieva, D. *Medicinal Plant Associated Endophytic Fungi: Metabolites and Bioactivity*; Elsevier: Amsterdam, The Netherlands, 2024.
15. Chow, C.; Padda, K.P.; Puri, A.; Chanway, C.P. An archaic approach to a modern issue: Endophytic archaea for sustainable agriculture. *Curr. Microbiol.* 2022, *79*, 322.
16. Kandel, S.; Joubert, P.; Doty, S. Bacterial endophyte colonization and distribution within plants. *Microorganisms* 2017, *5*, 77.
17. Rutkowska, N.; Drożdżyński, P.; Ryngajłło, M.; Marchut-Mikołajczyk, O. Plants as the extended phenotype of endophytes—The actual source of bioactive compounds. *Int. J. Mol. Sci.* 2023, *24*, 10096.
18. Jha, P.; Kaur, T.; Chhabra, I.; Panja, A.; Paul, S.; Kumar, V.; Malik, T. Endophytic fungi: Hidden treasure chest of antimicrobial metabolites — interrelationship of endophytes and metabolites. *Front. Microbiol.* 2023, *14*, 1227830.

ENZYMATIC CHARACTERISTICS OF BACTERIA ASSOCIATED WITH THE POTATO TUBER MOTH (*PHTHORIMAEA OPERCULELLA*)

Z.X. Qutlimurodova[1], S.A. Abdusamatov[2], Z. Eshbekova[2], J.U. Boyxonov[2]
Trainee Researcher, Urgench State University named after Abu Rayhan Beruni, Urgench, Uzbekistan[1]
National University of Uzbekistan named after Mirzo Ulugbek[2]
https://doi.org/10.5281/zenodo.20807979

Abstract. *In this study, bacterial isolates were obtained from the gut microbiota of the potato tuber moth (Phthorimaea operculella) and their morphological, biological, and enzymatic characteristics were investigated. A total of nine bacterial isolates were recovered from pest specimens, among which representatives belonging to the genera Bacillus, Enterobacter, and Brevibacillus were identified. The insecticidal activity of the isolated bacteria against the potato tuber moth was evaluated, and isolates N23, K10, and K7 exhibited the highest biological efficacy. In addition, the activities of chitinase, protease, and amylase enzymes were determined, with the highest values recorded for Bacillus thuringiensis isolates N23 and K10. The obtained results demonstrated that these bacterial isolates possess significant entomopathogenic potential and may serve as promising biological control agents against the potato tuber moth.*

Keywords: *phthorimaea operculella, potato tuber moth, entomopathogenic bacteria, Bacillus thuringiensis, Brevibacillus laterosporus, chitinase, protease, amylase, insecticidal activity, biological control.*

Literature review. Nowadays, protecting agricultural crops from pests is considered one of the important factors in ensuring food security. According to recent data, despite pesticide and non-chemical control measures, approximately 37% of crops are lost annually due to the impact of pests, of which 13% is attributed to insects, 12% to pathogens, and 12% to weeds. In potato cultivation as well, insect pests and diseases pose a constant threat, leading to a reduction in yield of up to 40% [1, 2].

Potato (*Solanum tuberosum* L.) is of great importance as an important food crop in world and Uzbekistan agriculture, and one of the main factors reducing its productivity is various insect pests. In particular, the potato tuber moth (*Phthorimaea operculella*) and the Colorado potato beetle (*Leptinotarsa decemlineata*) cause significant economic damage to potato crops, resulting in reductions in both yield quantity and quality.

Phthorimaea operculella damages potatoes both in the field and during storage. It reduces product quality and increases the risk of infection by pathogens. Because this pest simultaneously damages both leaves and tubers, crop yield is significantly reduced. Under warm climatic conditions, storage losses may even reach up to 100% [3, 4].

The main method used to control these pests has been the application of chemical insecticides. However, their prolonged use has resulted in several adverse effects, including the development of resistance in pest populations, environmental pollution, a reduction in beneficial organisms, and the accumulation of pesticide residues in food products. Therefore, the development of environmentally safe and biologically effective control strategies has become an

important scientific and practical priority. Modern agriculture faces two major challenges: increasing crop productivity and reducing negative environmental impacts. Pests and diseases are among the principal causes of food losses, leading to annual reductions of 20–40% in the global yields of major crops. Although synthetic chemical pesticides were initially employed as the primary means of insect pest control, their excessive and long-term use has contributed to the emergence of pesticide resistance, ecosystem contamination, biodiversity loss, and adverse effects on human and animal health [5].

In pest management, biopesticides—biological products that include metabolites synthesized by microorganisms, compounds of plant and animal origin, natural minerals, and semiochemicals—are also widely used [5]. Furthermore, microbiological biopesticides account for more than 55% of the total biopesticide market, confirming their important role in sustainable agriculture [6]. Recent technological advances, particularly in the fields of microbial fermentation, metabolomics, genomics, and synthetic biology, have accelerated the discovery and agricultural application of these natural compounds [7–9].

Bacteria used as biological control agents are functionally classified into facultative pathogens (*Pseudomonas aeruginosa*), obligate pathogens (*Bacillus popilliae*), crystal-forming spore-producing bacteria (*Bacillus thuringiensis*), and potential pathogens (*Serratia marcescens*). Among these groups, spore-forming bacteria are widely utilized because of their high efficacy, safety, and specificity [10].

Bacteria belonging to the families *Pseudomonadaceae*, *Streptococcaceae*, *Enterobacteriaceae*, *Bacillaceae*, and *Micrococcaceae* are commonly used in biological control. Among them, certain species of the genus *Bacillus*, particularly *Bacillus subtilis*, have been granted the status of "Generally Recognized as Safe" (GRAS) by the United States Food and Drug Administration (FDA) [11].

Approximately 90% of biopesticide products in the United States are based on *Bacillus thuringiensis* (Bt), which is widely used for pest control in medicine, agriculture, and forestry [12]. During the sporulation process, Bt produces insecticidal proteins in the form of parasporal crystals. These crystals are primarily composed of proteins known as Cry and Cyt toxins and are also referred to as δ-endotoxins [13]. Cry proteins are considered highly safe, selective, and sustainable alternative agents for pest management [14].

The β-exotoxin produced by *Bacillus thuringiensis*, known as thuringiensin, is a heat-stable secondary metabolite that exhibits insecticidal activity against insects belonging to the orders *Diptera*, *Coleoptera*, *Lepidoptera*, *Hymenoptera*, *Orthoptera*, and *Isoptera*, as well as against certain nematodes [15]. Another successful example is Spinosad, which is widely used as an insecticidal metabolite produced by *Saccharopolyspora spinosa* [16].

Furthermore, the insecticidal activity of metabolites produced by *Chromobacterium subtsugae*, identified as a novel insecticidal bacterium, has also been confirmed [13]. Various subspecies of *Bacillus thuringiensis* are effective against a broad spectrum of insect pests, including representatives of the orders *Lepidoptera*, *Coleoptera*, and *Diptera*, and are widely used in commercial biopesticide formulations. In addition, the toxin complex synthesized by *Xenorhabdus nematophilus* possesses insecticidal properties and enhances the pathogenicity of entomopathogenic nematodes through symbiotic interactions [14].

The application of biopreparations based on beneficial microorganisms in potato agroecosystems not only reduces pest populations but also improves soil microbiological activity. Compared with chemical insecticides, microbial preparations are environmentally friendly and

prevent the accumulation of toxic residues in agricultural products. Therefore, the importance of microbiological control methods within integrated pest management systems is continuously increasing [17].

Analysis of the scientific literature presented above indicates that the use of entomopathogenic bacteria is one of the most promising approaches for the control of potato pests. However, the composition of the microbiota associated with pests occurring in potato agroecosystems, as well as the biological characteristics and entomocidal activity of bacteria isolated from them, have not been sufficiently studied under local conditions. Therefore, in the present study, bacterial isolates were obtained from specimens of the potato tuber moth (*Phthorimaea operculella*), and their morphological and biological characteristics were investigated.

Materials and Methods

Isolation of Bacteria from *Phthorimaea operculella* Larvae

Standard microbiological methods were used for the isolation of bacterial strains. Specimens of *Phthorimaea operculella* collected under field conditions were transported to the laboratory in sterile containers. The external surfaces of the samples were sterilized with 70% ethanol for 1 min and subsequently rinsed several times with sterile distilled water. This procedure enabled the removal of external microflora and facilitated the selective isolation of internal microorganisms.

Under sterile conditions, *P. operculella* larvae were dissected, and gut tissues were aseptically removed. The isolated tissues were homogenized in sterile physiological saline solution containing 0.85% NaCl, and the resulting suspension was serially diluted to 10^{-1}–10^{-3}. Diluted samples were inoculated onto Nutrient Agar (NA), Tryptic Soy Agar (TSA), MacConkey agar, and Eosin Methylene Blue (EMB) agar media. The inoculated plates were incubated at 37°C for 24–48 h. After incubation, morphologically distinct colonies were selected and purified by repeated streaking to obtain pure cultures [18].

Determination of Hydrolytic Enzyme Activities (Chitinase, Protease, and Amylase) of Bacterial Isolates

Protease Activity. Proteolytic activity was determined using a hemoglobin substrate-based method with slight modifications. A 0.1% hemoglobin solution prepared in citrate buffer (pH 5.5) was used as the substrate. Enzyme activity was evaluated by measuring the amount of leucine released from hemoglobin. One unit (U) of protease activity was defined as the amount of enzyme required to release 1 mg of leucine at 37°C within 30 min. For the assay, 0.5 mL of crude enzyme extract was mixed with 3 mL of 1% hemoglobin solution and incubated at 37°C for 30 min. The reaction was terminated by adding 3 mL of 5% trichloroacetic acid (TCA), and the mixture was subsequently filtered. The filtrate was mixed with 0.5 mL of distilled water and 1 mL of ninhydrin reagent and then boiled for 20 min. After cooling, 5 mL of diluting solution (H_2O = 1:1) was added. Protease activity was determined by measuring the optical density at a wavelength of 570 nm [19].

Chitinase Activity. Chitinolytic activity was evaluated using the 3,5-dinitrosalicylic acid (DNS) method with colloidal chitin as the substrate, following the methodology of Shivalee et al. For this assay, 1.0 mL of enzyme solution was mixed with 1.0 mL of 0.5% colloidal chitin prepared in 0.1 M citrate buffer (pH 7.0) and incubated at 37°C in a shaking water bath for 30 min. The reaction was terminated by adding 2 mL of DNS reagent and heating the mixture in a boiling water bath for 10 min. After cooling, the mixture was centrifuged at 10,000 rpm for 10 min. The optical

density of the resulting supernatant was measured at 540 nm against a control sample. One unit (U) of chitinase activity was defined as the amount of enzyme producing reducing sugars in 1 mL of solution per minute under the assay conditions [20].

Amylase Activity. Amylolytic activity was determined using the standard 3,5-dinitrosalicylic acid (DNSA) method. To prepare the DNS reagent, 1.4 g of 3,5-dinitrosalicylic acid was dissolved in 70 mL of 0.5 N NaOH solution, followed by the addition of 30 g of sodium potassium tartrate, and the final volume was adjusted to 1000 mL. Standard maltose and test solutions consisting of 0.5 mL of 1% soluble starch solution and 1 mL of DNS reagent were incubated at 40°C for 15 min. Subsequently, 5 mL of distilled water was added, the mixture was cooled, and absorbance was measured at 540 nm. Based on the obtained results, the amount of reducing sugars released as a result of starch hydrolysis was calculated [21].

Results and Discussion

During the study, specimens of *Phthorimaea operculella* were collected from potato agroecosystems located in the Piskent, Bekabad, and Boka districts of the Tashkent region. Field observations revealed that the pest was widely distributed throughout the surveyed areas. The collected specimens were transported to the laboratory, where bacterial isolates were obtained from their gut microbiota for further investigation.

Bacterial isolation from the gut microbiota of *Phthorimaea operculella* was successfully performed. Following incubation on culture media, colonies exhibiting diverse morphological characteristics were observed. Morphologically distinct colonies were selected and purified through repeated streaking to obtain pure cultures (Figure 1).

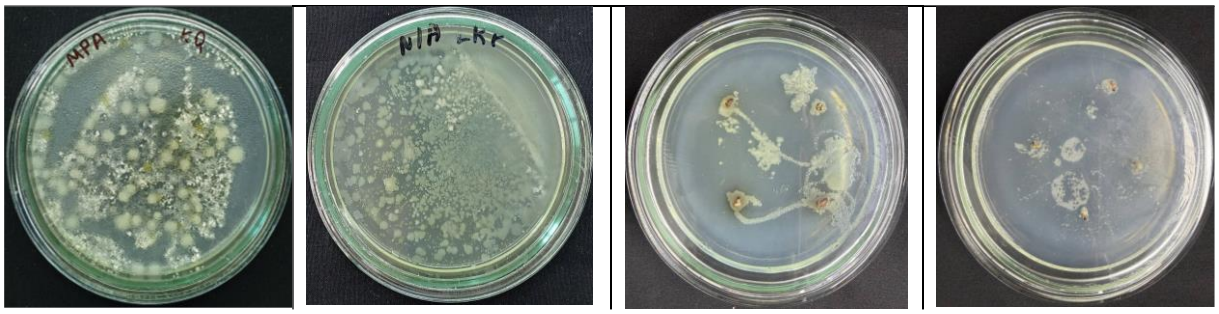


Figure 2. Isolation and purification of bacterial isolates from the gut microbiota of Phthorimaea operculella.

As a result, nine bacterial isolates were obtained from *P. operculella* specimens. The morphological and biological characteristics of the isolated strains were investigated, and selected isolates were subjected to further studies and microscopic examination (Figure 2).

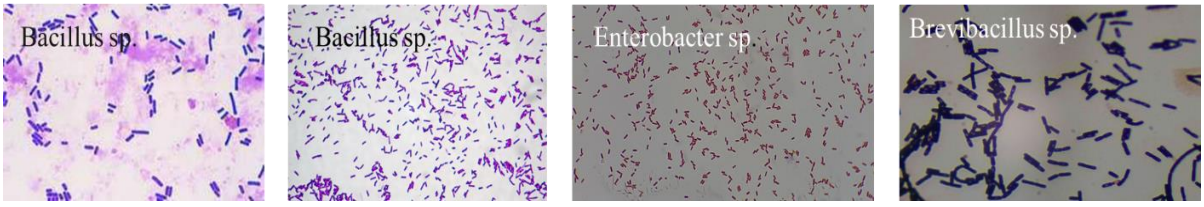


Figure 2. Morphological and cultural characteristics of bacterial isolates obtained from Phthorimaea operculella.

Gram staining and microscopic observations revealed the cell morphology and Gram reaction of the isolated bacterial strains (Figure 1). Among the investigated isolates, two representatives of *Bacillus* sp., one *Enterobacter* sp., and one *Brevibacillus* sp. were identified. The *Bacillus* isolates were Gram-positive and consisted of purple-stained rod-shaped cells. The

cells were observed either singly or arranged in short chains. In contrast, the *Enterobacter* sp. isolate exhibited a Gram-negative reaction and appeared as short pink-stained rod-shaped cells. The *Brevibacillus* sp. isolate was characterized by Gram-positive, relatively long rod-shaped cells, which were occasionally arranged in chains.

The obtained results confirmed that the isolates belonged to their respective bacterial groups based on their morphological characteristics and Gram-staining properties. The morphological features revealed through Gram staining were consistent with the results of molecular identification, allowing a preliminary taxonomic characterization of the isolates. These findings provide an important basis for subsequent physiological, biochemical, and molecular studies.

Disease Suppression Activity

The antagonistic activity of different bacterial isolates against the phytopathogen increased significantly over time (Figure 3). During the initial 3 days of the experiment, disease suppression levels were relatively low in all treatments, ranging from 4.5% to 20.3%. As the incubation period progressed, the protective efficacy of the isolates gradually increased, and the highest levels of disease suppression were observed on day 15.

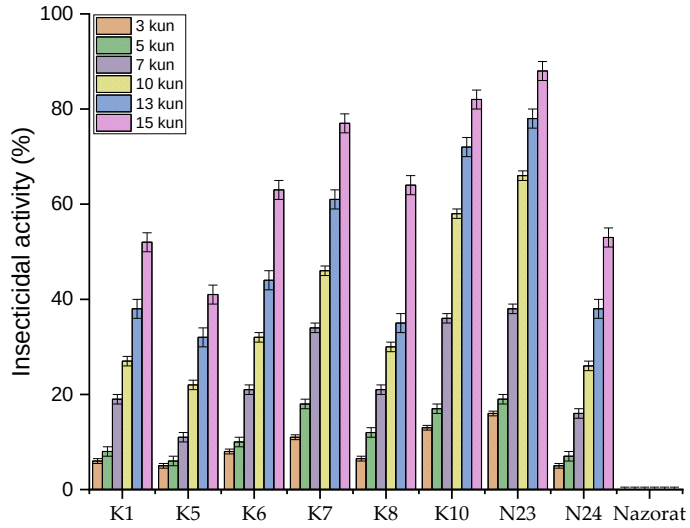


Figure 3. Insecticidal efficacy of bacterial isolates against the potato tuber moth (Phthorimaea operculella).

Among the investigated isolates, N23 exhibited the highest antagonistic activity. The disease suppression rate of this isolate was approximately 20% on day 3 and increased to 87–88% by day 15. Similarly, K10 and K7 also demonstrated high efficacy, achieving disease suppression rates of approximately 80% and 77%, respectively, at the end of the experiment. Positive results were also observed for K8 and K6, which successfully restricted disease development by 63–65% on day 15.

The antagonistic activities of isolates N24 and K1 were moderate, with disease suppression rates of approximately 53% and 52%, respectively, recorded at the end of the experiment. The lowest levels of activity were observed in the K5 isolate and the control treatment. While natural disease progression continued in the control treatment, the protective efficacy of K5 remained considerably lower than that of the more active isolates.

Overall, the results demonstrated that the ability of the bacterial isolates to suppress phytopathogen development increased over time and that isolates N23, K10, and K7 possess

considerable potential as biological control agents. These isolates represent promising candidates for the development of biocontrol products and for further investigation of their mechanisms of action.

Hydrolytic Enzyme Activities of Bacterial Isolates

The hydrolytic enzyme activities of nine bacterial isolates obtained from the gut microbiota of *Phthorimaea operculella* were evaluated. According to the preliminary screening results, *Bacillus thuringiensis* K10, *Bacillus thuringiensis* N23, and *Brevibacillus laterosporus* K7 exhibited high hydrolytic enzyme activities (Figure 4).

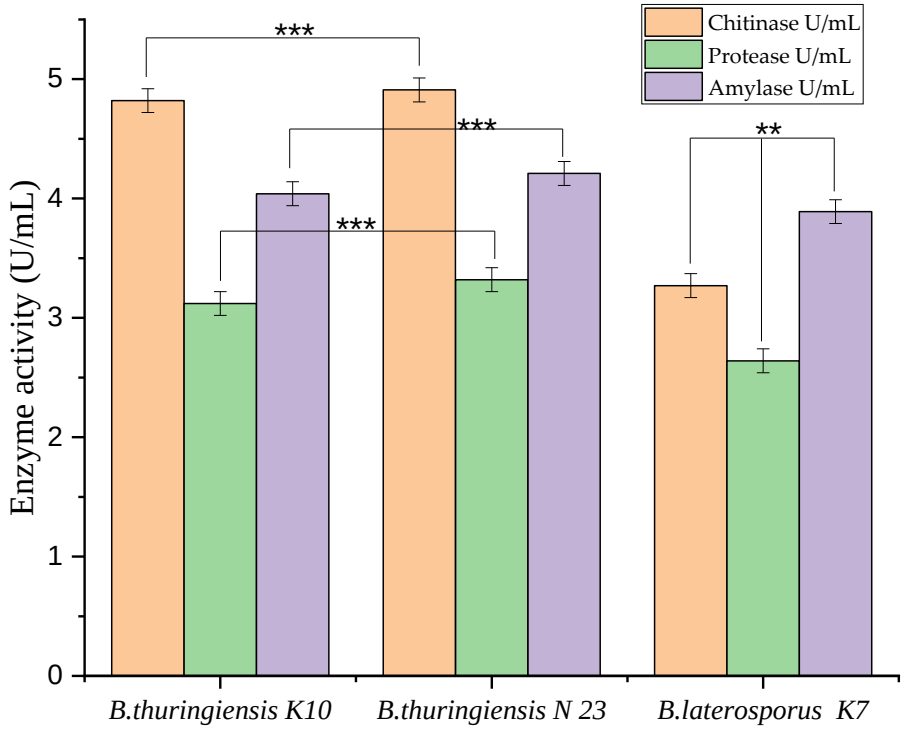


Figure 4. Activities of hydrolytic enzymes (chitinase, protease, and amylase) produced by bacterial isolates isolated from Phthorimaea operculella.

According to the obtained results, the highest chitinase activity was recorded in *Bacillus thuringiensis* N23, reaching 4.91 ± 0.12 U/mL. The corresponding values for isolate K10 and *Brevibacillus laterosporus* K7 were 4.82 ± 0.13 U/mL and 3.27 ± 0.21 U/mL, respectively.

Protease activity was also highest in isolate N23, with a value of 3.32 ± 0.08 U/mL. The activities recorded for K10 and K7 were 3.12 ± 0.07 U/mL and 2.64 ± 0.11 U/mL, respectively.

Similarly, isolate N23 exhibited the highest amylase activity, reaching 4.21 ± 0.11 U/mL. The enzyme activities of isolates K10 and K7 were 4.04 ± 0.20 U/mL and 3.89 ± 0.14 U/mL, respectively.

These results indicate that *B. thuringiensis* N23 and K10 possess a strong capacity for the synthesis of hydrolytic enzymes.

The findings of the present study demonstrated that *Bacillus thuringiensis* N23 and K10 isolates, obtained from the gut microbiota of *Phthorimaea operculella*, exhibited high chitinase, protease, and amylase activities. In particular, isolate N23 showed the highest values for all investigated enzymes. This observation suggests that these isolates may possess considerable entomopathogenic potential.

Our results are consistent with those reported by Liu et al. (2002), who demonstrated that chitinase enzymes are widely distributed among different *B. thuringiensis* strains and contribute

to enhanced insecticidal activity. According to their findings, chitinase-producing strains increased the larvicidal efficacy of *B. thuringiensis* toxins by up to 2.35-fold. This enhancement was attributed to the ability of chitinase to degrade the insect cuticle and peritrophic membrane, thereby facilitating toxin penetration and activity [22].

The importance of chitinase in entomopathogenicity has also been confirmed in subsequent studies. Qin et al. (2020) reported that chitin-binding proteins of *B. thuringiensis* interact with the peritrophic membrane of the insect gut and play an important role during the infection process [23]. Likewise, Nielsen-Leroux et al. (2012) noted that chitinolytic enzymes contribute to the disruption of gut barriers, thereby facilitating the access of bacteria and toxins to epithelial cells [24].

In the present study, *B. laterosporus* K7 also exhibited chitinase and protease activities, although these values were lower than those observed in *B. thuringiensis* isolates. Nevertheless, these findings support the entomopathogenic potential of *Brevibacillus laterosporus*. Prasanna et al. (2013) identified inducible extracellular chitinases in *B. laterosporus* strains and suggested that these enzymes contribute to the bacterium's biocontrol and insecticidal properties [25].

The protease activity observed in this study is also in agreement with previous reports. Malovichko et al. (2019) emphasized that, in addition to Cry toxins, proteases and chitinases represent important virulence factors of *B. thuringiensis*, contributing to the progression of infection within the insect host [26]. Similarly, Marche et al. (2018) demonstrated that the expression of chitinase and protease genes in *B. laterosporus* strains is associated with insecticidal activity [27].

Overall, the obtained results indicate that *B. thuringiensis* N23 and K10 possess high enzymatic activity, which may enhance their entomopathogenic potential. Comparison with previously published studies suggests that chitinase and protease enzymes play crucial roles in the degradation of insect cuticles and gut barriers. Therefore, these isolates may be considered promising biological agents for the development of biocontrol strategies against the potato tuber moth (*P. operculella*).

REFERENCES

1. EPA, Biopesticides, Environmental Protection Agency, 2024.
2. Barbara D.J., Clewes E., Plant pathogenic Verticillium species, Mol. Plant Pathol., 2003, pp. 297–305.
3. Brar S.K., Verma M., Tyagi R.D., Valero J.R., Advances in Bacillus thuringiensis biopesticides, Process Biochemistry, 2006, pp. 323–342.
4. Javorekova S., Kovacsova S., Medo J., Makova J., Petrova J., Hleba L., Kostalova D., Artimova R., Soil amended with organic fertilizers as a source of actinomycetes with biocontrol potential, Journal of Microbiology Biotechnology and Food Sciences, 2019, pp. 1352–1359.
5. Waghunde R.R., Shinde C.U., Pandey P., Singh C., Fungal biopesticides for agroenvironmental sustainability, Industrially Important Fungi for Sustainable Development, 2021, pp. 479–508.
6. Ayilara M.S., Akinola S.A., Adebajo M.T., Benefits and Drawbacks of Microbial Inoculant in Terms of Human Health and the Environment, Microbial Inoculants: Applications for Sustainable Agriculture, 2024, pp. 411–435.

7. Messing R., Brodeur J., Current challenges to the implementation of classical biological control, Biocontrol, 2018, pp. 1–9.
8. Kour D., Rana K.L., Yadav A.N., Yadav N., Kumar M., Kumar V., Vyas P., Dhaliwal H.S., Saxena A.K., Microbial biofertilizers: bioresources and eco-friendly technologies for agricultural sustainability, Biocatal. Agric. Biotechnol., 2020.
9. Hernández-Fernández M., Cordero-Bueso G., Ruiz-Muñoz M., Cantoral J.M., Culturable yeasts as biofertilizers and biopesticides for sustainable agriculture, Plants, 2021.
10. Pucheta D.M., Macias A.F., Navarro S.R., Mayra D.L.T., Mechanism of action of entomopathogenic fungi, Microbiol., 2006, pp. 2164–2171.
11. Sharma S., Malik P., Biopesticides: types and applications, 2012.
12. Mora M.A.E., Castilho A.M.C., Fraga M.E., Classification of entomopathogenic fungi, 2017.
13. Copping L.G., Menn J.J., Biopesticides: action and applications, Pest Manag. Sci., 2000, pp. 651–676.
14. Heuskin S., Lorge S., Godin B., Leroy P., Frère I., Verheggen F.J., Haubruge E., Wathelet J.P., Mestdagh M., Hance T., Lognay G., Semiochemical formulation optimization, Pest Manag. Sci., 2012.
15. Sivapragasm A., Biopesticides and their regulation in Malaysia, Asia-Pacific Biofertilizers and Biopesticides Information Platform, 2022.
16. Fenibo E.O., Ijoma G.N., Matambo T., Biopesticides in sustainable agriculture: current status and future prospects, New Developments in Biopesticide Research, 2022.
17. Pineda S., Alatorre R., Schneider M.L., Martinez A.M., Pathogenicity of entomopathogenic fungi, 2007, pp. 43–52.
18. Cappuccino, J. (2018). *Microbiology a laboratory manual*. Pearson.
19. Afrin, S., Tamanna, T., Shahajadi, U. F., Bhowmik, B., Jui, A. H., Miah, M. A. S., & Bhuiyan, M. N. I. (2024). Characterization of protease-producing bacteria from garden soil and antagonistic activity against pathogenic bacteria. *The Microbe*, *4*, 100123.
20. Xie, J., Zhang, L., Yang, K., Zhang, H., Jiang, M., Liao, S., ... & Shen, N. (2025). Enhanced chitinase production by Bacillus paralicheniformis GXMU-J23. 1: Optimization, genomic insights, and chitin degradation mechanism. *Bioresource Technology*, *418*, 131911.
21. Kim, J. A., Kim, M. J., Yim, J. H., Kim, I. C., Rhee, J. S., & Han, S. J. (2025). Isolation and Characterization of Low-Temperature and High-Salinity Amylase from Halomonas sp. KS41843. *Fermentation*, *11*(8), 465.
22. Liu, D., Cai, J., Xie, C., Liu, C., & Chen, Y. (2002). Purification and partial characterization of a 36-kDa chitinase from *Bacillus thuringiensis* subsp. *colmeri* and its biocontrol potential. *Enzyme and Microbial Technology, 31*(6), 828–834.
23. Qin, Y., Zhang, J., Liu, Y., Zhang, X., & Wang, Q. (2020). Chitin-binding proteins contribute to the insecticidal activity of *Bacillus thuringiensis*. *Toxins*, *12*(4), 252.
24. Nielsen-Leroux, C., Gaudriault, S., Ramarao, N., Lereclus, D., & Givaudan, A. (2012). How the insect pathogen bacteria *Bacillus cereus* and *Bacillus thuringiensis* induce host death. *Current Opinion in Microbiology*, *15*(3), 220–224
25. Prasanna, L., Eijsink, V. G. H., Meadow, R., & Gåseidnes, S. (2013). A novel chitinase from the entomopathogenic bacterium *Brevibacillus laterosporus*. *Microbiological Research*, *168*(6), 358–365.

BIOLOGICAL DEVELOPMENT OF MEDICINAL LEMON BALM (MELISSA OFFICINALIS L.) AND PATTERNS OF VEGETATIVE ORGAN FORMATION

F.I. Turdiyev
Associate Professor, Department of Medical Biology and Public Health, Kokand University Andijan Branch, PhD
https://doi.org/10.5281/zenodo.20838647

Abstract*. The study analyzes the biological development of medicinal lemon balm (Melissa officinalis L.) under open-field conditions, with special attention to the formation of vegetative organs that determine the value of the plant as herbal raw material. Thirty uniformly developed plants were selected for biometric observations. Phenological records were made every 7–10 days, while plant height, number of leaves, lateral shoots, root development and aboveground biomass were assessed by direct measurement or counting. Leaf surface area was recalculated using the non-destructive length–width method, $S = L \times W \times K$, where K was accepted as 0.75 for the broadly ovate to elliptic leaf shape of lemon balm. The vegetation period from spring regrowth to the pre-generative stage lasted 127 days. By the pre-generative stage, plant height reached 64.2 cm, the number of leaves was 236 per plant, lateral shoots reached 38.6, and aboveground biomass was 186.5 g per plant. The recalculated total leaf surface area was 4694.0 cm² per plant. The results indicate that the most biologically active period for vegetative organ formation occurred from late April through May, when branching and leaf mass expansion were most intensive. Because individual measurements for all 30 plants were not available in the source dataset, inferential statistics such as SD, SE, CV% and p-values are described methodologically but not artificially calculated.*

Keywords: *lemon balm, Melissa officinalis L., biological development, vegetative organs, leaf area, biomass, branching, medicinal raw material.*

INTRODUCTION. Medicinal and aromatic plants are not only a reserve of biologically active compounds, but also living biological systems whose raw-material value depends on the rhythm of growth, organ formation and the timing of harvest. For species cultivated mainly for leaves and young shoots, a general statement that the plant is “medicinal” is not sufficient. It is necessary to show how quickly the assimilative surface develops, when branching becomes active and whether the plant is able to accumulate enough aboveground mass before the transition to the generative phase.

Lemon balm (Melissa officinalis L.), a perennial herbaceous species of the Lamiaceae family, is widely used in phytotherapy, pharmacy, food production, cosmetics and aromatherapy. Its leaves and young shoots contain essential oil components, phenolic compounds, rosmarinic acid, flavonoids and other metabolites that form the pharmacological and aromatic profile of the raw material. From an agronomic point of view, however, the practical productivity of lemon balm is determined first of all by vegetative development: the number of leaves, branching intensity, total leaf surface area and aboveground biomass.

The present article focuses on this biological side of lemon balm cultivation. The author’s position is that the assessment of lemon balm under local open-field conditions should not be

limited to a final biomass value. A more useful evaluation must connect phenological phases with measurable morphological traits: plant height, lateral shoots, leaf number, leaf area and root development. Such an approach makes it possible to identify the period when the plant forms the main medicinal raw material and when cultivation measures are likely to have the strongest effect.

LITERATURE REVIEW. Earlier works on medicinal plants in Uzbekistan and neighboring regions have emphasized introduction, acclimatization and biological productivity as necessary stages before recommending a species for wider cultivation. These studies are important because the same medicinal plant can behave differently depending on soil moisture, temperature regime, planting density and local agronomic practice. For lemon balm, this point is especially relevant: the crop is perennial and capable of repeated regrowth, but the useful raw material is concentrated largely in the leaf-bearing shoots.

Modern studies confirm that lemon balm productivity is strongly controlled by the conditions under which vegetative organs are formed. Fallah et al. (2024), for example, showed that manure source affected biomass, nutrient content and essential oil production during consecutive harvests, indicating that nutrient availability changes not only yield quantity but also the quality of raw material [7]. Safaei et al. (2024) demonstrated under hydroponic conditions that nitrogen form substantially affected growth, biomass and phytochemical traits; the highest nitrate treatment produced the strongest growth and morpho-physiological response [8]. These findings support the view that leaf and shoot development should be treated as central indicators, not as secondary descriptive traits.

Research on light quality also shows the close connection between vegetative growth and secondary metabolism. Aghakarim et al. (2023) reported that end-of-day red and blue light treatments changed biomass, chlorophyll content, dry matter and essential oil characteristics of lemon balm [9]. Such results are useful for interpreting field observations: even when the present study does not manipulate light, the expansion of leaf area remains biologically meaningful because it defines the photosynthetic base from which biomass and metabolites are formed.

A separate methodological issue is the estimation of leaf area. Direct scanning gives the most accurate value, but non-destructive length–width models are widely used when repeated observation of the same plants is required. General studies of leaf-area estimation show that leaf length and width, combined with a correction coefficient reflecting leaf shape, can produce practical estimates for ordinary leaves [10]. For lemon balm, whose leaves are broadly ovate to elliptic and serrated, the coefficient must be stated explicitly; otherwise, the reported total leaf surface area cannot be reproduced.

The reviewed literature therefore points to a clear research gap. Many papers discuss the phytochemistry and pharmacological value of lemon balm, while fewer studies present local, phase-by-phase biometric evidence on vegetative organ formation. The present work addresses this gap by linking phenological development with final morphological indicators and by making the leaf-area calculation transparent.

The scientific novelty of the study lies in the local biometric characterization of Melissa officinalis L. under open-field conditions with emphasis on the formation of vegetative organs before the generative stage. The article specifies the duration of the main development phases, identifies the most active period of shoot and leaf formation, recalculates leaf surface area using an explicit coefficient, and links leaf number, branching and biomass accumulation to the practical production of medicinal raw material. The author’s contribution is the interpretation of lemon balm productivity not as a single final mass value, but as a sequence of biologically connected processes:

regrowth, stem elongation, branching, leaf-surface expansion and pre-generative biomass accumulation.

MATERIALS AND METHODS. The research object was medicinal lemon balm (Melissa officinalis L.) grown under open-field conditions. Plants were placed with a row spacing of 60 cm and an in-row spacing of 30 cm. For biometric observations, 30 healthy and uniformly developed plants were selected from the experimental field. Phenological observations were carried out every 7–10 days from spring regrowth until the pre-generative stage.

Plant height was measured from the soil surface to the upper growth point using a measuring ruler. The number of leaves, main stems and lateral shoots was determined by direct counting on the selected plants. Root length was recorded at the end of the observation period on sampled plants after careful removal from the soil. Aboveground vegetative biomass was determined as the fresh mass of stems, leaves and young shoots formed before the generative stage.

Leaf surface area was estimated by the non-destructive length–width method: $S = L \times W \times K$, where S is the area of one leaf (cm^2), L is leaf length (cm), W is maximum leaf width (cm), and K is the correction coefficient. Because lemon balm leaves are broadly ovate to elliptic, K was accepted as 0.75. With the recorded average leaf length of 6.8 cm and width of 3.9 cm, the calculated area of one leaf was 19.9 cm^2. Total leaf surface area per plant was calculated as $S_{total} = S \times N_{leaves}$, where N_{leaves} is the number of leaves per plant.

Statistical processing was planned for the 30-plant biometric dataset using the following indicators: arithmetic mean ($Mean = \Sigma xi/n$), standard deviation ($SD = \sqrt{\Sigma(xi - \bar{x})^2/(n-1)}$), standard error ($SE = SD/\sqrt{n}$), and coefficient of variation ($CV\% = SD/\bar{x} \times 100$). Where two or more treatments or stages are compared using plant-level repeated measurements, significance should be assessed by analysis of variance or an appropriate paired/repeated-measures test, with $p \leq 0.05$ accepted as statistically significant. In the present version, only mean values were available from the source document; therefore SD, SE, CV% and p-values were not calculated to avoid introducing unsupported numerical data.

RESULTS. The biological development of lemon balm from spring regrowth to the pre-generative stage lasted 127 days. Growth began on 20 March, and the first stage continued for 13 days. During this early period, plant height was 6.4 cm, showing that renewal growth started from the root collar and young overwintered buds. The following 27-day period was characterized by elongation of the main stem, during which plant height reached 18.7 cm.

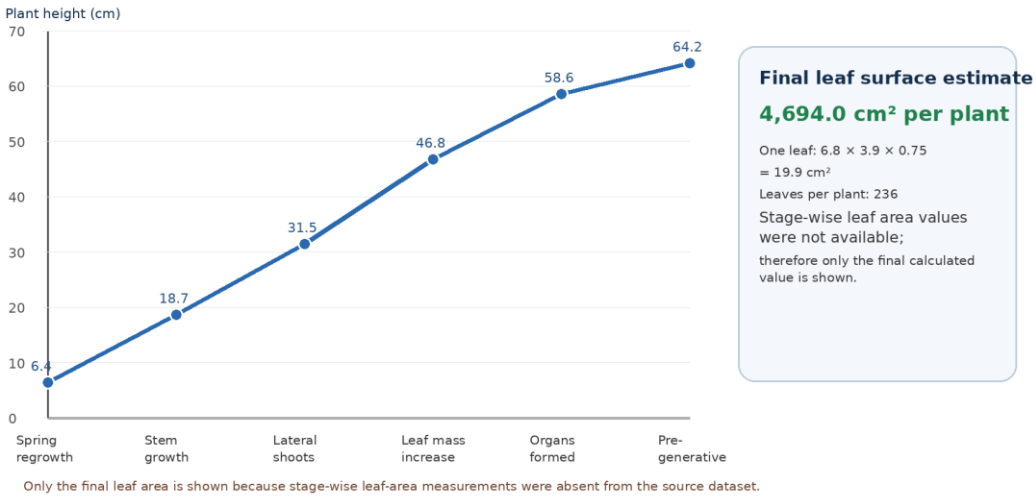
Table 1. Biological development stages of medicinal lemon balm.

No.	Development stage	Start	End	Duration, days	Plant height, cm
1	Spring vegetation	Mar 20	Apr 1	13	6.4
2	Main stem growth	Apr 2	Apr 28	27	18.7
3	Lateral shoots	Apr 29	May 20	22	31.5
4	Leaf mass increase	May 21	Jun 15	26	46.8
5	Vegetative organs formed	Jun 16	Jul 4	19	58.6
6	Pre-generative stage	Jul 5	Jul 24	20	64.2

The formation of lateral shoots was recorded between 29 April and 20 May, when plant height reached 31.5 cm. This phase is biologically important because the number of lateral shoots determines the number of nodes on which new leaves can be formed. The subsequent intensive increase in leaf mass continued until 15 June, and plant height reached 46.8 cm. By the stage of

complete vegetative organ formation, plants had reached 58.6 cm; at the pre-generative stage, height increased to 64.2 cm, after which vegetative elongation slowed.

Figure 1. Plant height dynamics and calculated final leaf surface area



The highest ten-day growth intensity was recorded during 11–20 May, when plant height increased by 13.1 cm. This period coincided with active branching and expansion of the leaf apparatus. After June, the growth rate gradually declined, indicating a redistribution of assimilates from rapid vegetative elongation toward consolidation of already formed organs and preparation for the generative phase.

Table 2. Final biometric indicators and statistical status of the dataset.

Indicator	**n**	**Mean / calculated value**	**Statistical status**
Plant height, cm	30	64.2	Raw data absent; SD, SE, CV% and p-value not calculated
Main stems, pcs	30	12.4	Raw data absent; SD, SE, CV% and p-value not calculated
Lateral shoots, pcs	30	38.6	Raw data absent; SD, SE, CV% and p-value not calculated
Leaves, pcs	30	236	Raw data absent; SD, SE, CV% and p-value not calculated
Average leaf length, cm	30	6.8	Raw data absent; SD, SE, CV% and p-value not calculated
Average leaf width, cm	30	3.9	Raw data absent; SD, SE, CV% and p-value not calculated
Calculated area of one leaf, cm²	30	19.9	Raw data absent; SD, SE, CV% and p-value not calculated
Calculated total leaf area, cm²	30	4694.0	Raw data absent; SD, SE, CV% and p-value not calculated
Root length, cm	30	24.7	Raw data absent; SD, SE, CV% and p-value not calculated

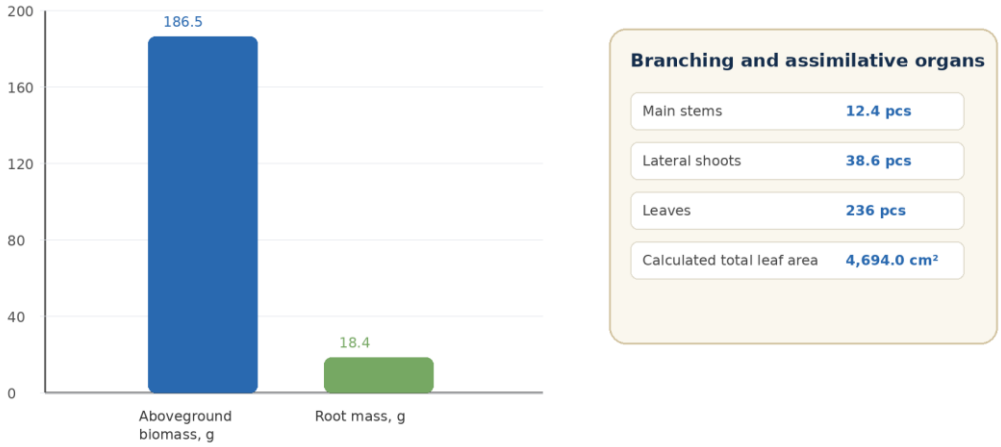
Root mass, g	30	18.4	Raw data absent; SD, SE, CV% and p-value not calculated
Aboveground vegetative biomass, g	30	186.5	Raw data absent; SD, SE, CV% and p-value not calculated

Note to Table 2. The table reports only values that can be supported by the source file. SD, SE, CV% and p-values require the individual measurements of all 30 plants and should be added after the raw biometric dataset is available.

At the end of the observation period, the average number of leaves was 236 per plant. Using K = 0.75, the area of one leaf was recalculated as 19.9 cm² and the total leaf surface area was 4694.0 cm² per plant. This corrected value is higher than the previously stated 2840 cm² and is mathematically consistent with the recorded leaf length, width and leaf number. The large assimilative surface explains the observed accumulation of aboveground biomass.

Figure 2. Vegetative biomass and branching structure

Final mean values recorded for the 30 selected plants; SD and SE require plant-level measurements.



Interpretation: high shoot number and broad assimilative surface explain the strong accumulation of aboveground raw biomass.

The final aboveground vegetative biomass was 186.5 g per plant, while root mass was 18.4 g and root length was 24.7 cm. The ratio between aboveground biomass and the strongly branched shoot system shows that lemon balm primarily invests in leaf-bearing shoots before the generative phase. This is biologically favorable for medicinal raw material production because leaves and young shoots are the most valuable harvested organs.

DISCUSSION. The obtained results confirm that the productivity of lemon balm should be interpreted through the coordination of shoot growth, branching and leaf-surface formation. The most active period in the present study occurred from late April through May. This agrees with the biological nature of perennial Lamiaceae species, in which spring regrowth is followed by rapid stem elongation and branching before flowering. The high number of lateral shoots (38.6 per plant) is particularly important, because branching increases the spatial distribution of leaves and improves the capacity for light interception.

Recent studies also support the connection between vegetative development and raw-material quality. Fallah et al. found that nutrient source influenced biomass and essential oil production across harvests, while Safaei et al. showed that nitrogen form affected both biomass and phytochemical parameters of lemon balm [7, 8]. These findings help interpret the present field

data: a large leaf surface is not only a morphological result, but also the structural basis for photosynthesis, carbohydrate production and secondary-metabolite formation.

The recalculation of leaf area is an important correction in the present manuscript. If the coefficient is not specified, total leaf area cannot be reproduced or compared with other studies. The accepted K = 0.75 is suitable for a practical non-destructive estimate of broadly ovate to elliptic leaves; nevertheless, future research should calibrate this coefficient by scanning lemon balm leaves and comparing actual area with L × W values. Such calibration would make the statistical interpretation stronger and would reduce methodological uncertainty.

The absence of plant-level measurements limits the statistical depth of the current dataset. Mean values show the direction and biological scale of development, but they do not show variation among the 30 plants. For this reason, SD, SE, CV% and p-values were not fabricated. In future work, recording individual measurements for each plant and each observation date will allow analysis of variability, confidence intervals and significant differences among development stages or cultivation treatments.

CONCLUSIONS:

• The vegetation period of Melissa officinalis L. from spring regrowth to the pre-generative stage lasted 127 days under open-field conditions. The most active vegetative development occurred from late April through May.

• Plant height increased from 6.4 cm at spring regrowth to 64.2 cm at the pre-generative stage. The maximum ten-day growth intensity was 13.1 cm during 11–20 May, indicating the peak period of shoot elongation and branching.

• At the final observation, one plant formed 236 leaves and 38.6 lateral shoots. With K = 0.75, the calculated area of one leaf was 19.9 cm^2 and the total leaf surface area reached 4694.0 cm^2 per plant.

• Aboveground vegetative biomass reached 186.5 g per plant, while root mass was 18.4 g and root length was 24.7 cm. These values show that lemon balm has a strong capacity to form leaf-bearing biomass before the generative phase.

• For practical cultivation, the period from late April to late May should be considered the key phase for agronomic care, because branching and leaf-surface expansion are most intensive during this interval.

• For future publication-quality statistical analysis, the 30 individual plant measurements should be included. Only then can SD, SE, CV% and p-values be reported with scientific reliability.

REFERENCES

1. Xolmatov H.X., Habibov Z.H. Medicinal Plants of Uzbekistan. Tashkent: Ibn Sino, 2017.
2. Abdullayev R.A., Xolmatov H.X. Biology of Medicinal Plants. Tashkent: Fan, 2018.
3. To‘xtayev B.Yo. Fundamentals of Plant Introduction and Acclimatization. Tashkent: Fan, 2019.
4. Serebryakov I.G. Morphology of Vegetative Organs of Higher Plants. Moscow: Nauka, 1962.
5. Rabotnov T.A. Phytocenology. Moscow: Moscow State University, 1992.
6. Shakeri A., Sahebkar A., Javadi B. Melissa officinalis L. — A review of its traditional uses, phytochemistry and pharmacology. Journal of Ethnopharmacology. 2016;188:204–228.

7. Fallah S., et al. Optimizing Lemon Balm (Melissa officinalis L.) Cultivation: Effects of Different Manures on Plant Growth and Essential Oil Production During Consecutive Harvests. Horticulturae. 2024;10(10):1105.
8. Safaei F., Alirezalu A., Noruzi P., Alirezalu K. Phytochemical and morpho-physiological response of Melissa officinalis L. to different NH4+ to NO3− ratios under hydroponic cultivation. BMC Plant Biology. 2024.
9. Aghakarim F., Sarikhani H., Azizi A. Effects of supplemental light quality at the end of day on herb production and some phytochemical properties of lemon balm (Melissa officinalis L.). International Journal of Horticultural Science and Technology. 2023;10(Special Issue):67–88.
10. Schrader J., et al. Leaf size estimation based on leaf length, width and shape. Annals of Botany. 2021.
11. Moradkhani H., Sargsyan E., Bibak H. Melissa officinalis L., a valuable medicinal plant: A review. Journal of Medicinal Plants Research. 2010;4(25):2753–2759.
12. Oniga I., Vlase L., Toiu A., et al. Phytochemical composition and antioxidant activity of Melissa officinalis L. Farmacia. 2017;65(5):711–715.
13. Wichtl M. Herbal Drugs and Phytopharmaceuticals. Stuttgart: Medpharm Scientific Publishers, 2004.

EFFECTIVE METHODS OF IN VITRO PROPAGATION OF ZINGIBER OFFICINALE ROSC: LITERATURE ANALYSIS AND PROSPECTIVE RESEARCH DIRECTIONS

Sh. Shamsiddinova
Karshi State University, Department of Microbiology and Biotechnology, Master's student in Biotechnology
https://doi.org/10.5281/zenodo.21274568

Abstract. *This article presents a systematic review of global scientific literature on the in vitro propagation of ginger (Zingiber officinale Rosc.). The study aims to identify optimal protocols for explant sterilization, rooting and acclimatization stages, and to evaluate the effects of plant growth regulators (BA, KIN, BAP, NAA, IBA) on in vitro multiplication. Literature analysis demonstrates that MS medium supplemented with 2.0 mg/L BA combined with 0.5 mg/L KIN provides the highest shoot proliferation parameters (11.3 shoots/explant, 22.8 leaves/shoot, plant height 16.4 cm). For root induction, half-strength MS medium supplemented with 1.0 mg/L NAA is optimal. Survival rate during acclimatization reached 96%. The findings serve as a scientific basis for developing an efficient biotechnological protocol for large-scale disease-free propagation of ginger, which is of high agricultural and pharmaceutical importance.*

Keywords: *zingiber officinale, in vitro propagation, Murashige-Skoog medium, benzyl adenine, kinetin, naphthalene acetic acid, acclimatization, plant growth regulators.*

1. INTRODUCTION

Ginger (Zingiber officinale Rosc.) is a member of the Zingiberaceae family and is one of the most important medicinal and food plants worldwide. It is widely distributed through rhizomes and is cultivated in tropical and subtropical climates, including South and Southeast Asia, Africa, South America, and the Mediterranean region (Purseglove, 1972). More than 3–4 million tons of ginger products are produced annually worldwide, with India, China, Nigeria, Indonesia, and Nepal being the main producers (FAO, 2022).

The rhizome of the plant contains phenolic compounds such as gingerol, shogaol, zingerone, as well as essential oils (alpha-zingiberene, beta-sesquiphellendrene, geraniol, cineole) and polysaccharides, which have a wide range of pharmacological properties. Scientific studies have confirmed the antioxidant, anti-inflammatory, antimicrobial, antidiabetic, hepatoprotective and anticancer properties of ginger (Anh et al., 2020).

However, Z. officinale faces a number of serious problems in traditional propagation. First, since the plant is propagated vegetatively - through rhizomes - pathogens (bacterial wilt - Ralstonia solanacearum, nematodes, viruses) are transmitted from generation to generation. Second, long-term vegetative propagation reduces genetic diversity, limiting the ability to renew varieties. Third, the low level of propagation by traditional methods does not allow for the provision of large-scale, high-quality planting material in sufficient quantities (Nayak and Naik, 2006). In fact, in some areas, bacterial wilt disease has destroyed more than 90% of the annual crop (Tariku et al., 2016).

In vitro propagation (tissue culture) is recognized as the most promising way to solve these problems. This method allows to obtain large quantities of disease-free, genetically identical plants

in a short time. In addition, in vitro technologies are increasingly used in the phytopharmaceutical industry for the production of valuable metabolites.

The purpose of this article is to conduct a literature review based on international scientific sources published in recent years on in vitro propagation of ginger, to identify optimal conditions for the stages of sterilization, propagation, root formation, and acclimatization, as well as to identify promising research directions in this area.

2. LITERATURE ANALYSIS AND DISCUSSION

2.1. Botanical description and distribution of ginger

*Zingiber officinale*Rosc. - A perennial herbaceous plant of the order Zingiberales. The underground part consists of branched lateral rhizomes, which reach a length of 10–15 cm and a width of 2–4 cm. The flower stalk rises to a height of 30–90 cm. The family Zingiberaceae includes at least 51 genera and more than 1500 species (Newman, 2001). The main center of diversity of the plant is Indo-Malaysia, from where it has spread to all tropical regions of the world.

Since most ginger cultivars are specialized for vegetative propagation, seed setting and flowering are very slow. This makes the creation of new cultivars by traditional breeding practically impossible and makes biotechnological approaches a necessary alternative (Simmonds, 1986).

2.2. Chemical composition and biological activity

*Z. officinale*The rhizome contains a wide range of pharmacologically important substances. According to scientific data, 34 different oleoresins have been identified in the novolatyl fraction of ginger, which accounts for 88.6% of the total composition. The main ones are gingerols (1-(4-hydroxy-3-methoxyphenyl)-5-hydroxyalkane-3-one), shogaols (1-(4-hydroxy-3-methoxyphenyl)-4-decen-3-one) and paradollars (Frontiers in Nutrition, 2022).

Gingerols are mainly abundant in fresh, undried rhizomes, while shogaols are formed by the dehydration reaction of gingerols during the drying process. 6-Shogaol has the strongest antioxidant and anti-inflammatory properties, which is due to the α,β-unsaturated ketone group in its chemical structure (Bode and Dong, 2011). The essential oil (1–3%) contains alpha-zingiberene (30–70%), beta-sesquiphellendrene, geraniol, cineole, borneol, and other terpenoids, which determine the characteristic odor of the plant.

Table 1. Main biologically active substances of Zingiber officinale

Type of attachment	Main representatives	Biological effects
Gingerols	6-, 8-, 10-gingerol	Antioxidant, anti-inflammatory, antimicrobial
Shogaols	6-, 8- Shogaol	Powerful antioxidant, anticarcinogenic, neuroprotective
Essential oils	α-zingiberene, geraniol	Deodorant, antimicrobial properties
Paradollars	Paradol	Hepatoprotective, antiparasitic
Polysaccharides	Starch (40–60%)	Energy source, technological application

Type of attachment	Main representatives	Biological effects
Vitamins and minerals	B6, C, potassium, magnesium	Immune boosting, general therapy

2.3. Scientific basis and historical development of in vitro reproduction

*Z. officinale*The first successful experiments on in vitro propagation of A. spp. were carried out by Hosoki and Sagawa (1977) using callus culture. Later, protocols for clonal propagation from meristem tips were developed by Pillai and Kumar (1982), Smith and Hamill (1996), and Balachandran et al. (1990). These studies demonstrated the potential of the in vitro method to produce disease-free, genetically stable planting material.

In vitro propagation technologies have improved significantly over the past decade. Modern research focuses not only on increasing propagation rates, but also on the formation of mycorrhizae, monitoring genetic stability using RAPD and ISSR markers, and on propagation in liquid media in bioreactors (PMC, 2013).

2.4. Selection and sterilization of explants

The success of in vitro propagation depends largely on the source of the explant and the effectiveness of the sterilization protocol. Various authors have used sprout buds, meristem tips, and nodal segments isolated from the rhizome as explants. Shoots of 1.5–2.0 cm in length are optimal, as such explants retain sufficient root-forming meristematic tissue and are resistant to microbial contamination (Shaik and Kanth, 2018).

The sterilization protocol is usually carried out in the following sequence: first, the explants are washed with running water and detergent (Tween-20 or Tween-80); then they are pretreated in 3% copper sulfate (CuSO4), ascorbic acid, and citric acid solutions - this reduces the oxidation of phenols and darkening. The next step is treatment with 70% ethanol for 1 minute, then with 30% sodium hypochlorite (5% active chlorine) for 15 minutes. All operations are performed under aseptic conditions in laminar air flow cabinets (Berihu, 2018).

2.5. Reproduction stage: nutrient medium and growth regulators

The most widely used medium for in vitro propagation of ginger is Murashige and Skoog's (1962) medium (MS medium). MS medium is supplemented with 30 g/L sucrose and 7 g/L agar, adjusted to pH 5.8, and autoclaved at 121°C for 15 minutes. Full strength MS medium is used during the growth phase.

The rate and quality of proliferation largely depend on the ratio of cytokines and auxins. Cytokines (BA, KIN, BAP, TDZ) stimulate shoot formation, while auxins (NAA, IBA, IAA) promote rooting. The balance between these two groups is the key to in vitro regeneration.

Table 2. Growth regulators used by various authors and the results obtained

Source	Cytokinin	Auxin	Best indicator
Berihu (2021)	2.0 mg/L BA	0.5 mg/L KIN	11.3 shoots/explant, 16.4 cm height
Shaik & Kanth (2018)	2.5 mg/L BAP	1.0 mg/L NAA	7.8 shoots/explant, 5.2 cm long
Biruk et al. (2012)	2.0 mg/L BA	1.0 mg/L IAA	8.2 shoots/explant, within 30 days

Source	Cytokinin	Auxin	Best indicator
Salim et al. (2024)	3.0 mg/L BAP	0.5 mg/L NAA	100% micronized formation
Zahid et al. (2021)	10 µM zeatin	-	Optimal for Bentong variety

The most widely used and effective cytokine is 6-benzyladenylate (BA or BAP). Berihu Mengs (2021) reported that in Z. officinale cv. Volvo, a combination of 2.0 mg/L BA and 0.5 mg/L KIN resulted in 11.3 shoots/explant, which is twice as high as BA alone (5.8 shoots/explant). This is due to the synergistic effect between BA and KIN, which together enhance cytokine-directed mitotic division and reduce apical dominance.

Regarding the effect of BAP concentration, Shaik and Kanth (2018) found that 2.5 mg/L BAP produced the most shoots (7.8 shoots/explant), while callus increased and shoot quality deteriorated when the concentration was increased above 3.0 mg/L. This indicates that the concentration of growth regulators should be within the optimal range.

In recent years, non-classical cytokines such as zeatin and TDZ (thidiazuron) have also been tested. Zahid et al. (2021) found that zeatin was more effective than other cytokines for the Bentong variety, indicating the need for optimization for different varieties.

2.6. Root formation stage

Once the shoots are fully formed, their rooting is an important step in the in vitro protocol. Half-strength (½ MS) medium is used for rooting-this increases carbon accumulation by reducing nitrogen content and stimulates root primordia (Gawel et al., 1990).

NAA (naphthaleneacetic acid) has been confirmed in many studies as the most effective auxin for promoting rooting. Berihu (2021) reported that 1.0 mg/L NAA produced the most roots (9.6 roots/shoot) and the longest roots (11.1 cm). IBA (indole-3-butyric acid) was also effective, with 1.0 mg/L IBA producing 8.3 roots/shoot. The rooting process usually takes 5–6 weeks.

2.7. Acclimatization stage

Plants grown in vitro need support in the transition from a heterotrophic to an autotrophic lifestyle. This transition process is called acclimation and is crucial for the survival of the plants (Hazarika, 2003).

In most studies, rooted seedlings are first transplanted into plastic pots filled with sterile coco coir or soil-sand-compost mixture (2:1:1) after washing off agar residues. Initially, 70–80% humidity and 28°C are maintained, and plastic covering is gradually introduced, requiring higher humidity. After four weeks, seedlings are transferred to a shade greenhouse. The final field cultivation success rate is up to 96% survival (Berihu, 2021).

A 2:1:1 mixture of forest soil, coffee husks, and sand has been found to be a suitable substrate for acclimatization. Coffee husks improve aeration and act as a source of organic matter. In a study by Shaik and Kanth (2018), a soil:sand:manure (1:1:1) mixture provided successful acclimatization for 6 weeks.

2.8. Genetic stability and somaclonal variation

One of the main advantages of in vitro propagation is the ability to maintain clonal uniformity. However, if propagation goes through a callus stage, the risk of somaclonal variation increases. Therefore, most modern protocols are aimed directly at organogenesis - the explant directly produces a shoot without callus. This method ensures maximum clonal uniformity.

Genetic analyses using RAPD, ISSR and SSR markers have shown that in vitro seedlings obtained through proper organogenesis are genetically identical to the original mother plant. This feature further enhances the practical value of the in vitro method in quality-controlled ginger propagation (PMC, 2013).

3. DISCUSSION

A review of the literature shows that in vitro propagation methods for ginger have made significant progress over the past thirty years. The main scientific results can be summarized as follows.

First, the explant source and sterilization protocol are the initial and critical factors determining the success of in vitro experiments. Actively sprouting shoots, especially specimens 1.5–2.0 cm long, show higher regeneration potential than other explant types. The pre-use of copper sulfate and organic acids during the sterilization step significantly reduces the level of contamination.

Secondly, in the growth phase, the combination of BA and KIN is much more effective than BA alone. The synergism of these two cytokines can double the rate of shoot growth. At the same time, it is necessary to maintain the concentration of growth regulators in the optimal range - excessive concentration leads to callus formation and deterioration of shoot quality.

Third, the optimal combination for rooting is half-strength MS medium and NAA (1.0 mg/L), which has been confirmed in many studies. The effectiveness of NAA is due to its ability to enhance the effect of endogenous auxin in stimulating root primordia.

Fourth, the acclimatization phase is often overlooked, but in practice, the adaptation of plants to the field determines the final effect of the entire in vitro protocol. The right substrate selection, gradual reduction of humidity and shading regime provide survival rates of up to 96%.

According to the current research trend, new directions are being developed, such as the cultivation of ginger in liquid media in bioreactors, integration with hydroponic systems, as well as the in vitro synthesis of valuable gingerols and shogaols. These directions are also of practical interest for the pharmaceutical, cosmetic, and food industries.

4. CONCLUSION

*Zingiber officinale*The analysis of the literature on in vitro propagation of Rosc. allows us to draw the following main conclusions:

1. The most effective explants for in vitro propagation of ginger are actively growing rhizome buds (1.5–2.0 cm). They have a high regeneration potential and are easy to clean from pathogens.
2. The optimal medium for propagation is: full strength MS + 2.0 mg/L BA + 0.5 mg/L KIN + 30 g/L sucrose + 7 g/L agar, pH 5.8. This combination provides a rate of 11.3 shoots/explant.
3. Optimal rooting medium: half strength (½) MS + 1.0 mg/L NAA. This composition provides 9.6 roots/shoot and 11.1 cm root length.
4. For acclimatization, a mixture of soil:coffee grounds:sand (2:1:1) and a gradually decreasing humidity regime of 70–80% provides a survival rate of 96%.
5. In vitro propagation provides rapid production of disease-free, genetically uniform planting material compared to the traditional method and is of practical importance to ginger farmers.

6. Prospective research directions include propagation in liquid media in bioreactors, production of microrhizomes in variable-density systems, and methods for monitoring genetic stability using modern molecular markers.

REFERENCES

1. Anh NH, Kim SJ, Long NP, et al. Ginger on human health: a comprehensive systematic review of 109 randomized controlled trials // Nutrients. - 2020. - Vol. 12. - P. 157. https://doi.org/10.3390/nu12010157
2. Balachandran SM, Baht SR, Chandel KPS In vitro clonal multiplication of turmeric (Curcuma spp.) and ginger (Zingiber officinale Rosc.) // Plant Cell Reports. - 1990. - Vol. 8. - P. 521–524.
3. Berihu Mengs. Control of Contamination and Explants Phenolics in Ginger accession (Zingiber officinale Rosc.) In Vitro Cultures // International Journal of Pharmaceutical Science and Research. - 2018. - Vol. 6(02). - P. 14–24.
4. Berihu Mengs. An Efficient Protocol for Micro Propagation of Ginger (Zingiber officinale Rosc.) cv. Volvo via Sprout Bud Culture // Journal of Natural Sciences Research. - 2021. - Vol. 12, No. 17. - P. 15–20. DOI: 10.7176/JNSR/12-17-02
5. Biruk A., Wondyifraw T., Kassahun B. In vitro propagation of Ethiopian ginger (Zingiber officinale Rosc.) cultivars: Evaluation of explant types and hormone combinations // African Journal of Biotechnology. - 2012. - Vol. 11(16). - P. 3911–3918.
6. Bode AM, Dong Z. The Amazing and Mighty Ginger. Herbal Medicine: Biomolecular and Clinical Aspects. - 2nd edition. - CRC Press, 2011.
7. FAO (Food and Agriculture Organization of the United Nations). World ginger production statistics. - Rome: FAO, 2022.
8. Frontiers in Nutrition. Potential Role of Ginger (Zingiber officinale Roscoe) in the Prevention of Neurodegenerative Diseases // Frontiers in Nutrition. - 2022. - Vol. 9. - P. 809621. DOI: 10.3389/fnut.2022.809621
9. Gawel NJ, Robacker CD, Corly WL In vitro propagation of Miscanthus sinensis // HortScience. - 1990. - Vol. 25(10). - P. 1291–1293.
10. Hartmann HT, Kester DE, Davis FT, Geneve RL Plant Propagation: Principles and Practices. 6th Ed. - Prentice-Hall, New Jersey, 1997.
11. Hazarika BN Acclimatization of tissue cultured plants // Current Science. - 2003. - Vol. 85. - P. 1705–1712.
12. Hosoki T., Sagawa Y. Clonal propagation of ginger (Zingiber officinale Rosc.) through tissue culture // HortScience. - 1977. - Vol. 12. - P. 451–452.
13. Koh et al. Zeatin–auxin synergy and growing media optimization enhanced micropropagation, acclimatization, and antioxidant properties of 'Bentong' ginger // Scientia Horticulturae. - 2024. Doi: 10.1016/j.scienta.2025.01.1665
14. Murashige T., Skoog F. A revised medium for rapid growth and bioassays with tobacco tissue cultures // Physiologia Plantarum. - 1962. - Vol. 15. - P. 473–497.
15. Nayak S., Naik PK Factors affecting in vitro microrhizome formation and growth in Curcuma longa L. and improved field performance of micropropagated plants // Science Asia. - 2006. - Vol. 32. - P. 31–37.
16. Newman M. Nomenclatural notes on Zingiberaceae // Journal of Botany. - 2001. - Vol. 58(1). - P. 173–174.

17. Pillai SK, Kumar KB Note on the clonal multiplication of ginger in vitro // Indian Journal of Agricultural Sciences. - 1982. - Vol. 52. - P. 397–399.
18. Purseglove JW Tropical crops: Monocotyledons. 1st edition. - Longman Group Limited, UK, London, 1972. - P. 52–54.
19. Salim NIS, Samah SNAA, Abdullah S., Yusuf NA Sterilization Protocols and in vitro Shoot and Root Induction of Zingiber officinale var. Rosc. using BAP and NAA // Journal of Agrobiotechnology. - 2024. - Vol. 15(1). - P. 1–10.
20. Shaik J., Kanth GR In vitro propagation of Zingiber officinale through rhizome and effect of plant growth regulators // Journal of Pharmacognosy and Phytochemistry. - 2018. - Vol. 7(5). - P. 2012–2014.
21. Simmonds NW Evolution of crop plants. - Longman Sci. & Tech., England, 1986. - P. 339.
22. Smith MK, Hamill SD Field evaluation of micropropagated and conventionally propagated ginger in subtropical Queensland // Australian Journal of Experimental Agriculture. - 1996. - Vol. 36. - P. 347–354.
23. Tariku H., Kassahun S., Gezahegne G. First report of ginger (Zingiber officinale) bacterial wilt disease in Ethiopia // Research Journal of Agriculture and Forestry Sciences. - 2016. - Vol. 4(4). - P. 5–9.
24. Zahid N. et al. Micropropagation of ginger (Zingiber officinale Roscoe) 'Bentong' and evaluation of its secondary metabolites and antioxidant activities // Plants. - 2021. - Vol. 10(5). DOI: 10.3390/plants10050978
25. Zhao DW High quality and production of ginger - theory and technology. - China Agricultural Publishing Company, Beijing, 2002. - P. 10–30.

CHEMICAL COMPOSITION, OIL CONTENT, AND AMINO ACID CONTENT OF CASTOR BEAN (RICINUS COMMUNIS L.) SEEDS CULTIVATED IN THE KHOREZM REGION

U.K. Abdurakhimov[1], D.A. Rakhimbayeva[2]
PhD., Senior Scientific Researcher, Khorezm Ma'mun Academy[1]
PhD student at Khorezm Mamun Academy[2]
https://doi.org/10.5281/zenodo.20809374

Abstract. *Castor bean (Ricinus communis L.) varieties are considered medicinal plants and represent a relatively new crop for the Khorezm region. Their cultivation technology, physiological characteristics, biochemical composition, and potential for cultivation under the soil and climatic conditions of the Khorezm region have not yet been sufficiently studied. Therefore, this article presents data on the content of macro- and microelements, oil content, as well as the composition and quantity of essential and non-essential amino acids in the seeds of four castor bean varieties-Zanzibarskaya, Gibsona, Impala, and the control variety Khersonskaya-10-grown on alluvial meadow soils of the Khorezm region.*

The results of the study demonstrated that the Impala variety showed a clear advantage in terms of the total content of macro- and microelements. The lowest values were generally observed in the Khersonskaya-10 variety, with the exception of calcium. However, higher concentrations of sodium and sulfur were recorded in the Gibsona variety, while the Zanzibarskaya variety contained relatively higher amounts of boron, iron, and chromium compared to the other studied varieties.

The highest oil content and oil yield were determined in the Impala and Gibsona varieties, reaching 46.3% and 56.4 kg/ha, and 45.5% and 55.1 kg/ha, respectively. The lowest values were recorded in the control variety Khersonskaya-10 (43.8% and 51.8 kg/ha). The acid value of the oil extracted from the seeds of the studied castor bean varieties complied with the standards specified in the National Pharmacopoeia of Uzbekistan and ranged from 0.79 to 1.85 mg KOH/g.

Laboratory analyses further revealed that the Impala variety significantly exceeded the other varieties in both essential and non-essential amino acid contents. In particular, the concentrations of several amino acids, including threonine, arginine, histidine, and tryptophan, were substantially higher than those in the control variety Khersonskaya-10, differing by several-fold. Nevertheless, the Khersonskaya-10 variety was distinguished by its considerably higher glutamine content compared with the other varieties studied.

Keywords: *medicinal plants, varietal differences, macroelements, microelements, oil content, acid value, oil yield, essential and non-essential amino acids.*

Introduction. Macroelements and microelements are essential nutrients required at all stages of plant growth and development. These include nitrogen, phosphorus, potassium, sulfur, magnesium, and iron, which are present in relatively large amounts in plants and play a crucial role in ensuring their normal growth and physiological functioning. Deficiency or insufficiency of these nutrients can negatively affect plant growth and development, resulting in reduced productivity and increased fruit or seed shedding [1]. The oil content and oil yield of medicinal plant seeds are among the most important indicators of their biological and economic value. Seed

oils serve not only as energy reserves for seed germination and early plant growth but are also widely utilized in the pharmaceutical, cosmetic, and food industries. Modern scientific studies have demonstrated that seed oil content is a variable trait influenced by genetic, biotic, and abiotic factors, including environmental stress conditions, cultivation practices, soil characteristics, climatic conditions, and applied agronomic techniques [5]. Amino acids are organic compounds that function as the fundamental building blocks of proteins. They participate in numerous metabolic processes within the human body and are indispensable for maintaining physiological functions. Contemporary biochemical research has established that amino acids perform not only structural (plastic) functions but also regulatory, energetic, and signaling roles in living organisms [18]. Under the conditions of Uzbekistan, castor bean (*Ricinus communis* L.) remains insufficiently studied from both medical and pharmacological perspectives. Consequently, scientific literature contains very limited information regarding its chemical composition, seed oil content, and particularly the quantitative characteristics of essential and non-essential amino acids under the environmental conditions of the Khorezm region.

Macro-and microelements act as important catalysts in numerous biochemical and metabolic processes. They contribute significantly to the maintenance of vital physiological functions in the human body, enhance disease resistance, and support the immune system [3]. Recent scientific investigations have emphasized that the oil content of medicinal plant seeds is one of the principal morphophysiological indicators determining both their biological value and commercial potential. Seed oils mainly consist of triglycerides, fatty acids, vitamins, and various biologically active compounds, which collectively contribute to the high value of seeds as industrial and pharmaceutical raw materials [13]. In recent years, interest in amino acids within the fields of nutrition science and clinical medicine has increased considerably due to their significant effects on immunity, metabolism, and overall human health [15]. Essential amino acids cannot be synthesized by the human body and therefore must be obtained through dietary sources. These include valine, leucine, isoleucine, lysine, methionine, threonine, tryptophan, phenylalanine, and histidine [4].

Literature review. Chemical elements can be classified into three groups according to their participation in physiological and biochemical processes in living organisms. The first group includes structural elements (macroelements), which constitute the major components of all organs and tissues of plants. The second group consists of essential elements (microelements) that are physiologically necessary for the vital activity of living organisms and perform numerous functions within cells. The third group comprises toxic elements, which may exert harmful effects even at very low concentrations and can cause toxicity. These include elements such as aluminum, lead, cadmium, chromium, silver, and beryllium [24]. The human body is unable to synthesize the macro- and microelements required for its normal functioning; therefore, these elements must be obtained through food or biologically active supplements [23]. Although microelements are required by plants only in very small quantities (fractions of milligrams), their role in physiological processes is indispensable. They are components of numerous enzymes and contribute significantly to photosynthesis and metabolic activities [11].

Microelements serve as important catalysts that regulate not only plant growth and development but also their internal biological activity. Despite their low concentrations in plant tissues, they directly participate in metabolic pathways, enzymatic reactions, and respiration processes. In particular, elements such as manganese and copper accelerate electron transport during photosynthesis, thereby enhancing the plant's energy reserves [16]. Adequate levels of

microelements improve cell membrane permeability and promote the efficient uptake of nutrients through the root system [9]. In crop production, plant resistance to environmental stresses—including drought, salinity, and extreme temperature fluctuations—is closely associated with elements such as zinc and boron. Zinc regulates the synthesis of natural plant growth hormones (auxins), while boron stimulates flowering and pollination processes and plays a crucial role in fruit and seed formation. Deficiency of any of these microelements weakens plant immunity, increases susceptibility to fungal and viral diseases, and consequently may lead to substantial reductions in crop productivity [14].

Furthermore, microelements significantly influence crop quality, particularly the protein and amino acid contents of seeds. For example, molybdenum regulates nitrogen metabolism and facilitates the conversion of nitrates into amino acids beneficial for plant growth. Therefore, proper mineral nutrition not only determines crop yield but also enhances its biological and nutritional value [17]. In summary, deficiencies of microelements in plants adversely affect productivity and reduce resistance to diseases and unfavorable environmental conditions. Consequently, the application of micronutrient fertilizers in modern crop production is considered an essential approach for obtaining high yields and producing environmentally safe, high-quality seeds and fruits [6]. The investigation of oil content and lipid composition in medicinal plant seeds contributes to improving the effectiveness of pharmacological products, optimizing cultivation technologies, and developing high-yielding varieties of medicinal plants. Modern analytical techniques allow accurate and reliable determination of both oil quantity and quality, which is of considerable scientific importance for their efficient utilization in industry, medicine, and pharmaceutical applications [21].

Research methodology. The oil content of medicinal plant seeds is directly associated with the quality of raw materials and their pharmacological value. Consequently, seed oils have broad applications in traditional medicine, modern healthcare, pharmaceutical manufacturing, and medicinal plant cultivation [26]. According to X. Wang, L. Chen [22] and other researchers, plant species and varietal differences significantly influence oil content and oil yield. For example, the oil content of fennel (*Foeniculum vulgare*) seeds ranges from 15–30%, whereas flax (*Linum usitatissimum*) seeds contain approximately 30–45% oil. Climatic conditions, soil characteristics, and agronomic practices such as fertilization and irrigation also substantially affect lipid biosynthesis. Dry climates and nutrient deficiencies can considerably reduce oil accumulation in seeds, thereby negatively affecting the quality and pharmacological properties of medicinal plant raw materials.

The quality of seed oils depends not only on their quantity but also on the composition of fatty acids, antioxidants, and biologically active compounds. From a pharmaceutical perspective, both the lipid content and the biochemical composition of seeds are of great importance. The highest oil accumulation generally occurs during the later stages of physiological maturation, particularly during fruit and seed ripening [19]. The acid value is a fundamental indicator reflecting the concentration of free fatty acids in oils and determining the extent of lipid hydrolysis. Its value is directly related to the quality, stability, and safety of oils used in pharmaceutical and medical applications [10]. International scientific and regulatory documents, including the **United States Pharmacopeia (USP)**, **European Pharmacopoeia (Ph. Eur.)**, **British Pharmacopoeia (BP)** and **Codex Alimentarius** recognize acid value as a mandatory parameter for quality control, standardization, and suitability assessment of oils. Therefore, this indicator is critically important

for ensuring the safety, efficacy, and stability of pharmaceutical products throughout all stages, from raw material processing to the production of finished medicinal preparations [2,7,8].

Recent studies indicate that branched-chain amino acids (BCAAs)-namely valine, leucine, and isoleucine-play a crucial role in muscle metabolism and energy homeostasis. Deficiency of essential amino acids in the human body may lead to negative nitrogen balance, impaired immune function, and dysfunction of various organs [20].

Non-essential amino acids are synthesized within the human body and include compounds such as alanine, asparagine, glutamate, and serine. Their synthesis primarily occurs in the liver and is closely associated with transamination processes [25].

Under certain physiological conditions, including stress, disease, injury, infection, and periods of rapid growth, the body's demand for specific amino acids increases significantly. Under such circumstances, amino acids such as arginine, glutamine, tyrosine, and cysteine are considered conditionally essential amino acids [12].

Analysis and results. Based on the objectives of the study, a comparative analysis of the macro- and microelement contents in the seeds of different castor bean (*Ricinus communis* L.) varieties revealed several notable differences. In the seeds of the Zanzibarskaya variety, the concentrations of macroelements were as follows: calcium – 2.712 mg/g, phosphorus – 53.463 mg/g, magnesium – 23.652 mg/g, sodium – 7.142 mg/g, sulfur – 6.716 mg/g, potassium – 146.712 mg/g, and boron – 0.252 mg/g. In the Gibsona variety, the corresponding values were calcium – 3.222 mg/g, phosphorus – 62.836 mg/g, magnesium – 26.117 mg/g, sodium – 9.150 mg/g, sulfur – 8.127 mg/g, potassium – 150.224 mg/g, and boron – 0.182 mg/g.

The Impala variety exhibited the highest concentrations of several macroelements, including calcium (4.443 mg/g), phosphorus (64.392 mg/g), magnesium (27.305 mg/g), and potassium (175.112 mg/g). The contents of sodium, sulfur, and boron in this variety were 8.300 mg/g, 6.254 mg/g, and 0.318 mg/g, respectively. In the control variety, Khersonskaya-10, the macroelement contents were comparatively lower and amounted to calcium – 3.155 mg/g, phosphorus – 52.196 mg/g, magnesium – 19.382 mg/g, sodium – 6.150 mg/g, sulfur – 5.646 mg/g, potassium – 135.112 mg/g, and boron – 0.164 mg/g (Table 1). A comparative analysis of the macroelement contents in the seeds of the studied castor bean (*Ricinus communis* L.) varieties revealed that the Impala variety showed a clear superiority in terms of overall macroelement accumulation. In contrast, the Khersonskaya-10 variety exhibited the lowest values for most macroelements, with the exception of calcium. However, the Gibsona variety was distinguished by its relatively higher concentrations of sodium and sulfur, while the Zanzibarskaya variety contained a comparatively higher amount of boron than the other varieties examined. These findings indicate significant varietal differences in mineral composition and nutrient accumulation capacity.

Table 1.

Comparative Macroelement Composition of Seeds of Different Castor Bean (*Ricinus communis *L.) Varieties (mg/10 g)

Ca 317.933 (mg/10g)	**P 213.617 (mg/10g)**	**Mg 285.213 (mg/10g)**	**Na 589.592 (mg/10g)**	**S 181.975 (mg/10g)**	**K 766.490 (mg/10g)**	**B 249.677 (mg/10g)**
Zanzibarskaya variety						
2,712	53,463	23,652	7,142	6,716	146,712	0,252

Gibsona variety						
3,222	62,836	26,117	9,150	8,127	150,224	0,182
Impala variety						
4,443	64,392	27,305	8,300	6,254	175,112	0,318
Khersonskaya-10 variety						
3,155	52,196	19,382	6,150	5,646	135,112	0,164

When the microelement contents of castor bean (*Ricinus communis* L.) seeds were analyzed, the seeds of the Zanzibarskaya variety contained copper – 0.143 mg/g, manganese – 0.124 mg/g, selenium – 0.209 mg/g, iron – 0.922 mg/g, zinc – 0.246 mg/g, cobalt – 0.007 mg/g, molybdenum – 0.383 mg/g, and chromium – 0.040 mg/g. In the Gibsona variety, the corresponding values were copper – 0.139 mg/g, manganese – 0.152 mg/g, selenium – 0.259 mg/g, iron – 0.761 mg/g, zinc – 0.441 mg/g, cobalt – 0.007 mg/g, molybdenum – 0.323 mg/g, and chromium – 0.020 mg/g. The seeds of the Impala variety contained copper – 0.171 mg/g, manganese – 0.216 mg/g, selenium – 0.319 mg/g, iron – 0.609 mg/g, zinc – 0.482 mg/g, cobalt – 0.006 mg/g, molybdenum – 0.646 mg/g, and chromium – 0.037 mg/g. In the control variety, Khersonskaya-10, the contents of these microelements were determined as follows: copper – 0.122 mg/g, manganese – 0.116 mg/g, selenium – 0.185 mg/g, iron – 0.561 mg/g, zinc – 0.231 mg/g, cobalt – 0.003 mg/g, molybdenum – 0.323 mg/g, and chromium – 0.022 mg/g (Table 2).

Table 2.

Comparative Microelement Composition of Seeds of Different Castor Bean (*Ricinus communis *L.) Varieties (mg/10 g)

Cu 327.393 (mg/10g)	**Mn 257.610 (mg/10g)**	**Se 196.026 (mg/10g)**	**Fe 238.204 (mg/10g)**	**Zn 206.200 (mg/10g)**	**Co 228.616 (mg/10g)**	**Mo 202.031 (mg/10g)**	**Cr 267.716 (mg/10g)**
Zanzibarskaya variety							
0,143	0,124	0,209	0,922	0,246	0,007	0,383	0,040
Gibsona variety							
0,139	0,152	0,259	0,761	0,441	0,007	0,323	0,020
Impala variety							
0,171	0,216	0,319	0,609	0,482	0,006	0,646	0,037
Xersonskaya variety							
0,122	0,116	0,185	0,561	0,231	0,003	0,323	0,022

A comparative analysis of the microelement contents in the seeds of the studied castor bean (*Ricinus communis* L.) varieties revealed that the Impala variety showed a clear superiority in terms of total microelement accumulation. The lowest concentrations were generally observed in the control variety, Khersonskaya-10. The Zanzibarskaya variety was distinguished by relatively higher contents of iron and chromium compared with the other varieties examined, whereas cobalt was found to be present at nearly the same level in all three experimental varieties. Based on the results obtained, it can be concluded that the observed varietal differences are associated with the genetic characteristics and geographical origin of the varieties, as well as with the soil and climatic conditions and agromeliorative practices applied during castor bean cultivation. In addition, the oil-related characteristics of the Zanzibarskaya, Gibsona, Impala, and control (Khersonskaya-10) varieties were comparatively evaluated, including oil content, oil yield, and acid value. The

experiments were conducted at the Applied Research Laboratory of the Institute of Bioorganic Chemistry of the Academy of Sciences of the Republic of Uzbekistan.

The seeds of the Zanzibarskaya variety contained 44.7% oil, with an oil yield of 53.3 kg/ha. In the Gibsona variety, these values were 45.5% and 55.1 kg/ha, respectively. The Impala variety exhibited the highest oil characteristics, with an average oil content of 46.3% and an oil yield of 56.4 kg/ha. In contrast, the control variety, Khersonskaya-10, showed the lowest values, with an oil content of 43.8% and an oil yield of 51.8 kg/ha (Figure 1, Appendix 1).

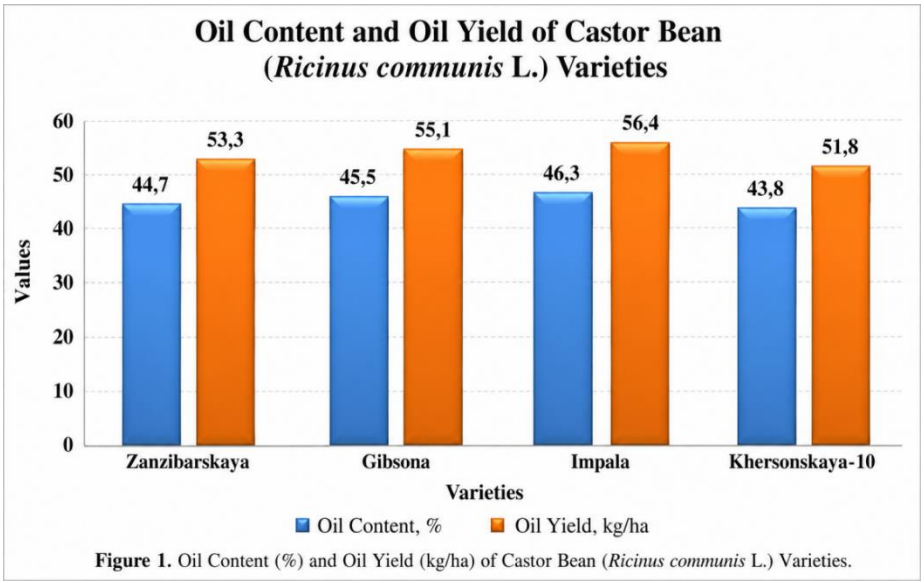


Figure 1. Oil Content (%) and Oil Yield (kg/ha) of Castor Bean (*Ricinus communis* L.) Varieties.

Figure 1. Oil Content of Castor Bean* (*Ricinus communis* L.) *Varieties

The results of our long-term experiments demonstrated that the acid value of oil extracted from castor bean (*Ricinus communis* L.) seeds was generally consistent with the standards specified in the National Pharmacopoeia of Uzbekistan, ranging from 0.79 to 1.85 mg KOH/g. According to pharmacopoeial requirements, the acid value should not exceed 0.65–1.50 mg KOH/g, as this parameter serves as an important indicator of oil quality and ensures the suitability of products intended for medical and cosmetic applications. The obtained results indicate that the seed oils of certain castor bean varieties can be classified as high-quality oils with favorable physicochemical characteristics (Figure 2).

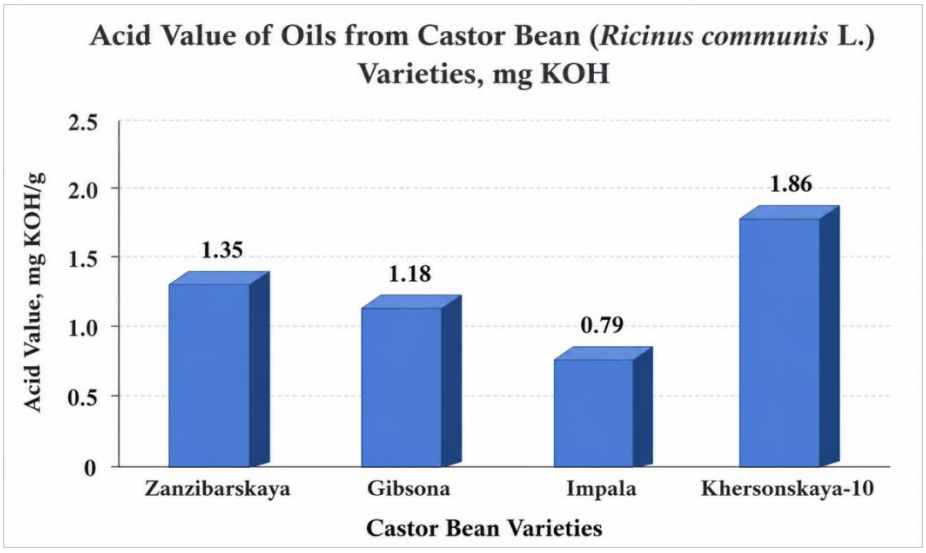


Figure 2. Comparative Analysis of the Acid Value of Oils from Different Castor Bean* (*Ricinus communis* L.) *Varieties (mg KOH/g)

Appendix 1.

Comparative Oil Content (%) and Oil Yield (kg/ha) of Castor Bean (*Ricinus communis *L.) Varieties, Average Data for 2026

Navlar	**M±m**	**V**	**L**	**S**
Oil Content, %				
Zanzibarskaya	44,7±0,28	0,51	41,3-45,8	0,32
Gibsona	45,5±0,03	0,40	25,1-25,4	0,10
Impala	46,3±0,03	0,48	22,0-22,3	0,10
Khersonskaya-10	43,8±0,03	0,48	22,0-22,3	0,10
Oil Yield, kg/ha				
Zanzibarskaya	53,3±0,03	0,04	265,8-266,1	0,10
Gibsona	55,1±0,05	0,05	312,8-313,4	0,17
Impala	56,4±0,06	0,07	267,6-268,2	0,19
Khersonskaya-10	51,8±0,06	0,07	267,6-268,2	0,19
Acid Value, mg KOH/g				
Zanzibarskay	1,35±0,03	0,50	0,31-0,32	0,01
Gibsona	1,18±0,05	0,23	0,26-0,27	0,06
Impala	0,79±0,06	0,18	0,29-0,30	0,06
Khersonskaya-10	1,86±0,06	0,18	0,29-0,30	0,06

***V – Coefficient of Variation (%);*L – Range (Minimum–Maximum); *S – Standard Deviation**

Based on the experimental results, significant varietal differences were observed in the oil-related characteristics of castor bean (***Ricinus communis*** L.) seeds. The highest oil content and oil yield were recorded in the Impala and Gibsona varieties, reaching 46.3% and 56.4 kg/ha, and 45.5% and 55.1 kg/ha, respectively. The lowest values for both parameters were observed in the control variety, Khersonskaya-10, with an oil content of 43.8% and an oil yield of 51.8 kg/ha. The Zanzibarskaya variety occupied an intermediate position, with corresponding values of 44.7% and 53.3 kg/ha. Furthermore, a comparative investigation of essential and non-essential amino acids was conducted in the seeds of the Zanzibarskaya, Gibsona, Impala, and Khersonskaya-10 varieties. Laboratory analyses revealed the presence of a total of 20 amino acids in castor bean seeds, including 10 essential and 10 non-essential amino acids, indicating that the seeds are a rich source of biologically active compounds. According to the results obtained for essential amino acids, the seeds of the Zanzibarskaya variety contained threonine – 0.60 mg/g, arginine – 0.12 mg/g, valine – 0.76 mg/g, methionine – 0.34 mg/g, histidine – 3.27 mg/g, isoleucine – 1.00 mg/g, leucine – 1.49 mg/g, tryptophan – 4.04 mg/g, phenylalanine – 0.58 mg/g, and lysine – 0.10 mg/g, with a total essential amino acid content of 12.3 mg/g. In the Gibsona variety, the corresponding values were threonine – 2.28 mg/g, arginine – 0.30 mg/g, valine – 1.01 mg/g, methionine – 0.58 mg/g, histidine – 3.48 mg/g, isoleucine – 1.07 mg/g, leucine – 1.73 mg/g, tryptophan – 4.70 mg/g, phenylalanine – 1.11 mg/g, and lysine – 0.14 mg/g, with a total essential amino acid content of 16.4 mg/g.

The Impala variety exhibited the highest concentration of essential amino acids, containing threonine – 5.47 mg/g, arginine – 0.63 mg/g, valine – 1.20 mg/g, methionine – 0.70 mg/g, histidine – 6.96 mg/g, isoleucine – 1.07 mg/g, leucine – 1.91 mg/g, tryptophan – 5.50 mg/g, phenylalanine – 1.33 mg/g, and lysine – 0.20 mg/g, with a total content of 25.0 mg/g. In contrast, the control variety, Khersonskaya-10, contained considerably lower amounts of essential amino acids:

threonine – 0.16 mg/g, arginine – 0.06 mg/g, valine – 0.43 mg/g, methionine – 0.30 mg/g, histidine – 1.40 mg/g, isoleucine – 0.66 mg/g, leucine – 1.02 mg/g, tryptophan – 1.36 mg/g, phenylalanine – 0.27 mg/g, and lysine – 0.09 mg/g, with a total essential amino acid content of only 5.75 mg/g (Figure 3).

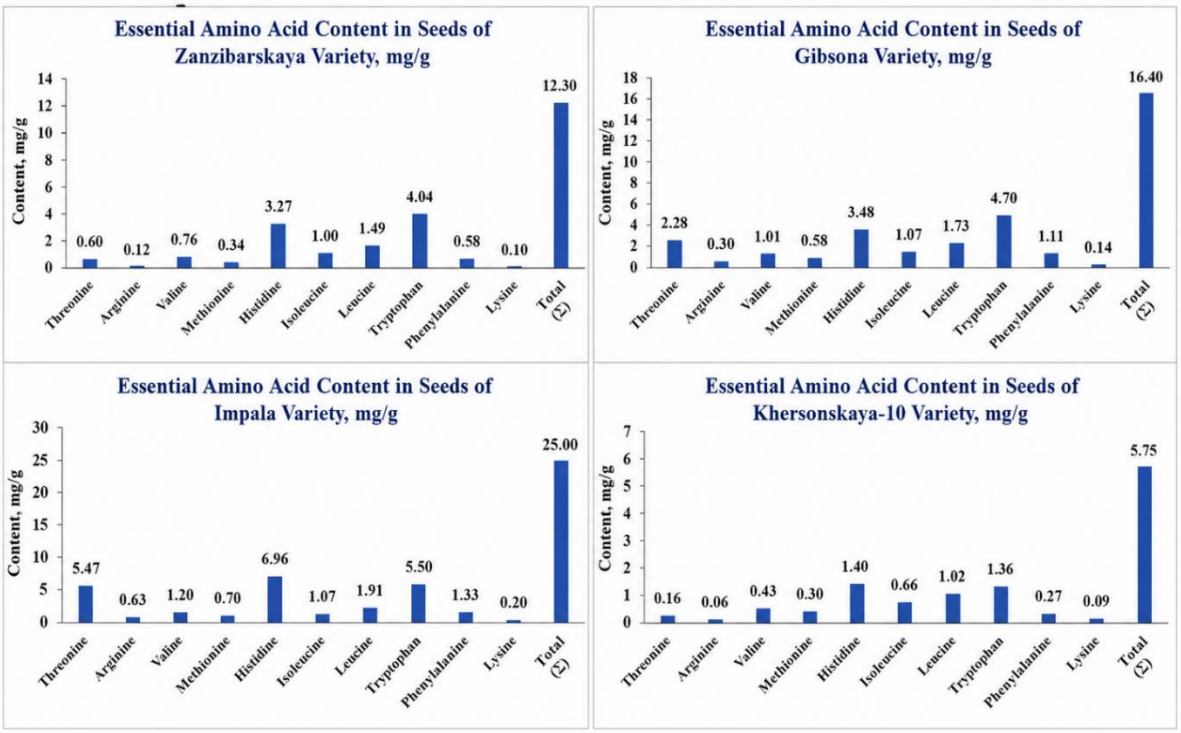


Figure 3. Comparative Analysis of Essential Amino Acid Contents in Seeds of Different Castor Bean (Ricinus communis L.) Varieties (mg/g)

Appendix 2.

Comparative Essential Amino Acid Composition of Seeds of Different Castor Bean (Ricinus communis L.) Varieties (mg/g)

Amino Acid Name	Zanzibarskaya, mg/g	Gibsona, mg/g	Impala, mg/g	Khersonskaya-10, mg/g
Threonine	0,60	2,28	5,47	0,16
Arginine	0,12	0,30	0,63	0,06
Valine	0,76	1,01	1,20	0,43
Methionine	0,34	0,58	0,70	0,30
Histidine	3,27	3,48	6,96	1,40
Isoleucine	1,00	1,07	1,07	0,66
Leucine	1,49	1,73	1,91	1,02
Tryptophan	4,04	4,70	5,50	1,36
Phenylalanine	0,58	1,11	1,33	0,27
Lysine	0,10	0,14	0,20	0,09
Total (Σ)	**12,3**	**16,4**	**25,0**	**5,75**

According to the laboratory analyses, the highest concentrations of all essential amino acids were generally recorded in the Impala variety. The only exception was isoleucine, whose content in the Impala variety was identical to that of the Gibsona variety, reaching 1.07 mg/g.

Among the essential amino acids, the highest concentration of threonine was observed in the Impala variety (5.47 mg/g). This value was approximately two times higher than that of the

Gibsona variety (2.28 mg/g) and substantially greater than that of the Zanzibarskaya variety (0.60 mg/g). The lowest threonine content was recorded in the control variety, Khersonskaya-10 (0.16 mg/g). The highest levels of arginine and valine were also detected in the Impala variety, reaching 0.63 mg/g and 1.20 mg/g, respectively. In contrast, the lowest values were found in the Khersonskaya-10 variety, amounting to 0.06 mg/g and 0.43 mg/g, respectively.

Similarly, the highest concentrations of methionine, histidine, and leucine were observed in the Impala variety, with values of 0.70 mg/g, 6.96 mg/g, and 1.91 mg/g, respectively. The lowest concentrations of these amino acids were recorded in the Khersonskaya-10 variety (0.30 mg/g, 1.40 mg/g, and 1.02 mg/g, respectively), while relatively low values were also observed in the Zanzibarskaya variety (0.34 mg/g, 3.27 mg/g, and 1.49 mg/g, respectively). In the case of isoleucine, both the Impala and Gibsona varieties exhibited the same value of 1.07 mg/g, whereas the Zanzibarskaya variety showed a comparable concentration of 1.00 mg/g.

The Impala variety also demonstrated the highest levels of tryptophan, phenylalanine, and lysine, reaching 5.50 mg/g, 1.33 mg/g, and 0.20 mg/g, respectively. The Gibsona variety occupied an intermediate position, with corresponding values of 4.70 mg/g, 1.11 mg/g, and 0.14 mg/g. Lower tryptophan concentrations were observed in the Zanzibarskaya variety compared with the Impala and Gibsona varieties. Regarding lysine content, the Zanzibarskaya variety exhibited a value comparable to that of the control variety, Khersonskaya-10, amounting to 0.10 mg/g and 0.09 mg/g, respectively.

Overall, the Impala variety showed a pronounced superiority over the other varieties in terms of essential amino acid content. In particular, the concentrations of threonine, arginine, histidine, and tryptophan were several-fold higher than those recorded in the control variety, Khersonskaya-10. When compared with the Gibsona variety, however, the differences were less pronounced, indicating a relatively similar nutritional profile between these two varieties.

Based on the obtained results, it can be concluded that the Impala and Gibsona varieties possess the highest concentrations of essential amino acids and therefore exhibit superior nutritional value among the studied castor bean varieties. Considering these findings, the contents of non-essential amino acids in castor bean seeds were also investigated.

The results revealed significant varietal differences in the concentrations of non-essential amino acids. Among the studied varieties, the highest total content of non-essential amino acids was recorded in the Impala variety, reaching 21.6 mg/g. The Gibsona and Khersonskaya-10 varieties exhibited relatively similar values, amounting to 14.5 mg/g and 14.1 mg/g, respectively. The lowest total content was observed in the Zanzibarskaya variety, with a value of 10.3 mg/g (Appendix 3). The highest concentration of aspartic acid was also found in the Impala variety, reaching 5.29 mg/g. The corresponding values for the Gibsona, Zanzibarskaya, and Khersonskaya-10 varieties were 3.20 mg/g, 2.76 mg/g, and 1.61 mg/g, respectively.

Appendix 3.

Comparative Non-Essential Amino Acid Composition of Seeds of Different Castor Bean (Ricinus communis L.) Varieties (mg/g)

Amino Acid Name	Castor Bean Varieties			
	Zanzibarskaya, mg/g	Gibsona, mg/g	Impala, mg/g	Khersonskaya-10, mg/g
Aspartic Acid	2,76	3,20	5,29	1,61
Glutamic Acid	0,60	1,15	2,34	9,48

Serine	1,22	2,07	3,23	0,28
Glycine	1,27	1,47	1,85	0,40
Asparagine	1,25	1,48	1,87	0,42
Glutamine	0,53	0,55	0,60	0,32
Cysteine	0,12	0,42	0,52	0,03
Alanine	0,96	2,43	2,65	0,68
Proline	1,00	1,20	2,25	0,54
Tyrosine	0,61	0,51	0,97	0,33
Total (Σ)	10,3	14,5	21,6	14,1

The control variety, Khersonskaya-10, exhibited a pronounced superiority over the other varieties in terms of glutamic acid content. The concentration of glutamic acid reached 9.48 mg/g, accounting for more than 67% of the total non-essential amino acid content. In contrast, the concentrations of glutamic acid in the Impala, Gibsona, and Zanzibarskaya varieties were considerably lower, amounting to 2.34 mg/g, 1.15 mg/g, and 0.60 mg/g, respectively.

Significant varietal differences were also observed in the content of serine. The highest concentration was recorded in the Impala variety (3.23 mg/g), followed by the Gibsona variety (2.07 mg/g) and the Zanzibarskaya variety (1.22 mg/g). The lowest serine content was found in the control variety, Khersonskaya-10, where it amounted to 0.28 mg/g.

The concentrations of glycine and asparagine varied considerably among the studied varieties. Glycine content ranged from 0.40 to 1.85 mg/g, while asparagine content ranged from 0.42 to 1.87 mg/g. The highest concentrations of both amino acids were observed in the Impala variety (1.85 mg/g and 1.87 mg/g, respectively). The lowest concentrations were recorded in the control variety, Khersonskaya-10, with values of 0.40 mg/g and 0.42 mg/g, respectively. The Gibsona (1.47 mg/g and 1.48 mg/g) and Zanzibarskaya (1.27 mg/g and 1.25 mg/g) varieties occupied intermediate positions.

The concentration of glutamine did not differ substantially among the varieties. The highest value was observed in the Impala variety (0.60 mg/g), which was comparable to those recorded in the Gibsona (0.55 mg/g) and Zanzibarskaya (0.53 mg/g) varieties. In the Khersonskaya-10 variety, the glutamine content was 0.32 mg/g.

Particular attention was drawn to the accumulation patterns of sulfur-containing and related amino acids, namely cysteine, proline, and tyrosine. Among these, cysteine was present in the lowest concentrations in all varieties. Nevertheless, its content in the Impala (0.52 mg/g) and Gibsona (0.42 mg/g) varieties was substantially higher than in the control variety (0.03 mg/g) and several times greater than that observed in the Zanzibarskaya variety (0.12 mg/g).

A similar trend was observed for proline and tyrosine. The Impala variety once again demonstrated superior biosynthetic performance, accumulating 2.25 mg/g of proline and 0.97 mg/g of tyrosine. In contrast, the lowest concentrations of these amino acids were recorded in the Khersonskaya-10 variety, amounting to 0.54 mg/g and 0.33 mg/g, respectively.

The concentration of alanine ranged from 0.68 to 2.65 mg/g among the studied varieties. The highest value was recorded in the Impala variety (2.65 mg/g), followed closely by the Gibsona variety (2.43 mg/g). The Zanzibarskaya variety contained 0.96 mg/g, whereas the control variety, Khersonskaya-10, contained 0.68 mg/g of alanine.

Overall, the results demonstrated that the Impala variety possessed the highest concentrations of most non-essential amino acids, indicating a rich amino acid composition and

superior nutritional quality. The Gibsona variety occupied an intermediate position for most parameters, while the Zanzibarskaya variety was characterized by relatively balanced amino acid levels. Although the control variety, Khersonskaya-10, exhibited lower concentrations of most amino acids, it was distinguished by its exceptionally high glutamic acid content compared with the other varieties investigated.

Conclusion. The results of the present study demonstrated that the Impala variety of castor bean (*Ricinus communis* L.) exhibited a clear superiority in terms of macroelement accumulation. In contrast, the lowest concentrations of most macroelements were recorded in the Khersonskaya-10 variety, with the exception of calcium. However, the Gibsona variety was characterized by relatively higher contents of sodium and sulfur, while the Zanzibarskaya variety contained a comparatively greater amount of boron than the other varieties investigated.

A comparative analysis of microelement composition revealed that the Impala variety also possessed the highest concentrations of most microelements. The lowest values were generally observed in the control variety, Khersonskaya-10. The Zanzibarskaya variety was distinguished by relatively high concentrations of iron and chromium, whereas cobalt was present at similar levels among the studied varieties.

The highest oil content and oil yield were recorded in the Impala and Gibsona varieties, reaching 46.3% and 56.4 kg/ha, and 45.5% and 55.1 kg/ha, respectively. The lowest values were observed in the control variety, Khersonskaya-10 (43.8% and 51.8 kg/ha). The Zanzibarskaya variety occupied an intermediate position, with an oil content of 44.7% and an oil yield of 53.3 kg/ha.

The acid value of oils extracted from castor bean seeds ranged from 0.79 to 1.85 mg KOH/g, which generally corresponded to the requirements established by the National Pharmacopoeia of Uzbekistan and confirmed the satisfactory quality of the obtained oils.

Laboratory analyses further demonstrated that the Impala variety possessed significantly higher concentrations of essential amino acids compared with the other varieties. In particular, the contents of threonine, arginine, histidine, and tryptophan were several times higher than those recorded in the control variety, Khersonskaya-10.

Similarly, the Impala variety exhibited the highest levels of most non-essential amino acids, indicating its superior nutritional and biochemical value. The Gibsona variety generally occupied an intermediate position, while the Zanzibarskaya variety was characterized by relatively balanced amino acid contents. Although the Khersonskaya-10 variety showed lower concentrations of most amino acids, it was distinguished by its markedly higher glutamic acid content compared with the other varieties studied.

Overall, the results indicate that the Impala and Gibsona varieties are the most promising castor bean varieties for cultivation under the soil and climatic conditions of the Khorezm region due to their favorable mineral composition, high oil content, and rich amino acid profile.

REFERENCES:

1. Abdul Ghani, Zulfaqar Ali, Muhammad Ishtiaq, Mehwish Maqbool, Saira Parveen. Estimation of macro and micro nutrients in some important medicinal plants of Soon Valley, District Khushab, Pakistan. African Journal of Biotechnology. 2012, Vol. 11, p. 78.
2. American Oil Chemists' Society (USA). Official Methods and Recommended Practices of the AOCS. – 6th ed. (method section). – Urbana, IL: USA Press, 2017. – P. 362-369.;

3. Anna Leśniewicz, Katarzyna Jaworska, Wieslaw Żyrnicki Macro- and micro-nutrients and their bioavailability in polish herbal medicaments // Food Chemistry, 2006, Volume 99, Issue 4, Pages 670-679.
4. Berg J.M., Tymoczko J.L., Gatto G.J. Biochemistry. – 9th ed. – New York: W.H. Freeman, 2019.-328-341.
5. Bhardwaj R., Kumar S., Singh P. Bioactive compounds in seed oils of medicinal plants. Journal of Medicinal Plants Research, 2020. Vol. 14, No. 3, pp. 150–162.
6. Bhaskarwar AC, Chopde N, Patokar MJ, Bayaskar S. Studies on effect of zinc sprays on growth and yield of rose cv. Centenary. Plant Archives. 2017;17(1): 196-198.
7. British Pharmacopoeia Commission. British Pharmacopoeia. – London: The Stationery Office, 2020. – P. 215–217.
8. European Pharmacopoeia Commission. European Pharmacopoeia. – 10th ed. – Strasbourg: Council of Europe, 2020. – P. 143–145.;
9. Fahad S, Ahmad M, Akbar Anjum M, Hussain S. The effect of micronutrients (B, Zn and Fe) foliar application on the growth, flowering and corm production of gladiolus (Gladiolus grandiflorus L.) in calcareous soils. Journal of Agricultural Science and Technology. 2014;16(7): 1671-1682.
10. Gunstone F. D., Harwood J. L., Dijkstra A. J. The Lipid Handbook. – 3rd ed. – Boca Raton: CRC Press, 2007. – P. 98–102.
11. Halder NK, Ahmed R, Sharifuzzaman SM, Bagam KA, Siddiky MA. Effect of boron and zinc fertilization on corm and cormel production of gladiolus in grey terrace soils of Bangladesh. Int. J. Sustain. Crop Prod. 2007; 2(5):85-89.
12. Kimball S.R., Jefferson L.S. Signaling pathways and molecular mechanisms // J. Nutr. – 2006. – Vol. 136. – P. 227–231.
13. Li H., Zhao Y., Chen X. Integrative approaches to maximize oil yield in medicinal plants. Frontiers in Plant Science, 2021, Vol. 12, Article 678901, pp. 1–12.
14. Maurya R, Kumar A. Effect of micronutrients on growth and corm yield of gladiolus. Plant Archives. 2014;14(1):529- 531.
15. Nelson D.L., Cox M.M. Lehninger Principles of Biochemistry. – New York: W.H. Freeman, 2021. pp-238.
16. Pal S, Barad AV, Singh AK, Khadda BS, Kumar D. Effect of foliar application of Fe and Zn on growth, flowering and yield of gerbera (Gerbera jamesonii) under protected condition. Indian Journal of Agricultural Sciences. 2016;86 (3):394-398.
17. Rudani K, Vishal P, Kalavati P. The importance of zinc in plant growth-A review. Int. Res.J. Nat. Appl. Sci. 2018;5 (2):38-48.
18. Salder P.C. Branched-chain amino acids and immunity // J. Nutr. – 2006. – Vol. 136. – P. 288–293.
19. Sharma A., Singh V. Seed oil composition and pharmacological potential. Phytochemistry Letters, 2016, Vol. 17, pp. 45–52.
20. Shimomura Y., et al. Branched-chain amino acids and exercise // J. Nutr. – 2006. – Vol. 136. – P. 529–532.
21. Singh P., Kumar R. Harvesting stage effects on oil content in medicinal plants. Industrial Crops and Products, 2018, Vol. 122, pp. 678–686.
22. Wang X., Chen L., Zhao J. Genetic variability and seed oil content in Foeniculum vulgare. Plant Science, 2017, Vol. 258, pp. 45–53.

DIGITAL MONITORING OF IRRIGATED AGRICULTURAL LANDS USING REMOTE SENSING TECHNOLOGIES: RESULTS AND ANALYSIS FROM AMUDARYA DISTRICT, KARAKALPAKSTAN

N.M. Djumabekova
Tashkent State Agrarian University, Tashkent, Uzbekistan
https://doi.org/10.5281/zenodo.20809560

Abstract. *Effective monitoring of irrigated agricultural lands is critical for sustainable land resource management, particularly in arid regions facing soil salinization, water scarcity, and land degradation. This study presents a comprehensive digital monitoring system for the irrigated lands of Amudarya District (Karakalpakstan Republic, Uzbekistan) developed using Sentinel-2 MSI and Landsat-8/9 OLI/TIRS satellite data processed through Google Earth Engine (GEE) and integrated with ArcGIS Pro and ArcGIS Dashboard platforms. Three key spectral indices were applied: the Normalized Difference Vegetation Index (NDVI), Normalized Difference Moisture Index (NDMI), and Land Surface Temperature (LST), covering the period 2020–2024. Digital mapping revealed that actual irrigated land area (41,240 ha) exceeds official cadastral records (39,516 ha) by 1,724 ha (98.97% accuracy), while total territory mapping accuracy reached 96.68%. Strong correlation analysis (n = 1,200 pixels) confirmed: LST–NDVI (r = -0.98, R^2 = 0.96), NDMI-NDVI (r = +0.92, R^2 = 0.85), and NDMI-LST (r = -0.87, R^2 = 0.75) relationships at p < 0.001. An interactive ArcGIS Dashboard geoportal was developed and registered with the Karakalpakstan Land Resources Authority, enabling real-time monitoring, automated threshold alerts, and seasonal reporting. Compared to conventional field monitoring, the geoportal system reduces costs 5-8 times and accelerates data processing 30–90 times while increasing monitoring frequency to every 5 days across 100% of district territory.*

Keywords: *remote sensing; NDVI; NDMI; LST; Sentinel-2; Landsat-8; GIS; ArcGIS Dashboard; irrigated land monitoring; soil salinization; Aral Sea basin; Uzbekistan.*

1. Introduction

Irrigated agricultural lands constitute a cornerstone of global food production systems. According to the Food and Agriculture Organization of the United Nations (FAO), approximately 352 million hectares worldwide are designated for irrigation, comprising around 20-22% of total cropland yet supplying over 40% of global agricultural output (FAO, 2022). In arid and semi-arid regions such as Central Asia, where rainfall is insufficient for rainfed agriculture, irrigation is the only means of ensuring sustainable crop production.

The Amudarya District, located in the Karakalpakstan Republic of Uzbekistan, is situated in one of the world's most ecologically stressed regions: the Aral Sea basin. The progressive desiccation of the Aral Sea has generated a new desert-the "Aral Kum"-from which tens of millions of tons of salt-laden dust are transported annually across the region, accelerating soil salinization and land degradation (UNEP, 2023). Combined with an extreme continental climate (annual precipitation 90-120 mm, evapotranspiration 1,000-1,200 mm/year), rising groundwater

mineralization, and declining inflows from the Qoshtapa Canal (reduced from 8.0 to 6.1 billion m^3 over 20 years), the district's irrigated agricultural lands face severe and compounding threats.

Traditional cadastral and field-based monitoring methods are insufficient for addressing these challenges at the required spatial and temporal scales. This gap has created demand for satellite-based, automated, and cost-effective monitoring solutions. Recent advances-particularly the freely available Sentinel-2 and Landsat-8/9 datasets combined with Google Earth Engine (GEE)-have revolutionized land monitoring capabilities (Bazzi et al., 2021; Zhu et al., 2024).

Despite growing global interest in this domain-with over 2,654 publications from China alone in Scopus and Web of Science databases during 2021-2025-only one publication from Uzbekistan was identified in the international literature on this topic. The objective of this study is to develop and validate a comprehensive digital monitoring system for the irrigated agricultural lands of Amudarya District using multi-source satellite data and GIS platforms, assess its accuracy against official cadastral records, quantify spectral index correlations, and demonstrate the operational utility of the resulting ArcGIS Dashboard geoportal.

2. Materials and Methods

2.1. Study Area

The Amudarya District is situated in the southern part of Karakalpakstan Republic, along the left bank of the Amu Darya River. The district covers 102,119 ha of which 71,428 ha (69.9%) are agricultural lands. An extreme continental climate characterizes the region: mean annual temperature +12-13 °C, summer maximum up to +47 °C, annual precipitation 90-120 mm, and evapotranspiration 1,000-1,200 mm/year. The district lies within the Aral Sea ecological crisis zone, subject to salt-dust deposition from the Aral Kum desert and secondary soil salinization.

2.2. Satellite Data

Two primary datasets were used: Sentinel-2 MSI Level-2A (10 m resolution, 5-day revisit, 2020-2024 growing season, cloud cover <10%) and Landsat-8/9 OLI/TIRS (30 m resolution for TIRS thermal bands). All data were processed in Google Earth Engine with atmospheric correction applied. Spectral indices were exported as GeoTIFF and integrated with ArcGIS Pro via Zonal Statistics as Table.

2.3. Spectral Indices

Three indices were calculated:

$NDVI = (NIR - RED) / (NIR + RED)$ [Rouse et al., 1973]

$NDMI = (NIR - SWIR) / (NIR + SWIR)$ [Gao, 1996]

LST derived from Landsat-8 TIRS bands with emissivity correction: $\varepsilon = 0.004 \times Pv + 0.986$

The combined NDVI×NDMI Intersect algorithm was used to distinguish irrigated croplands from forests, grasslands, and water bodies. Only pixels exceeding both thresholds ($NDVI > 0.30$; $NDMI > 0.10$) were classified as irrigated cropland.

2.4. Correlation Analysis

Pearson correlation and linear regression were performed on 1,200 pixel observations (2023-2024) to quantify inter-index relationships at $p < 0.001$.

3. Results

3.1. Digital Contour Mapping

A comprehensive digital contour database was created in ArcGIS Pro EPSG:32642 coordinate system from Sentinel-2 imagery and cadastral materials, covering all agricultural land parcels in Amudarya District (Figure 1).

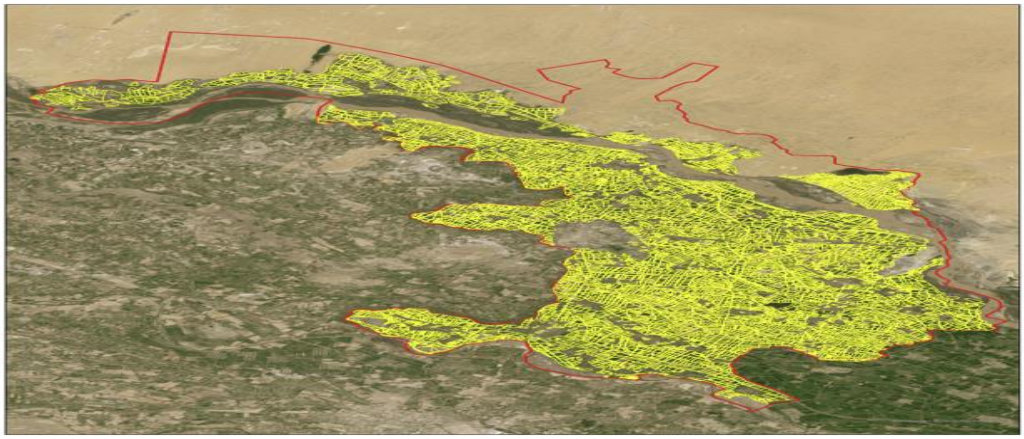


Figure 1. Digital land contour map of Amudarya District generated in ArcGIS Pro (EPSG:32642, WGS 84 UTM Zone 42N). Red outline: administrative boundary; yellow polygons: agricultural contours.

3.2. Accuracy Assessment: Monitoring vs. Cadastral Records

Comparison of satellite-based monitoring results with the National Land Report 2025 revealed significant discrepancies indicating the superior spatial completeness of remote sensing-based inventory (Table 1).

Table 1. Comparison of official cadastral records and monitoring results

Indicator	Cadastral Data	Monitoring Results	Difference / Accuracy (%)
Total territory (ha)	102,119	105,510	+3,391 / 96.68%
Irrigated croplands (ha)	39,516	41,240	+1,724 / 98.97%
Irrigated land share (%)	38.69%	39.08%	-
Cropland area (ha)	32,497	32,466	−31 / 96.70%

The monitoring system identified 41,240 ha of active irrigated croplands. Figure 2 shows the spatial distribution of irrigated land area as mapped from satellite contours.



Figure 2. Irrigated cropland area of Amudarya District based on digital contour monitoring (ha). Source: Sentinel-2 and Landsat-8 imagery, ArcGIS Pro analysis.

3.3. NDVI Analysis: Vegetation Dynamics

NDVI was calculated for each growing season from 2020 to 2024. Figure 3 shows the spatial distribution of NDVI across irrigated croplands in 2024, while Figure 4 presents inter-annual dynamics.

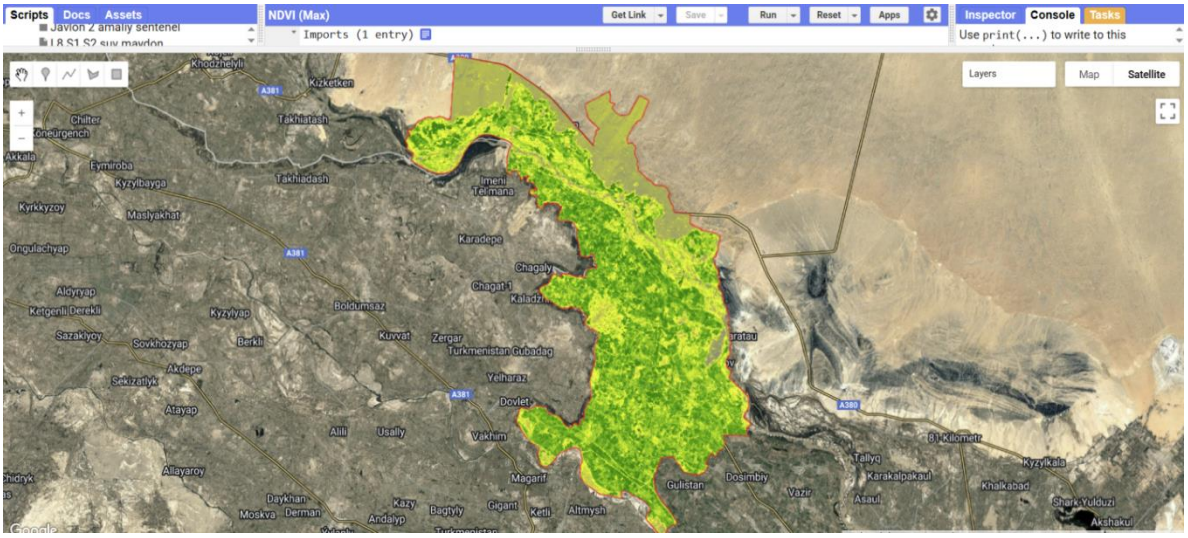


Figure 3. NDVI distribution map of Amudarya District irrigated croplands (2024). Classes: red = low (<0.33), yellow = moderate (0.33–0.60), green = high (>0.60). Source: Sentinel-2 Level-2A, GEE processing.



Figure 4. Multi-year mean NDVI dynamics of Amudarya District irrigated croplands (2020–2024). Minimum: 0.50 (2021 drought); maximum: 0.70 (2022 optimal conditions).

Table 2. Vegetation categories by NDVI class (2020–2024)

NDVI Category	Area (ha)	Characterization
Low (<0.33)	15,157	Degraded, sparse, or saline croplands
Moderate (0.33–0.60)	18,689	Average productivity; risk of moisture stress
High (>0.60)	19,950	Dense, healthy vegetation; well-irrigated

3.4. LST Analysis: Thermal Dynamics

LST was derived from Landsat-8/9 TIRS bands. A declining thermal trend was observed from 2021 (peak 46°C mean) to 2024 (37°C mean), reflecting improved vegetation cover and moisture conditions (Figure 5). In 2024, 63% of irrigated croplands fell within the optimal LST range (30-33°C).

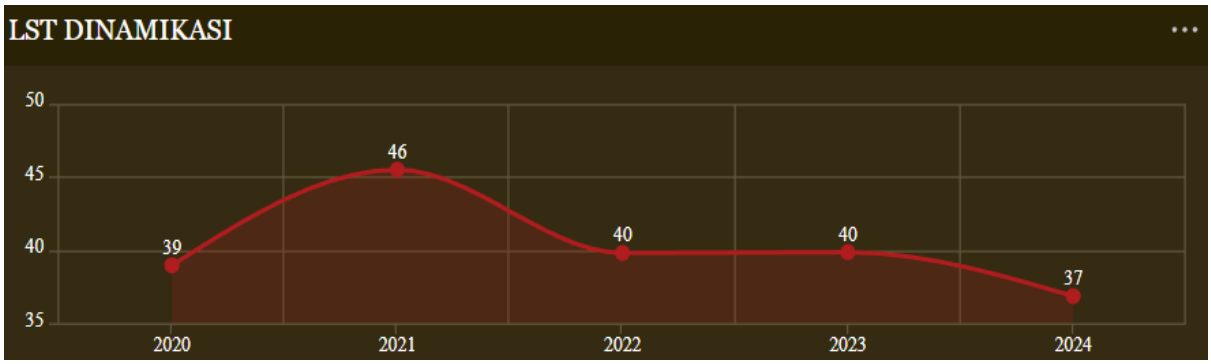


Figure 5. Annual Land Surface Temperature (LST) dynamics in Amudarya District irrigated croplands (2020-2024, °C). Peak thermal stress observed in 2021 (46°C); lowest in 2024 (37°C).

3.5. Irrigated Land Identification Algorithm

The combined NDVI×NDMI Intersect methodology is illustrated in Figure 6. Only pixels exceeding both thresholds (NDVI > 0.30 AND NDMI > 0.10) were retained as irrigated cropland, eliminating false positives from forests and grasslands.

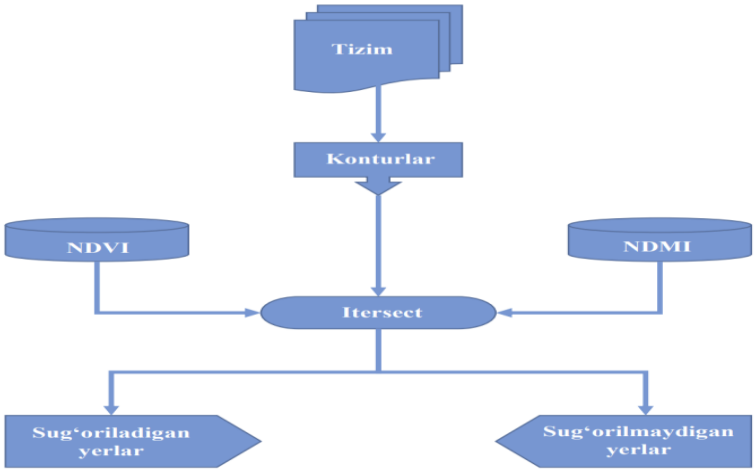


Figure 6. Block scheme of irrigated land identification methodology using NDVI and NDMI Intersect operation (GEE + ArcGIS Pro integration).

Figure 7 illustrates the proportional distribution of irrigated versus non-irrigated lands identified through the monitoring system.

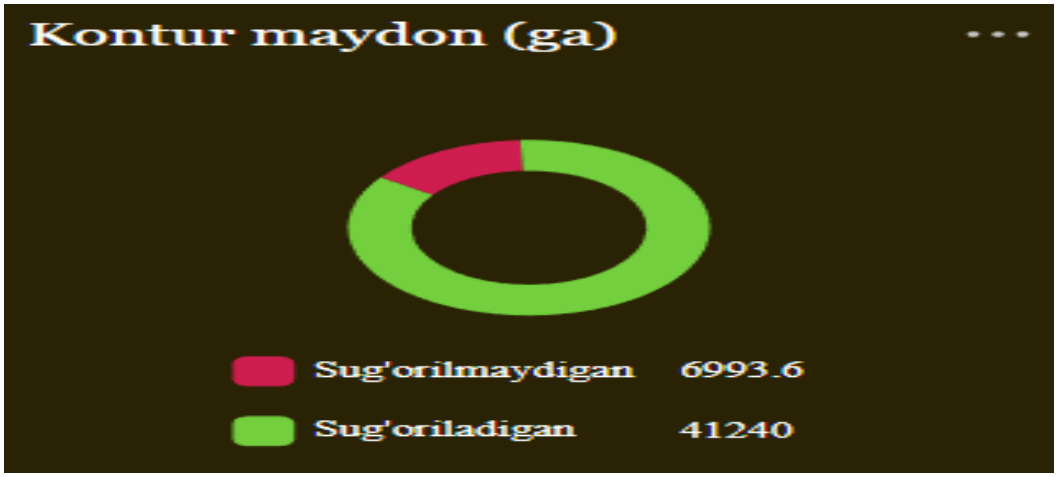


Figure 7. Proportional distribution of irrigated (41,240 ha, 85.5%) and non-irrigated former croplands (6,993.6 ha, 14.5%) in Amudarya District, as identified by satellite monitoring.

3.6. Correlation Analysis of Spectral Indices

Pearson correlation analysis was performed on 1,200 pixel observations from 2023-2024 data.

Table 3. Correlation statistics between spectral indices (Amudarya District, 2024; n = 1,200 pixels)

Variable Pair	r	R^2	Regression Equation	p-value
NDVI ↔ LST	−0.98	0.96	NDVI = −0.0142×LST + 0.847	<0.001
NDVI ↔ NDMI	+0.92	0.85	NDVI = 0.684×NDMI + 0.312	<0.001
NDMI ↔ LST	−0.87	0.75	NDMI = −0.0089×LST + 0.741	<0.001

The LST–NDVI scatter plot (Figure 8) demonstrates the strongest relationship (R^2 = 0.96): each 1°C rise in LST reduces NDVI by 0.0142 units.

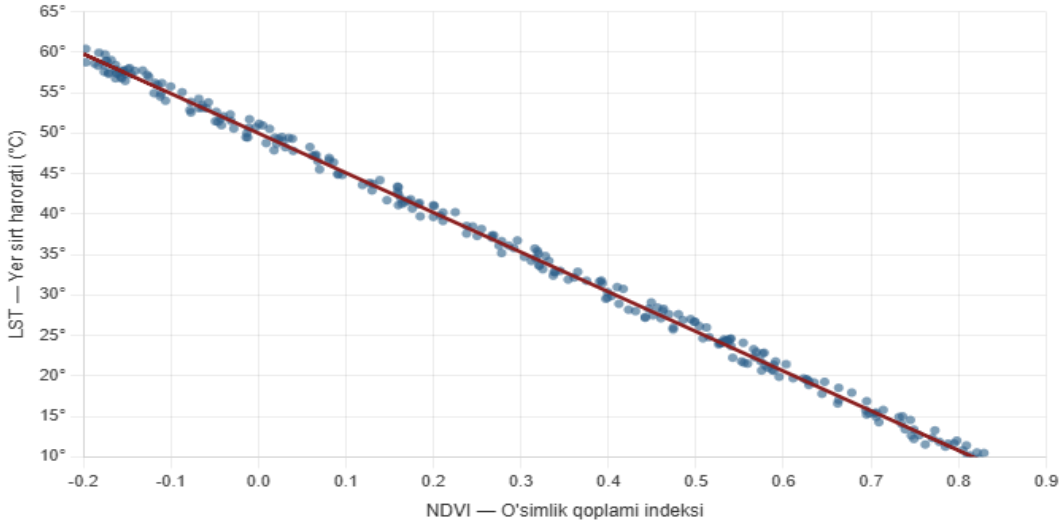


Figure 8. Correlation between Land Surface Temperature (LST) and NDVI in Amudarya District (R^2 = 0.96, n = 1,200 pixels, 2024). Regression: NDVI = −0.0142×LST + 0.847; p < 0.001.

The NDMI–NDVI relationship (Figure 9) confirms moisture as the primary driver of vegetation productivity: 85% of NDVI variation is explained by soil and plant moisture content.

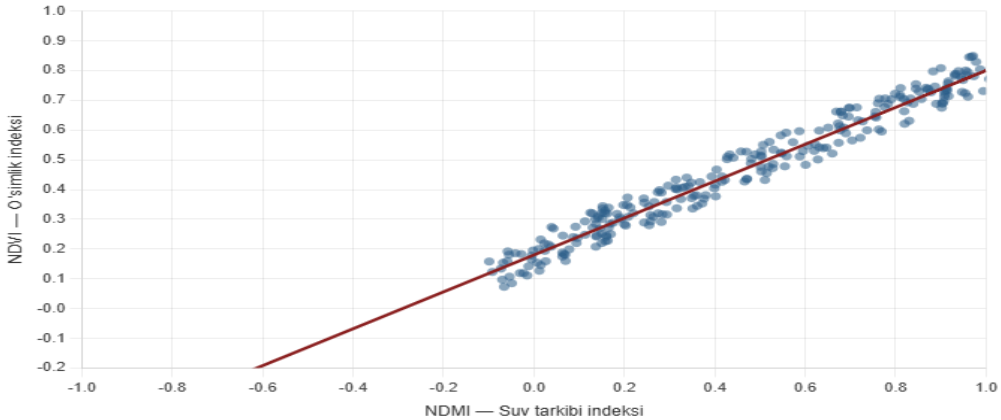


Figure 9. Correlation between NDMI and NDVI in Amudarya District (R^2 = 0.85, n = 1,200 pixels, 2024). Regression: NDVI = 0.684×NDMI + 0.312; p < 0.001. Source: Sentinel-2 L2A data.

The NDMI-LST relationship (Figure 10) quantifies thermal control over moisture balance (R^2 = 0.75): rising temperatures drive accelerated evapotranspiration and topsoil moisture depletion.

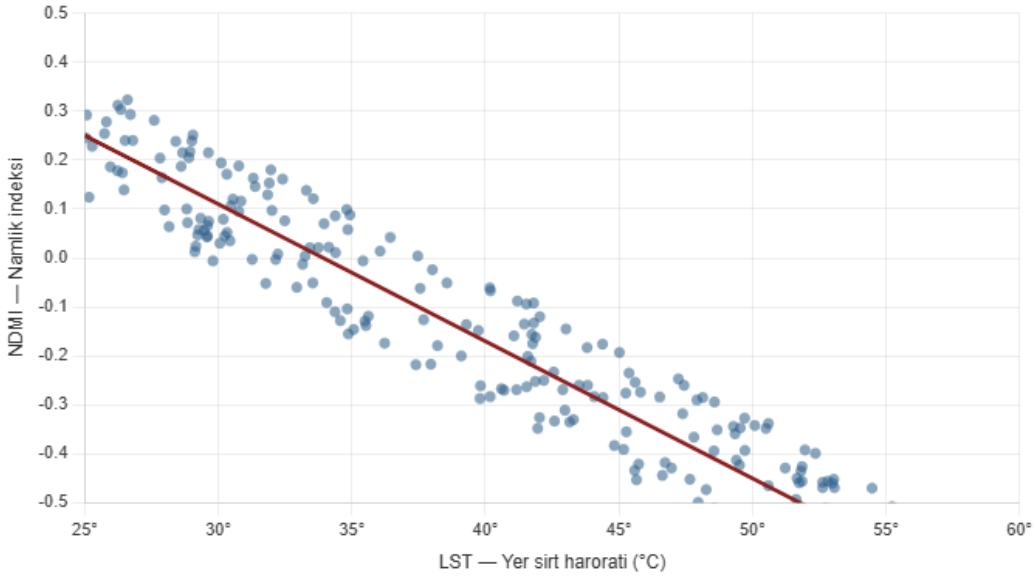


Figure 10. Correlation between NDMI and LST in Amudarya District (R^2 = 0.75, n = 1,200 pixels, 2024). Regression: NDMI = −0.0089×LST + 0.741; p < 0.001.

Seasonal dynamics of all three indices through 2024 are shown in Figure 11, demonstrating the phenological cycle from spring green-up (March-May) through peak cotton growth (June–August) to autumn senescence (September-December).

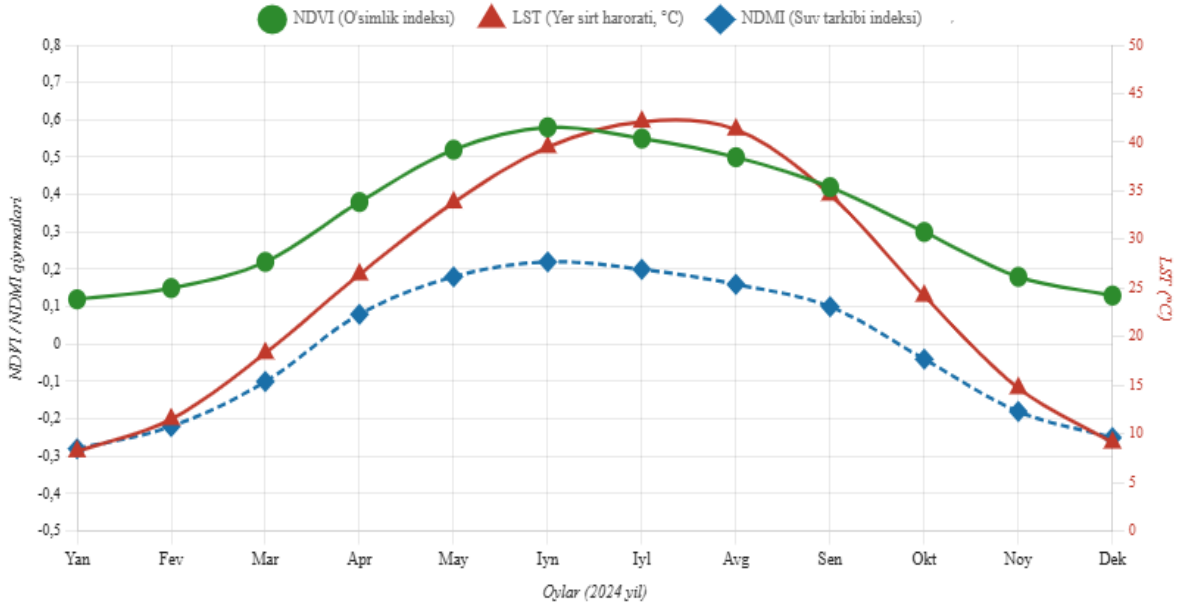


Figure 11. Seasonal dynamics of NDVI, LST, and NDMI in Amudarya District irrigated croplands by month (2024). NDVI peak in June (0.58); LST peak in July (42.5°C); winter minimum NDVI = 0.13. Source: Sentinel-2 and Landsat-8 data, ArcGIS Pro.

3.7. Geoportal System

The ArcGIS Dashboard geoportal integrates all monitoring outputs into a unified real-time platform (Figure 12). The system enables: spatial visualization of NDVI, NDMI and LST automated alerts when indices cross predefined thresholds crop type classification; and monthly/seasonal report generation.

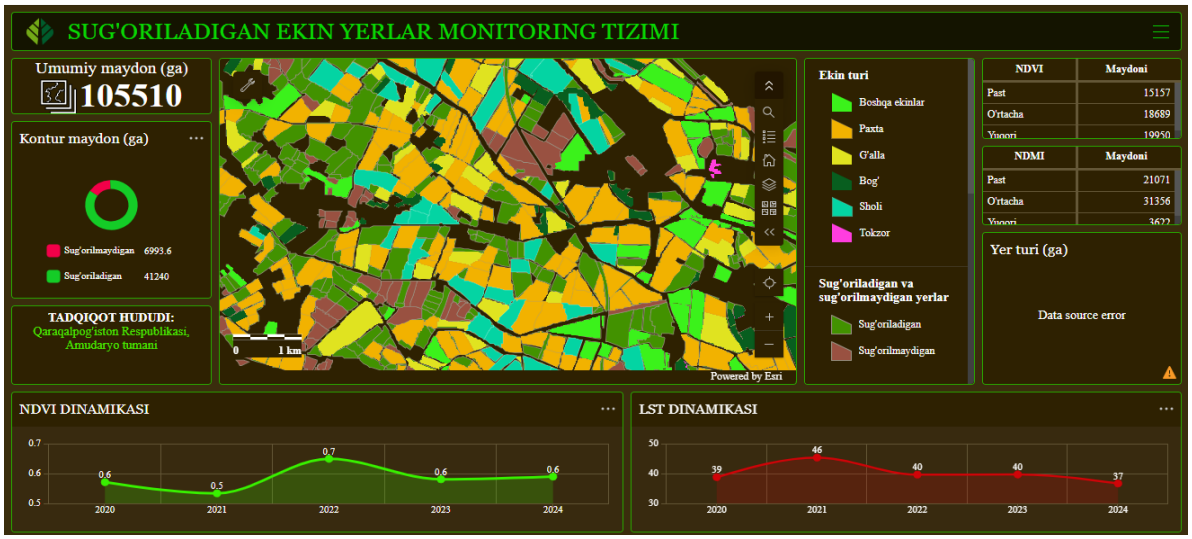


Figure 12. Main interface of the "Irrigated Agricultural Land Monitoring System" geoportal (ArcGIS Dashboard). Panels show: irrigated/non-irrigated distribution (top left), NDVI/NDMI class areas (right), multi-year NDVI and LST trend graphs (bottom). Developed by the author; registered with Karakalpakstan Land Resources Authority, 2025.

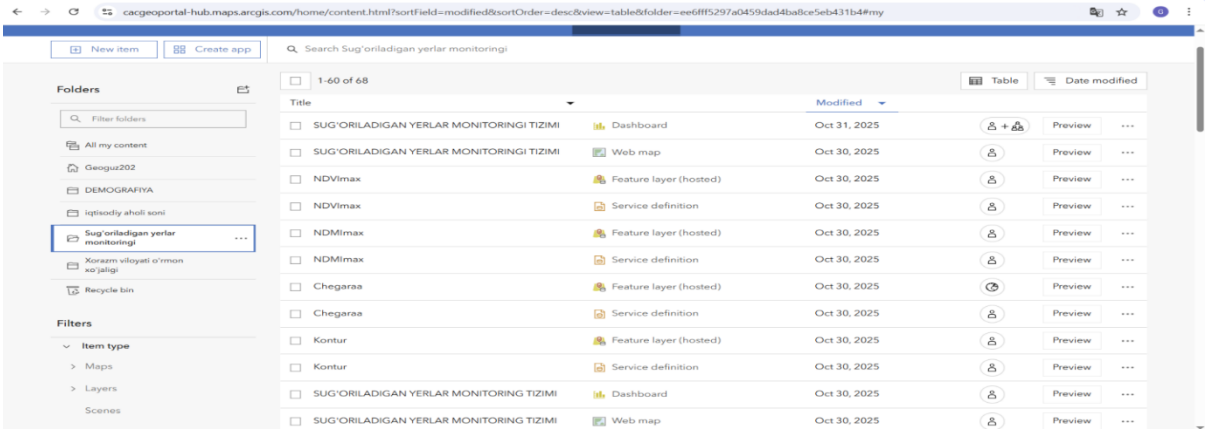


Figure 13. Dashboard view of irrigated (green) and non-irrigated (orange) land contours across Amudarya District. Each polygon is attributed with NDVI, NDMI, LST values and crop type classification.

Table 4. Comparison of conventional field monitoring and geoportal system

Indicator	**Conventional Method**	**Geoportal System**	**Improvement**
Area mapping accuracy	70-85%	96.68%	+7-12 pp
Monitoring frequency	1-2×/year	Every 5 days	36-72× higher
Processing duration	60-90 days	1-3 days	30-90× faster
Cost per inspection	25-40 M UZS	3-5 M UZS	5-8× lower
Territorial coverage	Partial sampling	100% of district	Full coverage
Degradation detection	Post-event	10-15 days prior	Proactive

4. Discussion

The results demonstrate that combined NDVI×NDMI Intersect methodology substantially outperforms single-index approaches, achieving 98.97% accuracy for irrigated cropland delineation exceeding the 80-95% range typically reported for single-index methods. The 1,724

ha discrepancy between monitoring and cadastral records has direct policy implications for water allocation, land taxation, and agricultural planning.

The exceptionally strong LST-NDVI correlation ($R^2 = 0.96$) is higher than values typically reported in temperate contexts ($R^2 = 0.60$-0.85), attributable to the extreme thermal amplitude of the Aral Sea basin environment. The identification of 6,993.6 ha as inactive former irrigated land is a finding with immediate policy relevance for land reclamation programs. Automated integration of threshold alerts into the geoportal translates these correlations into actionable irrigation scheduling recommendations.

Limitations include intermittent cloud cover and the 30 m spatial resolution of Landsat-8 TIRS for very small parcels (<1 ha). Future integration of UAV imagery would enhance delineation accuracy for such parcels.

5. Conclusions

1. The combined NDVI×NDMI Intersect methodology accurately delineated irrigated cropland at 98.97% accuracy, revealing a 1,724 ha discrepancy relative to cadastral records and identifying 6,993.6 ha of degraded former irrigated land requiring reclamation.

2. Strong correlations were confirmed: LST-NDVI ($R^2 = 0.96$), NDVI–NDMI ($R^2 = 0.85$), NDMI-LST ($R^2 = 0.75$) at $p < 0.001$, enabling predictive modeling of vegetation condition 10-15 days in advance.

3. NDMI analysis revealed 37.6% of territory (21,071 ha) with chronic moisture deficit; LST mapping identified critical thermal stress zones during the July-August peak growing period.

4. The ArcGIS Dashboard geoportal reduces monitoring costs 5-8×, accelerates processing 30-90×, and achieves 100% territorial coverage at 5-day intervals-officially registered and recommended for regional deployment.

5. Satellite-based monitoring with GIS integration is technically superior, economically viable, and institutionally scalable for water-stressed agricultural landscapes of Central Asia.

REFERENCES

1. Bazzi, H., Baghdadi, N., Zribi, M., Demarez, V., & Belhouchette, H. (2021). Mapping irrigated areas using Sentinel-1 and Sentinel-2 time series data. Remote Sensing, 13(13), 2584–2605.
2. Chakhar, A., Baghdadi, N., Zribi, M., & El Hajj, M. (2024). Machine learning for irrigation mapping: A comparative study. Remote Sensing Applications, 33, 88–104.
3. FAO. (2020). Remote sensing for evapotranspiration monitoring: A technical guide. FAO, Rome.
4. FAO.(2022). WaPOR database methodology. FAO, Rome. https://doi.org/10.4060/cb8756en
5. Gao, B.-C. (1996). NDWI-A normalized difference water index. Remote Sensing of Environment, 58(3), 257-266.
6. Gorelick, N., et al. (2017). Google Earth Engine: Planetary-scale geospatial analysis. Remote Sensing of Environment, 202, 18–27.
7. IPCC. (2021). Climate Change 2021: The Physical Science Basis. Cambridge University Press.
8. Kumar, R., & Singh, A. (2023). Bibliometric analysis of remote sensing in irrigation. Water Resources Management, 37, 45–62.
9. Pettorelli, N., et al. (2011). Using the satellite-derived NDVI to assess ecological responses. Trends in Ecology & Evolution, 20(9), 503–510.

10. Rouse, J. W., et al. (1973). Monitoring vegetation systems in the Great Plains with ERTS. NASA SP-351, 309–317.
11. Sharopov, R. N. (2025). Organization of rainfed and irrigated land resource use: Regional models (DSc dissertation abstract). Tashkent.
12. Sodikova, G., et al. (2025). GIS assessment of soil erosion in Uzbekistan's rainfed lands. BIO Web of Conferences, 173, 4–11.
13. UNEP. (2023). Digital monitoring for sustainable agriculture. UNEP, Geneva.
14. World Bank. (2023). Resilient agriculture in the Aral Basin. World Bank Group, Washington, DC.
15. Xie, Y., et al. (2021). Mapping annual irrigation from Landsat imagery. Remote Sensing of Environment, 256, 112316.
16. Yu, L., et al. (2024). Identification of irrigated areas using Sentinel-2 and machine learning. Journal of Hydrology, 620, 129450.
17. Zhu, W., et al. (2024). Large-scale irrigation area mapping. Agricultural Water Management, 278, 108168.

ECONOMIC EFFICIENCY OF NEW EARLY-MATURING, HIGH-YIELDING MAIZE VARIETIES AND THEIR PRIMARY SEED PRODUCTION

Kh.K. Nazarov[1], T.Kh. Farmanov[2], K.K. Azizov[3]
Tashkent State Agrarian University, Associate Professor of the Department of Genetics, Breeding and Seed Production of Agricultural Crops, Doctor of Agricultural Sciences (DSc)[1]
Tashkent State University of Economics, Professor, Doctor of Economics[2]
Research Institute of Cereals and Leguminous Crops, Deputy Director for Research and Innovation, Doctor of Agricultural Sciences (DSc), Senior Researcher[3]
https://doi.org/10.5281/zenodo.20812058

Abstract. *This article examines scientific research on maize cultivation for grain and green fodder production, the research developments of scientists, and the newly developed early-maturing and high-yielding maize variety "Kelajak 100", which is intended for grain and green fodder production. A comparative analysis was conducted between the new variety and the widely cultivated standard variety "Uzbekistan 601 ECB". The study analyzes varietal differences, yield levels, production costs, total income, net profit, and overall economic efficiency. On the basis of the obtained results, the economic effectiveness of the new "Kelajak 100" variety is scientifically substantiated.*

Keywords: *maize grain, seed production, yield, output, green fodder, production costs, income, profit, profitability level, value, promising variety, hybrid variety.*

1. Introduction

Maize is one of the most widely cultivated cereal crops in the world and is grown for fodder, food, and industrial purposes. Its grain contains 65-70% carbohydrates, 9-12% protein, 4-8% oil, mineral salts, and vitamins. In terms of cultivated area and yield, the United States ranks first, China second, and Brazil third.

Maize (Zea mays L.) remains a major food source in many regions of the world. According to United Nations data cited in the source text, global grain production is approximately 2.45 billion tonnes, of which around 2.194 billion tonnes are accounted for by cereal crops, including maize.

Globally, 116 million tonnes of maize are used as food. In addition, maize is an important source of starch for the pharmaceutical, paper, mining, and construction industries.

In scientific research on maize breeding worldwide, considerable attention is paid to developing promising early-maturing varieties and hybrids with high grain and green-mass yields, resistance to diseases and pests, and improved seed-production systems.

Under conditions of global climate change, the development and practical introduction of maize varieties resistant to different stress factors, including drought, diseases, and pests, have substantial scientific and practical significance for ensuring food security.

In Uzbekistan, local productive varieties of maize have been developed by plant breeders to supply the population with food, industry with raw materials, and livestock and poultry production with nutritious feed. Nevertheless, a large proportion of the area occupied by maize is still sown with imported seed.

The Laws of the Republic of Uzbekistan “On Seed Production” of 16 February 2019 and “On Breeding Achievements” of 29 August 2002, Presidential Decree No. PF-5853 of 23 October 2019 “On the Strategy for the Development of Agriculture of the Republic of Uzbekistan for 2020-2030”, Resolution No. PQ-3683 of 27 April 2018 “On Measures for the Fundamental Improvement of the Seed Production System in the Republic of Uzbekistan”, Resolution No. PQ-106 of 28 January 2022 “On Additional Measures for the Further Development of Seed Production of Agricultural Crops”, and other regulatory documents adopted in this field define the creation of new local maize varieties, alongside other agricultural crops, as a priority direction.

Presidential Decree No. PF-158 of 11 September 2023 “On the Uzbekistan-2030 Strategy” sets tasks such as sharply increasing productivity and profitability in agriculture, raising the average income obtained from one hectare to USD 5,000, increasing agricultural exports to USD 10 billion annually, and attracting a total of USD 15 billion of investment into the agrarian sector.

Scientific investigations aimed at developing effective innovative technologies for maize breeding and seed production have been conducted at leading research centers, institutions, and universities worldwide. These include institutions and organizations in the United States, Australia and CIMMYT, China, Pakistan, Serbia, Ukraine, Moldova, Yugoslavia, Hungary, Bulgaria, the Czech Republic, Slovakia, Russia, Kazakhstan, as well as well-known international maize seed companies in the United States, the United Kingdom, Germany, France, Serbia, and Hungary. In Uzbekistan, research has been carried out at the Research Institute of Plant Genetic Resources and at the Maize Breeding and Seed Production Scientific Experimental Station. Comprehensive breeding work on early-maturing maize varieties and hybrids has also been conducted by the Ukrainian Research Institute of Maize Production and the Research Institute of Plant Genetic Resources.

The results of these studies have scientifically and practically demonstrated that the use of hybrids, synthetic varieties, and populations in maize breeding makes it possible to create productive varieties that are early-maturing and resistant to cold, drought, diseases, and pests.

However, an analysis of previous research indicates that the scientific basis for hybridizing geographically distant maize samples with local varieties, creating new early-maturing and productive hybrids and varieties with high grain and green-mass yields, and improving their primary seed production has not yet been sufficiently developed by national researchers.

Maize plays an important role in satisfying food demand. In world agriculture, it is among the major crops after wheat and rice. In the 1990s, maize was cultivated on 109 million hectares worldwide, producing 412 million tonnes of output. Over the subsequent decade, the maize area increased to 146 million hectares, and gross production reached 686 million tonnes in 2003-2005. Among agricultural crops, maize occupies the third position, with a share exceeding 30%.

By cultivated area, maize ranks after wheat and rice globally. In Asia, maize is cultivated on 55.0 million hectares; in North America, on more than 36.8 million hectares; in Africa, on 27.8 million hectares; in South America, on 25.5 million hectares; and in Europe, on 12.3 million hectares. In 2019, the United States ranked first in maize area with 35.5 million hectares, China second with 33.2 million hectares, and Brazil third with 15.3 million hectares. In Uzbekistan, the maize area in 2014 was 35.5 thousand hectares, with a yield of 50 c/ha.

Maize is considered a crop of American origin. The first written information about maize was recorded by Christopher Columbus during the discovery of America in 1492. At that time, dent, starchy, sweet, and popcorn groups of maize were known. Subsequently, maize began to spread throughout the world as a cultivated crop.

The history of maize origin covers a long period. Under favorable cultivation conditions, maize can produce high grain yields. In nature, maize has almost no independent mechanism for reproduction and adaptation to the external environment; under ordinary natural conditions, most plants perish and do not produce a harvest.

To date, science has not identified the wild ancestors of maize with certainty, and its origin spans millennia. This is supported by data from radioactive decay analysis of 5,000-year-old maize cobs found in Mexico. Some sources indicate that maize may have originated in the mountainous regions of Peru, Bolivia, and Ecuador, where many local forms of maize are found.

Other studies recognize southern Mexico and Central America as the center of origin of maize, because these regions contain teosintes with a chromosome number similar to maize (2n = 20) and numerous local forms related to them.

In Central Asia, maize began to be cultivated in the late eighteenth and early nineteenth centuries. Early records of maize cultivation in the Fergana Valley were made by Votkhonu (1835) and Chekotillo (1931). As in Transcaucasia and Moldova, maize was not widely grown as a main crop across large areas in Central Asian countries. It was planted around field borders and among fruit, vegetable, and melon crops. The local population paid greater attention to sorghum than to maize, using its green mass as livestock feed and its grain for food.

The first variety-testing experiments on maize in Uzbekistan were conducted by M.M. Bushuev and R.R. Schroeder in 1910-1914 at the experimental plots of the desert zones and at Turkestan agricultural experimental stations. Until 1917, maize was not widely distributed in Uzbekistan because local flint and semi-dent forms were low-yielding. Maize was planted on small areas in the Fergana Valley and in Syrdarya. Later, N.N. Ballashev studied 43 maize varieties at the Uzbekistan Agricultural Station. In addition, S.K. Samokhvalenko at the Uzbekistan Research Institute of Animal Husbandry and F.S. Parkhomenko at the Uzbekistan Research Institute of Cotton Growing studied maize collection samples at the former SoyuzNIKHI Central Experimental Station.

Increasing maize productivity is an important global objective. To achieve this, breeders need to create high-yielding varieties and hybrids. Breeding is understood as the purposeful selection and creation by humans of plant varieties that can be used for food and animal feed.

Regarding the importance of breeding, N.I. Vavilov described plant breeding as “evolution created by human hands”.

In terms of feed and productivity quality, maize is one of the most valuable crops in the world. By land area, it ranks third after wheat and rice, occupying more than 114.5 million hectares and accounting for 31% of the global cultivated area.

America accounts for 45.7% of total maize grain production, more than two-thirds of which is produced in the United States, where the highest grain yields in the world, 5.3-7.5 t/ha, are obtained.

Maize grain is also one of the main crops in Brazil, Mexico, Argentina, Colombia, Venezuela, Paraguay, Peru, Guatemala, and Honduras; however, grain yields in these countries are relatively low, at 1.2-2.0 t/ha.

In Asia, maize occupies 38.6 million hectares, with an average yield of 2.8 t/ha, an annual gross output of 107.2 million tonnes, and a 26.4% share of world production. The main grain producer in Asia is China, accounting for 63.8%, with yields of 3.0-3.9 t/ha.

In the CIS countries, maize occupies 4.2 million hectares, with an average yield of 3.8 t/ha and a global share of 3.1-3.9%.

In Uzbekistan, 895.5 thousand tonnes of maize grain and 29.4 thousand tonnes of white sorghum grain were produced in 2024.

According to analyses by agricultural economists, the cultivation of agricultural crops, including maize, under the conditions of Uzbekistan is highly profitable. In addition to maize grain, its leaves and stems are valuable feed for livestock, and maize also plays an important role in satisfying the population's food demand.

2. Materials and Methods

Research on maize was conducted during 2010-2021 at the Maize Breeding and Seed Production Scientific Experimental Station in Zangiota district, Tashkent region. The climate of Tashkent region is sharply continental and is characterized by abundant heat and light throughout the growing season. According to observations of the Tashkent Observatory, average annual sunshine duration is 2,870 hours; the maximum duration occurs in summer and reaches up to 380 hours in July, or 95% of the possible value. Winter is relatively unstable, with cold periods alternating with warm periods.

The average duration of the period with air temperatures above 0°C is 330 days, while the vegetation period for heat-loving plants, defined by temperatures above 10°C, is 214 days.

Summers are hot and dry. In the hottest month, July, the average monthly air temperature is 28-29°C. The abundance of thermal resources, heat, and light in the artificially irrigated conditions of the Tashkent oasis makes it possible to obtain accurate data by applying intensive cultivation and processing technologies to different heat-loving plants, including maize.

During the experimental years, air temperature was favorable for maize growth and development. According to long-term averages, total precipitation was 35.1 mm, most of which occurred in late autumn, winter, and early spring. Stable snow cover is observed only in some winters; its thickness does not exceed 10-12 cm and it remains for 30-34 days. In most years, snow cover is uneven and melts quickly. The climate is dry, and the main share of precipitation falls in winter and spring. The highest precipitation is observed in March. The continental nature of the climate is reflected in annual, monthly, and daily meteorological variation across different years.

Total precipitation during the experimental years was lower than the long-term average. In 2018, precipitation was 35.9 mm, with the lowest value, 0.4 mm, recorded in July. The highest annual average precipitation was observed in 2016, at 39.9 mm.

In the maize experiments, no precipitation was observed during the flowering period, namely in August.

Table 1. Agrochemical characteristics of the experimental field soil at the Maize Breeding and Seed Production Scientific Experimental Station, Zangiota district, Tashkent region

Soil layer, cm	Humus, %	Nitrogen, %	Phosphorus, %	Potassium, %	CO2, %	Mobile nitrogen, mg/kg	Mobile phosphorus, mg/kg	Mobile potassium, mg/kg
0-30	0.927	0.063	0.275	0.682	7.87	16.2	20.8	132.0
30-50	0.542	0.036	0.250	0.682	7.81	9.4	7.36	103.0

To conduct in-depth scientific research in this area, experiments were carried out in the experimental field of the Maize Breeding and Seed Production Scientific Experimental Station in Zangiota district, Tashkent region.

The experimental field consisted of typical sierozem soil with a heavy loam mechanical composition. The 30-cm arable layer was moderately supplied with total nutrient reserves: humus 1.2%, nitrogen 0.1%, phosphorus 0.160%, and potassium 1.60%. The amounts of mobile forms of phosphorus, potassium, and nitrates in the 0-30 cm soil layer were as follows: P2O5 - 35.5 mg/kg, K2O - 290 mg/kg, and N2O3 - 28.2 mg/kg; in the 30-50 cm layer, the corresponding values were 32 mg/kg, 180 mg/kg, and 8.25 mg/kg (Table 1).

The moisture capacity of the soil in this field was 22%, and groundwater occurred at a depth of 13-15 m.

The experiments used the new promising high-grain-yielding maize variety “Kelajak 100”, included in the State Register of the Republic of Uzbekistan. In developing this variety, “VC 6661” was used as the maternal form and “MJ 600” as the paternal form.

The high-green-mass-yielding variety “Esdalik 80” was also used; in creating this variety, the maternal form was “Uzbekistan 100” and the paternal form was the “Uzbekistan 601 ECB” hybrid. Repeated crosses were conducted using the simple hybridization method.

The research methods were mainly laboratory and field based. The scientific studies used the generally accepted field-laboratory experiments and phenological observations described in the methodological manual “Methods of Field Experiments with Maize” (Dnipropetrovsk, 1984). Seed-quality indicators were determined according to O‘zDSt 2823:2014, “Seeds of Agricultural Crops: Methods for Determining Germination”.

In addition, the following methods were used: “Methodology of Breeding Experiments with Maize” by I.V. Savchenko (2012); the guidance on “Duration of the Vegetation Period and Valuable Economic Traits of New Early-Maturing Maize Hybrids” of the Uzbekistan Research Institute of Plant Science (2010); the method of individual selection in primary seed-production work of the All-Russian Research Institute of Grain Crops; and the phytopathological methods of Chumakov A.E. et al., “Basic Methods of Phytopathological Research” (Moscow, 1974), for identifying diseases.

The obtained results were statistically analyzed using B.A. Dospekhov’s “Methodology of Field Experiment” (Moscow, 1985) and modern ANOVA (analysis of variance). Yield was determined using StatView software (SAS Institute Inc.).

Agrotechnical measures in the experiment were developed on the basis of standard technological maps for the care of agricultural crops and production of agricultural output for 2016-2020.

As in other annual plants, the growth and development stages of maize are characterized by a series of successive morphological changes. The length of the growing season, the duration of each stage, and varietal traits of the plant are closely linked to the climatic conditions of the spring-summer-autumn period.

The more favorable the conditions for plant growth and development, the faster all life stages are completed; that is, the duration of each stage is shorter. Conversely, under unfavorable conditions, the plant remains longer in each developmental stage and its yield organs form more slowly.

To conduct the agrotechnical measures in the experimental field at the recommended times for cultivating maize varieties, the field was plowed to a depth of 28-30 cm.

Before plowing, 75% of the generally recommended phosphorus and potassium fertilizers were applied (P2O5 - 225 kg and KCl - 112.5 kg), while the remaining 25% (P2O5 - 75 kg and KCl - 37.5 kg) was applied together with seed sowing.

In early spring, the field was chiseled to a depth of 18-22 cm, leveled, and furrows and irrigation channels were prepared.

The prepared land plot was divided into experimental plots, and the seeds were sown manually. Because soil moisture was sufficient, pre-sowing irrigation was not applied.

The sown seeds germinated completely within 10-12 days. When the seedlings produced 4-5 leaves, the first cultivation was carried out at a depth of 10-12 cm.

During crop care, weeding was performed manually to control weeds, and light thinning was conducted to equalize plant density.

For the first fertilization, 230 kg of urea per hectare was applied and irrigation was carried out. When the plants produced 8-10 leaves, the second cultivation and fertilization were performed.

During the vegetation period, the maize crop was irrigated 5-6 times. Phenological observations were conducted from April to September, and the obtained results were recorded in the field journal.

3. Results and Discussion

As a result of high-quality implementation of all agrotechnical measures, mineral fertilization, inter-row cultivation, control of diseases and pests, and irrigation, the “Kelajak 100” variety produced 9.63 t/ha of grain, or up to 2.3 c/ha more grain yield than the standard “Uzbekistan 601 ECB” hybrid.

According to agricultural economists, maize cultivation is a competitive crop under the conditions of Uzbekistan. In addition, because maize leaves and stems, apart from its grain, serve as a feed source for livestock, the crop provides additional economic benefit.

When the funds spent on cultivating agricultural crops under the conditions of Uzbekistan are compared with exchange prices, cotton, maize, and wheat occupy leading positions under irrigated conditions and are considered economically efficient crops.

The costs incurred, income received, and net profit obtained from producing commercial grain of the promising “Kelajak 100” maize variety on 1 ha under production conditions were calculated relative to the standard variety. The results are presented in Table 2.

In the standard “Uzbekistan 601 ECB” hybrid, net profit was 17.7 million UZS/ha, whereas in the promising “Kelajak 100” variety it was 25.3 million UZS/ha. The profitability level was 108.2% and 154.6%, respectively.

According to the calculations, the new maize variety “Kelajak 100” was economically efficient for grain production and is recommended for cultivation to obtain high maize grain yield.

Table 2. Economic efficiency of grain production from maize varieties and hybrids

No.	**Crop/indicator**	**Unit**	**Standard “Uzbekistan 601 ECB” hybrid**	**“Kelajak 100” variety**	**Difference, +/-**
1	Sown area	ha	1	1	0
2	Total maize grain yield	t	8.4	10.7	+2.3
	Income from maize grain (3,500 UZS/kg)	thousand UZS	29,400	37,450	+8,050

No.	Crop/indicator	Unit	Standard "Uzbekistan 601 ECB" hybrid	"Kelajak 100" variety	Difference, +/-
3	Dry fodder	t	23.4	21.2	-2.2
	Value (200 UZS/kg)	thousand UZS	4,680.0	4,240.0	-440
4	Total income	thousand UZS	34,080.0	41,690.0	+7,610.0
5	Production costs				
5.1	Seed	kg	25	25	0
	Value (15,000 UZS/kg)	thousand UZS	375.0	375.0	0
5.2	Mineral fertilizers, total				
5.2.1	Urea	kg	460	460	0
	Value (4,600 UZS/kg)	thousand UZS	2,116.0	2,116.0	0
5.2.2	Phosphorus	kg	469	469	0
	Value (8,000 UZS/kg)	thousand UZS	3,752.0	3,752.0	0
5.2.3	Potassium	kg	153	153	0
	Value (2,500 UZS/kg)	thousand UZS	0.383	0.383	0
6	Organic fertilizer (manure)	t	20	20	0
	Value (300 UZS/t)	thousand UZS	6.0	6.0	0
7	Diesel fuel	L	169.5	169.5	0
	Value (9,500 UZS/L)	thousand UZS	1,610.2	1,610.2	0
8	Total cost	thousand UZS	14,235.7	14,235.7	0
9	Unexpected costs (15% of total cost)	thousand UZS	2,148.8	2,148.8	0
10	All costs	thousand UZS	16,371.1	16,371.1	0
11	Profit	thousand UZS	17,708.9	25,318.9	+7,610.8
12	Profitability level	%	108.2	154.6	+46.4 p.p.

Similarly, under production conditions, the costs incurred, income obtained, and net profit from cultivating the promising “Esdalik 80” variety for green mass (silage) on 1 ha were calculated relative to the standard variety. The results are presented in Table 3.

For green-mass production, net profit was 13.9 million UZS/ha in the standard “Uzbekistan 100” variety and 16.9 million UZS/ha in “Esdalik 80”. The profitability level was 89.9% for the standard variety and 108.9% for “Esdalik 80”.

The new promising maize variety “Esdalik 80” was evaluated as economically efficient for green-mass (silage) production and was recommended for cultivation across the republic.

Table 3. Economic efficiency of green-mass production from maize varieties and hybrids

No.	**Crop/indicator**	**Unit**	**Standard “Uzbekistan 100” variety**	**“Esdalik 80” variety**	**Difference, +/-**
1	Sown area	ha	1	1	0
2	Silage mass yield	t	73.9	81.3	+7.4
	Total income (400 UZS/kg)	thousand UZS	29,560	32,520	+2,960
3	Costs				
3.1	Seed	kg	30	30	0
	Value (15,000 UZS/kg)	thousand UZS	450.0	450.0	0
4	Mineral fertilizers, total				
4.1	Urea	kg	460	460	0
	Value (4,600 UZS/kg)	thousand UZS	2,116.0	2,116.0	0
4.2	Phosphorus	kg	469	469	0
	Value (8,000 UZS/kg)	thousand UZS	3,752.0	3,752.0	0
4.3	Potassium	kg	153	153	0
	Value (2,500 UZS/kg)	thousand UZS	382.5	382.5	0
4.4	Organic fertilizer, manure	t	20	20	0
	Value (300 UZS/kg)	thousand UZS	6,000	6,000	0
5	Diesel fuel	L	152.5	152.5	0
	Value (9,500 UZS/L)	thousand UZS	1,448.7	1,448.7	0
6	Total cost	thousand UZS	14,149.2	14,149.2	0

No.	Crop/indicator	Unit	Standard "Uzbekistan 100" variety	"Esdalik 80" variety	Difference, +/-
7	Unexpected costs (10% of total cost)	thousand UZS	1,414.9	1,414.9	0
8	All costs	thousand UZS	15,564.2	15,564.2	0
9	Profit	thousand UZS	13,995.8	16,955.8	+2,960
10	Profitability level	%	89.9	108.9	+19 p.p.

According to experiments conducted in 2019-2021 on the "Kelajak 100" variety grown for grain, seed germination energy ranged from 96.7% to 97.3%, while in the standard "Uzbekistan 601 ECB" hybrid it ranged from 96.0% to 96.8%. Seed germination in "Kelajak 100" was 97.9-98.1%, while in the standard "Uzbekistan 601 ECB" hybrid it was 97.5-97.8%.

The germination energy of seeds of the promising "Kelajak 100" variety and the standard "Uzbekistan 601 ECB" hybrid showed that the average germination energy of "Kelajak 100" was 97.1%, which was 0.6% higher than that of the standard hybrid. Seed germination was also 0.3% higher than in the standard "Uzbekistan 601 ECB" hybrid. The results show that, when developing new promising varieties and hybrids, an in-depth analysis of laboratory results helps preserve positive indicators and supports the long-term stability of varieties without loss of varietal traits.

In the newly developed promising "Esdalik 80" variety grown for green mass (silage), seed germination energy was 94.0-95.0%, while in the standard "Uzbekistan 100" variety it was 94.5-96.0%. Seed germination in "Esdalik 80" was 95.3-96.7%, whereas in "Uzbekistan 100" it ranged from 95.0% to 96.0%.

The data obtained for germination energy in the promising "Esdalik 80" and the standard "Uzbekistan 100" varieties show that the average germination energy of "Esdalik 80" was 94.7%, which was 0.4% higher than the standard. Its seed germination was also 0.5% higher than that of "Uzbekistan 100".

The yield indicators of the newly developed promising "Kelajak 100" and "Esdalik 80" varieties were also high, and these varieties produced high results in all experimental plots where they were sown and tested (Table 4).

Table 4. Yield indicators of the new promising maize varieties "Kelajak 100" and "Esdalik 80"

No.	Location	Variety	2019	2020	2021	Average yield (c/ha)
	Grain production (wax-ripeness stage)					

No.	Location	Variety	2019	2020	2021	Average yield (c/ha)
1	Maize Breeding and Seed Production Scientific Experimental Station, Tashkent region	Kelajak 100	97.0	109.5	107.4	104.6
2	“Oqsuv” farm, Qurgontepa district, Andijan region	Kelajak 100	78.1	98.9	104.4	93.8
3	“Energo Nasl Chorva” farm, Khavos district, Syrdarya region	Kelajak 100	78.1	93.6	100.4	90.7
	Average yield					96.3
	Green mass for silage (milk-ripeness stage)					
1	Maize Breeding and Seed Production Scientific Experimental Station, Tashkent region	Esdalik 80	802	816	824	814

No.	Location	Variety	2019	2020	2021	Average yield (c/ha)
2	“Oqsuv” farm, Qurgontepa district, Andijan region	Esdalik 80	733	746	798	759
3	“Energo Nasl Chorva” farm, Khavos district, Syrdarya region	Esdalik 80	730	751	795	758
	Average yield					777

Because the economic indicators presented above were effective for farmers, the “Esdalik 80” maize variety was planted during 2019-2021 for silage and green mass on 7.0 ha at the “Oqsuv” farm in Qurgontepa district, Andijan region, and on 18.0 ha at the “Energo Nasl Chorva” farm in Khavos district, Syrdarya region. The variety produced 81.0 t/ha of green mass, which was 5.1-5.6 t/ha higher than the standard “Uzbekistan 100” variety.

According to the research results, the proper selection of parental forms and the analysis of their valuable economic traits in the development of new promising varieties and hybrids help preserve positive results and ensure that varieties remain stable for many years without losing their varietal characteristics.

4. Conclusion

High efficiency was achieved as a result of scientific research on the development of new early-maturing and high-yielding maize varieties and hybrids and the improvement of their primary seed production. The main conclusions are as follows:

1. The germination energy and seed germination were 97.1% and 98.1% in “Kelajak 100”, 96.5% and 97.8% in the standard “Uzbekistan 601 ECB” hybrid, 94.7% and 95.9% in “Esdalik 80”, and 94.3% and 95.4% in the standard “Uzbekistan 100” variety. Compared with the standard, these indicators were 0.6% and 0.3% higher in “Kelajak 100” and 0.4% and 0.5% higher in “Esdalik 80”.

2. The “Kelajak 100” variety matured five days earlier than the standard variety; its grain yield was 2.3 c/ha higher, green-mass yield was 9 c/ha higher, and grain output was 2% higher, while its 1,000-grain weight was 22 g lower. The “Esdalik 80” variety matured six days earlier than the standard “Uzbekistan 100” variety; its grain and green-mass yields were 4.2 and 7.4 c/ha higher, and its grain output and 1,000-grain weight were 1% and 13 g higher, respectively.

3. Under production conditions, “Kelajak 100” produced 96.3 c/ha of grain, which was up to 2.3 c/ha more than the standard.

4. When the grain of the promising “Kelajak 100” variety was sold as commercial grain, net profit amounted to 25.3 million UZS/ha and profitability reached 154.6%. When the green

mass of the promising “Esdalik 80” variety was sold for silage, net profit per hectare was 16.9 million UZS/ha and profitability was 108.9%.

5. In addition, when “Kelajak 100” and the standard variety were grown for seed grain on 1 ha, net profit was 26.3 million UZS/ha in the standard variety and 36.3 million UZS/ha in “Kelajak 100”, with a profitability level of 217.4%.

6. When “Esdalik 80” was grown for seed production on 1 ha for silage purposes, net profit in “Esdalik 80” was reported as 36,488,000 UZS/ha and profitability was 209.6%.

7. The newly developed promising maize variety “Kelajak 100” is recommended for agricultural use for grain production, and “Esdalik 80” is recommended for green-mass production.

8. On the basis of results obtained in the primary seed-production system, it is proposed to improve the seed-production system and introduce a shortened four-year system in place of the existing five-year elite-seed production system.

REFERENCES

1. Massino, A. I., & Massino, I. A. (2015). Selection of hybrid maize for irrigated conditions of Uzbekistan [Selektsiya gibridnoy kukuruzy dlya oroshayemykh usloviy Uzbekistana]. Tashkent. 235 p. [in Russian].
2. Dwyer, L. M., & Stewart, D. W. (1984). Indicators of water stress in corn [Zea mays L.]. Canadian Journal of Plant Science, 64, 537-546.
3. State Statistics Committee of the Republic of Uzbekistan. (2019). Final data on maize harvest in the Republic in 2018. Tashkent, 21 February 2019. [in Uzbek/Russian].
4. Du Toit, L. J., & Pataky, J. K. (1999). Effects of silk maturity and pollination on infection of silks to maize ears by U. maydis. Plant Disease, 83(7), 621-626.
5. Chumak, M. V., & Suprunov, A. I. (2012). Combining ability of populations of different selection cycles for early flowering. Kukuruza i sorgo, 3, 9-12. [in Russian].
6. Vavilov, N. I. (1987). Theoretical foundations of breeding. Moscow: Nauka, 172-194. [in Russian].

ELEVATOR-SUCTION AS A NEW HYBRID INSTRUMENT IN THE CONTEMPORARY PRACTICE OF SURGICAL DENTISTRY

Sh.Yu. Abdullaev[1], A.V. Zhdanov[2], M.G. Khatypova[1], F.A. Dzhumaev[1], A.A. Hodjimetov[1]
Tashkent State Medical University[1]
Tashkent International University KIMYO[2]
https://doi.org/10.5281/zenodo.20624686

Abstract. *In implantology, the formation of a mucoperiosteal flap is an important step for obtaining the necessary access, viewing the surgical field and minimizing tissue damage. The result and injuries of periosteal detachment in the majority depend on the instruments used by the surgeon, as well as the presence of aspiration of the surgical field. This article is devoted to the analysis of modern types of spreaders (elevators) for working with the mucoperiosteal flap with an assessment of their design features, the presence of advantages and disadvantages in comparison with the model of a new hybrid tool we have proposed in the practice of surgical dentistry - spreader-suction.*

The systematization of data on the design of spreaders and features of aspiration systems helped us in the development of the design of our instrument - a spreader with integrated aspiration, aimed at increasing ergonomics, reducing operational injury and optimizing the conditions of surgical intervention.

Keywords: elevator-suction; hybrid surgical instrument; surgical dentistry; mucoperiosteal flap; aspiration system; periosteal elevator; dental implantology.

Introduction Manipulation of the mucoperiosteal flap is one of the most important stages of surgical interventions in dentistry and maxillofacial surgery. The degree of visualization of the surgical field, atraumatization and ergonomics is determined mainly by this stage of surgery. The main tool used to separate the mucoperiosteal flap from the bone surface is the periosteal elevators (spreaders). Clinicians have developed a large number of different types of elevator, with different designs of the working part, sizes, bending angle and shape of the handle. Most of them were developed by well-known surgeons and became widespread among medical practitioners. Despite the variety of designs and the use of existing tools, there is a problem of maximum performance without traumatic detachment and a full-fledged review of the surgical field [1]. The elevators presented in practice can be classified according to several basic features. (Fig. 1) According to the structure of the working part, spade-shaped, pointed, rounded and curved elevators are distinguished. In terms of the number of working ends, they can be one-way or two-way. According to their intended purpose, there are universal elevators, instruments for delicate detachment of the periosteum, elevators for working with dense tissues, as well as instruments used in extensive maxillofacial surgical interventions. The Molt Periosteal Elevator tool (Fig. 1.1) gained great popularity. This spreader is a two-sided tool, one of its working parts has a wide and flat shape, and the other is narrow and pointed. Due to this, this tool can be used both for the initial step of detachment of the mucoperiosteal flap after an incision of the mucous membrane, and for further opening of the surgical access. The advantages of this tool include its versatility, the

convenience of dosing pressure by a surgeon and great effectiveness in most maxillofacial surgical interventions. [2].

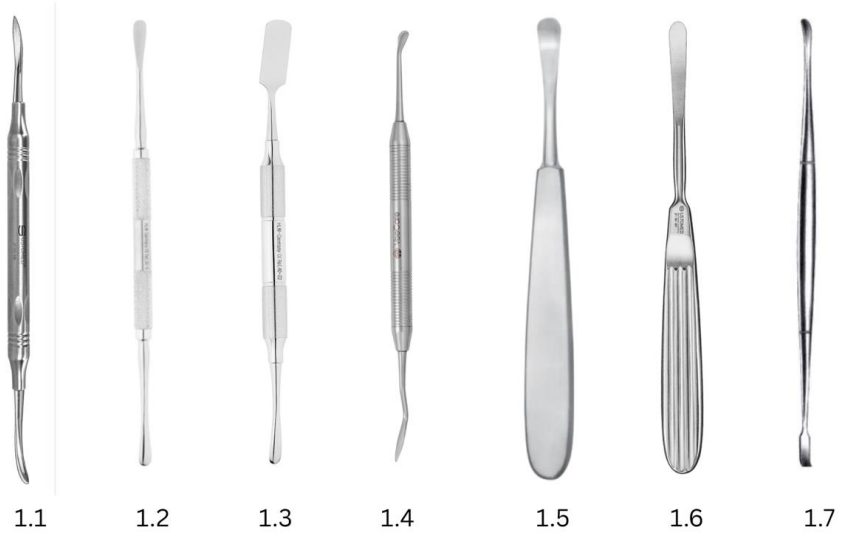


Fig. 1

The other most widely recognized tool is the Freer Periosteal Elevator (Fig. 1.2). This elevator has a thin working part and a moderate bending of its ends, which provides high accuracy and delicacy of manipulations. This elevator is widely used in operations that require gentle and gentle detachment of tissues, as well as when the operating space is limited. The main advantage of this tool is the maximum atraumatism of soft tissues. Also, its use may not be effective enough in working with a tightly attached periost [2,4]. Prichard Periosteal Elevator is also widely used in surgery (Fig. 1.3). This elevator has a wide shovel-like working part designed to separate more rigid tissues and form large mucoperiosteal flaps. Due to its design features, it works as a lever and is perfectly effective when working with a tight attachment of the periosteum to the underlying bone. However, this tool should be used very carefully when working with thin tissues in complex areas, so if not carefully used, this spreader can lead to increased damage to soft tissues [3]. For more delicate precise work, surgeons prefer to use the Woodson Periosteal Elevator (Fig. 1.4). It has a thin working part with small rounded ends. This tool is used mainly for periodontal procedures and operations in aesthetic areas where high accuracy of work and minimal risk of tissue damage are important. Its main advantage is the accuracy and precision of manipulations, but the tool cannot be used with a dense periosteum [4]. Seldin Periosteal Elevator is also one of the instruments used in dental surgery (Fig. 1.5). This tool has a thin working part with a slight bend and is used for neat detachment of the mucoperiosteal flap. Thanks to this design, the surgeon can easily control movements and perform delicate tissue manipulation during tooth removal or implantological interventions. The positive aspects of this tool include the ergonomics and accuracy of the detachment performed, however, as in the aforementioned type of spreader, its effectiveness in rigid tissues is slightly limited [2]. In maxillofacial surgery, Obwegeser Periosteal Elevator is also used (Fig. 1.6). This tool is widely used in extensive surgical operations due to its long and wide working part. Its main advantage is the ability to work deep in the operating wound. However, for normal manipulations in oral surgery, this tool is too rough. A separate group of this toolkit includes the elevators used in work in hard-to-reach areas of the wound surface - this is the Howarth Periosteal Elevator (Fig. 1.7). This elevator has a long narrow working part and a slight bend, all this allows it to be used with limited access. It is applied in most surgical disciplines. It

is also convenient to work with accurate tissue detachment. At the same time, its versatility in standard dental interventions is limited [4].In addition to high-quality ergonomic elevator, surgical manipulations require an aspiration system and an aspiration tip that meet the requirements of the surgeon [2].

Ensuring the removal of blood, saliva and irrigation solutions from the surgical field, aspiration systems play an important role in surgical dentistry, which allows maintaining good visibility of the surgical field, reduces the risk of infection and increases the efficiency of surgical interventions. Aspiration systems are classified according to several characteristics: aspiration power, tip design, manufacturing material and degree of sterility. Distinguish between high-volume and low-volume aspiration systems by aspiration power. High-volume aspirators are used mainly for surgical operations, such as tooth removal, osteotomy, implantation and other operations. They provide removal of a large amount of fluid, blood and irrigation solution during manipulations [2]. Low-volume aspirators (Saliva ejectors) are used mainly for therapeutic dental procedures and are designed to remove saliva and a small amount of fluid [2]. By design, aspiration tips are divided into several types, among which Frazier suction tip and Yankauer suction tip are widespread. Frazier suction tip (Fig. 2.1) is a thin metal aspiration tip of small diameter, designed for accurate aspiration in limited areas of the surgical field.



2.1 2.2

Fig. 2

The design of the tool is a long narrow tube with a small hole at the end and an additional ventilation hole on the handle. This opening serves the surgeon to regulate the force of aspiration by closing or opening it with a finger. Thanks to its design, the Frazier tip has found wide application in microsurgical interventions, including oral and maxillofacial surgery, neurosurgery and otorhinolaryngology. It provides accurate removal of blood and fluid without damaging surrounding tissues [5]. Yankauer suction tip (Fig. 2.2) has a wider aspiration tip with a curved shape and a rounded end. It usually has several lateral openings, which prevents damage to soft tissues during aspiration. This tip is used to remove a large volume of fluid, blood and irrigation solutions from the operating field. In dental and maxillofacial surgery, the Yankauer tip is used when rapid and effective aspiration is required, that is, for extensive surgical procedures, [2,5]. Tips in the aspiration system are divided into metal and plastic. Metal tips are usually made of stainless steel, they are characterized by high mechanical strength, durability and resistance to sterilization. They are used predominantly in surgical procedures. Plastic tips are more often used

in everyday dental practice. Aspiration tips can be either disposable or reusable, and are used primarily to remove saliva or a small amount of fluid.

Materials and methods Based on the above types of auxiliary instruments for performing surgery in the oral cavity, it should be noted that the simultaneous use of several types of instruments in the same operating field significantly reduces the visual view of the surgeon and constrains him in carrying out various manipulations. In view of this, we have a need to create a hybrid toolkit that allows us to level the above disadvantages. Such a hybrid tool is a tool that combines the functions of a tip for aspiration and a elevator of soft tissues - Elevator-suction (patent FAP 2021 0140 UZ.). This surgical accessory is a tool necessary for the simultaneous suction of various fluids in the oral cavity (blood, saliva, etc.), since it is a tubular structure, and the soft tissues of the oral cavity are moved away from the surgical field due to the curved tubular part of the "scapula" attached to the end of it, which allows the operating dentist to work in a "dry" surgical field and not injure the soft tissues with other mechanically rotating instruments (boron, cutter, etc.), which the doctor uses together with the suction spreader (Figure 3). The model itself is connected through a hose, which is put on the shank of the model to the suction device, which creates negative pressure.

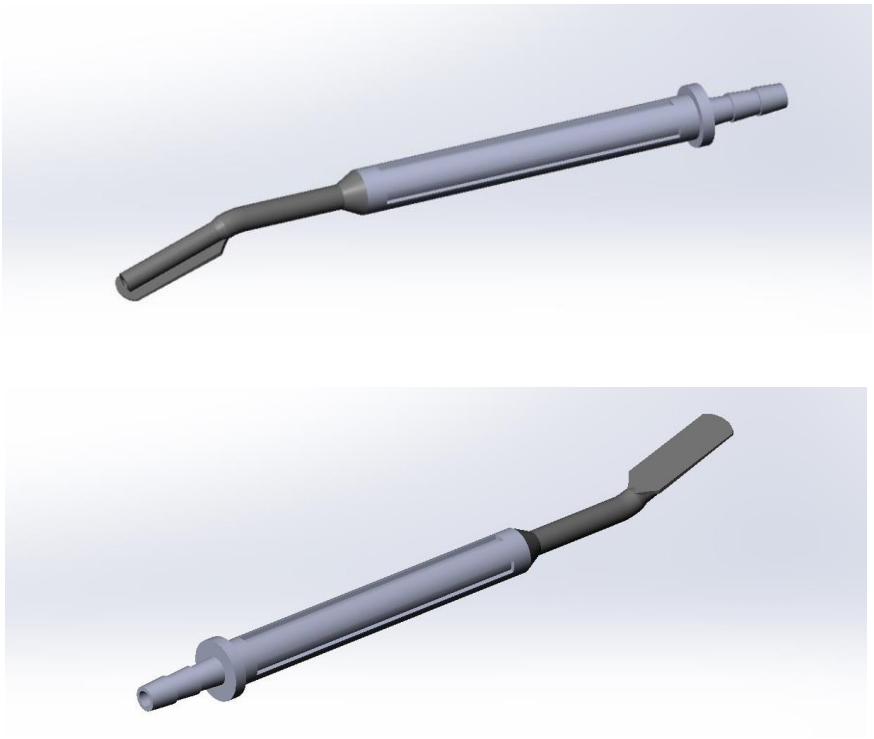


Fig.3

One of the functions of the elevator-suction tool is to retract, which means the first part of the name of the tool. The working part in the form of a spreader is used to separate the mucoperiosteal flap from the bone base and hold it (Fig.) The working part in the form of a small diameter tube connected to the working part-retractor performs an exclusively aspiration function, i.e., the ability to absorb, conduct through itself and remove various types of liquids from various cavities of the human body. The task of using this useful model is to retract, i.e., to hold a soft-tissue flap or soft-tissue structures in the operating field and simultaneously aspirate (aspirate) biological or other fluids entering the operating field, as well as to preserve soft-tissue structures

from damage by rotary instruments (turbine, mechanical tips) under liquid irrigation and create good visualization when conducting various manipulations that require "dry" "spaces. (Fig. 4)

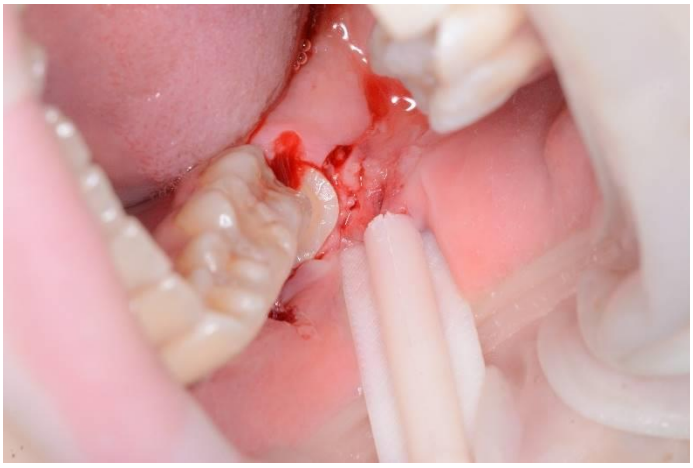


Fig.4

The introduction of this tool in dental practice made it possible to facilitate the manipulation of the dentist in the oral cavity, reduced the number of instruments in the oral cavity, created improved visualization of the procedure, and reduced the risk of soft tissue injuries with rotary instruments.

Results The introduction of this type of instrumentation into our dental practice has created a number of advantages in the work of a dental surgeon:

Firstly, the ergonomics of the instrument contributed to better control of surgical manipulation by the surgeon, eliminating the need for the presence of medical personnel responsible for aspiration in the surgical field

Second, the use of a tool combining the functions of two tools reduced the number of simultaneously applied tools in the operating field, which improved visualization.

Finally, the simplicity and cheapness of the design made it possible to produce a budget version of the plastic tool, which requires a standard 3D printer for manufacturing (printing).

Conclusions Thus, the introduction of this new type of instrument does not diminish the significance of the above types of elevators and aspiration tips, but adds more opportunities to facilitate and accelerate the work of a dental surgeon when manipulating soft and hard tissues in the oral cavity.

REFERENCES

1. LOZIER M. The role of periosteal elevators in the practice of oral surgery. Oral Surg Oral Med Oral Pathol. 1952 Apr;5(4):359-62. doi: 10.1016/0030-4220(52)90291-0. PMID: 14920027.
2. Contemporary Oral and Maxillofacial Surgery — Hupp J.R., Ellis E., Tucker M. Contemporary Oral and Maxillofacial Surgery. 7th ed. St. Louis: Elsevier; 2019.
3. Oral and Maxillofacial Surgery — Fonseca R.J. Oral and Maxillofacial Surgery. 3rd ed. Philadelphia: Elsevier; 2018.
4. Oral Surgery — Fragiskos F.D. Oral Surgery. Berlin: Springer; 2007.
5. Peterson’s Principles of Oral and Maxillofacial Surgery Miloro M., Ghali G. E., Larsen P. E., Waite P. D. Peterson’s Principles of Oral and Maxillofacial Surgery. — 3rd ed. — Shelton: PMPH-USA, 2012.

RATIONAL ANTIMICROBIAL USE IN OBSTETRIC CARE AS A STRATEGY FOR MATERNAL SEPSIS PREVENTION: RESULTS OF A POINT PREVALENCE SURVEY

T.F. Abduraimov
Republican Specialized Scientific and Practical Medical Center for Maternal and Child Health, Tashkent, Uzbekistan
https://doi.org/10.5281/zenodo.20696968

Abstract. *Antimicrobial resistance is one of the most pressing global health issues, requiring the rational use of antibacterial drugs and the improvement of antimicrobial control programs. The aim of this study was to evaluate the practice of prescribing antibiotics, quality indicators of antimicrobial therapy, and compliance with clinical recommendations in a specialized obstetric and gynecological hospital of the Republic of Uzbekistan. The study was conducted using the Point Prevalence Survey (PPS) method in accordance with the standardized methodology of the World Health Organization. Patients from six inpatient obstetric-genetic departments were included in the analysis. The frequency of antibiotic prescription, purpose of use, compliance with clinical recommendations, and indicators of rational use of antimicrobial drugs were evaluated. The obtained data made it possible to characterize the structure of antibiotic consumption in the obstetric-genetic hospital and to identify existing problems in antimicrobial practice. The research results emphasize the importance of regular monitoring of antibiotic prescriptions for the prevention of maternal sepsis, reducing the risk of developing antimicrobial resistance, and improving the quality of medical care.*

Keywords: *antimicrobial resistance, antibiotics, rational use of antibiotics, obstetrics, gynecology, maternal sepsis, Point Prevalence Survey, PPS, infection control, quality of medical care, Uzbekistan.*

Introduction

Antimicrobial resistance (AMR) is one of the most pressing global health threats; multidrug-resistant infections impact clinical outcomes and substantially elevated mortality risk compared to those with susceptible infections. Beyond these immediate clinical consequences, AMR carries significant economic burdens through increased healthcare expenditures, extended hospital stays, and lost productivity [1]. Multiple interconnected factors drive the emergence and spread of AMR, including overprescribing and inappropriate dispensing of antimicrobials by healthcare professionals, poor infection prevention and control practices, limited access to diagnostic testing, and a lack of effective surveillance systems [1,2]. In response to this crisis, several UN resolutions have tried to promote general awareness and implement measures to contain AMR; however these objectives can only be reached when accurate data on use and resistance are available [3].

To address critical data gaps on hospital antimicrobial use (AMU), particularly in low- and middle-income countries (LMICs), the WHO developed a standardised Point Prevalence Survey (PPS) methodology in 2018. The PPS approach provides a pragmatic alternative to continuous surveillance by capturing a snapshot of antibiotic use at a specific point in time. It requires substantially fewer resources than continuous surveillance systems [4]. This

methodology enables meaningful comparisons of antibiotic use across multiple parameters-including time, institutions, districts, countries, and regions-while facilitating standardisation in data collection, analysis, and interpretation. [4,5].

While antibiotic prescribing in general hospitals has been extensively characterised, AMU patterns in specialised obstetric-gynaecological (O&G) settings warrant specific attention. O&G wards show different prescribing profiles compared to other hospital departments, reflecting the predominance of surgical prophylaxis for caesarean delivery and gynaecological procedures over therapeutic prescriptions for infections. Additionally, patients admitted to these wards may present with common infections, such as community-acquired pneumonia or urinary tract infections. Finally, for accurate antibiotic selection, local resistance patterns must be considered, and pregnancy must be taken into account for dosage adjustment, potential teratogenicity of the substance, or interference with lactation.

In Nigeria, a 2020 PPS across multiple centres documented an overall antibiotic prevalence of 80.1%, but with substantially lower prevalence in obstetrics and gynaecology wards (72.9%) [9]. In Sierra Leone's national 2023 PPS, O&G wards showed the lowest antibiotic prevalence among all ward types at 65.7%, consistent with a pattern where O&G prescribing differs fundamentally from general hospital departments; the most common indications in O&G settings were surgical prophylaxis for obstetric and gynaecological procedures, representing 23.8% of all antibiotic prescriptions in one analysis [11].

A Latin American multicentre study documented that O&G patients exhibited distinct prescribing patterns, with surgical prophylaxis requiring particular scrutiny regarding the appropriateness of duration and spectrum [12]. In Mexico, a recent multicentre survey documented O&G departments as one of five key clinical areas studied, with obstetrics and gynaecology prophylaxis representing a significant portion of total antibiotic use [15]. In South Africa's 2021 multicentre survey, obstetrics and gynaecology prophylaxis comprised 14.0% of antibiotic indications [13], while in Pakistan, obstetric or gynaecological prophylaxis represented 16.5% of antibiotic indications [18].

While recent PPS studies have increasingly provided granular data on antibiotic use in general hospitals and specific wards, a significant evidence gap remains regarding specialised O&G hospitals. Published PPS data from specialised O&G hospital settings-particularly those in resource-limited contexts where both diagnostic capacity and guideline implementation may be constrained-are virtually absent from the literature. This gap is notable because O&G hospitals serve fundamentally different patient populations and have prescribing patterns that differ from those of general hospitals, and therefore, their antimicrobial stewardship needs differ from those of other hospitals.

The objective of this study is to address this knowledge gap by conducting a comprehensive assessment of antibiotic prescribing practices, quality indicators, and guideline adherence in a specialised obstetric-gynaecological hospital in Tashkent, Uzbekistan, using a WHO-standardised PPS methodology adapted to the local context.

Methods

Study design. This was a single-centre, cross-sectional point prevalence survey (PPS) of antimicrobial use conducted at the Republican Specialised Scientific and Practical Medical Centre of Maternal and Child Health State Institution in Tashkent, Uzbekistan. The study followed the standardised World Health Organization (WHO) methodology for PPS on antibiotic use in hospitals, version 1.1 (2018). This methodology was selected for its suitability in resource-limited

settings and its established use in comparable healthcare facilities across low- and middle-income countries.

Study setting and facility characteristics. The study was conducted at a specialised obstetric-gynaecological hospital in Uzbekistan. The institution operates a total of 160 inpatient beds distributed across six acute care departments with specialised intensive care capabilities. According to the WHO methodology, facilities with fewer than 500 inpatient beds require complete enumeration without patient sampling, and this hospital met this criterion.

Ward selection and study population. Six acute care inpatient wards met the inclusion criteria and were included in the survey. These comprised: (1) Obstetric Departments (50 beds, classified as adult medical wards or mixed adult/paediatric wards); (2) Gynaecology Departments (50 beds, classified as adult surgical wards for procedural patients and adult medical wards for medical management); (3) Pathology of Pregnant Women Departments (40 beds, classified as adult high-risk wards with expected elevated antibiotic utilization due to high-risk pregnancies); (4) Neonatal Pathology Department (20 beds, classified as neonatal medical ward); (5) Obstetric Intensive Care Unit (12 beds, classified as adult intensive care unit); and (6) Neonatal Intensive Care Unit (6 beds, classified as neonatal intensive care unit). The scientific and advisory polyclinic services were excluded as outpatient facilities per the WHO inclusion criteria.

The study population inclusion criteria specified that all patients hospitalised as inpatients at or before 08:00 hours on the survey day were included across all participating wards. Neonates born before 08:00 hours were counted as separate patients from their mothers, creating distinct patient records for maternal-neonatal dyads as per the WHO methodology for pregnant patients and their newborns.

Variables and data collection. Data collection followed the WHO PPS standardised forms, capturing information on patient demographics, hospitalisation status, and antibiotic prescriptions. For each patient, the following data were systematically extracted: (1) patient age and gender; (2) ward classification; (3) antibiotic agent name and dosage; (4) route of administration; (5) frequency of dosing; (6) indication for therapy (community-acquired infection, hospital-associated infection, medical prophylaxis, or surgical prophylaxis); and (7) evidence of microbiological confirmation. Special attention was given to surgical prophylaxis documentation, including classification as single preoperative dose (SP1), multiple doses within 24 hours (SP2), or extended administration beyond 24 hours (SP3).

Exclusion criteria followed WHO guidance and included topical applications, drops, and vaginal suppositories, which are not considered systemic antimicrobial therapy appropriate for prevalence assessment.

Data collection procedures. A research team was assembled, comprising a hospital coordinator with senior clinical experience and infectious disease expertise, or specialised knowledge in obstetric-gynaecological antimicrobial therapy; an infectious disease physician or consultant; a hospital pharmacist with knowledge of the obstetric-gynaecological formulary; and experienced ward nursing staff with access to patient medical records. The hospital coordinator assumed responsibility for institutional ethical clearance, team coordination, and dissemination of results.

Before the survey, a pilot study involving 10 patients across representative wards was conducted to establish inter-rater reliability and standardise data extraction procedures. This pilot emphasised the critical distinction between maternal and neonatal antibiotic administration and proper classification of surgical versus medical prophylaxis.

The survey was conducted over a maximum of three consecutive weeks, with each ward completed within a single day to minimise artefacts from patient movement. According to the recommendations, the survey timing avoided weekends and holiday periods to maintain a representative distribution of elective surgical procedures and prophylaxis patterns typical of normal operations. A sequential ward-by-ward approach was implemented, with investigator team capacity matched to ward size; larger departments were assigned multiple investigators to ensure single-day completion of each ward.

Data collection involved no direct interaction between the investigator team and patients, and the process did not interrupt patient care. Patient medical records and associated documentation were reviewed to extract relevant information. No patient identifiers were collected; instead, unique codes were assigned to each patient record to maintain anonymity throughout data collection and analysis.

Quality assurance and data validation. Comprehensive quality assurance measures were implemented to ensure the accuracy and reliability of data. These measures included systematic documentation of antibiotic indication compliance with local guidelines, assessment of the appropriateness of surgical prophylaxis duration, and evaluation of ratios of empirical prescriptions to culture-directed therapy.

A quality indicators assessment evaluated prescribing appropriateness, including adherence to local and WHO treatment guidelines, timing of surgical prophylaxis relative to the procedure, duration of prophylaxis relative to guideline recommendations, and the proportion of prescriptions with microbiological confirmation of the indication.

Definitions of key metrics. Antimicrobial use (AMU) prevalence refers to the percentage of hospitalised in-patients who received one or more antimicrobial agents (for prophylactic or therapeutic purposes) at the time of the survey. This metric quantifies the burden of antimicrobial exposure within a hospital population and enables comparison across different healthcare facilities and patient populations. For example, a 40.8% prevalence indicates that approximately 4 of every 10 hospitalised patients are exposed to antimicrobials on any given day.

Antimicrobial consumption density (also termed “antimicrobial courses per treated patient”) represents the average number of distinct antimicrobial courses prescribed to each patient receiving antimicrobial therapy at the time of survey. It is calculated as: (total number of antimicrobial courses) / (number of patients on antimicrobials). This metric captures the complexity and intensity of antimicrobial prescribing, independent of prevalence. A consumption density of 1.4 courses per treated patient indicates that patients on antimicrobials are receiving an average of 1.4 distinct treatment courses, reflecting combination therapy in some patients or sequential monotherapy in others. For example, a patient receiving both intravenous ceftriaxone AND oral metronidazole simultaneously would represent two courses; a patient receiving only ceftriaxone would represent one course.

Ethical considerations. Institutional ethical review was obtained for the study with particular attention to patient privacy in specialised care settings. The study implemented a "no-blame" approach to evaluate prescribing practices, ensuring that the assessment of antimicrobial use was conducted for quality improvement purposes without stigmatising individual prescribers or clinical teams.

Patient anonymisation protocols were implemented and required careful attention due to the potentially identifiable nature of rare conditions or procedures in a specialised obstetric-gynaecological setting.

The study was registered and conducted in accordance with institutional policies and national antimicrobial stewardship guidelines.

Results

Patient demographics. The point-prevalence survey was conducted in November 2025 at a 160-bed specialised obstetric-gynaecological hospital. The survey captured 142 hospitalised inpatients distributed across six acute care ward types: intensive care units (n=10), surgical wards (n=86), paediatric/neonatal wards (n=15), and therapeutic/high-risk pregnancy wards (n=31).

The study population included 124 adults (87.3%) and 18 children (12.7%). Among the 142 inpatients, 58 (40.8%; 95% CI 32.6–49.2%) were receiving antimicrobial therapy or prophylaxis at the time of the survey. The prevalence of antimicrobial use differed between age groups, with 55.5% (10/18) of children and 38.7% (48/124) of adults receiving antimicrobial agents, though this difference was not statistically significant ($\chi^2 = 1.24$, $p > 0.05$).

Table 1. Patient demographics and antimicrobial use by age group (n=142). AM, antimicrobial

Age group	Without AM (n)	On AM (n)	Prevalence (%)	Total (n)
Children	8	10	55.5	18
Adults	76	48	38.7	124
TOTAL	84	58	40.8	142

Overall antimicrobial use density.

The 58 patients on antimicrobial therapy were prescribed a total of 82 distinct treatment courses utilising 16 different antimicrobial agents. The overall AMU density was 1.4 courses per treated patient. Analysis by age group revealed that AMU density was higher in children (1.8 courses per treated child) than in adults (1.3 courses per treated adult), reflecting the complexity of paediatric and neonatal infections, which often require combination therapy.

AMU prevalence and density varied across different ward categories. Intensive care units demonstrated the highest prevalence (100%) with 1.8 courses per treated patient; paediatric and therapeutic wards demonstrated an intermediate prevalence (45–47%) and higher consumption density (1.2–2.4 courses per treated patient; surgical wards, despite managing high-acuity obstetric and gynaecological procedures, demonstrated the lowest AMU prevalence (31.3%) but with moderate consumption density (1.3 courses per treated patient), reflecting the predominance of surgical prophylaxis over therapeutic use in these settings.

Table 2. Antimicrobial Prevalence and Consumption Density by ward category. "Cons. Density", consumption density (courses per treated patient); "Prophyl", prophylactic antimicrobial use percentage (see Methods)

Ward Type	Patients (n)	On AM (n)	AMU Prevalence (%)	Cons. Density	Prophyl. (%)
Intensive Care Units	10	10	100	1.8	50
Paediatric Wards	15	7	46.7	2.4	43
Therapeutic Wards	31	14	45.1	1.2	7

Surgical Wards	86	27	31.3	1.3	70
TOTAL	142	58	40.8	1.4	48

Prophylactic and therapeutic use. The overall distribution of antimicrobial prescribing in this 160-bed specialised O&G hospital showed nearly equal division between prophylactic and therapeutic uses. Of the 58 patients on antimicrobials, 28 (48.3%) received prophylactic agents, while 30 (51.7%) received therapeutic antimicrobials. However, this overall facility-level balance masked substantially different prescribing patterns across individual ward types (see Table 2).

Intensive care units demonstrated balanced prophylaxis-to-therapy ratios (50%). Still, surgical wards were heavily prophylaxis-focused with 70% of antimicrobial courses administered for surgical prophylaxis, as expected given the predominance of caesarean deliveries and gynaecological surgical procedures. In contrast, therapeutic wards managing high-risk pregnancies were predominantly therapy-focused, with only 7% of antimicrobial courses used for prophylaxis and 93% directed toward treatment of documented or suspected infections. Paediatric wards showed an intermediate pattern with 43% of courses representing prophylactic purposes.

Antimicrobial distribution according to the WHO AWaRe classification. The 82 antimicrobial courses distributed across 16 distinct agents demonstrated substantial variation in prescribing patterns. The five most frequently prescribed antimicrobials accounted for almost three-quarters of all prescriptions (70.7%). Ceftriaxone was the most common agent (20/82; 24.4%), followed by cefazolin (11/82; 13.4%), cefoperazone + sulbactam (9/82; 11.0%), nitroxoline (8/82; 9.8%), and ampicillin (6/82; 7.3%).

The predominance of broad-spectrum agents was evident, with 40.2% of prescriptions including a *Watch* category antibiotic and 35.4% *Access* category antibiotics. It should be highlighted that 20.7% of the antibiotics belonged to the Unclassified category. This distribution indicates that 60.9% of antimicrobial prescriptions (50/82 courses) included broad-spectrum or unclassified agents, suggesting prescribing patterns characterised by empiric, rather than targeted, indication-specific selection.

Table 3. Antimicrobial agent distribution according to the WHO AWaRe Classification, number of courses and age.

Antimicrobial Agent	**Courses n (%)**	**Adults n (%)**	**Children n (%)**	**TOTAL**
Ceftriaxone	20	20	0	20
Cefazolin	11	11	0	11
Cefoperazone+Sulbactam*	9	4	5	9
Nitroxoline	8	8	0	8
Ampicillin	6	0	6	6
Gentamycin				5
Erythromycin				4
Ampicillin+Sulbactam				4
Metronidazole				4
Fosfomycin				3
Vancomycin				3
Cefotaxim				1
Azithromycin				1

Cefepime				1
Clarithromycin				1
TOTAL	**82**			**82**

*Cefoperazone + sulbactam is currently classified as "not recommended" by the WHO.

Adults predominantly received ceftriaxone (24.4%), cefazolin (13.4%), and nitroxoline (9.8%). In contrast, children more frequently received combination agents including cefoperazone + sulbactam (27.8%), ampicillin (27.8%), and gentamicin (27.8%).

Indication-specific prescribing patterns and appropriateness. Cross-tabulation of antimicrobial agents and clinical indications shows clear prescribing patterns. Ceftriaxone was mostly used for surgical prophylaxis (16/20 indications), respiratory tract infections (2/20), and surgical site infections (2/20). The Access cefazoline was used only for surgical prophylaxis (11 indications). The combination of cefoperazone + sulbactam was most commonly used for UTIs (8/9 indications), and nitroxoline was used for urinary tract infections (7/7 indications) (see Table 4).

Table 4. Antimicrobial agents prescribed for different clinical indications (n=82 courses). RTI, respiratory tract infection; UTI, urinary tract infection; SI, surgical infection; Surg Pr, surgical prophylaxis; Med Pr, medical prophylaxis; Cef+Sulb, cefoperazone + sulbactam.

Antimicrobial Agent	**UTI**	**Surg Pr**	**Med Pr**	**RTI**	**SI**	**TOTAL**
Ceftriaxone	1	12	—	6	1	20
Cefazolin	1	10	—	—	—	11
Cefoperazone+Sulbactam	1	—	3	5	—	9
Nitroxolin	8	—	—	—	—	7
Ampicillin	—	—	4	2	—	6
Gentamycin	—	—	—	4	1	5
Erythromycin	—	—	—	-	—	4
Ampicillin+Sulbactam	—	—	—	4	—	4
Metronidazole	—	2	—	2	—	4
Fosfomycin	2	—	—	1	—	**20**
Vancomycin	—	—	—	2	1	**11**
Cefuroxime	—	1	—	-	—	**9**
Cefotaxim	—		—	1	—	**8**
Azithromycin	—	1	—	—	—	**6**
Cefepime	—	—	—	—	—	**5**
Clarithromycin	—	—	—	1	—	**4**
TOTAL	**13**	**26**	**11**	**29**	**3**	**4**

Table 4 X presents the distribution of antimicrobial agents according to the indication for use. A total of 82 antimicrobial prescriptions were recorded during the study period, with respiratory tract infections (RTIs) accounting for the largest proportion of prescriptions (n=29), followed by surgical prophylaxis (n=26), urinary tract infections (UTIs) (n=13), medical prophylaxis (n=11), and skin infections (SIs) (n=3).

For the management of UTIs, four antimicrobial agents were prescribed. Nitroxoline was the most frequently used drug (n=8), followed by fosfomycin (n=2), while ceftriaxone, cefazolin, and cefoperazone/sulbactam were each prescribed once. Surgical prophylaxis was primarily based on ceftriaxone (n=12) and cefazolin (n=10), which together accounted for 84.6% of all

prescriptions for this indication. Metronidazole (n=2), cefuroxime (n=1), and azithromycin (n=1) were used less frequently.

Medical prophylaxis included 11 prescriptions and was mainly represented by ampicillin (n=4) and cefoperazone/sulbactam (n=3), while the remaining prescriptions were distributed among other agents. RTIs represented the most common indication for antimicrobial therapy, with ceftriaxone (n=6) and cefoperazone/sulbactam (n=5) being the most frequently prescribed antibiotics. Gentamicin and ampicillin/sulbactam were each used in four prescriptions, whereas vancomycin, metronidazole, fosfomycin, cefotaxime, and clarithromycin were prescribed less often.

Only three prescriptions were related to skin infections, for which ceftriaxone, gentamicin, and vancomycin were prescribed. Overall, ceftriaxone was the most commonly used antimicrobial agent (n=20), followed by cefazolin (n=11), cefoperazone/sulbactam (n=9), nitroxoline (n=7), and ampicillin (n=6). The predominance of third-generation cephalosporins reflects their extensive use both for prophylactic purposes and for the treatment of respiratory and urinary tract infections.

Surgical prophylaxis duration. As shown in Table 5, among the 28 patients receiving antimicrobial prophylaxis, 24 (85.7%) received it for surgical procedures, predominantly caesarean deliveries and gynaecological surgery.

Table 5. Surgical prophylaxis duration. Compliance (n=24 surgical prophylaxis cases). SP1, single preoperative dose (guideline-compliant); SP2, double dose within 24 hours (non-compliant); SP3, extended beyond 24 hours (non-compliant).

Duration Category	Clinical Definition	Number (n)	%
SP1 (Guideline-Compliant)	Single preoperative dose, no continuation	6	25.0
SP2 (Non-Compliant)	Two doses administered within 24 hours	4	16.7
SP3 (Non-Compliant)	Multiple doses extending beyond 24 hours	11	45.8
Unknown/Unclear Documentation	Unable to classify duration	3	12.5
NON-COMPLIANT (SP2+SP3)		15	62.5

Only six patients (25.0%) received guideline-compliant single-dose surgical prophylaxis (SP1), the evidence-supported standard. Four patients (16.7%) received double-dose prophylaxis within 24 hours (SP2), and 11 patients (45.8%) received multiple doses extending beyond 24 hours (SP3). This SP3 pattern of extended prophylaxis was documented in 62.5% of surgical prophylaxis cases (15/24).

Therapeutic indications and microbiological confirmation. Therapeutic antimicrobial use (30 courses) was concentrated in three primary infection sites: respiratory tract infections (60%, 18/30 courses), urinary tract infections (36.7%, 11/30 courses), and surgical infections (3.3%, 1/30 courses). Respiratory tract infections were the predominant therapeutic indication, accounting for 18 courses: 13 in adults and 5 in children, reflecting the high prevalence of pneumonia and respiratory tract infections in hospitalised populations. Urinary tract infections accounted for 11 courses, exclusively in adult patients. A single surgical infection was identified and managed.

Infection site-specific microbiological confirmation rates revealed important diagnostic patterns and significant opportunities for improvement. Respiratory tract infections demonstrated the highest confirmation rate at 44.4% (8/18 cases with documented microbiological evidence, such as sputum culture or lower respiratory tract sampling). Urinary tract infections demonstrated a substantially lower rate of confirmation at 27.3% (3/11 cases), despite the relative accessibility and ease of urine culture diagnostics. The single case of surgical infection lacked microbiological confirmation. Overall, only 36.7% (11/30) of the 30 therapeutic courses demonstrated documented microbiological confirmation through positive culture or serology, indicating that 63.3% of therapy was empirically prescribed without documented laboratory evidence of causative organisms.

Table 6. Microbiological confirmation rates for therapeutic antimicrobial courses by infection site. Microbiological confirmation includes a documented positive culture or serology that supports the antimicrobial selection. Overall confirmation rate: 36.7% (11/30 therapeutic cases); empiric therapy without confirmation: 63.3%.

Infection Site	**Total Cases (n)**	**Microbiologically Confirmed (n)**	**Confirmation Rate (%)**	**Adults/Children**
Respiratory Tract Infections	18	8	44.4	13/5
Urinary Tract Infections	11	3	27.3	11/0
Surgical Infections	1	0	0	1/0
Total therapeutic use	30	11	36.7	25/5

Guideline concordance. Overall guideline concordance-defined as antimicrobial selection appropriate for documented indication, patient age, and renal function-was 72.4% (42/58 patients), indicating reasonable but improvable adherence to evidence-based practices. Concordance was significantly higher in adult patients (77.1%, 37/48) compared to paediatric patients (50%, 5/10), suggesting that paediatric prescribing represents a particular stewardship vulnerability requiring enhanced guideline-based education and clinical decision support.

Ward-level analysis revealed substantial variation in concordance, with critical performance gaps identified in specific units, and these results will be used for stewardship purposes.

Documentation quality and guideline adherence. Medical record documentation of key antimicrobial prescribing parameters was generally strong throughout the facility. Indications for antimicrobial use were documented in 89.6% of prescriptions (52/58 cases), and discontinuation or review dates were documented in 89.6% of cases (52/58). Appropriate dosing for the indicated infection and antimicrobial agent was confirmed in 100% of cases (58/58), and appropriate route of administration (intravenous versus oral) was confirmed in 100% (58/58 cases). These high documentation rates regarding indication, dosing, and route suggest strong basic prescribing documentation practices within the facility, providing a solid foundation for stewardship improvement initiatives.

In contrast, microbiological confirmation rates—defined as documented evidence of positive culture, serology, or antigen detection supporting the antimicrobial selection—were substantially limited. Of 30 therapeutic courses, only 11 (36.7%) had microbiological confirmation, indicating that approximately two-thirds of therapeutic prescriptions were empirically selected without documented laboratory evidence.

Discussion

To our knowledge, this represents one of the first point prevalence surveys conducted in a specialised obstetric-gynaecological hospital with neonatal services in a resource-limited setting. This survey documented an overall antimicrobial prevalence of 40.8% (95% CI 32.6-49.2%) at this 160-bed specialised facility in Uzbekistan. The antimicrobial use density was 1.4 courses per treated patient, higher in children (1.8) than adults (1.3). A substantial ward-level variation was observed: as expected, intensive care units had a 100% prevalence, while, surprisingly, surgical wards had a 31.3% prevalence. The concordance with the existing guidelines was reasonable at 72.4% overall (77.1% adults vs. 50% children), with a range of 33.3-100% across wards, which means that there is space for improvement through antimicrobial stewardship actions.

The 40.8% prevalence is lower than published AMU data, according to PPS research in general hospitals; for example, Sierra Leone's 2023 national PPS reported 65.7% in obstetrics and gynaecology wards, and Nigeria's 2020 multicentre study documented 72.9% [6,7]. It should be highlighted that the low surgical ward use prevalence (31.3%) observed in this PPS in Uzbekistan likely reflects the inclusion of immediate post-operative patients requiring no therapeutic intervention beyond prophylaxis.

Surgical prophylaxis comprised 48% of all courses, consistent with the surgical nature of obstetric-gynaecological practice. Latin American multicentre studies similarly documented O&G prophylaxis as a significant portion of total antimicrobial use [8].

Surgical prophylaxis. A critical finding is the suboptimal adherence to surgical prophylaxis guidelines. Of 24 surgical prophylaxis cases, only 25.0% received guideline-compliant single-dose prophylaxis (SP1). In contrast, 62.5% received extended prophylaxis beyond 24 hours (SP3), and 16.7% received double-dose prophylaxis (SP2). Current evidence-based guidance consistently recommends single-dose perioperative prophylaxis for major obstetric and gynaecological procedures;[12] extended prophylaxis increases antimicrobial exposure without demonstrable clinical benefit. This 62.5% non-compliance rate found in this PPS substantially exceeds compliance gaps documented in some high-income countries, representing a highly actionable stewardship opportunity.

Diagnostic confirmation and empirical therapy. Only 36.7% (11/30) of therapeutic antimicrobial courses had microbiological confirmation, indicating that 63.3% were empiric therapy without laboratory evidence. Urinary tract infections were particularly poorly confirmed (27.3%) despite the availability of urine culture. Respiratory tract infections were confirmed in 44.4% of cases. Microbiology samples should be collected before starting empiric antibiotic therapy [13]; this is important because it is the best way to switch treatment if necessary once the results arrive, if the infection has not been solved yet, and, additionally, it is the best way to obtain systematic microbiology data to have data on the local aetiology and resistance patterns. Our findings highlight a gap in diagnostic-driven prescribing that compromises de-escalation strategies, a cornerstone of antimicrobial stewardship. Low confirmation rates suggest either inadequate diagnostic utilisation or system delays in communicating results, preventing clinicians from acting on available data. The lack of local resistance data is a driver of inappropriate

prescribing, pushing clinicians toward broad-spectrum or last-resort antibiotics due to uncertainty about the local resistance patterns. [14, 15]

Broad-spectrum agents comprised 60.9% of prescriptions, with *Watch* category at 40.2% (primarily ceftriaxone 24.4%, cefoperazone + sulbactam 11.0%) and *Access* category at 35.4%. This distribution indicates empirical rather than targeted selection. Ceftriaxone use for conditions such as uncomplicated urinary tract infection suggests possible overuse, as WHO AWaRe Access agents are preferred for such indications.[16] Notably, cefoperazone + sulbactam, traditionally classified by WHO as "not recommended, comprised 11% of courses. Although there can be local adaptations to practices recommended by the WHO, it is important that these adaptations are based on high-level evidence or local resistance data. However, the WHO Expert Group is reconsidering the classification of this fixed-dose combination under the Watch category, given its extended use, particularly in Asian countries [17].

Documentation quality. The facility demonstrates strong documentation of basic parameters. For example, the indication of use, one of the added values of PPS compared with other drug utilisation methods, was complete in 90% of cases, a proportion higher than in other surveys, such as a three-year PPS in Chinese hospitals, where the indication of use was available in only 55% of cases. [18] Other variables, such as discontinuation/review dates, dosing appropriateness, and route selection, were collected in 90-100% of patients. However, there is a relevant gap between documented indications (90%) and microbiological confirmation (36.7%), suggesting that prescribers document the clinical suspicion but do not obtain samples for microbiological testing, or don’t record or analyse these data. Diagnostic stewardship is a relatively new concept that involves interventions to improve the appropriate use of microbiological testing and diagnostics to guide clinical decisions. Underutilisation of diagnostic tests can negatively affect patient outcomes. [19] This is an opportunity to strengthen the review processes, assessing whether culture results are obtained and acted upon.

Study limitations. PPS has several advantages over other quantitative drug utilisation studies, but they also have well-known limitations. This single-centre, single-day snapshot per the WHO methodology cannot assess temporal variation, seasonal differences, or practice changes over time, unless the PPS is repeated periodically. The 142-patient sample, while representing complete enumeration, yields wide confidence intervals (32.6-49.2%) and limits power in small subgroups, particularly the 18 paediatric patients. Cluster effects within wards are not accounted for.

As previously highlighted, one of the PPS’s added values is information about the indication of use; however, the indication relies on the investigator's assessment of the documented clinical rationale. The WHO-AWaRe “unclassified” antimicrobial category accounted for 20.7% of the antimicrobials used in this study; the predominant substances in this classification were nitroxoline and the fixed-dose combination of cefoperazone and sulbactam. However, it should be noted that the AWaRe classification is dynamic and depends on the available evidence; WHO has already received a petition to reconsider some substances in this category. [17] Microbiological confirmation depends on documentation in the medical record; unreported results would underestimate the use of diagnostic-driven therapy.

Finally, the assessment required the investigator's judgment regarding "appropriateness. Reliance on documented clinical data meant that missing information (renal function, allergy history) could limit the assessment's completeness.

The way forward. The results of this PPS should serve as the basis for designing specific stewardship activities in the study hospital. Additionally, the method, piloted in this centre, could be replicated in other branches of the hospital or in other types of hospitals. Even this study could be considered a successful pilot for adaptation by other countries in the Region.

According to the main results, the hospital's stewardship implementation should prioritise optimising surgical prophylaxis protocols (to address 62.5% non-compliance), enhancing diagnostic-driven therapy through microbiological confirmation, and improving paediatric prescribing practices, supported by a formal stewardship committee with quarterly audit-and-feedback mechanisms. Secondary priorities include restricting the use of inappropriate broad-spectrum agents (particularly cefoperazone + sulbactam) and establishing system-level performance indicators to track compliance, de-escalation rates, and clinical outcomes longitudinally.

Conclusion

This survey identified substantial opportunities for antimicrobial stewardship improvement in surgical prophylaxis duration (62.5% non-compliance), diagnostic confirmation of therapeutic indications (63.3% empirical), and paediatric prescribing (50% concordance). The facility has demonstrated reasonable guideline concordance (72.4%) and appropriate agent selection, suggesting prescriber awareness of evidence-based practices provides a foundation for targeted interventions.

The five priority recommendations—surgical prophylaxis optimisation, diagnostic-driven therapy, paediatric guidelines, broad-spectrum agent stewardship, and system-level implementation—are aligned with WHO stewardship principles and are feasible for specialised facilities in resource-limited settings.] As one of the first detailed point prevalence surveys from a specialised obstetric-gynaecological hospital with neonatal services in a resource-limited setting, this study addresses a critical evidence gap and provides findings that can inform antimicrobial stewardship practice in similar specialised facilities throughout Central Asia and comparable healthcare systems.

REFERENCES

1. Antimicrobial Resistance Collaborators. Global burden of bacterial antimicrobial resistance in 2019: a systematic analysis. *Lancet*. 2022 Feb 12;399 (10325):629-655. doi: 10.1016/S0140-6736(21)02724-0. Epub 2022 Jan 19.
2. World Health Organization. Global action plan on antimicrobial resistance. Geneva: WHO; 2015. Available at: https://www.who.int/publications/i/item/9789241509763
3. Figueras A. A. Global Call to Action on Antimicrobial Resistance at the UN General Assembly. *Antibiotics (Basel)*. 2024 Sep 24;13(10):915. doi: 10.3390/antibiotics13100915.
4. World Health Organization. WHO Methodology for Point Prevalence Survey on Antibiotic Use in Hospitals. Geneva: WHO; 2018. Available at: https://www.who.int/publications-detail-redirect/WHO-EMP-IAU-2018.01
5. Elias C., Ha N.T., Sengvilaipaserth O., et al. Antibiotic prescribing practices and antibiotic use quality indicators in Luang Prabang, Lao PDR: a point prevalence survey in a tertiary care hospital. *BMC Infect Dis*. 2024 Aug 13;24(1):818. doi: 10.1186/s12879-024-09614-4.
6. Abubakar U. Antibiotic use among hospitalized patients in northern Nigeria: a multicenter point-prevalence survey. *BMC Infect Dis*. 2020 Jan 30;20(1):86. doi: 10.1186/s12879-020-4815-4.

7. Kamara I.F., Kanu J., Maruta A., Fofanah BD. Antibiotic use among hospitalised patients in Sierra Leone: a national point prevalence survey using the WHO survey methodology. *BMJ Open*. 2023 Dec 30;13(12):e078367. doi: 10.1136/bmjopen-2023-078367.
8. Levy Hara G, Rojas-Cortés R., at al. Latin American Point Prevalent Survey Study Group. Point prevalence survey of antibiotic use in hospitals in Latin American countries. *J Antimicrob Chemother*. 2022 Feb 23;77(3):807-815. doi: 10.1093/jac/dkab459.
9. Venegas-Esquivel G..A., Berumen-Lechuga M.G., Molina-Pérez C.J., et al. A Point Prevalence Survey of Antimicrobial Use in Second-Level Mexican Hospitals: A Multicenter Study. *Antibiotics (Basel)*. 2024 Nov 9;13(11):1065. doi: 10.3390/antibiotics13111065.
10. Mthombeni T.C., Burger J.R., Lubbe M.S., Julyan M. Antibiotic prescribing to inpatients in Limpopo, South Africa: a multicentre point-prevalence survey. *Antimicrob Resist Infect Control*. 2023 Sep 16;12(1):103. doi: 10.1186/s13756-023-01306-z.
11. Saleem Z., Hassali M.A., Versporten A., Godman B., Hashmi F.K., Goossens H., Saleem F. A. multicenter point prevalence survey of antibiotic use in Punjab, Pakistan: findings and implications. *Expert Rev Anti Infect Ther*. 2019 Apr;17(4):285-293. doi: 10.1080/14787210.2019.1581063. Epub 2019 Feb 22.
12. Leaper D.J., Edmiston C.E. World Health Organization: global guidelines for the prevention of surgical site infection. *J Hosp Infect*. 2017 Feb;95(2):135-136. doi: 10.1016/j.jhin.2016.12.016. Epub 2016 Dec 24.
13. Schoffelen T., Papan C., Carrara E., et al; ESCMID Study Group for Antimicrobial Stewardship (ESGAP). European society of clinical microbiology and infectious diseases guidelines for antimicrobial stewardship in emergency departments (endorsed by European association of hospital pharmacists). *Clin Microbiol Infect.* 2024 Nov;30(11):1384-1407. doi: 10.1016/j.cmi.2024.05.014. Epub 2024 Jul 17.
14. Panda P.K. Wrong diagnosis - Wrong antimicrobials: Rise in antimicrobial resistance in developing countries. *IDCases*. 2025 Jul 6;41:e02313. doi: 10.1016/j.idcr.2025.e02313.
15. Mori V., Grant G., Hattingh L. Evaluation of antimicrobial resistance surveillance data sources in primary care setting: a scoping review. *Fam Pract*. 2025 Feb 7;42(2):cmaf013. doi: 10.1093/fampra/cmaf013.
16. WHO. The WHO AWaRe (Access, Watch, Reserve) antibiotic book. The WHO AWaRe (Access, Watch, Reserve) antibiotic book.
17. WHO. Proposal to the 2025 Expert Committee on Selection and Use of Essential Medicines to classify antibiotics not currently included in the WHO AWaRe classification. https://cdn.who.int/media/docs/default-source/2025-eml-expert-committee/late-papers/l.4_aware-classifications.pdf?sfvrsn=28b75898_1
18. Jing F.H., Wang Q., He T.J., Xin N., Wang Y.W., Han Y., Wang X., Li Z. Three-Year Point Prevalence Survey of Antimicrobial Use in a Chinese University Hospital. Can J Infect Dis Med Microbiol. 2024 Feb 8;2024: 6698387. doi: 10.1155/2024/6698387.
19. WHO. Diagnostic stewardship: a guide to implementation in antimicrobial resistance surveillance sites. Geneva, 2018. https://www.who.int/publications/i/item/WHO-DGO-AMR-2016.3

MICRORNAS AS LIQUID BIOMARKERS OF CANCER: A REVIEW OF CURRENT APPROACHES TO CIRCULATING MICRORNAS IN ONCOLOGICAL DIAGNOSTICS

M.R. Ruzibakieva[1], J.J. Ramziddinov[2], A.J. Jangavarov[3], F.T. Ryskulov[4], K.E. Grigoryants[5]
DSc, Leading Researcher at the Laboratory of Genomic and Cellular Technologies[1]
Junior Researcher at the Department of Cell Therapy[2]
Junior Researcher at the Department of Cell Therapy[3]
Junior Researcher at the Laboratory of Genomic and Cellular Technologies[4]
PhD, Senior Researcher at the Laboratory of Genomic and Cellular Technologies[5]
Institute of Immunology and Human Genomics of the Academy of Sciences of the Republic of Uzbekistan[1,2,3,4,5]
https://doi.org/10.5281/zenodo.20697446

Abstract. *Cancer remains one of the leading causes of death worldwide, and the stage at which a tumour is detected continues to be among the strongest determinants of patient survival. Although early diagnosis markedly improves outcomes, the screening tools currently in routine use are frequently limited by insufficient sensitivity and specificity. This shortfall has fuelled an active search for minimally invasive biomarkers capable of flagging malignancy at an early, ideally pre-symptomatic, stage. Circulating microRNAs - short non-coding RNAs that are readily detectable in blood and other body fluids - have drawn particular attention in this regard. Owing to their remarkable stability and their tumour-type-specific expression patterns, these molecules are widely viewed as promising candidates for a blood-based "liquid biopsy". The present review brings together current evidence on the diagnostic value of circulating microRNAs across the major categories of malignancy and weighs the prospects for translating them into clinical practice. As the surveyed data show, circulating microRNAs - especially when assembled into multi-marker panels or combined with conventional tumour markers - can deliver sensitivity and specificity high enough to make them a credible tool for minimally invasive cancer diagnostics.*

Keywords: *microRNA, circulating microRNAs, cancer biomarkers, liquid biopsy, oncological diagnostics, early cancer detection, non-invasive biomarkers, tumour markers, miRNA panels, serum biomarkers, plasma biomarkers, personalized oncology.*

INTRODUCTION

MicroRNAs (miRNAs) are a class of short non-coding RNAs, typically 19-24 nucleotides in length, that govern gene expression at the post-transcriptional level. Once processed within the cell, a mature miRNA is loaded into the RNA-induced silencing complex (RISC) and guided to complementary sequences in target messenger RNAs (mRNAs), where it triggers either transcript degradation or translational repression. Through this mechanism miRNAs help orchestrate a broad range of physiological processes, and their dysregulation has been linked to numerous diseases, malignant tumours among them. Cancer cells harbour both oncogenic miRNAs (so-called oncomiRs), whose overexpression silences tumour-suppressor genes, and tumour-suppressive miRNAs, whose loss drives unchecked proliferation, impaired apoptosis and enhanced angiogenesis - changes that together favour tumour progression [35].

Of particular interest is the detection of miRNAs outside the cell, in the circulating blood. The first evidence that tumour-derived miRNAs are present in-patient serum - and that they persist there in a form resistant to RNase activity - was obtained in 2008 [22]. miRNAs released by tumours can be recovered from plasma or serum, where they are shielded from degradation either by binding to proteins such as Argonaute2 or by packaging into extracellular vesicles (exosomes and microvesicles). This stability underlies their considerable promise as non-invasive cancer biomarkers. Over the past ten to fifteen years, research on circulating miRNAs in oncology has expanded rapidly, uncovering numerous associations between blood miRNA profiles and the presence of a tumour, its histological type, stage and prognosis. It has been proposed that characteristic shifts in the levels of particular miRNAs may signal an early, still asymptomatic tumour or a recurrence following treatment [33].

MICRORNAS AND CANCER

miRNAs perform key regulatory roles across cellular processes [4, 11, 18]. The biogenesis of miRNAs and the ways in which they take part in the control of gene expression have been described in detail elsewhere [3, 13]. Since the first miRNAs were identified in *C. elegans*, roughly 1,500 such molecules have been catalogued in humans [26].

The earliest studies - centred on lin-4 and let-7 - revealed the part these miRNAs play in embryogenesis and developmental timing in C. elegans, where they operate within intricate circuits of gene regulation [23]. Biochemical work subsequently showed that such small RNAs can both inhibit protein translation and influence mRNA stability [19]. Current estimates suggest that miRNAs regulate the expression of about half of all protein-coding genes in humans [23].

The pioneering work of Calin and et al. in 2002 was the first to demonstrate a central role for miRNAs in oncogenesis. They found that miR-15 and miR-16 are markedly reduced in chronic lymphocytic leukaemia (CLL) as a consequence of deletions at the 13q14 locus [5]. These early observations also showed that more than half (52%) of miRNA genes lie within genomic regions that are frequently disrupted in cancer; later mapping reinforced the point, pinpointing 186 miRNAs located at fragile sites and other vulnerable parts of the genome [5].

In the years since, miRNAs have been tied to a wide variety of cancers, contributing to neoplastic transformation, tumour progression and clinical outcome [7, 16, 20, 32]. Depending on the set of target genes it regulates, a given miRNA may act either as an oncogene that promotes malignant growth or as a tumour suppressor that restrains carcinogenesis, placing miRNAs at the very heart of the signalling networks that drive cancer.

The involvement of miRNAs in gene regulation underscores their importance both in maintaining normal physiology and in the emergence of disease [19, 24]. Single-nucleotide polymorphisms within the 3′ untranslated regions of mRNAs can, moreover, alter the way miRNAs exert their regulatory effects - a phenomenon that has been associated with an elevated risk of cancer [10].

CIRCULATING MICRORNAS

Drawing a blood sample remains the most accessible and least invasive way to obtain biomarkers. A large body of work has confirmed that distinctive circulating miRNA profiles accompany various pathological states, with expression levels that track disease stage [12, 28, 31]. In oncology, the appearance of specific circulating miRNA signatures reflects the passive escape of these molecules from tumour cells as a result of their heightened proliferation and apoptosis. Contemporary views on the biogenesis, classification and analysis of circulating microRNAs, together with their diagnostic potential, have been reviewed extensively [1, 21, 38].

A comparative analysis by Yu and et al. highlighted appreciable differences between the metabolite profiles of plasma and serum, with serum showing higher metabolite concentrations and, correspondingly, greater diagnostic sensitivity [42]. The study by Lawrie and co-workers was the first to report a diagnostically meaningful rise in serum miR-155, miR-210 and miR-21 in patients with diffuse large B-cell lymphoma relative to healthy donors [22].

Subsequently, miRNA expression profiles were obtained from the serum or plasma of patients with a range of malignancies, including acute leukaemia [36], breast cancer [43], colorectal cancer [29], gastric cancer [37], glioblastoma [34], hepatocellular carcinoma [40], lung cancer [8], ovarian cancer [30] and prostate cancer [27].

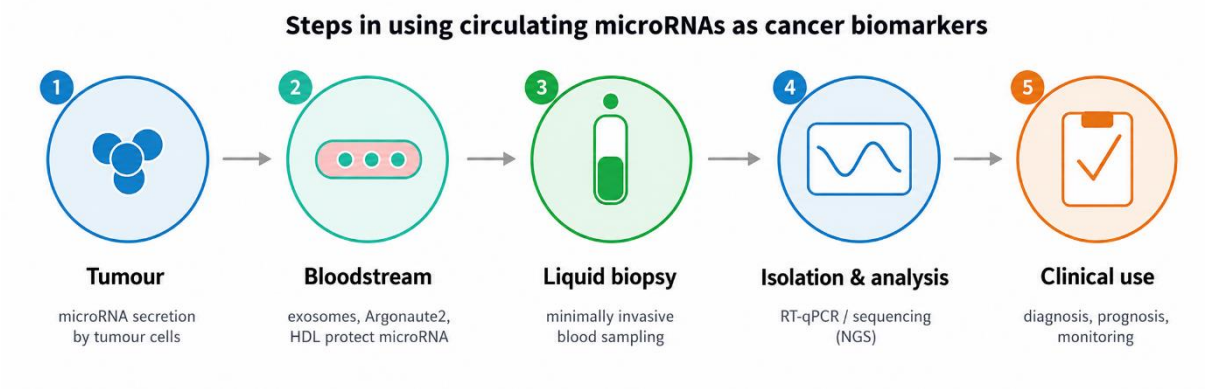


Figure 1. Schematic overview of the steps involved in using microRNAs as cancer biomarkers [9]

CLINICAL EVIDENCE ON THE USE OF MICRORNAS IN ONCOLOGICAL DIAGNOSTICS

Breast cancer (BC), the most common malignancy in women, was among the first tumours for which circulating miRNAs were proposed as diagnostic biomarkers. Breast tumour tissue frequently shows dysregulation of miR-21, miR-155, miR-10b and others, all of which promote invasion and metastasis. These same miRNAs are likewise found at elevated concentrations in the blood of BC patients compared with healthy controls.

In 2021, Canatan and et al. examined the expression of nine candidate miRNAs in the serum of BC patients and identified three - miR-21, miR-125a and miR-155 - that were significantly elevated and offered the greatest diagnostic accuracy [6]. In their data, miR-155 separated patients from healthy individuals with a sensitivity of 83% and a specificity of 82%, while the corresponding figures for miR-125a were 78% and 84%.

Circulating microRNAs are also being explored within diagnostic panels: Hagrass and et al. showed that a serum miRNA panel comprising miR-155, miR-10b and miR-34a reliably distinguishes BC patients from healthy women. Taken together, circulating miR-21, miR-125a and miR-155 are regarded as promising non-invasive markers for the early detection of breast cancer [17].

Lung cancer is the leading cause of cancer death worldwide, in large part because it is so difficult to detect early. Circulating miRNAs are under intensive study as potential early markers of non-small-cell lung cancer (NSCLC) and its other forms [25]. In 2018, Yu and et al. conducted a systematic review of 17 studies on the early diagnosis of lung cancer with miRNAs in Western populations, drawing together data on 35 individual miRNA markers and 19 marker combinations. Single miRNAs achieved a median sensitivity of 78% and specificity of 79%, whereas multi-miRNA panels performed better, with a median sensitivity of 83% and specificity of 85% [42].

Combinations of two to five circulating miRNAs thus detected early lung cancer considerably more accurately than individual markers; the miR-223/miR-20a/miR-21 panel, for instance, reached an AUC of 0.90 in NSCLC patients relative to healthy smokers [42]. The use of miRNA expression ratios proved a further useful strategy: as Yu and et al. noted, computing the ratio between paired miRNAs helps offset inter-individual variability and improves the reproducibility of the test.

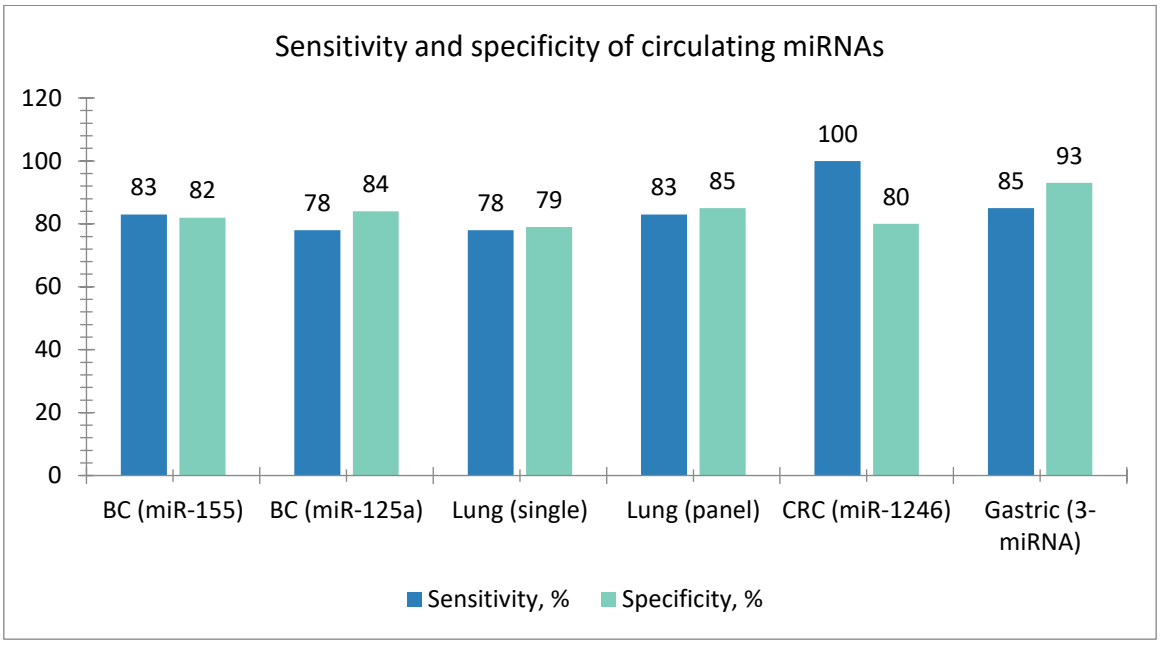


Figure 2. Sensitivity and specificity of circulating miRNAs across different cancer types.

Colorectal cancer (CRC) is one of the most common malignancies of the gastrointestinal tract, and blood miRNAs are being actively studied to enable its early detection. In their 2024 meta-analysis, AlZaabi and Shalaby reported that the circulating miRNA profiles of CRC patients differ substantially from those of healthy individuals, with frequent increases in miR-21, miR-20a and miR-223 and decreases in a number of other miRNAs. miR-21 has attracted special attention, as it is detected consistently in CRC and is linked to tumour progression. The same meta-analysis noted that the diagnostic performance of miR-21 varies widely across studies, from a modest AUC of 0.55 to a very high 0.97. More reproducible markers were nonetheless identified: circulating miR-1246, for example, showed strong diagnostic accuracy in several reports, and in one study it detected CRC with an AUC of 0.924 at 100% sensitivity and 80% specificity - figures comparable to, or better than, those of established non-invasive tests such as the faecal occult blood test [2].

Gastric cancer (GC) carries high mortality, again largely because of late detection. Circulating miRNAs are being assessed as a possible tool for the non-invasive screening of early gastric cancer. In the blood of GC patients, increases in miR-21, miR-20a, miR-221/222, miR-423-5p and several others are reported most often, alongside reductions in the tumour-suppressive miR-375, miR-148a and others. In 2021, Yao and et al. analysed miRNA expression profiles in two independent cohorts of GC patients and healthy individuals and, using machine learning, singled out three key miRNAs (miR-320a, miR-1260b and miR-6515-5p) that together delivered excellent diagnostic performance. In both cohorts this trio separated gastric cancer patients with an AUC above 0.95 at a sensitivity exceeding 85% and a specificity above 93%. Validation on additional datasets further showed that each of the three markers individually provided a sensitivity of 92-100% with a specificity of 89-100%, while their combined use approached 100% accuracy

(AUC 0.99) [41]. Pancreatic cancer (PaC), and pancreatic ductal adenocarcinoma (PDAC) in particular, is notable for its extremely aggressive course and the lack of effective methods for early diagnosis. Circulating miRNAs are of special interest here, since the conventional marker CA 19-9 is insufficiently sensitive at early stages.

In 2021, Vieira and et al. demonstrated the diagnostic value of several miRNAs in PDAC: plasma levels of miR-181c and miR-210 were markedly elevated in patients relative to healthy controls and could be used to flag the presence of a tumour. Strikingly, in pancreatic tissue samples the combined expression of miR-21 and miR-210, considered together with serum CA 19-9, achieved 100% accuracy in diagnosing pancreatic cancer. This suggests that pairing classical tumour markers with a miRNA profile can substantially improve diagnostic reliability. Overall, miR-21, miR-155, miR-181c and miR-210 are viewed as leading candidates for multi-marker panels in pancreatic cancer; their use, especially alongside CA 19-9, could improve early detection of this tumour - a matter of considerable importance given its rapid progression [39].

Prostate cancer (PC) is among the most common malignancies in men. The standard screening marker, prostate-specific antigen (PSA), has limited specificity, so the search for additional non-invasive biomarkers is relevant for improving early diagnosis and curbing overdiagnosis.

In a large 2025 study, Gomez-Acebo and et al. analysed 46 candidate miRNAs in 203 prostate cancer patients and 54 controls, then built predictive models from the best-performing markers. They identified 14 miRNAs robustly associated with the presence of prostate cancer. Among them were miR-199a-5p, which was elevated in patients, and miR-150-5p, which was conversely reduced across all risk categories. Several miRNAs - miR-145-5p, miR-93-5p and miR-182-5p, for example - already differed significantly at early disease stages, pointing to their potential for detecting localised cancer. Logistic models built on panels of several miRNAs performed well: for the low-risk (early-stage) group the classifier reached an AUC of 0.93, whereas the overall model distinguished patients from healthy individuals with an AUC of 0.82 [15].

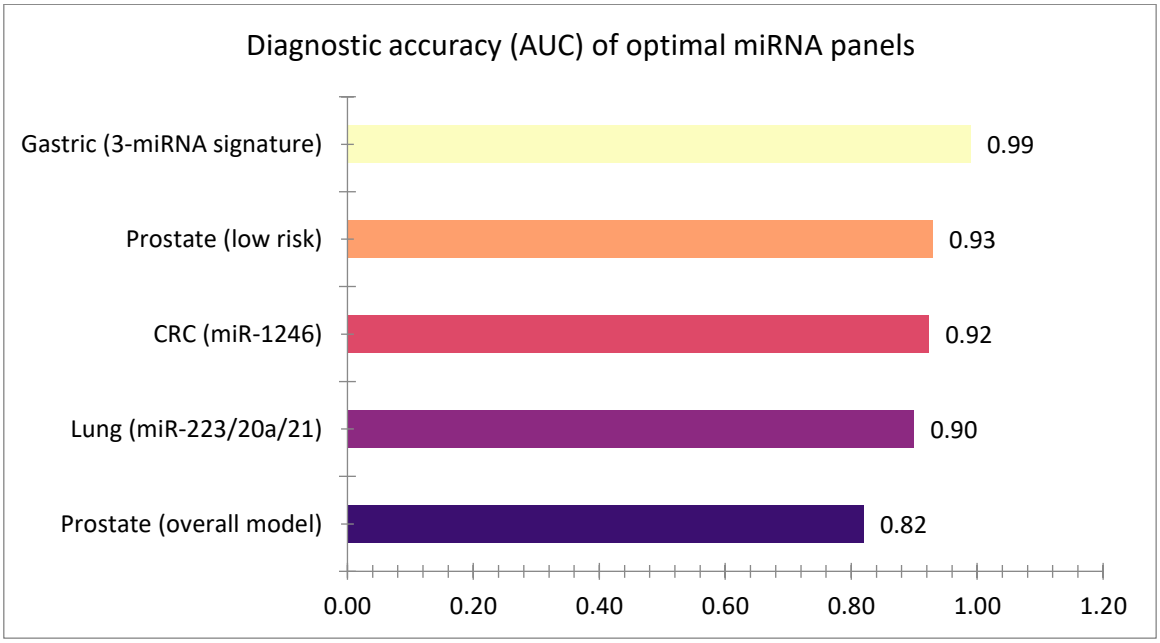


Figure 3. Diagnostic accuracy (AUC) of optimal miRNA panels by cancer type.

Ovarian cancer (OC) is frequently diagnosed at an advanced stage because it lacks specific symptoms and reliable screening tests. The main marker in current use, CA 125, is not sensitive enough for early detection.

In their 2023 meta-analysis, Frisk and et al. pooled data from 44 studies of circulating miRNAs in OC, 22 of which entered the quantitative analysis. The authors highlighted nine miRNAs that were most reproducibly altered in ovarian cancer - miR-21, miR-125b, miR-141, miR-145, miR-200a, miR-200b, miR-200c, miR-205 and miR-328 - all of which were significantly higher in-patient blood than in healthy controls; miR-21 and miR-205 ranked among the most consistently confirmed markers. The same meta-analysis showed that integrating a miRNA (such as miR-205 or miR-132) with CA 125 raised the AUC to 0.95-0.98, compared with 0.85 for CA 125 alone [14].

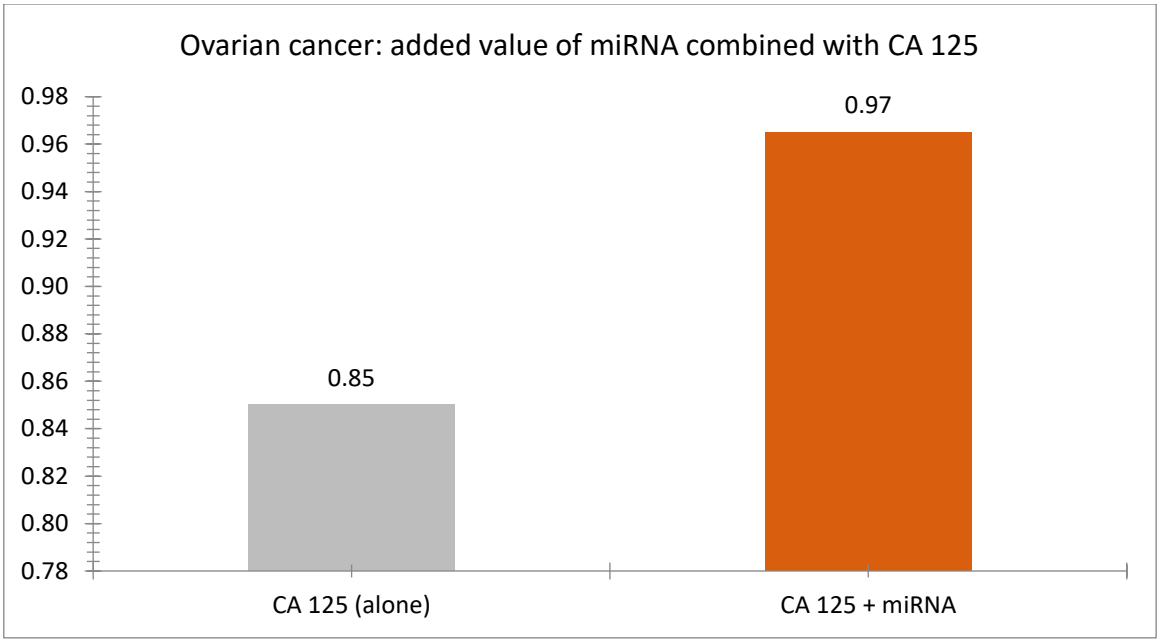


Figure 4. Improvement in diagnostic accuracy when miRNA is added to the CA 125 tumour marker (ovarian cancer) [14].

Table 1. Examples of circulating miRNAs in the diagnosis of various cancers.

Disease	**microRNA**	**Diagnostic role of microRNA**	**Study**
Breast cancer	miR-21 ↑ miR-125a ↑ miR-155 ↑	Early BC diagnosis; distinguish patients from healthy controls with high sensitivity and specificity	Canatan et al. 2021 [6]
Lung cancer (NSCLC)	miR-21 ↑	Non-invasive screening of early lung cancer; 2-4-miRNA panels give AUC 0.80-0.85	Yu et al. 2018 [42]

Colorectal cancer	miR-1246 ↑	Detection of colorectal cancer; one of the most accurate markers (AUC 0.92, 100% sens., 80% spec.)	AlZaabi & Shalaby, 2024 [2]
Gastric cancer	miR-320a ↑ miR-1260b ↑ miR-6515-5p ↑	Three-miRNA signature for early diagnosis; validation showed >95% detection accuracy	Yao et al. 2021 [41]
Pancreatic cancer	miR-21 ↑ miR-155 ↑	PDAC markers; associated with tumour presence and aggressiveness, proposed for early diagnosis (combined with CA 19-9)	Vieira et al. 2021 [39]
Prostate cancer	miR-199a-5p ↑ miR-150-5p ↓	Early diagnosis and risk stratification of PC; part of a 14-miRNA set for discriminating prostate cancer	Gómez-Acebo et al. 2025 [15]
Ovarian cancer	miR-21 ↑ miR-125b ↑ miR-200c ↑	Screening of epithelial OC; combining several miRNAs with CA 125 improves early-diagnosis accuracy	Frisk et al. 2023 [14]

CONCLUSION

Recent research has made a compelling case that circulating miRNAs hold considerable promise as early cancer biomarkers. For virtually all of the major tumour types - lung, breast, colorectal, pancreatic, ovarian and prostate cancer among them - specific blood miRNA patterns have been identified that set patients apart from healthy individuals. These short RNAs are highly stable in plasma and serum, and their profiles mirror the molecular and genetic alterations characteristic of the corresponding tumours. In this review we have surveyed current approaches to miRNA detection and presented examples of diagnostic panels that achieve sensitivity and specificity matching or surpassing those of conventional markers. It is worth emphasising that the most promising direction lies in combining several miRNAs and in integrating miRNAs with classical tumour markers and clinical variables, an approach that appreciably increases diagnostic accuracy.

That said, a number of hurdles must be cleared before miRNA tests can enter routine clinical practice. These include standardising the methods used to isolate and analyse circulating

RNA, developing reliable normalisation controls, validating the identified biomarkers at scale in prospective patient cohorts, and accounting for the influence of comorbidities and other conditions on miRNA levels. Meeting these challenges will demand concerted effort from research groups and clinicians alike, as well as well-designed multicentre studies.

In closing, circulating miRNAs open up new possibilities for non-invasive cancer diagnosis. They offer several clear advantages - minimally invasive sampling, high stability, tissue specificity and the ability to capture the dynamics of disease. Within the next few years one can anticipate the emergence of miRNA-panel-based test systems for the early detection of cancer, the monitoring of treatment response and the identification of recurrence. Further research and clinical trials will reveal whether these molecules can live up to the hopes placed in them and secure a lasting place in the diagnostic arsenal of personalised oncology.

REFERENCES

1. Alemayehu E., Fasil A., Ebrahim H., Gebeyehu A., Belachew F. Circulating microRNAs as promising diagnostic biomarkers for hepatocellular carcinoma: a systematic review and meta-analysis // Frontiers in Molecular Biosciences. - 2024. - Vol. 11. - Art. 1353547. - DOI: 10.3389/fmolb.2024.1353547.
2. AlZaabi A., Shalaby A. A systematic review of diagnostic performance of circulating microRNAs in colorectal cancer detection with a focus on early-onset colorectal cancer // International Journal of Molecular Sciences. - 2024. - Vol. 25, № 17. - P. 9565. - DOI: 10.3390/ijms25179565.
3. Ambros V. The functions of animal microRNAs // Nature. - 2004. - Vol. 431. - P. 350-355. - DOI: 10.1038/nature02871.
4. Bartel D.P., Chen C.Z. Micromanagers of gene expression: the potentially widespread influence of metazoan microRNAs // Nature Reviews Genetics. - 2004. - Vol. 5. - P. 396-400. - DOI: 10.1038/nrg1328.
5. Calin G.A., Dumitru C.D., Shimizu M. et al. Frequent deletions and down-regulation of micro-RNA genes miR-15 and miR-16 at 13q14 in chronic lymphocytic leukemia // Proceedings of the National Academy of Sciences of the USA. - 2002. - Vol. 99. - P. 15524-15529. - DOI: 10.1073/pnas.242606799.
6. Canatan D., Yılmaz Ö., Sönmez Y. et al. Circulating microRNAs as potential non-invasive biomarkers for breast cancer detection // Acta Biomed. - 2021. - Vol. 92, № 2. - P. e2021028. - DOI: 10.23750/abm.v92i2.9678.
7. Chan E., Patel R., Nallur S. et al. MicroRNA signatures differentiate melanoma subtypes // Cell Cycle. - 2011. - Vol. 10. - P. 1845-1852. - DOI: 10.4161/cc.10.11.15777.
8. Chen X., Ba Y., Ma L. et al. Characterization of microRNAs in serum: a novel class of biomarkers for diagnosis of cancer and other diseases // Cell Research. - 2008. - Vol. 18. - P. 997-1006. - DOI: 10.1038/cr.2008.282.
9. Condrat C.E., Thompson D.C., Barbu M.G. et al. miRNAs as biomarkers in disease: latest findings regarding their role in diagnosis and prognosis // Cells. - 2020. - Vol. 9, № 2. - P. 276. - DOI: 10.3390/cells9020276.
10. Conne B., Stutz A., Vassalli J.D. The 3′ untranslated region of messenger RNA: a molecular “hotspot” for pathology? // Nature Medicine. - 2000. - Vol. 6. - P. 637-641. - DOI: 10.1038/76211.

11. Croce C.M. Causes and consequences of microRNA dysregulation in cancer // Nature Reviews Genetics. - 2009. - Vol. 10. - P. 704-714. - DOI: 10.1038/nrg2634.
12. Dieckmann K.P., Spiekermann M., Balks T. et al. MicroRNAs miR-371-3 in serum as diagnostic tools in the management of testicular germ cell tumours // British Journal of Cancer. - 2012. - Vol. 107. - P. 1754-1760. - DOI: 10.1038/bjc.2012.469.
13. Flynt A.S., Lai E.C. Biological principles of microRNA-mediated regulation: shared themes amid diversity // Nature Reviews Genetics. - 2008. - Vol. 9. - P. 831-842. - DOI: 10.1038/nrg2455.
14. Frisk N.L.S., Sørensen A.E., Pedersen O.B.V., Dalgaard L.T. Circulating microRNAs for early diagnosis of ovarian cancer: a systematic review and meta-analysis // Biomolecules. - 2023. - Vol. 13, № 5. - P. 871. - DOI: 10.3390/biom13050871.
15. Gómez-Acebo I., Valero-Domínguez S., Llorca J. et al. Role of circulating microRNAs in prostate cancer diagnosis and risk stratification in the MCC Spain study // Scientific Reports. - 2025. - Vol. 15. - Art. 17517. - DOI: 10.1038/s41598-025-01373-9.
16. Guttilla I.K., White B.A. Coordinate regulation of FOXO1 by miR-27a, miR-96 and miR-182 in breast cancer cells // Journal of Biological Chemistry. - 2009. - Vol. 284. - P. 23204-23216. - DOI: 10.1074/jbc.M109.031427.
17. Hagrass H.A., Sharaf S., Pasha H.F. et al. Circulating microRNAs - a new horizon in molecular diagnosis of breast cancer // Genes & Cancer. - 2015. - Vol. 6, № 5-6. - P. 281-287. - DOI: 10.18632/genesandcancer.66.
18. Hobert O. miRNAs play a tune // Cell. - 2007. - Vol. 131. - P. 22-24. - DOI: 10.1016/j.cell.2007.09.031.
19. Hwang H.W., Mendell J.T. MicroRNAs in cell proliferation, cell death, and tumorigenesis // British Journal of Cancer. - 2006. - Vol. 94. - P. 776-780. - DOI: 10.1038/sj.bjc.6603023.
20. Kefas B., Godlewski J., Comeau L. et al. microRNA-7 inhibits the epidermal growth factor receptor and the Akt pathway and is down-regulated in glioblastoma // Cancer Research. - 2008. - Vol. 68. - P. 3566-3572. - DOI: 10.1158/0008-5472.CAN-07-6639.
21. Kim V.N. Small RNAs: classification, biogenesis, and function // Molecules and Cells. - 2005. - Vol. 19. - P. 1-15. - PMID: 15750334.
22. Lawrie C.H., Gal S., Dunlop H.M. et al. Detection of elevated levels of tumour-associated microRNAs in serum of patients with diffuse large B-cell lymphoma // British Journal of Haematology. - 2008. - Vol. 141. - P. 672-675. - DOI: 10.1111/j.1365-2141.2008.07077.x.
23. Lujambio A., Lowe S.W. The microcosmos of cancer // Nature. - 2012. - Vol. 482. - P. 347-355. - DOI: 10.1038/nature10888.
24. Maccani M.A., Padbury J.F., Marsit C.J. miR-16 and miR-21 expression in the placenta is associated with fetal growth // PLoS ONE. - 2011. - Vol. 6, № 6. - e21210. - DOI: 10.1371/journal.pone.0021210.
25. Metcalf G.A.D. MicroRNAs: circulating biomarkers for the early detection of imperceptible cancers via biosensor and machine-learning advances // Oncogene. - 2024. - Vol. 43, № 29. - P. 2135-2142. - DOI: 10.1038/s41388-024-03076-3.
26. miRBase: The microRNA database [Электронный ресурс]. - Режим доступа: http://www.mirbase.org (дата обращения: 15.11.2012).
27. Mitchell P.S., Parkin R.K., Kroh E.M. et al. Circulating microRNAs as stable blood-based markers for cancer detection // Proceedings of the National Academy of Sciences of the USA. - 2008. - Vol. 105, № 30. - P. 10513-10518. - DOI: 10.1073/pnas.0804549105.

28. Mo M.H., Chen L., Fu Y. et al. Cell-free circulating miRNA biomarkers in cancer // Journal of Cancer. - 2012. - Vol. 3. - P. 432-448. - DOI: 10.7150/jca.4919.
29. Ng E.K., Chong W.W., Jin H. et al. Differential expression of microRNAs in plasma of patients with colorectal cancer: a potential marker for colorectal cancer screening // Gut. - 2009. - Vol. 58. - P. 1375-1381. - DOI: 10.1136/gut.2008.167817.
30. Resnick K.E., Alder H., Hagan J.P., Richardson D.L., Croce C.M., Cohn D.E. The detection of differentially expressed microRNAs from the serum of ovarian cancer patients using a novel real-time PCR platform // Gynecologic Oncology. - 2009. - Vol. 112, № 1. - P. 55-59. - DOI: 10.1016/j.ygyno.2008.08.036.
31. Russo F., Di Bella S., Nigita G. et al. miRandola: extracellular circulating microRNAs database // PLoS ONE. - 2012. - Vol. 7, № 10. - Art. e47786. - DOI: 10.1371/journal.pone.0047786.
32. Schultz J., Lorenz P., Gross G. et al. MicroRNA let-7b targets important cell-cycle molecules in malignant melanoma cells and interferes with anchorage-independent growth // Cell Research. - 2008. - Vol. 18, № 4. - P. 549-557. - DOI: 10.1038/cr.2008.45.
33. Siniscalco D., Galderisi U., Peluso G., Finicelli M. Circulating microRNAs in cancer: a 5-year update with a focus on breast and lung cancers // International Journal of Molecular Sciences. - 2024. - Vol. 25, № 6. - P. 3140. - DOI: 10.3390/ijms25063140.
34. Skog J., Wurdinger T., van Rijn S. et al. Glioblastoma microvesicles transport RNA and proteins that promote tumour growth and provide diagnostic biomarkers // Nature Cell Biology. - 2008. - Vol. 10. - P. 1470-1476. - DOI: 10.1038/ncb1800.
35. Sundarbose K., Kartha R.V., Subramanian S. MicroRNAs as biomarkers in cancer // Diagnostics. - 2013. - Vol. 3, № 1. - P. 84-104. - DOI: 10.3390/diagnostics3010084.
36. Tanaka M., Oikawa K., Takanashi M. et al. Down-regulation of miR-92 in human plasma is a novel marker for acute leukemia patients // PLoS ONE. - 2009. - Vol. 4, № 5. - Art. e5532. - DOI: 10.1371/journal.pone.0005532.
37. Tsujiura M., Ichikawa D., Komatsu S. et al. Circulating microRNAs in plasma of patients with gastric cancers // British Journal of Cancer. - 2010. - Vol. 102. - P. 1174-1179. - DOI: 10.1038/sj.bjc.6605608.
38. Valihrach L., Androvic P., Kubista M. Circulating miRNA analysis for cancer diagnostics and therapy // Molecular Aspects of Medicine. - 2020. - Vol. 72. - P. 100825. - DOI: 10.1016/j.mam.2019.10.002.
39. Vieira N.F., Serafini L.N., Novais P.C. et al. The role of circulating miRNAs and CA19-9 in pancreatic cancer diagnosis // Oncotarget. - 2021. - Vol. 12. - P. 1638-1650. - DOI: 10.18632/oncotarget.28038.
40. Yamamoto Y., Kosaka N., Tanaka M. et al. MicroRNA-500 as a potential diagnostic marker for hepatocellular carcinoma // Biomarkers. - 2009. - Vol. 14. - P. 529-538. - DOI: 10.3109/13547500903150771.
41. Yao Y., Ding Y., Bai Y. et al. Identification of serum circulating microRNAs as novel diagnostic biomarkers of gastric cancer // Frontiers in Genetics. - 2021. - Vol. 11. - Art. 591515. - DOI: 10.3389/fgene.2020.591515.
42. Yu H., Guan Z., Cuk K. et al. Circulating microRNA biomarkers for lung cancer detection in Western populations // Cancer Medicine. - 2018. - Vol. 7, № 10. - P. 4849-4862. - DOI: 10.1002/cam4.1782.

PRODUCTIVITY TRAITS IN F1 HYBRIDS DERIVED FROM COTTON CULTIVARS, A WILD SPECIES, AND INTROGRESSIVE FORMS

A.A. Mamajonov
Department of Medical Biology and Public Health, Andijan Branch, Kokand University, Andijan, Uzbekistan, Acting Associate Professor
https://doi.org/10.5281/zenodo.20664878

Abstract. *This study investigated the formation and inheritance of productivity traits in F_1 hybrids obtained from cotton cultivars, wild species, and introgressive forms. The total number of bolls per plant, the number of opened bolls, the number of seeds per boll, and the percentage of fully developed seeds were evaluated. Reciprocal and stepwise hybridization methods were applied in the study. The results demonstrated that hybrids involving the cultivars Golib, Andijon-35, Namangan-77, and Qizil Baraka exhibited high productivity indicators. In contrast, some hybrids involving G. mustelinum and T-85 showed relatively lower productivity performance. Positive and negative overdominance, dominance, and intermediate inheritance patterns were identified in the inheritance of the studied traits, and promising initial breeding materials were recommended for selection programs.*

Keywords: *cotton, F_1 hybrids, productivity, reciprocal crossing, stepwise hybridization, inheritance, breeding, Gossypium.*

Introduction

Cotton is one of the most important industrial crops in agriculture, and increasing its yield remains one of the primary objectives of modern breeding programs. Productivity is a complex quantitative trait that is determined by numerous genetic and environmental factors. The number of bolls per plant, the number of opened bolls, the proportion of fully developed seeds, and other biological characteristics are considered major components of yield performance. Wild cotton species and introgressive forms represent valuable sources of genetic diversity, and their hybridization with cultivated varieties provides opportunities for obtaining promising breeding materials. Therefore, the investigation of productivity traits in F_1 hybrids derived from cotton cultivars, wild species, and introgressive forms, as well as the determination of their inheritance patterns and the identification of promising hybrid combinations, is of considerable scientific and practical importance.

Literature Review

According to Sirojidinov and co-authors, productivity in cotton is determined by the plant's genetic potential and is formed through the interaction of several traits and characteristics [1].

Seyitmusayev and Tishin [2], as well as Ernazarova [3], reported that productivity is largely determined by the number of opened bolls, the number of fully developed seeds in each boll, and fiber content.

Azimov [4], while studying wilt resistance and boll number in interspecific cotton hybrids, demonstrated that the development and inheritance of this trait depend on the parental genotypes selected for crossing. He further noted that greater differences between parental forms in boll

number increase the probability of obtaining highly heterozygous hybrid populations in subsequent generations. The author emphasized the importance of conducting genetic and breeding studies using such heterogeneous populations.

Umbetayev, Eleshev, and Atakulov [5] investigated the productivity of cultivars belonging to *Gossypium hirsutum* L. under different mineral nutrition conditions and found that the number of bolls per plant increased proportionally under both minimum and maximum fertilizer regimes.

Karimova [6] studied the development of cotton cultivars and lines under drought-prone soil conditions and observed a substantial reduction in both the number of bolls per plant and the proportion of fully developed seeds under water-deficit conditions.

Saidov [7], while investigating the genetic and physiological potential of cotton cultivars and hybrids under various ecological conditions, reported that boll number and boll size are primarily determined by the genotype and tend to be expressed according to their inherent genetic potential regardless of environmental influences.

Rao and Gopinath [8] confirmed the relationship between cotton yield and fiber quality and demonstrated that the number of bolls per plant plays a more important role in yield improvement than the weight of cotton per boll.

Avtonomov and Kimsanbayev [9] emphasized that the number of bolls per plant should be considered one of the principal components determining cotton productivity and, therefore, warrants detailed investigation.

Chorshanbiyev [10] studied this trait in F_1 and F_2 hybrids of *Gossypium barbadense* L. cultivars and found that the number of bolls per plant was inherited with positive overdominance in the F_1 generation. Furthermore, he demonstrated that cytoplasmic genes also participate in the genetic regulation of this trait in reciprocal hybrid combinations.

Murtaza [11] investigated the genetic effects controlling boll number and boll weight through diallel crosses involving eight different genotypes of *Gossypium hirsutum* L. He concluded that the inheritance of these traits in diallel hybrid populations is a complex process and emphasized that the achievement of high productivity depends on proper parental selection and the use of mature, well-developed seeds.

Materials and Methods

The formation and inheritance of productivity-related traits, including the total number of bolls per plant, the number of opened bolls per plant, the total number of seeds per boll, and the numbers of fully developed and undeveloped seeds, were investigated in cultivars, lines, and F_1 hybrid plants obtained through reciprocal and stepwise hybridization methods.

Phenological observations were conducted to determine the total number of bolls and the number of opened bolls per plant. The data collected during these observations, together with the results obtained from seed analyses of individual bolls, were subjected to statistical evaluation.

Results and Discussion

Among the tetraploid cultivars belonging to *Gossypium hirsutum* L., the total number of bolls per plant ranged from 13.5 to 23.7, whereas the number of opened bolls varied between 9.1 and 12.5. Namangan-77 exhibited the highest value for total boll number (23.7 bolls per plant), while Golib and Andijan-35 showed intermediate values of 15.2 and 18.4 bolls per plant, respectively. Qizil Baraka displayed the lowest value, with 13.8 bolls per plant.

Although the wild species *Gossypium mustelinum* Miers ex Watt produced a relatively high total number of bolls (17.1 per plant), it exhibited a comparatively low number of opened bolls

(7.8 per plant). The T-85 line showed the poorest performance among the experimental materials, with only 11.1 total bolls and 5.2 opened bolls per plant (Table 1).

Table 1. Productivity traits in F_1 cotton hybrids

No.	Genotypes and Hybrid Combinations	Plants (n)	Total Bolls per Plant	Opened Bolls per Plant	Analyzed Bolls (n)	Total Seeds per Boll	Fully Developed Seeds per Boll	Unfilled Seeds pe	Percentage of Fully Developed Seeds per Boll (%)				
									X±m%	min±max	S	V%	*hp*
Parental Forms													
1	Golib	10	15,2	9,7	10	33,2	32	1,2	96,5±0,7	91,7-100,0	2,3	2,4	
2	Andijon-35	10	18,4	10,2	10	34,3	32,5	1,8	94,8±1,5	80,6-100,0	4,8	5,1	
3	Namangan-77	10	23,7	12,5	10	32,3	29,5	2,8	91,5±1,2	83,8-96,7	3,9	4,2	
4	Qizil baraka	10	13,8	9,1	10	30,1	27,9	2,2	93,02±2,6	66,7-100,0	8,1	8,7	
5	*G.mustelinum* Miers ex Watt	10	17,1	7,8	10	29,4	22,7	6,7	77,1±2,7	62,5-94,4	8,5	11,0	
6	T-85	10	11,1	5,2	10	20,5	17,3	3,2	84,4±2,1	77,3-94,4	6,7	7,9	
Reciprocal hybridization combinations of F_1 plants													
1	Golib x Andijon-35	30	16,3	9,1	30	35,4	33,6	1,8	94,8±1,5	88,2-100	4,6	4,9	-0,6
2	Andijon-35 x Golib	30	18,5	10,3	30	31,8	31,1	0,7	97,8±0,67	93,5-100	2,10	2,15	2,5
3	Golib x Namangan-77	30	17,3	11,2	30	36	34,6	1,4	96,1±0,56	92,1-97,6	1,8	1,9	0,6
4	Namangan77 x Golib	30	19,1	12,1	30	37,5	35,5	2	94,6±1,3	85-97,6	4,1	4,2	0,1
5	Golib x Qizil baraka	30	16,4	10,2	30	34,3	32,6	1,7	96,9±2,78	79,4-100	4,78	5,1	1,2
6	Qizil baraka x Golib	30	15,1	9,5	30	32,4	31,1	1,3	96,1±1,60	78,6-100	5,05	5,25	0,8
7	Golib x *G.mustllinum* Miers. ex Watt.	30	14,1	7,8	30	34,5	28,1	6,4	81,4±1,69	72,2-100	5,33	6,54	-0,6
8	*G.mustllinum* Miers. ex Watt. x Golib	30	14,4	8,1	30	31,8	26,2	5,6	82,3±3,34	63,6-96,9	10,55	12,82	-0,5
9	T-85 x Golib	30	7,8	3,4	30	28,5	23,3	5,2	81,5±3,5	60-100	11,14	13,66	-1,6
10	Andijon-35 x Namangan-77	30	21,3	12,7	30	30,1	28,9	1,2	96,4±2,50	92-100	2,41	2,50	1,9
11	Namangan-77 x Andijon-35	30	19,8	13,4	30	31,4	30,2	1,2	96,1±1,24	81,5-100	3,91	4,06	1,8
12	Andijon-35 x *G.mustllinum* Miers. ex Watt.	30	18,7	8,9	30	29,7	23,9	5,8	80,6±2,37	64,5-96,4	7,48	9,28	-0,6
13	*G.mustllinum* Miers. ex Watt. x Andijon-35	30	16,6	7,1	30	31,6	24,4	7,2	76,9±1,9	66,7-86,5	6	7,81	-1,1
14	Namangan-77 x Qizil baraka	30	22,3	11,8	30	35,9	34,2	1,7	95,6±1,19	85,7-100	3,77	3,94	4,4
15	Qizil baraka x Namangan-77	10	16,3	9,8	10	32,4	31,5	0,9	97,2±0,8	90,3-100,0	2,7	2,8	6,5
16	Namangan-77 x *G.mustelinum* Miers ex Watt	10	15,1	9,5	10	32,7	25,5	6,2	77,9±1,9	66,7-94,4	6,0	7,4	-0,4
17	*G.mustelinum* Miers ex Watt x Namangan-77	10	19,1	11,2	10	29,2	24,2	5,0	82,7±5,7	48,3-96,7	17,9	21,7	-0,2
18	Namangan-77 x T-85	10	15,8	4,3	10	30,9	27,8	3,1	89,9±2,8	73,1-100,0	8,9	9,9	0,5
19	T-85 x Namangan-77	10	16,3	5,4	10	28,2	24,1	4,1	85,2±4,3	62,9-96,5	13,7	16,1	-0,9
20	Qizil baraka x *G.mustelinum* Miers ex Watt	10	14,9	9,5	10	30,9	26,9	4,0	87,4±2,0	69,7-100,0	6,5	7,4	-0,4
21	*G.mustelinum* Miers ex Watt x Qizil baraka	10	13,7	8,8	10	29,3	24,1	5,2	82,3±1,8	71,4-96,4	5,8	7,0	-0,3
22	Qizil baraka x T-85	10	11,3	5,2	10	25,1	23	2,1	91,7±1,1	85,2-100,0	3,5	3,8	0,7
23	T-85 x Qizil baraka	10	10,3	4,1	10	29,7	22,1	7,6	73,2±4,7	46,2-94,4	14,8	20,2	-3,9
24	*G.mustelinum* Miers ex Watt x T-85	10	13,1	3,1	10	28,6	25,8	2,8	90,5±3,2	58,6-100,0	10,9	11,1	2,4
25	T-85 x *G.mustelinum* Miers ex Watt	10	12,6	4,2	10	29,1	20	9,1	68,8±3,3	53,3-82,8	10,5	15,3	-3,1
19	T-85 x Namangan-77	10	16,3	5,4	10	28,2	24,1	4,1	85,2±4,3	62,9-96,5	13,7	16,1	-0,9
20	Qizil baraka x *G.mustelinum* Miers ex Watt	10	14,9	9,5	10	30,9	26,9	4,0	87,4±2,0	69,7-100,0	6,5	7,4	-0,4
21	*G.mustelinum* Miers ex Watt x Qizil baraka	10	13,7	8,8	10	29,3	24,1	5,2	82,3±1,8	71,4-96,4	5,8	7,0	-0,3
22	Qizil baraka x T-85	10	11,3	5,2	10	25,1	23	2,1	91,7±1,1	85,2-100,0	3,5	3,8	0,7
23	T-85 x Qizil baraka	10	10,3	4,1	10	29,7	22,1	7,6	73,2±4,7	46,2-94,4	14,8	20,2	-3,9
24	*G.mustelinum* Miers ex Watt x T-85	10	13,1	3,1	10	28,6	25,8	2,8	90,5±3,2	58,6-100,0	10,9	11,1	2,4
25	T-85 x *G.mustelinum* Miers ex Watt	10	12,6	4,2	10	29,1	20	9,1	68,8±3,3	53,3-82,8	10,5	15,3	-3,1
Stepwise hybridization combinations of F_1 plants													
1	(Golib x Andijon-35) x Qizil baraka	10	12,3	8,2	10	30,2	29	1,2	95,9±1,2	86,2-100,0	3,8	4,0	1,1
2	(Golib x Andijon-35) x *G.mustelinum* Miers ex Watt	10	16,3	6,3	10	31,4	25,5	5,9	81,1±1,9	70,3-92,6	5,9	7,36	-0,5
3	(Golib x Andijon-35) x T-85	10	12,3	4,4	10	29,8	24,9	4,9	83,3±3,2	62,1-100,0	10,1	12,2	-1,3

4	(Andijon-35 x Golib) x Qizil baraka	10	15,1	9,2	10	31,9	30,6	1,3	95,8±1,3	76,0-100,0	4,2	4,4	0,2
5	(Andijon-35 x Golib) x *G.mustelinum* Miers ex Watt	10	17,5	8,2	10	30,9	25,2	5,7	82,1±2,8	64,5-100,0	8,9	10,9	-0,5
6	(Golib x Namangan-77) x Qizil baraka	10	18,2	10,2	10	32,2	30,1	1,1	93,5±1,8	73,1-100,0	5,7	5,9	1,0
7	(Golib x Namangan-77) x *G.mustelinum* Miers ex Watt	10	17,1	7,5	10	33,1	26,2	6,9	79,4±2,5	64,3-92,1	8,0	10,1	-0,7
8	(Golib x Namangan-77) x T-85	10	12,1	4,8	10	25,4	22,1	3,3	86,7±2,7	61,5-97,8	8,6	9,9	-0,7
9	(Andijon-35 x Namangan-77) x Qizil baraka	10	15,1	9,6	10	30,9	29,8	1,1	96,7±0,9	90,2-100,0	2,8	2,9	1,2
10	(Andijon-35 x Namangan-77) x *G.mustelinum* Miers ex Watt	10	17,8	9,1	10	28,7	23,5	5,2	81,9±1,8	68,9-93,3	5,5	6,8	-0,5
11	(Andijon-35 x Namangan-77) x T-85	10	10,1	3,7	10	24,1	21,2	2,9	88,3±2,7	70,4-100,0	8,7	9,8	-0,4
12	(Namangan-77 x Andijon-35) x Qizil baraka	10	14,4	8,8	10	32,1	30,4	1,7	94,7±1,4	83,3-100,0	4,3	4,5	0,1
13	(Namangan-77 x Andijon-35) x *G.mustelinum* Miers ex Watt	10	16,9	9,5	10	31,7	25,1	6,6	79,1±2,5	63,3-100,0	7,8	9,8	-0,8
14	(Namangan-77 x Andijon-35) x T-85	10	11,5	4,8	10	29,1	23,4	5,7	80,8±3,3	66,7-95,4	10,4	12,9	-1,7

Note: CV - coefficient of variation; hp - degree of dominance; values are presented as mean ± standard error.

Regarding the percentage of fully developed seeds per boll, the cultivar Golib exhibited the highest value (96.5%), whereas the wild species *G. mustelinum* Miers ex Watt demonstrated the lowest value (77.1%). In terms of variation amplitude, Golib, Andijan-35, and Namangan-77 displayed relatively narrow and similar ranges (80.6-100.0%), indicating greater genetic uniformity. In contrast, Qizil Baraka, *G. mustelinum*, and T-85 exhibited wider ranges of variation (62.5-100.0%), suggesting greater genetic divergence among these genotypes.

The coefficient of variation (V%) was lowest in Golib (2.4%) and highest in *G. mustelinum* Miers ex Watt (11.0%). These findings indicate that Golib possesses a more stable genetic system controlling seed development, whereas the wild species displays greater phenotypic variability. Such differences may substantially influence the expression and inheritance of productivity traits in hybrid populations.

The stability of a gene or gene complex responsible for the phenotypic expression of any quantitative trait can be assessed through the coefficient of variation of that trait. Low values of variation for quantitative characteristics generally indicate that the genes controlling their phenotypic expression are predominantly in a homozygous state and that the genotype has reached a high degree of varietal stabilization.

Based on the above-mentioned data and the results presented in Table 3.2, the cultivars Golib, Andijan-35, and Namangan-77 exhibited stable varietal characteristics for the traits under investigation. In contrast, the cultivar Qizil Baraka, the wild species *Gossypium mustelinum* Miers ex Watt, and the T-85 line appeared to possess less stable genetic systems controlling seed development within the boll. Such genetic differences among the experimental materials significantly influenced the expression of productivity traits in the resulting hybrid populations.

In reciprocal hybrids involving the cultivar Golib and various cultivars and lines, the total number of bolls per plant ranged from 7.8 to 19.1, while the number of opened bolls varied from 3.4 to 12.1. The highest performance was observed in reciprocal hybrids involving Namangan-77, whereas the lowest values were recorded in combinations with the T-85 line, where the total number of bolls and opened bolls amounted to only 7.8 and 3.4 per plant, respectively.

The percentage of fully developed seeds per boll in hybrids derived from Golib ranged from 81.4% to 97.8%. Higher values for this trait were observed in F_1 hybrids involving Andijan-

35, Namangan-77, and Qizil Baraka. In contrast, the hybrids Golib × *G. mustelinum* Miers ex Watt and Golib × T-85 exhibited comparatively lower percentages of fully developed seeds [12].

The broad variation amplitude (60-100%) and relatively high coefficients of variation (12.8% and 13.7%) observed in hybrids involving *G. mustelinum* Miers ex Watt and the T-85 line suggest considerable genetic divergence between these forms and the cultivar Golib with respect to the genes controlling seed development.

Analysis of inheritance patterns for the percentage of fully developed seeds per boll in F_1 populations derived from Golib and other parental forms revealed positive and negative overdominance, weak, moderate, and strong positive dominance, as well as moderate negative dominance.

The productivity traits observed in F_1 hybrids between Andijan-35 and Namangan-77, as well as those involving *G. mustelinum* Miers ex Watt, were generally comparable to the results obtained from Golib-derived hybrids. In reciprocal combinations of Andijan-35 × Namangan-77, the percentage of fully developed seeds per boll exhibited positive overdominance in both crossing directions (hp = 1.9 and 1.8). Even stronger overdominance effects were observed in F1 hybrids between Namangan-77 and Qizil Baraka, where hp values reached 4.4 and 6.5.

Similar trends were observed in reciprocal hybrids involving Namangan-77 and Qizil Baraka crossed with *G. mustelinum* Miers ex Watt and the T-85 line. The total number of bolls per plant ranged from 10.3 to 22.3. Among these combinations, Namangan-77 × Qizil Baraka, *G. mustelinum* Miers ex Watt × Namangan-77, and Qizil Baraka × *G. mustelinum* Miers ex Watt exhibited satisfactory numbers of opened bolls, averaging 11.8, 11.2, and 9.5 bolls per plant, respectively.

The highest coefficients of variation were recorded in F1 hybrids involving Namangan-77 and Qizil Baraka crossed with *G. mustelinum* Miers ex Watt and T-85, reaching 16.1%, 21.7%, and 20.2%, respectively (Table 1). These elevated values indicate substantial genetic variability within the hybrid populations and suggest considerable opportunities for obtaining recombinant genotypes valuable for future breeding programs.

Reciprocal F_1 hybrids obtained between the geographically distant and genomically divergent forms, namely the wild species *Gossypium mustelinum* Miers ex Watt and the T-85 line, produced 12.6-13.1 bolls per plant, whereas the number of opened bolls ranged from 3.1 to 4.2 per plant. In hybrids where *G. mustelinum* Miers ex Watt served as the maternal parent, the percentage of fully developed seeds per boll reached 90.5%, representing a relatively high value. However, due to the very low average number of opened bolls, this result cannot be considered favorable from a breeding perspective. Overall, all productivity-related traits evaluated in these reciprocal hybrids exhibited undesirable performance (Table 1).

To further investigate productivity traits in F1 hybrids, stepwise hybridization was carried out using F_1 progenies derived from reciprocal crosses among the cultivars Golib, Andijan-35, and Namangan-77, followed by crossing with the cultivar Qizil Baraka, the wild species *G. mustelinum* Miers ex Watt, and the T-85 line. The resulting F0 hybrid seeds were planted, F1 plants were obtained, and their productivity characteristics were subsequently evaluated (Table 1).

As a result of stepwise hybridization involving F_1 Golib × Andijan-35 plants crossed with Qizil Baraka, *G. mustelinum* Miers ex Watt, and T-85, the total number of bolls per plant ranged from 12.3 to 16.3, while the number of opened bolls varied from 4.4 to 8.2. The percentage of fully developed seeds per boll ranged from 81.1% to 95.9%.

The variation amplitude for this trait ranged from 62.1% to 100.0%, whereas the coefficient of variation varied between 4.0% and 12.2%. Analysis of inheritance patterns for the percentage of fully developed seeds per boll in the F_1 populations revealed positive and negative overdominance as well as moderate negative dominance.

The productivity traits observed in the stepwise hybrid combination F_1 (Golib × Andijan-35) × Qizil Baraka demonstrated the highest values among the studied populations. Intermediate performance was recorded in F_1 (Golib × Andijan-35) × *Gossypium mustelinum* Miers ex Watt, whereas the lowest productivity was observed in F_1 (Golib × Andijan-35) × T-85 hybrids. Based on these findings, it can be inferred that the genomic constitution of the F_1 Golib × Andijan-35 hybrid is genetically closer to the cultivar Qizil Baraka, moderately divergent from the wild species *G. mustelinum* Miers ex Watt, and substantially different from the T-85 line.

Similar patterns were observed in the remaining stepwise hybrid combinations. In general, F_1 progenies derived from reciprocal crosses among Golib, Andijan-35, and Namangan-77 exhibited superior productivity when crossed with Qizil Baraka, intermediate performance when crossed with *G. mustelinum* Miers ex Watt, and lower productivity when crossed with the T-85 line.

Conclusion.

Among the reciprocal F_1 hybrids, the highest productivity, as determined by total boll number per plant, number of opened bolls, and percentage of fully developed seeds per boll, was observed in hybrid combinations involving the cultivars Golib, Andijan-35, Namangan-77, and Qizil Baraka. Similarly, superior productivity performance was recorded in the stepwise hybrid combinations F_1 (Andijan-35 × Golib) × Qizil Baraka, F_1 (Golib × Namangan-77) × Qizil Baraka, F_1 (Andijan-35 × Namangan-77) × Qizil Baraka, F_1 (Andijan-35 × Namangan-77) × *G. mustelinum* Miers ex Watt, and F_1 (Namangan-77 × Andijan-35) × *G. mustelinum* Miers ex Watt.

These hybrid combinations were characterized by narrow ranges of variation for the percentage of fully developed seeds per boll, low coefficients of variation, and positive overdominance effects. Therefore, they can be recommended as promising initial breeding materials for cotton improvement programs aimed at increasing yield potential.

Analysis of reciprocal and stepwise F_1 hybrid populations revealed diverse inheritance patterns for the percentage of fully developed seeds per boll, including positive and negative overdominance as well as weak, moderate, and strong positive and negative dominance effects. In most cases, this trait tended to shift toward the parental genotype exhibiting lower expression values.

The results further demonstrated that hybridization between geographically distant forms creates opportunities for obtaining recombinant populations with broad genetic variability and enhanced breeding potential for productivity traits.

Moreover, the substantial genomic divergence among the parental forms used in the present study provides valuable novel genetic resources for future cotton breeding programs.

REFERENCES

1. Sirojidinov B., Rizayeva S., Abdullayev A. Avstraliya va Hindi-Xitoy g‘o‘za turlarining filogenetik munosabatlari. Monografiya. - Toshkent: Navro‘z, 2018. - 40 b.

2. Seyitmusaev A.I., Tishin A.I. Otbor na skorospelost i produktivnost staryx pokoleniyax gibridov // Voprosy genetiki, seleksii i semenovodstva xlopchatnika. - Tashkent, 1996. - S. 59-64.
3. Ernazarova Z.A. Mejvidovoe rodstvo C-genomnix xlopchatnikov i ix filogeneticheskie vzaimootnosheniya s D-genomnimi vidami: Dis. … kand. biol. nauk. - Tashkent: IG i EBR AN RUz, 1998. - 153 s.
4. Azimov A.A. Sopryajennost vilt-ustoychivosti s priznakom «Kolichestvo korobochek na rastenii» u mejvidovix gibridov xlopchatnika // Evraziyskiy Soyuz Uchenix. - 2019. - № 10(67). - S. 9-12.
5. Xolmatov X. Nasledovanie indeksa i vixoda volokna v F_1 mejlineynix gibridov xlopchatnika // O‘zbekiston biologiya jurnali. - 1978. - S. 73-75.
6. Karimova I.S. Vliyanie prodoljitelnoy pochvennoy zasuxi na fiziologicheskie protsessi u razlichnix sortov i liniy xlopchatnika: Avtoref. dis. … kand. biol. nauk. - Dushanbe, 2009. - 31 s.
7. Saidov R.F. Ekologogeneticheskiy analiz sistem attraksii, mikroraspredeleniya assimilantov i adaptivnosti u xlopchatnika i vyyavlenie tsennix donorov dlya seleksii: Avtoref. dis. … kand. s.-x. nauk. - Dushanbe, 2011. - 23 s.
8. Rao J.M., Gopinath P.M. Association analysis of yield and fibre quality characters in upland cotton (Gossypium hirsutum L.) // Australian Journal of Basic and Applied Sciences. - 2013. - Vol. 7, No. 8. - P. 787-790.
9. Avtonomov V.A., Kimsanbaev M.X. Nasledovanie chisla korobochek i produktivnosti xlopka-sirtsa odnogo rasteniya u geograficheski otdalyonnix gibridov F_1-F_2 Gossypium barbadense L. // Vestnik Agrarnoy Nauki Uzbekistana. - 2005. - No. 4(22). - S. 31-37.
10. Chorshanbiev N.E. Nasledovanie i izmenchivost priznaka «Kolichestvo korobochek na rastenii» u gibridov F_1-F_2 sortov Gossypium barbadense L. // Problemy sovremennoy nauki i obrazovaniya. - 2017. - № 4(86). - S. 19-22.
11. Murtaza N. Study of gene effects for boll number, boll weight and seed index in cotton // Journal of Central European Agriculture. - 2005. - Vol. 6, No. 3. - P. 255-262.
12. Mamajonov A.A., Muminov A.A. Urojaynost u postoyannix i mejvidovix gibridov F_1 u xlopchatnika // Nauka molodix - nauka budushchego: materialy III Mejdunarodnoy nauchno-prakticheskoy konferensii. - Petrozavodsk: MCNP «Novaya nauka», 2023. - S. 286-290.

OPTIMIZATION OF POSTOPERATIVE REHABILITATION AFTER HYSTERECTOMY IN WOMEN WITH BENIGN UTERINE TUMORS: A COMPARATIVE ANALYSIS OF LAPAROSCOPIC AND OPEN SURGICAL APPROACHES

D. Rahmatullayeva
First-year Master's student, Department of Obstetrics and Gynecology, Tashkent State Medical University
https://doi.org/10.5281/zenodo.20694618

Abstract. *Benign uterine tumors remain among the most prevalent gynecological disorders affecting women of reproductive and perimenopausal age. Despite significant advances in conservative treatment and organ-preserving interventions, hysterectomy continues to be one of the most frequently performed gynecological operations worldwide. The choice of surgical access plays a decisive role not only in the immediate postoperative outcome but also in the duration and quality of rehabilitation. In recent decades, laparoscopic hysterectomy has become increasingly widespread due to its minimally invasive nature and reduced surgical trauma. However, abdominal hysterectomy performed through laparotomy still maintains clinical relevance in complicated cases involving large uterine masses, severe adhesions, or combined pelvic pathology. The present article examines modern approaches to optimizing postoperative rehabilitation in women with benign uterine tumors and provides a comparative analysis of laparoscopic and laparotomic hysterectomy. Particular attention is given to postoperative pain syndrome, psychoemotional adaptation, recovery dynamics, quality of life indicators, and the role of ERAS protocols in improving rehabilitation outcomes. The findings demonstrate that minimally invasive surgery significantly accelerates physical and social recovery, while multidisciplinary rehabilitation strategies contribute to better long-term clinical results.*

Keywords: *benign uterine tumors, hysterectomy, laparoscopy, laparotomy, rehabilitation, quality of life, ERAS protocol, gynecological surgery.*

INTRODUCTION

Benign uterine tumors constitute a significant medical and social problem in contemporary gynecology due to their high prevalence, recurrent clinical course, and considerable impact on women's physical and psychological health. Uterine leiomyoma, adenomyosis, and endometrial hyperplasia are among the most common benign gynecological diseases requiring surgical treatment. Epidemiological observations indicate that uterine fibroids may occur in more than half of women over the age of forty, while adenomyosis is increasingly diagnosed among women of active reproductive and working age. Although modern pharmacological therapy and minimally invasive interventions have expanded treatment possibilities, hysterectomy remains the definitive therapeutic method in patients with persistent symptoms, recurrent bleeding, chronic pelvic pain, rapid tumor growth, or resistance to conservative management. Hysterectomy is currently the most common gynecological procedure performed globally. Even though this procedure is clinically effective, there are frequently a number of physiological and psychological difficulties during the postoperative phase. Significant postoperative pain, delayed mobilization, hormonal imbalance,

chronic exhaustion, mental instability, sleep difficulties, anxiety, and a lower quality of sexual life are all possible outcomes for women having hysterectomies. In many patients, the removal of the uterus is linked to severe psychological stress pertaining to social adaption, reproductive identity, and femininity perception in addition to physical damage. As a result, one of the main concerns in contemporary gynecological surgery is the optimization of postoperative rehabilitation. The approach to postoperative care in gynecology has significantly changed due to the quick development of minimally invasive surgical technology. Because laparoscopic hysterectomy enables the surgeon to carry out intricate procedures with less tissue damage, smaller incisions, and a lower inflammatory reaction, it has grown in popularity. Laparoscopic surgery is typically linked to less blood loss, less postoperative pain, a shorter hospital stay, and a quicker return to normal activity when compared to standard abdominal hysterectomy with laparotomy. However, in complex instances, such as those involving enormous uterine fibroids, significant pelvic adhesions, severe obesity, or anatomical abnormalities that impede laparoscopic visualization, laparotomy is still clinically warranted.

MATERIALS AND METHODS

The present study analyzed postoperative rehabilitation outcomes in women with benign uterine tumors who underwent hysterectomy through either laparoscopic or open abdominal approaches. The analysis included 120 patients aged between 35 and 55 years. Sixty women underwent laparoscopic hysterectomy, while the remaining sixty patients were treated using conventional laparotomy. The study evaluated postoperative pain intensity, blood loss, duration of hospitalization, psychoemotional condition, quality of life, and rehabilitation dynamics.

RESULTS AND DISCUSSION

Clinical observations demonstrated substantial differences between the two surgical approaches. Patients who underwent laparoscopic hysterectomy generally showed more favorable postoperative recovery. Reduced surgical trauma contributed to earlier mobilization and significantly lower pain intensity during the first postoperative days. Women treated laparoscopically required fewer narcotic analgesics and demonstrated earlier restoration of gastrointestinal function and physical independence. In contrast, patients after laparotomy more frequently experienced prolonged weakness, abdominal discomfort, delayed mobilization, and higher emotional distress caused by extensive surgical wounds and longer hospitalization. The mean intraoperative blood loss in laparoscopic surgery remained significantly lower than in open surgery, according to the comparison analysis. While patients following a laparotomy frequently needed more than a week of inpatient care, the laparoscopic group's typical hospital stay was three to four days. Patients who underwent laparoscopic surgery recovered to full physical activity almost twice as quickly as those who underwent abdominal hysterectomy.

Clinical Indicators	Laparoscopy	Laparotomy
Average blood loss	120 ± 35 ml	340 ± 60 ml
Mean hospital stay	3–4 days	7–10 days
Postoperative pain intensity	Mild to moderate	Moderate to severe
Recovery of physical activity	2–3 weeks	6–8 weeks
Frequency of postoperative	Lower	Higher

complications		

Psychoemotional adaption is a crucial component of postoperative rehabilitation. Many patients expressed mental instability following surgery, worries about sexual function, and anxiety related to changes in body image. Due to prominent postoperative scars, protracted pain syndrome, and delayed social reintegration, these symptoms were more noticeable in women who had laparotomies. Numerous patients expressed worry about their future quality of life and dread of losing their femininity, according to clinical interviews. These results demonstrate that effective surgical rehabilitation requires psychological care and counselling in addition to physical recuperation.

In recent years, the concept of quality of life has become one of the key indicators for evaluating surgical outcomes in gynecology. Assessment using internationally recognized scales such as SF-36 demonstrated that women after laparoscopic hysterectomy achieved significantly better results in physical functioning, emotional stability, social activity, and overall life satisfaction. Most patients from the minimally invasive surgery group returned to professional and family activities earlier and reported less fatigue, improved sleep quality, and higher postoperative self-confidence. Particular attention in modern surgical practice is currently directed toward ERAS (Enhanced Recovery After Surgery) protocols, which represent an evidence-based multidisciplinary approach to perioperative care. The ERAS strategy includes detailed preoperative counseling, shortened fasting periods, minimally invasive surgical techniques, multimodal analgesia, prevention of thromboembolic complications, early nutrition, and early mobilization. The integration of ERAS principles into gynecological surgery has significantly improved postoperative outcomes and reduced complication rates. Women managed according to ERAS protocols demonstrated shorter hospitalization, reduced opioid consumption, faster intestinal recovery, and higher satisfaction with treatment results. Early beginning of physical activity is critical to the success of rehabilitation following a hysterectomy. Early mobilization reduces the incidence of venous thrombosis, increases intestinal motility, enhances lung ventilation, and improves emotional state. Postoperative stability is greatly aided by respiratory exercises, a gradual increase in walking activity, physiotherapy techniques, and customized rehabilitation plans. Simultaneously, multimodal pain treatment is essential for enhancing the quality of rehabilitation since sufficient analgesia allows patients to continue exercising and lessens stress reactions following surgery.

Indicators	**Standard Management**	**ERAS Protocol**
Hospital stay	7.5 days	3.6 days
Postoperative complications	18%	7%
Opioid analgesic use	High	Reduced
Recovery of physical activity	Delayed	Accelerated
Patient satisfaction	Moderate	High

Overall, the findings of the present analysis confirm that laparoscopic hysterectomy offers substantial benefits in postoperative rehabilitation compared with conventional laparotomy. Reduced operative trauma, lower inflammatory response, faster mobilization, improved cosmetic outcomes, and better psychoemotional adaptation collectively contribute to enhanced quality of

life and earlier social reintegration. Nevertheless, optimal rehabilitation outcomes are achieved not only through surgical technique itself but also through comprehensive perioperative management integrating physical rehabilitation, psychological support, effective pain control, and ERAS-based recovery strategies.

CONCLUSION

The optimization of postoperative rehabilitation after hysterectomy in women with benign uterine tumors remains one of the most important challenges in contemporary gynecological practice. The growing prevalence of uterine leiomyoma, adenomyosis, and endometrial hyperplasia among women of reproductive and perimenopausal age significantly increases the need for effective surgical treatment methods combined with comprehensive rehabilitation strategies. Although hysterectomy continues to be a highly effective and frequently performed operation, postoperative recovery largely determines the long-term physical, emotional, and social outcomes for patients. The findings of the present study demonstrate that laparoscopic hysterectomy provides considerable clinical advantages compared with conventional abdominal hysterectomy performed through laparotomy. Reduced surgical trauma, lower intraoperative blood loss, minimal postoperative pain, shorter hospitalization, and faster restoration of physical activity contribute to improved rehabilitation efficiency and earlier return to daily and professional activities. In addition, minimally invasive surgery is associated with better cosmetic outcomes and reduced risk of postoperative adhesions and infectious complications, which further enhances patient satisfaction and quality of life.

REFERENCES

1. Aarts J.W., Nieboer T.E., Johnson N., Tavender E., Garry R., Mol B.W., Kluivers K.B. Surgical approach to hysterectomy for benign gynecological disease. Cochrane Database of Systematic Reviews. 2015;8:CD003677.
2. Donnez J., Dolmans M.M. Uterine fibroid management: from the present to the future. Human Reproduction Update. 2016;22(6):665–686.
3. Wright J.D., Herzog T.J., Tsui J., et al. Nationwide trends in the performance of inpatient hysterectomy in the United States. Obstetrics & Gynecology. 2013;122(2):233–241.
4. Nieboer T.E., Johnson N., Lethaby A., et al. Surgical approach to hysterectomy for benign gynaecological disease. BJOG: An International Journal of Obstetrics and Gynaecology. 2009;116(7):902–910.
5. Kehlet H., Wilmore D.W. Evidence-based surgical care and the evolution of fast-track surgery. Annals of Surgery. 2008;248(2):189–198.
6. Nelson G., Altman A.D., Nick A., et al. Guidelines for postoperative care in gynecologic oncology surgery: Enhanced Recovery After Surgery (ERAS) Society recommendations. Gynecologic Oncology. 2016;140(2):323–332.
7. Stewart E.A., Cookson C.L., Gandolfo R.A., Schulze-Rath R. Epidemiology of uterine fibroids: a systematic review. BJOG. 2017;124(10):1501–1512.
8. Vitale S.G., Tropea A., Rossetti P., Carnelli M., Cianci A. Management of uterine leiomyomas in pregnancy: review of literature. Updates in Surgery. 2013;65(3):179–182.
9. Carlson K.J., Miller B.A., Fowler F.J. The Maine Women’s Health Study: outcomes of hysterectomy. Obstetrics & Gynecology. 1994;83(4):556–565.
10. Kluivers K.B., Hendriks J.C., Mol B.W., Bongers M.Y., Vierhout M.E., Brölmann H.A. Quality of life and surgical outcome after total laparoscopic hysterectomy versus total

abdominal hysterectomy for benign disease. Journal of Minimally Invasive Gynecology. 2007;14(2):145–152.

11. Ljungqvist O., Scott M., Fearon K.C. Enhanced Recovery After Surgery: A Review. JAMA Surgery. 2017;152(3):292–298.
12. Kalogera E., Dowdy S.C. Enhanced Recovery Pathways in Gynecologic Surgery: Improving Outcomes Through Evidence-Based Medicine. Obstetrics and Gynecology Clinics of North America. 2016;43(3):551–573.
13. Flory N., Bissonnette F., Binik Y.M. Psychosocial effects of hysterectomy: literature review. Journal of Psychosomatic Research. 2005;59(3):117–129.
14. Walsh C.A., Walsh S.R., Tang T.Y., Slack M. Total abdominal hysterectomy versus total laparoscopic hysterectomy for benign disease: systematic review and meta-analysis. European Journal of Obstetrics & Gynecology and Reproductive Biology. 2009;144(1):3–7.
15. Johnson N., Barlow D., Lethaby A., Tavender E., Curr E., Garry R. Methods of hysterectomy: systematic review and meta-analysis of randomised controlled trials. BMJ. 2005;330(7506):1478.
16. Gambone J.C., Reiter R.C., Lench J.B., Moore J.G. The impact of hysterectomy on quality of life in women. Obstetrics & Gynecology. 2000;96(1):1–6.
17. Tinelli R., Malvasi A., Mynbaev O.A., et al. The surgical outcome of intracapsular cesarean hysterectomy versus total hysterectomy. Archives of Gynecology and Obstetrics. 2014;289(3):517–523.
18. Uccella S., Cromi A., Bogani G., et al. Systematic implementation of laparoscopic hysterectomy independent of uterus size. Journal of Minimally Invasive Gynecology. 2013;20(4):505–516.
19. Barber E.L., Van Le L. Enhanced Recovery Pathways in Gynecology and Gynecologic Oncology. Obstetrics and Gynecology Clinics. 2015;42(1):173–185.
20. Kho R.M., Abrão M.S. Intraoperative and postoperative complications of hysterectomy. Clinical Obstetrics and Gynecology. 2014;57(1):43–57.

NON-ALCOHOLIC FATTY LIVER DISEASE: A REVIEW OF EPIDEMIOLOGY, PATHOPHYSIOLOGY, CLINICAL COURSE AND DIAGNOSIS METHODS

B.I. Urinov[1], N.M. Djuraeva[2]
Radiologist, the 1st Central Consultative and Diagnostic Polyclinic under the Main Medical Directorate of the Administration of the President of the Republic of Uzbekistan[1]
DSc, Head of Department of Computed and Magnetic Resonance Imaging in State Institution "Republican Specialized Scientific and Practical Medical Center for Surgery named after Academician V. Vakhidov"[2]
https://doi.org/10.5281/zenodo.20808668

Abstract. *With the increasing prevalence of obesity and diabetes in many countries around the world, non-alcoholic fatty liver disease (NAFLD) is becoming one of the leading causes of liver cirrhosis and hepatocellular cancer. Effective management of NAFLD requires a broad understanding of its development mechanisms, as well as the use of advanced diagnostic and therapeutic methods, making this topic relevant to the scientific and medical community. The use of a variety of radiological techniques, such as MRI with fatty infiltration and elastography, provides a reliable alternative to liver biopsy. An integrated approach to the problem of NAFLD helps to improve the efficiency of diagnosis and develop individual strategies for the treatment and prevention of this disease. The article presents a literature review covering current aspects of multimodal radiodiagnosis of non-alcoholic fatty liver disease.*

Keywords: *non-alcoholic fatty liver disease, steatohepatitis, radiation diagnostics, magnetic resonance imaging, transient elastography.*

Introduction. Liver disease remains a global concern across all age demographics [1]. In the late 1990s and early 2000s, there was a fivefold increase in the incidence of non-alcoholic fatty liver disease (NAFLD) among individuals aged 18–39 years [2, 3]. As individuals reach the age of 50, the incidence of fatty liver disease tends to rise, reaching its peak in the 50–59 age group.

According to the World Gastroenterological Organization, NAFLD and non-alcoholic steatohepatitis (NASH) became the predominant liver diseases in Western countries by the mid-2000s. During this period, the overall prevalence of NAFLD doubled, while the prevalence of other chronic liver diseases either remained stable or declined [4]. The escalating global incidence of NAFLD has spurred increased interest in non-invasive methods for accurately assessing liver fat content in vivo.

Definition of the pathological condition, epidemiological, and etiopathogenetic aspects of NAFLD.

The term "non-alcoholic fatty liver disease (NAFLD)" encompasses various liver pathologies of metabolic origin, confirmed by morphological evidence of steatosis, steatohepatitis, fibrosis, cirrhosis, or adenocarcinoma, in the absence of exogenous toxic factors damaging the liver [5]. Until 2020, debates persisted regarding the clarity of the term "NAFLD."

In 2020, a consortium of experts from 22 countries proposed a new consensus concept, Metabolically Associated Fatty Liver Disease (MAFLD), which encompasses etiological factors

such as overweight, type 2 diabetes, and metabolic syndrome leading to fatty liver disease, primarily not associated with chronic alcohol consumption [6].

MAFLD and NAFLD refer to distinct patient populations: MAFLD applies to patients with designated metabolic risk factors and steatosis, while NAFLD encompasses patients without metabolic risk factors but with steatosis. The revised interpretation of MAFLD facilitates tailored treatment and diagnostic approaches for individual patients with various comorbidities associated with MAFLD [6].

Advocates of the MAFLD criteria contend that they outperform NAFLD criteria in identifying patients at high risk of liver fibrosis, a key determinant of mortality in fatty liver disease [7]. However, it is suggested that WHO-approved ICD-11 disease codes be used in routine practice.

According to Z.M. Younossi et al. (2016), the global prevalence of NAFLD in 2016 was 24% [5]. A more recent study indicated an incidence of NAFLD of up to 32%, suggesting that NAFLD will dominate clinical hepatology in the 21st century [8].

The high prevalence of NAFLD is primarily attributed to the rising rates of obesity and diabetes mellitus. Surprisingly, even among individuals with a normal body mass index (BMI), the incidence of NAFLD in 2022 was 9%. Furthermore, the incidence of NAFLD has risen across all regions, with the most significant increases observed in the Middle East, North America, and East Asia [9].

In the United States, the prevalence of NAFLD in adults was 24.13% in 2016 and is projected to rise to 33.5% by 2030, with an estimated 100.9 million cases of NAFLD by that year [10]. A modeling study predicts a 56% increase in the prevalence of NASH by 2030, accompanied by a twofold rise in associated mortality. The current overall prevalence of NAFLD in Asia stands at 27.37% [5].

The escalating prevalence of MAFLD is attributed, in part, to chronic hepatitis B (CHB) being the primary cause of chronic liver diseases in Asia. Although virological outcomes in patients with CHB and MAFLD are favorable, MAFLD has been independently associated with fibrosis progression and poorer prognoses in patients with CHB.

Mortality rates for NAFLD and NASH in 2022 were 0.77 per 1000 and 11.77 per 1000 person-years, and 15.44 per 1000 and 25.56 per 1000 person-years, respectively. Patients with NAFLD have a 34-69% higher likelihood of death within the next 15 years compared to the general population [11]. Several studies have compared the prevalence of MAFLD and NAFLD, generally finding that the prevalence of MAFLD closely mirrors that of NAFLD, albeit slightly higher for obvious reasons [7].

Overall, information on the prevalence of NAFLD/MAFLD and NASH varies widely in terms of definitions, characteristics of study populations, diagnostic methods used, and follow-up periods.

In modern gastroenterology, NAFLD is considered an etiologically heterogeneous disease, characterized by the excessive accumulation of neutral fat - triglycerides and free fatty acids - both inside hepatocytes and extracellularly. This process is accompanied by progressive aseptic inflammation and subsequent fibrosis, triggering a cascade of pathological processes. NAFLD is closely associated with demographic changes (aging population), unhealthy lifestyle (overeating, lack of exercise), and cardiovascular and metabolic diseases (type 2 diabetes, hypertension, dyslipidemia).

Currently, the pathogenesis of NAFLD is considered multifactorial, including processes such as insulin resistance (IR), lipotoxicity, inflammation, imbalance of cytokines and adipokines, activation of innate immunity and microbiota, exposure to environmental and genetic factors.

Clinical course and comorbidity in NAFLD.

In NAFLD, hepatic steatosis occurs without signs of inflammation, whereas in NASH, hepatic steatosis is associated with lobular inflammation and apoptosis, which can lead to liver fibrosis and cirrhosis [12].

NASH can progress and predispose to the development of hepatocellular carcinoma (HCC), which can develop in the absence of cirrhosis. By 2030, the incidence of HCC associated with NAFLD is projected to increase sharply in China, France, and the United States, with increases of 82%, 117%, and 122% compared with 2016, respectively [13].

Age-related characteristics are of great importance in predicting the course and outcome of NAFLD [2]. Several studies have revealed significant gender differences in the clinical manifestations of NAFLD. The prognosis for the development of NAFLD in premenopausal women is more favorable compared to postmenopausal women and men. It has been established that NAFLD more often affects men [14].

Over the past two decades, there has been an increasing trend in the incidence of MAFLD among Asians, who accumulate liver fat at a lower body mass index (BMI) than other races. In such patients, the disease is more severe with more pronounced inflammation and balloon degeneration [15].

NAFLD and MetS are often described as an interrelated process because they share a common pathophysiological mechanism, but each predicts and worsens the outcome of the other, significantly increasing the risk of cardiovascular events and cardiovascular disease (CVD) [16].

Recently, hepatic steatosis has been considered an independent risk factor for cardiovascular disease, but also for kidney disease and cancer [17].

It has been established that NAFLD is associated with the main markers of CVD, namely: endothelial dysfunction, increased impulse wave velocity, and increased calcification of the coronary arteries. At the same time, it should be noted that the issue of the connection between NAFLD/MAFLD and an increase in non-fatal cardiovascular events and death is still a matter of debate [18].

In 2016, the European Association for the Study of the Liver (EASL) published clinical practice guidelines for the management of patients with NAFLD in the setting of obesity, which is a major risk factor for the development and progression of NAFLD and insulin resistance [19].

At the first stage of diagnosis, it is necessary to differentiate NAFLD from alcoholic fatty liver disease (AFLD). When diagnosing NAFLD in non-obese patients, the recommendation of the American Gastroenterological Association (2022) should be taken into account, namely: to determine the presence of other causes of fatty liver, in particular: the presence of metabolic syndrome, HIV, lipodystrophy, lysosomal acid lipase deficiency, familial hypobetalipoproteinemia, and hepatic steatosis, caused by drugs such as methotrexate, amiodarone, tamoxifen, and steroids.

NAFLD/MAFLD and Liver Transplantation

There is no doubt that NAFLD/MAFLD and NASH, and in case of their progression, cirrhosis, and primary liver cancer require expensive treatment, including liver transplantation [9]. The number of patients with terminal or progressive liver disease associated with NAFLD who

require liver transplantation is growing, outpacing the need for transplantation in patients with hepatitis C [20].

Since NAFLD is the second most common pathology requiring liver transplantation and, according to forecasts, will become the leading one over the next decade, an accurate assessment of the possibility of developing steatohepatosis in such patients plays a decisive role in the prognosis of NAFLD and the success of therapy [21].

On the other hand, it is extremely important in this aspect to study potential living donors who donate a liver fragment during related transplantation for NAFLD. Most studies from leading transplant centers around the world have shown that donors with mild steatosis have an increased risk of NAFLD and that liver grafts from these donors may negatively impact liver transplant success [20].

Diagnostic Aspects of NAFLD

Histological examination is still considered the gold standard for diagnosing fatty liver [22]. Various approaches can be used to obtain a liver tissue sample. These include biopsy guided by ultrasonography (ultrasound) or computed tomography (CT).

An endoscopic approach using ultrasound (EUS) has been described [23]. In modern clinical practice, biopsy is a reliable method for differentiating NAFLD from NASH and detecting fibrosis. However, a biopsy is an invasive and painful procedure and requires six or more hours of bed rest.

In addition, its cost and risk of complications should be taken into account, as well as the uneven distribution of fibrosis in the liver, which makes it difficult to create a holistic picture of liver damage [24].

In addition, estimates made from biopsy results are subject to significant intraobserver and interobserver variability. There is also a fairly wide list of conditions when this procedure is contraindicated. Absolute contraindications to liver biopsy include: infectious and inflammatory diseases of the abdominal organs, suspicion of vascular lesions, hemostasis disorders, severe hypofibrinogenemia, sepsis, and ascites. Relative contraindications include cardiac or respiratory failure, respiratory tract infections, and anemia. In clinical practice, to identify NAFLD, track disease processes, and monitor the effectiveness of treatment, preference is often given to effective non-invasive diagnostic methods.

Thus, it has been established that liver fat content, determined using magnetic resonance imaging (MRI) and magnetic resonance spectroscopy (MRS), closely correlates with histological assessments of liver fat content in populations of patients with NAFLD, as well as with each other [25].

Diagnostic Value of Radioimaging Methods in the Assessment of NAFLD/MAFLD

Ultrasound (US) is the main screening method for the visual diagnosis of moderate to severe NAFL/NASH. Ultrasound diagnostic criteria for identifying NAFL/NASH include several key features such as echo attenuation, liver hyperechogenicity, increased echogenicity, and changes in vascular pattern. However, it should be noted that the presence of fibrosis may complicate the diagnosis as the texture of the liver echo becomes coarser.

The level of fatty infiltration also affects the effectiveness of ultrasound. The sensitivity of this method increases with increasing degree of fatty infiltration, but in obesity its diagnostic accuracy may decrease. With mild steatosis, the sensitivity of ultrasound may be low, and with steatosis less than 20% it may not be detected [26]. It is interesting to note that in the early stages of NAFL/NASH, new approaches are being used for more accurate diagnosis and prognosis,

including the calculated ratio of ultrasound characteristics of the liver and kidneys, as well as the frequency of attenuation of the ultrasound intensity of the liver. In general, ultrasound is an accessible and relatively inexpensive method for diagnosing NAFL/NASH, but its disadvantages include the inability to quantify, dependence on the level of fatty infiltration, and limited ability to distinguish the initial stages of steatosis from NASH, as well as the influence of hemochromatosis and methodological factors on the results of the study.

A review of the literature highlights the importance of elastography, particularly transient elastography (TE) and acoustic radiation force imaging (ARFI). The TRE method, which includes field of study requirements, may be limited in obesity and some other circumstances. Point shear wave elastography (pSWE) has also been used to diagnose liver fibrosis, demonstrating good sensitivity and specificity, especially for cirrhosis.

However, this method has its limitations, including the inability to quantify and the inability to determine tissue composition [27]. An alternative is two-dimensional shear wave elastography (2D-SWE), which has several advantages, including the ability to select the area of interest and create a color map. This method is also used to assess fibrosis stage and predict recurrence of hepatocellular carcinoma.

Despite their effectiveness, elastography methods are susceptible to false-positive results caused by various factors, such as elevated transaminase levels, extrahepatic cholestasis, and others. In addition, some studies offer criteria to identify unreliable liver stiffness measurements. Overall, elastography remains an important tool for diagnosing and assessing the degree of liver fibrosis, but its use requires consideration of various factors that affect the accuracy of the results.

A study of factors influencing the accuracy of liver stiffness measurements highlights older age, increased body mass index (BMI), and non-hepatitis B liver damage as independent but less powerful predictors of errors. Other researchers have also identified a number of factors that negatively affect the accuracy of such measurements, including a BMI greater than 30 kg/m2, female gender, age over 50 years, and others. However, the effect of steatosis on transient elastography (TRE) results remains controversial.

In cases with equivocal results, single-photon emission computed tomography (CT) of the liver is used, which can detect steatosis by several signs, including changes in liver radiation density and others. Despite this, the specificity of CT in assessing fatty liver disease may be poor and is more often recommended when liver neoplasms are suspected. Some studies also indicate the high ability of CT to detect steatosis without contrast enhancement, but the method has limitations, including radiation exposure and others.

Magnetic resonance imaging (MRI), which has high sensitivity and specificity, is often used to reliably diagnose NAFL/NASH [28]. However, estimates of MRI accuracy may vary depending on the machine model and patient characteristics. MRI has a number of advantages and disadvantages, such as high cost, scanning time, and dependence on the experience of the specialist.

MRI elastography is a promising method for assessing the degree of liver fibrosis, although its use is also limited by certain factors, such as the patient's excess body weight and the presence of metal implants.

It is recommended to detect NASH in patients with type 2 diabetes using MRI, using the assessment of fatty infiltration by calculating the proton density of fat, and determining the degree of liver fibrosis using the MRI elastography method [29]. This method has advantages such as the

ability to evaluate the entire liver and high yield in cirrhosis, although it also has the disadvantages of MRI.

There is inconsistency in comparing the effectiveness of MRI elastography and TrE, which requires further research. Some researchers have stated that acoustic radiofrequency indexing (ARFI) provides better results in liver assessment. A meta-analysis of 13 studies on liver fibrosis by S. Bota et al. (2013) did not reveal significant differences between pSWE/ARFI and TrE [30].

Developments in magnetic resonance imaging techniques include in-phase/out-of-phase (IP/OP) imaging, Dixon technique, and hydrogen MR spectroscopy (H1-MRS) [31]. The main advantage of these methods over ultrasound and computed tomography is the use of a calculated ratio of liver fat proton density to total liver proton density [32]. H1-MRS is capable of detecting even minor lipid accumulation in the liver parenchyma, while its sensitivity and specificity are comparable to biopsy (95-98% and 94-96%, respectively) [33]. These results have been confirmed by several studies [34].

Factors such as age, gender, BMI, and comorbidity do not have a significant impact on the diagnostic accuracy of MRI-PDFF in NAFLD [35]. MRI spectroscopy is a promising method for diagnosing NAFLP, allowing one to study metabolic processes in the liver [8].

Ultrahigh-precision MRS can detect changes in energy metabolism in patients with NASH but requires consideration of various interferences, especially in the early stages of steatosis [36]. Some clinics use bioelectrical impedance analysis for the initial diagnosis of NASH in patients with sarcopenic obesity, although this method is not yet widely used [37].

Despite some limitations, MRI-PDFF is considered the most accurate method for detecting fatty liver disease, while MRE can more accurately assess the extent of liver damage. The combination of MRI-PDFF and MRE allows risk stratification in patients with NAFLD. However, cost and wait times for results remain a challenge for many healthcare institutions [38].

Conclusion.

Timely radiological diagnosis of NAFLD and identification of potential risk factors for poor prognosis play a key role in preventing disease progression. This allows you to detect liver damage in the early stages, choose the appropriate treatment method, and prevent further deterioration of the patient’s condition.

Optimizing the combined use of quantitative imaging modalities, taking into account medical, technical, and social aspects, may provide a reliable and safe alternative to liver biopsy for the diagnosis and monitoring of NAFLD, thereby increasing the effectiveness of treatment.

With an integrated approach to the problem of NAFLD and a deeper understanding of the pathological processes associated with this disease, the collection of information is accelerated, the diagnostic process is improved, and individualized treatment and prevention methods are identified for different age and gender groups of patients with NAFLD.

REFERENCES

1. Vassilopoulos A, Kalligeros M, Vassilopoulos S et al. Prevalence of Steatotic Liver Disease Among US Adults with Rheumatoid Arthritis. Dig Dis Sci. 2024 Jan 6; doi: 10.1007/s10620-023-08225-4.
2. Allen AM, Therneau TM, Larson JJ et al. Nonalcoholic fatty liver disease incidence and impact on metabolic burden and death: a 20 year-community study. Hepatology. 2018;67(5):1726–1736. doi: 10.1002/hep.29546.

3. Leoni S, Tovoli F, Napoli L. et al. Current guidelines for the management of non-alcoholic fatty liver disease: A systematic review with comparative analysis. World J Gastroenterol. 2018; 24:3361–3373, doi:10.3748/wjg. v24.i30.3361.
4. LaBrecque D, Abbas Z, Anania F et al. Global Guidelines Nonalcoholic Fatty Liver Disease and Nonalcoholic Steatohepatitis. World Gastroenterology Organization. J Clin Gastroenterol. June 2014; 48(6). doi:10.1097/MCG.0000000000000116.
5. Younossi ZM, Koenig AB, Abdelatif D et al. Global epidemiology of nonalcoholic fatty liver disease – meta-analytic assessment of prevalence, incidence, and outcomes. Hepatology. 2016 Jul;64(1): 73-84.doi: 10.1002/hep.28431.
6. Eslam M, Sanyal AJ, George J. MAFLD: a consensus driven proposed nomenclature for metabolic associated fatty liver disease. Gastroenterology. 2020 Feb 8. doi: 10.1053/j.gastro.2019.11.312.
7. Alharthi J, Gastaldelli A, Cua IH et al. Metabolic dysfunction-associated fatty liver disease: a year in review. Curr Opin Gastroenterol 2022; 38:000–000. doi:10.1097/MOG.0000000000000823.
8. Thiagarajan P, Bawden SJ, Aithal GP. Metabolic Imaging in Non-Alcoholic Fatty Liver Disease: Applications of Magnetic Resonance Spectroscopy. J Clin Med. 2021 Feb 7;10(4):632. doi: 10.3390/jcm10040632.
9. Riazi K, Azhari H, Charette JH et al. The prevalence and incidence of NAFLD worldwide: a systematic review and meta-analysis. Lancet Gastroenterol Hepatol. 2022 7(9):851–861. https://doi.org/10.1016/S2468-1253(22)00165-0.
10. Estes C, Anstee QM, Arias-Loste MT et al. Modeling NAFLD disease burden in China, France, Germany, Italy, Japan, Spain, United Kingdom, and United States for the period 2016-2030. J Hepatol. 201; 69(4):896–904. https://doi.org/10.1016/j.jhep.2018.05.036.
11. Benedict, M.; Zhang, X. Non-alcoholic fatty liver disease: An expanded review. World journal of hepatology 2017, 9, 715. doi: 10.4254/wjh.v9.i16.715.
12. Machado MV, Diehl AM. Pathogenesis of nonalcoholic steatohepatitis. Gastroenterology. 2016;150(8):1769–77. doi: 10.1053/j.gastro.2016.02.066.
13. Huang, D.Q., El-Serag, H.B. & Loomba, R. Global epidemiology of NAFLD-related HCC: trends, predictions, risk factors and prevention. Nat Rev Gastroenterol Hepatol. 2021;18, 223–238. https://doi.org/10.1038/s41575-020-00381-6.
14. Yang JD., Abdelmalek MF., Pang H. et al. Gender and menopause impact severity of fibrosis among patients with nonalcoholic steatohepatitis. Hepatology. 2014;59(4):1406–1414. doi: 10.1002/hep.26761.
15. Gao E, Hercun J, Heller T, Vilarinho S. Undiagnosed liver diseases. Transl Gastroenterol Hepatol. 2021; 6: 28.doi: 10.21037/tgh.2020.04.04.
16. Fresneda, S, Abbate M., Busquets-Cortés C. et al. Sex and age differences in the association of fatty liver index-defined non-alcoholic fatty liver disease with cardiometabolic risk factors: a cross-sectional study. Biol Sex Differ. 2022;13, 64. https://doi.org/10.1186/s13293-022-00475-7.
17. Byrn CD. Targher G. NAFLD: a multisystem disease. Journal of Hepatology. 2015;62(1S): 47–64. doi: 10.1016/j.jhep.2014.12.012.
18. Francque SM, van der Graaff D , Kwanten WJ. Non-alcoholic fatty liver disease and cardiovascular risk: Pathophysiological mechanisms and implications. J Hepatol. 2016 Aug;65(2):425-43. doi: 10.1016/j.jhep.2016.04.005.

19. EASL-EASD-EASO Clinical Practice Guidelines for the management of non-alcoholic fatty liver disease. J Hepatol. 2016; 64:1388–1402. doi: 10.1016/j.jhep.2015.11.004.
20. Burra P, Becchetti C, Germani G et al. NAFLD and liver transplantation: Disease burden, current management and future challenges. JHEP Rep. 2020 Oct 9; 2(6):100192. doi: 10.1016/j.jhepr.2020.100192.
21. Starekova, J, Reeder SB. Liver fat quantification: where do we stand? Abdom Radiol (NY) 2020; 45:3386–3399, doi:10.1007/s00261-020-02783-1.
22. Pouwels S, Sakran N, Graham Y et al. Non-alcoholic fatty liver disease (NAFLD): a review of pathophysiology, clinical management and effects of weight loss. BMC Endocr Disord. 2022;22, 63. https://doi.org/10.1186/s12902-022-00980-1.
23. Chandan S, Deliwala S, Khan SR et al. EUS-guided versus percutaneous liver biopsy: A comprehensive review and meta-analysis of outcomes. Endosc Ultrsound. 2023. Mar-Apr;12(2): 171-180.doi: 10.4103/EUS-D-21-00268.
24. Tyagi A, Yeganeh O, Levin Y et al. Intra- and inter-examination repeatability of magnetic resonance spectroscopy, magnitude-based MRI, and complex-based MRI for estimation of hepatic proton density fat fraction in overweight and obese children and adults. Abdominal imaging 2015, 40, 3070–3077. doi: 10.1007/s00261-015-0542-5/
25. Stine JG, Munaganuru N, Barnard A et al. Change in MRI-PDFF and Histologic Response in Patients With Nonalcoholic Steatohepatitis: A Systematic Review and Meta-Analysis. Clin Gastroenterol Hepatol. 2021 Nov;19(11):2274-2283.e5. doi: 10.1016/j.cgh.2020.08.061
26. Kleiner DE, Brunt EM, Wilson LA, et al. Association of histologic disease activity with progression of nonalcoholic fatty liver disease. JAMA Netw Open. 2019.2(10). e1912565. doi:10.1001/jamanetworkopen.2019.12565.
27. Schneider A, Feussner H. Diagnostic Procedures. Chapter 5 In: Biomedical Engineering in Gastrointestinal Surgery, 2017: 87-220. Academic Press. https://doi.org/10.1016/B978-0-12-803230-5.00005-1.
28. Caussy C, Reeder SB, Sirlin CB, Loomba R. Noninvasive, quantitative assessment of liver fat by MRI-PDFF as an endpoint in NASH trials. Hepatology 2018; 68(2):763–772. https://doi.org/10. 1002/hep.29797.
29. Doycheva I, Cui J, Nguyen P et al. Non-invasive screening of diabetics in primarycare for NAFLD and advanced fibrosis by MRI and MRE. Alimentary Pharmacology and Therapeutics. 2016. Vol. 43 (1). P. 83–95. doi: 10.1111/apt.13405.
30. Bota S, Herkner H, Sporea I et al. Meta-analysis: ARFI elastography versus transient elastography for the evaluation of liver fibrosis. Liver Int. 2013; 33: 1138-1147. doi: 10.1111/liv.12240.Bota et al., 2013
31. Jones JG. Non-Invasive Analysis of Human Liver Metabolism by Magnetic Resonance Spectroscopy. Metabolites. 2021 Oct 29;11(11):751. doi: 10.3390/metabo11110751.
32. Dulai PS, Sirlin CB, Loomba R. MRI and MRE for non-invasive quantitative assessment of hepatic steatosis and fibrosis in NAFLD and NASH: Clinical trials to clinical practice. J Hepatol. 2016 Nov;65(5):1006-1016. doi: 10.1016/j.jhep.2016.06.005.
33. Pasanta D, Htun, KT, Pan J et al. Magnetic Resonance Spectroscopy of Hepatic Fat from Fundamental to Clinical Applications. Diagnostics. 2021; 11:842. https://doi.org/10.3390/diagnostics11050842.

MODERN APPROACHES TO THE EARLY DIAGNOSIS OF MYOCARDIAL INFARCTION AND THEIR CLINICAL SIGNIFICANCE

M.A. Zikrillayev
Lecturer, Tashkent Branch of the University of Business and Science
https://doi.org/10.5281/zenodo.20808950

Abstract. *This scientific study was conducted based on clinical observations, examinations, and analyses of 125 patients admitted to the Emergency Department of City Clinical Hospital No. 1. The study compared conventional and modern diagnostic methods and demonstrated the effectiveness of coronary angiography in the diagnosis of myocardial infarction (MI). Myocardial infarction is one of the most serious cardiovascular diseases and remains a leading cause of severe complications and premature mortality worldwide. This article discusses the pathophysiology of acute coronary syndrome, early clinical manifestations, electrocardiographic changes, the diagnostic value of high-sensitivity cardiac troponin assays, and the role of coronary angiography in the early diagnosis of myocardial infarction. The findings presented in this study may serve as an important diagnostic guideline for healthcare professionals working in emergency medical services, primary healthcare centers, emergency departments, cardiology, internal medicine, and intensive care units. During the study, it was observed that atypical clinical presentations of myocardial infarction occurred more frequently among women, elderly patients, and individuals with diabetes mellitus, which contributed to difficulties in establishing an early diagnosis. In conclusion, the early detection of myocardial infarction requires a comprehensive approach that integrates clinical assessment, electrocardiography, high-sensitivity cardiac troponin testing, and modern imaging techniques. The combined application of these diagnostic methods significantly improves diagnostic accuracy, facilitates timely initiation of treatment, and contributes to better clinical outcomes and prognosis for patients.*

Keywords: *myocardial infarction, acute coronary syndrome, troponin, myoglobin, symptoms, electrocardiography (ECG), coronary angiography, echocardiography, ST-segment elevation, ST-segment depression, T-wave inversion, revascularization, myocardium, reperfusion.*

Introduction

Myocardial infarction (MI) is one of the most severe and life-threatening cardiovascular diseases, contributing significantly to disability and mortality worldwide. According to the World Health Organization (WHO), cardiovascular diseases remain the leading cause of death globally, with myocardial infarction accounting for a substantial proportion of these deaths. The pathogenesis of MI is primarily associated with acute myocardial ischemia and necrosis resulting from the rupture of atherosclerotic plaques or the development of thrombosis within the coronary arteries.

A diagnosis of myocardial infarction requires a rise and/or fall in cardiac troponin levels, with at least one value exceeding the 99th percentile upper reference limit, accompanied by at least one of the following criteria:

- Symptoms consistent with myocardial ischemia;
- Newly developed ischemic changes on electrocardiography (ECG);

• Development of pathological Q waves;
• Imaging evidence of new loss of viable myocardium or new regional wall motion abnormalities presumed to be of ischemic origin;
• Identification of a coronary thrombus by coronary angiography or autopsy (not applicable to type 2 and type 3 myocardial infarction).

The presence of acute atherothrombosis in the coronary artery supplying the infarcted myocardium during autopsy confirms the diagnosis of type 1 myocardial infarction.

Type 2 myocardial infarction is diagnosed when there is an imbalance between myocardial oxygen supply and demand in the absence of acute atherothrombosis.

Type 3 myocardial infarction refers to cardiac death occurring in patients with symptoms suggestive of myocardial ischemia and new ischemic ECG changes before cardiac troponin results become available or before troponin levels have risen sufficiently to be detected.

Clinical outcomes in myocardial infarction largely depend on how early and accurately the diagnosis is established. Reperfusion therapy administered during the initial hours of ischemia, including percutaneous coronary intervention (PCI) or thrombolytic therapy, significantly reduces myocardial damage, prevents the development of heart failure, and improves patient survival. Therefore, the principle of “time is muscle” remains a cornerstone of modern cardiology.

Traditional diagnostic methods, including clinical assessment, electrocardiographic findings, and conventional biomarkers such as creatine kinase-MB (CK-MB) and myoglobin, are often insufficient. Diagnostic challenges are particularly evident during the early stages of the disease and in patients with atypical clinical presentations. Women, elderly individuals, and patients with diabetes mellitus frequently present with non-specific symptoms, making timely diagnosis more difficult and increasing the risk of delayed treatment and adverse clinical outcomes.

In recent years, significant advances have been made in the diagnosis of myocardial infarction. The introduction of high-sensitivity cardiac troponin (hs-cTn) assays, rapid diagnostic algorithms (0/1-hour and 0/2-hour protocols), and improved clinical risk stratification tools have greatly enhanced the ability to identify MI during its earliest stages. These approaches are strongly recommended by international clinical guidelines, including those of the European Society of Cardiology (ESC) and the American College of Cardiology/American Heart Association (ACC/AHA), and have become integral components of clinical practice.

Furthermore, modern diagnostic strategies not only facilitate the early detection of myocardial infarction but also help differentiate myocardial injury from other acute and chronic conditions. This reduces the likelihood of misdiagnosis and supports individualized treatment planning. Advances in artificial intelligence, telemedicine, and novel biomarkers are expected to further improve the accuracy and efficiency of MI diagnosis in the future.

The aim of this article is to analyze contemporary approaches to the early diagnosis of myocardial infarction, evaluate their clinical significance, and discuss their practical application based on the latest international clinical guidelines.

Literature Review

In recent decades, the early diagnosis of myocardial infarction (MI) and acute coronary syndrome (ACS) has remained one of the most important and rapidly developing areas in cardiology. According to the World Health Organization (WHO), cardiovascular diseases are the leading cause of global mortality, with myocardial infarction accounting for a significant

proportion of these deaths. Therefore, numerous studies have been conducted to improve early detection and effective management strategies for MI.

The Fourth Universal Definition of Myocardial Infarction (Thygesen et al., 2018) established that the diagnosis of MI is based on the detection of a rise and/or fall in cardiac troponin levels above the 99th percentile upper reference limit, combined with clinical or instrumental evidence of myocardial ischemia. This definition significantly strengthened the role of biomarkers in the diagnostic process.

Katus, Giannitsis, and Jaffe (2017) demonstrated that the introduction of high-sensitivity cardiac troponin (hs-cTn) assays has significantly improved the ability to detect myocardial infarction within the first 1–3 hours after symptom onset. According to their findings, hs-cTn assays provide superior sensitivity and diagnostic accuracy compared to conventional biomarkers such as CK-MB and myoglobin. In particular, rapid diagnostic algorithms (0/1-hour and 0/2-hour protocols) have been shown to significantly accelerate clinical decision-making.

The 2023 European Society of Cardiology (ESC) guidelines recommend the use of rapid troponin-based algorithms as the primary diagnostic strategy for the management of acute coronary syndrome. These protocols allow rapid classification of patients into “rule-in” and “rule-out” groups, thereby improving patient triage and treatment initiation.

According to the American College of Cardiology/American Heart Association (ACC/AHA) guidelines (Amsterdam et al., 2014), electrocardiography (ECG) remains the first-line diagnostic tool in suspected MI cases. ST-segment changes play a crucial role in differentiating types of myocardial infarction. However, ECG alone is often insufficient, particularly in non-ST-elevation myocardial infarction (NSTEMI) and atypical clinical presentations, necessitating additional laboratory and imaging studies.

Braunwald (2022), in *Heart Disease: A Textbook of Cardiovascular Medicine*, emphasized that the pathogenesis of MI is primarily driven by atherosclerotic plaque rupture and subsequent coronary thrombosis, leading to myocardial ischemia and necrosis. He also highlighted the critical importance of the “time is muscle” principle in determining clinical outcomes.

In recent years, advanced imaging modalities such as coronary computed tomography angiography (CCTA), echocardiography, and invasive coronary angiography have become essential tools in MI diagnosis. Studies have shown that coronary angiography not only confirms the diagnosis but also enables immediate therapeutic intervention through percutaneous coronary intervention (PCI).

Overall, the literature review indicates that the most effective approach to early MI diagnosis is a multimodal strategy combining clinical assessment, electrocardiography, high-sensitivity troponin testing, and modern imaging techniques. All authors consistently emphasize that an integrated diagnostic approach is essential, particularly in atypical cases, to reduce diagnostic errors and improve patient outcomes.

Research Methods

The main objective of this scientific article is to systematically analyze modern diagnostic approaches used in the early diagnosis of myocardial infarction, evaluate their clinical effectiveness and practical significance, and present optimal diagnostic strategies based on the latest international clinical guidelines.

Within the framework of this study, 125 patients were selected and examined. The role of high-sensitivity cardiac troponin (hs-cTn) assays in the early detection of myocardial infarction

within the first hours, the clinical applicability of rapid diagnostic algorithms (0/1-hour and 0/2-hour protocols), and their significance in patient risk stratification were thoroughly analyzed.

Special attention was also given to the integration of electrocardiography, laboratory biomarkers, and modern imaging techniques, including echocardiography, treadmill testing, coronary computed tomography angiography (CCTA), and invasive coronary angiography, in improving diagnostic accuracy.

Another important aim of the study was to identify the challenges of early diagnosis of myocardial infarction in patients presenting with atypical clinical manifestations, particularly among women, elderly patients, and individuals with diabetes mellitus, as well as to evaluate the role of modern diagnostic approaches in overcoming these challenges.

For this purpose, follow-up results from coronary angiography examinations of 75 patients were analyzed. In addition, issues related to differential diagnosis were addressed, considering that troponin levels may also be elevated in non-myocardial infarction conditions. This emphasizes the necessity of a comprehensive approach in clinical decision-making.

The analysis was based on the following diagnostic methods: This study included 125 patients aged 50 years and older who were admitted to the emergency department of the 1st City Clinical Hospital with suspected acute coronary syndrome or myocardial infarction. Inclusion criteria were the presence of clinical symptoms suggestive of myocardial ischemia, performance of a 12-lead electrocardiogram (ECG), and assessment of cardiac biomarkers, including troponin I/T and creatine kinase-MB (CK-MB). The exclusion criteria included patients younger than 50 years of age, individuals who declined participation in the study, patients with acute myocarditis, severe chronic kidney disease, active infectious or inflammatory disorders, traumatic cardiac injury, and conditions associated with elevated troponin levels due to non-coronary causes.

Statistical Analysis: The collected data were analyzed using statistical software. Quantitative variables were expressed as mean ± standard deviation (M ± SD). Differences between groups were evaluated using Student's t-test, while categorical variables were analyzed using the chi-square (χ^2) test. The sensitivity, specificity, and diagnostic accuracy of the diagnostic methods were calculated. A p-value of <0.05 was considered statistically significant, whereas p-values <0.001 were regarded as highly statistically significant.

Discussion

The findings of this study confirmed the high clinical effectiveness of modern diagnostic approaches in the early diagnosis of myocardial infarction (MI). The data obtained during the study demonstrated that the combined use of high-sensitivity cardiac troponin (hs-cTn) assays, electrocardiography (ECG), echocardiography, and coronary angiography significantly improves the diagnostic accuracy of MI and enables rapid and reliable risk stratification of patients.

Among all imaging modalities evaluated, coronary angiography demonstrated the highest diagnostic performance. The sensitivity and specificity of coronary angiography were both 99%. Significant coronary artery stenosis or complete occlusion was identified in 94.7% of the 75 patients who underwent coronary angiographic evaluation, further confirming coronary atherothrombosis as the principal etiological mechanism underlying MI.

Particularly in patients presenting with STEMI, coronary angiography serves not only as a diagnostic procedure but also as a therapeutic intervention, allowing prompt revascularization through percutaneous coronary intervention (PCI). Future advances in artificial intelligence technologies, telecardiology systems, portable ECG devices, and novel cardiac biomarkers are expected to further improve the early detection of MI.

In particular, the implementation of prehospital ECG and troponin monitoring by emergency medical service teams may substantially reduce the time to reperfusion therapy and improve patient outcomes.

Overall, the results of this study demonstrate that the integrated application of high-sensitivity cardiac troponin assays, electrocardiography, echocardiography, and coronary angiography provides the highest diagnostic accuracy for the early detection of myocardial infarction.

These approaches facilitate rapid risk stratification, timely revascularization, and a reduction in cardiovascular complications and mortality, thereby offering substantial clinical benefits for patients with acute myocardial infarction.

Table 1. Time to MI Diagnosis in Patients with Typical and Atypical Symptoms

Group	**Time to diagnosis (hours)**
Patients with typical symptoms	2.1 ± 0.8
Patients with atypical symptoms	4.7 ± 1.4

It was observed that the time to diagnosis in patients with atypical symptoms was almost twice as long ($p < 0.001$).

Table 2. Prevalence of Atypical Clinical Presentations

Patient group	**Atypical symptoms (%)**
Women	30.2
>65 years	34.8
Patients with diabetes mellitus	41.5
General population	21.6

These findings indicate that relying solely on clinical symptoms in diagnosing MI among women, elderly patients, and individuals with diabetes mellitus may lead to incorrect clinical decisions.

Table 3. Results of the Integrated Diagnostic Approach

Diagnostic combination	**Accuracy (%)**
ECG only	84.0
ECG + Troponin	94.8
ECG + Troponin + Echocardiography	97.2
ECG + Troponin + Echocardiography + Angiography	99.1

The integrated diagnostic approach significantly improved diagnostic accuracy ($\chi^2 = 18.4$; $p < 0.001$).

Overall, the findings demonstrate that the integration of high-sensitivity troponin assays, electrocardiography, and modern imaging techniques enables earlier detection of myocardial infarction, more effective risk stratification, and timely implementation of revascularization procedures.

The obtained results confirm the clinical effectiveness of the 0/1-hour troponin algorithm recommended by ESC and AHA guidelines and highlight the necessity of its widespread use in clinical practice.

Results

A total of 125 patients were included in the study. The mean age of the patients was 61.4 ± 11.2 years. Among them, 72 (57.6%) were male and 53 (42.4%) were female.

Table 4. Demographic characteristics of the study population (n = 125)

Variable	n	%
Males	**72**	**57,6**
Females	**53**	**42,4**
Age <50 years	**24**	**19,2**
Age 50–65 years	**58**	**46,4**
Age > 65 years	**43**	**34,4**
Diabetes mellitus	**41**	**32,8**
Arterial hypertension	**78**	**62,4**

Table 5. Frequency of clinical symptoms among patients

Clinical symptom	n	%
Typical chest pain	98	78.4
Dyspnea	56	44.8
Cold sweating	48	38.4
Nausea	21	16.8
Atypical symptoms	27	21.6

According to the analysis, 27 patients (21.6%) presented with atypical clinical manifestations of myocardial infarction.

Table 6. Diagnostic performance of methods for MI detection

Diagnostic method	Sensitivity (%)	Specificity (%)
ECG	84.0	88.0
hs-cTn I/T	98.4	94.7
CK-MB	82.3	86.1
Echocardiography	87.2	89.5
CT coronary angiography	92.1	91.8
Coronary angiography	99.0	99.0

High-sensitivity troponin assays demonstrated significantly higher diagnostic accuracy compared to other biomarkers ($p < 0.001$).

Table 7. Clinical effectiveness of troponin algorithms

Algorithm	MI confirmation (%)	MI exclusion (%)
0/1-hour hs-cTn	96.8	98.2
0/3-hour hs-cTn	93.4	95.7

The 0/1-hour algorithm showed significantly better performance in rapid patient risk stratification ($p = 0.02$).

Table 8. Coronary angiography findings (n = 75)

Finding	n	%
Single-vessel stenosis	24	32.0
Double-vessel stenosis	19	25.3
Triple-vessel stenosis	17	22.7
Total occlusion	11	14.7

Hemodynamically insignificant stenosis	4	5.3

According to coronary angiography results, clinically significant coronary artery stenosis or occlusion was identified in 94.7% of patients.

Conclusion. Early and accurate diagnosis of myocardial infarction is of crucial importance in saving patients' lives and preventing severe complications. In modern cardiology, the diagnostic process is not based on a single method but rather on the integrated and coordinated use of clinical assessment, electrocardiography, laboratory biomarkers, and imaging techniques. In particular, the introduction of high-sensitivity cardiac troponin (hs-cTn) assays has significantly expanded the ability to detect myocardial infarction within the first hours of symptom onset.

Electrocardiography plays a key role in the initial evaluation of myocardial infarction and remains the primary tool for differentiating STEMI and NSTEMI. Meanwhile, echocardiography is essential for detecting regional wall motion abnormalities of the myocardium, thereby confirming the diagnosis and assessing complications. Coronary angiography, especially in STEMI cases, allows precise identification of the culprit coronary artery and enables timely reperfusion therapy.

For patients with suspected myocardial infarction, the following rapid and structured diagnostic algorithm based on international clinical guidelines is recommended:

1. Clinical assessment of the patient and evaluation of symptoms
2. Performance of a 12-lead ECG within 10 minutes after admission
3. Application of the 0/1-hour high-sensitivity troponin diagnostic protocol
4. Confirmation of myocardial injury using echocardiography
5. In STEMI cases, coronary angiography and reperfusion therapy within 90 minutes

Strict adherence to this algorithm shortens diagnostic time, improves treatment effectiveness, and reduces both mortality and disability rates among patients. In conclusion, the widespread implementation of modern diagnostic approaches in the early detection of myocardial infarction plays a key strategic role in reducing adverse clinical outcomes associated with cardiovascular diseases.

REFERENCES

1. National clinical protocol for the diagnosis and treatment of acute coronary syndromes. Ministry of Health of the Republic of Uzbekistan. Tashkent, 2022.
2. Collet J.P., Thiele H., Barbato E., et al. 2023 ESC Guidelines for the management of acute coronary syndromes. *European Heart Journal*. 2023;44(38):3720–3826. doi:10.1093/eurheartj/ehad191
3. Thygesen K., Alpert J.S., Jaffe A.S., et al. Fourth Universal Definition of Myocardial Infarction (2018). *European Heart Journal*. 2019;40(3):237–269. doi:10.1093/eurheartj/ehy462
4. Amsterdam E.A., Wenger N.K., Brindis R.G., et al. 2014 AHA/ACC Guideline for the management of patients with non–ST-elevation acute coronary syndromes. *Circulation*. 2014;130(25):e344–e426. doi:10.1161/CIR.0000000000000134
5. Ibanez B., James S., Agewall S., et al. 2017 ESC Guidelines for the management of acute myocardial infarction in patients presenting with ST-segment elevation. *European Heart Journal*. 2018;39(2):119–177. doi:10.1093/eurheartj/ehx393

IN SILICO EVALUATION OF THE ANTIDIABETIC ACTIVITY OF THE C-4 COMPOSITION

L.U. Makhmudov[1], R.A. Yakubova[2], N.A. Tagayalieva[3]
Academician O.S. Sodikov Institute of Bioorganic Chemistry, Academy of Sciences of the Republic of Uzbekistan[1]
Academician O.S. Sodikov Institute of Bioorganic Chemistry, Academy of Sciences of the Republic of Uzbekistan[2]
Academician O.S. Sodikov Institute of Bioorganic Chemistry, Academy of Sciences of the Republic of Uzbekistan[3]
https://doi.org/10.5281/zenodo.20696870

Abstract. *Diabetes mellitus is a widespread endocrine-metabolic disorder characterized by persistent hyperglycemia, and the search for new effective and safe antidiabetic agents remains an urgent task. The present study was carried out to evaluate, using in silico molecular docking analysis, the possible antidiabetic mechanisms of the main components of the C-4 composition — L-carnitine, ammonium glycyrrhizinate, quercetin, and cysteine — which were investigated in an alloxan-induced experimental diabetes model. Two target proteins directly involved in antihyperglycemic mechanisms were selected: alpha-glucosidase, represented by human maltase-glucoamylase (PDB ID: 2QMJ), and dipeptidyl peptidase-IV (DPP-4, PDB ID: 1X70). Receptor and ligand structures were prepared using PyMOL and AutoDock Tools, and docking calculations were performed with AutoDock 4.2; the results were evaluated on the basis of binding free energy and the non-covalent interactions formed with active-site amino acid residues. Among the studied ligands, ammonium glycyrrhizinate showed the strongest binding to both targets, with binding energies of −10.2 kcal/mol for alpha-glucosidase and −13.2 kcal/mol for DPP-4, followed by quercetin (−8.4 and −7.6 kcal/mol, respectively). L-carnitine (−4.7 and −4.8 kcal/mol) and cysteine (−4.0 and −4.1 kcal/mol) exhibited weaker binding. These findings suggest that the antidiabetic potential of the C-4 composition may be mediated through several complementary mechanisms, including the inhibition of intestinal carbohydrate hydrolysis and the support of incretin-mediated insulin secretion, with ammonium glycyrrhizinate and quercetin acting as the main contributing components. The in silico results provide additional molecular evidence supporting the hypoglycemic effect observed under experimental conditions, while further experimental studies are required to confirm these interactions.*

Keywords: *diabetes mellitus, alloxan-induced diabetes, C-4 composition, molecular docking, in silico analysis, alpha-glucosidase, DPP-4, ammonium glycyrrhizinate, quercetin, L-carnitine, cysteine, antidiabetic activity.*

Introduction: Diabetes mellitus is one of the most widespread endocrine-metabolic disorders, characterized mainly by persistent elevation of blood glucose levels, known as hyperglycemia. This pathological condition is associated with disturbances in carbohydrate, lipid, and protein metabolism and may lead to the development of various complications affecting the cardiovascular system, kidneys, liver, and nervous system. Therefore, the search for new effective and safe agents aimed at controlling blood glucose levels remains an urgent task in the treatment and prevention of diabetes mellitus. In experimental pharmacology, alloxan is widely used to

induce experimental diabetes mellitus. Alloxan exerts a toxic effect on pancreatic β-cells, leading to decreased insulin secretion and the development of hyperglycemia. For this reason, the alloxan-induced diabetes model is considered an important experimental model for evaluating the hypoglycemic activity of new antidiabetic compounds.

The development of hyperglycemia in diabetes mellitus is not only related to insulin deficiency but also to intestinal carbohydrate digestion and glucose absorption into the bloodstream. In this process, alpha-glucosidase plays an important role, as it participates in the breakdown of complex carbohydrates into glucose. Inhibition of this enzyme can slow glucose absorption and help reduce postprandial hyperglycemia. In addition, the incretin system plays a significant role in the regulation of blood glucose levels. Dipeptidyl peptidase-IV (DPP-4) rapidly degrades incretin hormones such as glucagon-like peptide-1 (GLP-1) and glucose-dependent insulinotropic polypeptide (GIP). Inhibition of DPP-4 may prolong the biological activity of GLP-1, support glucose-dependent insulin secretion, and contribute to the reduction of blood glucose levels. In recent years, in silico approaches, particularly molecular docking analysis, have been widely used to support experimental findings at the molecular level. Molecular docking makes it possible to evaluate the binding energy between a ligand and a target protein, the orientation of the ligand within the active site, and its interactions with amino acid residues. This approach is important for explaining the possible mechanism of action of biologically active compounds. In the present study, molecular docking analysis was performed to evaluate the possible molecular mechanisms underlying the antidiabetic activity of the main components of the C-4 composition, including L-carnitine, ammonium glycyrrhizinate, quercetin, and cysteine, which were studied in an alloxan-induced experimental diabetes model. For this purpose, two protein targets involved in antihyperglycemic mechanisms were selected: alpha-glucosidase, represented by human maltase-glucoamylase (PDB ID: 2QMJ), and dipeptidyl peptidase-IV, DPP-4 (PDB ID: 1X70). The formation of hyperglycemia in diabetes mellitus is a complex pathophysiological process and is not limited only to reduced insulin secretion or impaired insulin action in peripheral tissues. Intestinal enzymatic degradation of carbohydrates, glucose absorption into the bloodstream, and changes in incretin hormone activity also play important roles. From this point of view, the investigation of key molecular targets involved in glucose homeostasis is relevant for evaluating compounds with potential antidiabetic effects. Thus, the present in silico molecular docking study was carried out to explain the possible molecular basis of the hypoglycemic effect observed under experimental conditions. The selected targets, alpha-glucosidase and DPP-4, are directly involved in two important antidiabetic mechanisms: inhibition of intestinal carbohydrate hydrolysis and support of incretin-mediated insulin secretion. This approach provides additional molecular evidence for the experimentally observed hypoglycemic activity and helps to assess the antidiabetic potential of the studied compounds.

Alpha-glucosidase is considered one of the main enzymes involved in the hydrolysis of poly- and oligosaccharides into glucose in the intestine. A decrease in the activity of this enzyme reduces the rate at which carbohydrates are converted into glucose, which in turn makes it possible to limit the absorption of glucose from the intestine into the blood and to decrease the level of postprandial hyperglycemia. For this reason, alpha-glucosidase was selected as an important inhibitory target for evaluating antidiabetic activity. For the docking analysis of this enzyme, the crystal structure of human maltase-glucoamylase in complex with acarbose — PDB ID: 2QMJ — was used as the basis.

DPP-4 is an important enzyme that regulates the activity of the incretin system; it participates in the rapid degradation of incretin hormones such as glucagon-like peptide-1 (GLP-1) and glucose-dependent insulinotropic polypeptide (GIP). Inhibition of DPP-4 activity prolongs the biological effect of GLP-1 in the blood, enhances glucose-dependent insulin secretion, suppresses glucagon release, and thereby contributes to the reduction of blood glucose levels. From this point of view, DPP-4 was selected as the second important target for evaluating antidiabetic activity at the molecular level. For this target, the crystal structure of human dipeptidyl peptidase-IV in complex with an inhibitor — PDB ID: 1X70 — was selected.

In the molecular docking analysis, L-carnitine, ammonium glycyrrhizinate, quercetin, and cysteine were selected as ligands. Their binding ability with alpha-glucosidase and DPP-4 protein targets was evaluated based on binding energy, conformational orientation within the active site, and interactions with amino acid residues, including hydrogen bonds, hydrophobic contacts, and other types of non-covalent interactions. This approach allows the possible molecular mechanisms underlying the antidiabetic effect observed under in vivo conditions to be clarified and provides additional support for the experimental findings.

Aim of the study: The aim of this study was to evaluate the possible antidiabetic mechanisms of the main components of the C-4 composition, including L-carnitine, ammonium glycyrrhizinate, quercetin, and cysteine, using in silico molecular docking analysis in an alloxan-induced experimental diabetes model. In this study, the binding energies, active-site orientations, and interactions of these compounds with amino acid residues of alpha-glucosidase and DPP-4 target proteins were analyzed.

Materials and methods. The computational part of the study was performed using freely available academic research tools. The three-dimensional structures of the antidiabetic target proteins were obtained from the Protein Data Bank (PDB), a widely used structural database for biological macromolecules. Based on their important roles in glucose metabolism and antidiabetic mechanisms, two target proteins were selected for molecular docking analysis: alpha-glucosidase, represented by human maltase-glucoamylase (PDB ID: 2QMJ), and dipeptidyl peptidase-IV (DPP-4, PDB ID: 1X70). Alpha-glucosidase was selected because this enzyme participates in the enzymatic hydrolysis of carbohydrates into glucose in the intestine. Inhibition of alpha-glucosidase may slow intestinal glucose absorption and reduce postprandial hyperglycemia. DPP-4 was selected due to its important role in the degradation of incretin hormones, particularly glucagon-like peptide-1 (GLP-1) and glucose-dependent insulinotropic polypeptide (GIP). Inhibition of DPP-4 may prolong incretin hormone activity, enhance glucose-dependent insulin secretion, and contribute to the reduction of blood glucose levels.

L-carnitine, ammonium glycyrrhizinate, quercetin, and cysteine were selected as ligands for molecular docking analysis. The molecular structures of these compounds were prepared and optimized before docking. The target protein structures downloaded in PDB format were inspected using PyMOL. During receptor preparation, crystallographic water molecules, unnecessary heteroatoms, and other non-relevant components were removed from the protein structures. PyMOL was also used for visualization of receptor structures and post-docking analysis of ligand–protein interactions. Further preparation of receptors and ligands was carried out using AutoDock Tools. At this stage, polar hydrogen atoms were added to the protein structures, partial charges were assigned, rotatable bonds in ligands were defined, and the prepared receptor and ligand structures were converted into the required docking format. Molecular docking calculations were

performed using AutoDock 4.2 to determine the most favorable binding conformations of the studied ligands within the active regions of alpha-glucosidase and DPP-4.

For alpha-glucosidase docking, the grid box center was set at center_x = −21.417000, center_y = 7.904000, and center_z = −31.219399. For DPP-4 docking, the grid box center was set at center_x = 51.046000, center_y = 56.003000, and center_z = 44.224154. Docking results were evaluated based on binding free energy values expressed in kcal/mol, as well as hydrogen bonds, electrostatic interactions, hydrophobic contacts, π-interactions, and other non-covalent interactions formed between the ligands and amino acid residues of the target proteins. The obtained molecular docking results were used to support the possible antidiabetic mechanisms of the studied compounds at the molecular level. The binding results with alpha-glucosidase were interpreted in relation to the potential inhibition of intestinal carbohydrate hydrolysis and glucose absorption. The binding results with DPP-4 were interpreted in relation to the possible support of glucose-dependent insulin secretion through the incretin system. Thus, in silico molecular docking analysis provided additional molecular evidence for the hypoglycemic effect observed in the alloxan-induced experimental diabetes model.

Prior to molecular docking analysis, all target protein structures retrieved from the Protein Data Bank were subjected to a standardized preparation procedure, since raw PDB files are generally not directly suitable for docking calculations. The downloaded protein structures may contain crystallographic water molecules, co-crystallized ligands, ions, missing hydrogen atoms, and other unnecessary heteroatoms. If these components are not properly removed, they may affect the accuracy of docking results [10]. Therefore, all additional molecules that were not directly related to the target protein structure were removed before docking. In this study, two antidiabetic target proteins were used: human maltase-glucoamylase/alpha-glucosidase (PDB ID: 2QMJ) and dipeptidyl peptidase-IV (DPP-4, PDB ID: 1X70). These proteins were selected because of their important roles in glucose metabolism and antidiabetic mechanisms. Alpha-glucosidase is involved in the enzymatic breakdown of carbohydrates into glucose in the intestine, whereas DPP-4 plays an important role in the degradation of incretin hormones such as GLP-1 and GIP.

During receptor preparation, crystallographic water molecules, unnecessary heteroatoms, ions, and other non-protein components were removed from the structures. Co-crystallized ligands were also deleted before docking calculations. When necessary, the original ligands present in the crystal structures were saved separately and used as reference molecules for comparison or docking validation. The removal of these additional components is important because they may occupy the ligand-binding pocket, partially block the active site, create artificial steric hindrance, or produce non-physiological interactions with the tested ligands. The prepared receptor structures were visually inspected using PyMOL. At this stage, the structural integrity of the proteins and the condition of their active or functionally important regions were evaluated [11]. No major structural defects that could significantly affect the docking analysis were observed in the selected receptor structures. After visual inspection, the protein structures were imported into AutoDock Tools for further preparation. Polar hydrogen atoms were added to the receptors, and Kollman united atom charges were assigned to properly represent the electrostatic properties of the target proteins. Protonation states were adjusted according to the standard AutoDock Tools preparation workflow to approximate physiological conditions. The final prepared receptor structures were saved in .pdbqt format, which contains atom type information and partial charges required for AutoDock docking calculations. For alpha-glucosidase docking, the grid box center was set at center_x =

−21.417000, center_y = 7.904000, and center_z = −31.219399. For DPP-4 docking, the grid box center was set at center_x = 51.046000, center_y = 56.003000, and center_z = 44.224154.

Ligand structures were prepared using a similar protocol [12]. The selected compounds, including L-carnitine, ammonium glycyrrhizinate, quercetin, and cysteine, were imported into AutoDock Tools. Hydrogen atoms were added to the ligands, Gasteiger charges were assigned, and non-polar hydrogen atoms were merged according to the standard AutoDock procedure. Rotatable bonds and root atoms were automatically identified by AutoDock Tools and manually checked when necessary to ensure proper ligand flexibility during docking. Finally, all prepared ligand structures were saved in .pdbqt format and used for molecular docking simulations. These preparation steps ensured that the docking results reflected the direct interactions between the selected antidiabetic target proteins, alpha-glucosidase and DPP-4, and the studied compounds. The resulting ligand–protein complexes were analyzed based on binding free energy, hydrogen bonds, electrostatic interactions, hydrophobic contacts, π-interactions, and other non-covalent interactions formed within the active site.

Results

L-carnitine

L-carnitine molecule was subjected to molecular docking analysis with the alpha-glucosidase target protein. During the docking procedure, the active site coordinates were set as center_x = −21.417000, center_y = 7.904000, and center_z = −31.219399. According to the obtained results, L-carnitine bound to the active site of alpha-glucosidase in an energetically favorable position and showed a binding energy of −4.7 kcal/mol. The negative value of the binding energy indicates that the formation of the ligand–protein complex is thermodynamically favorable. The binding energy of −4.7 kcal/mol suggests that L-carnitine has a moderate binding affinity toward alpha-glucosidase. This result indicates that L-carnitine may partially suppress alpha-glucosidase activity, thereby potentially slowing the breakdown of carbohydrates into glucose. The 2D interaction analysis showed that L-carnitine interacted with several amino acid residues within the active site of alpha-glucosidase. In particular, conventional hydrogen bond and carbon hydrogen bond interactions were observed with ASP A:772 and TRP A:290 residues. In addition, electrostatic attractive charge interactions were formed with GLU A:774 and ARG A:748 residues. These interactions may contribute to the relatively stable positioning of the ligand within the active site of the enzyme.

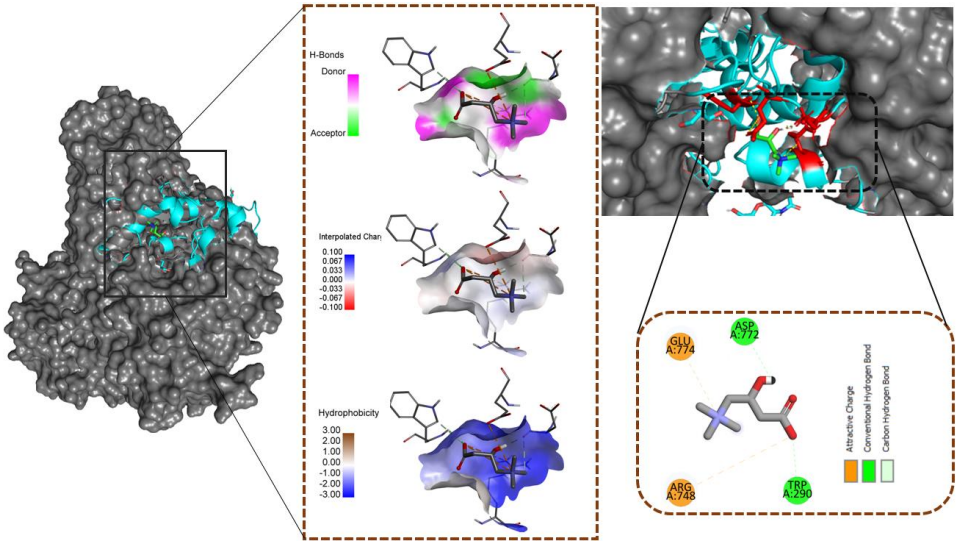


Figure 1. Molecular docking results of L-carnitine with alpha-glucosidase

These results indicate that L-carnitine has the ability to interact with the alpha-glucosidase target. Since alpha-glucosidase plays an important role in the intestinal breakdown of carbohydrates into glucose, inhibition of this enzyme may contribute to the reduction of postprandial hyperglycemia. From this point of view, the interaction of L-carnitine with alpha-glucosidase can be considered as an additional molecular basis for its possible antidiabetic mechanism. In the molecular docking analysis performed with the DPP-4 target protein, the binding properties of L-carnitine within the active site of this enzyme were evaluated. For docking, the active site coordinates were set as center_x = 51.046000, center_y = 56.003000, and center_z = 44.224154. According to the calculation results, L-carnitine showed a binding energy of −4.8 kcal/mol with the DPP-4 enzyme. The negative binding energy indicates that the formation of the ligand–protein complex between L-carnitine and DPP-4 is energetically favorable. The value of −4.8 kcal/mol reflects a moderate binding affinity of this molecule toward the active site of DPP-4. This finding suggests that L-carnitine may partially suppress DPP-4 enzyme activity and thereby participate in antidiabetic mechanisms related to the incretin system.

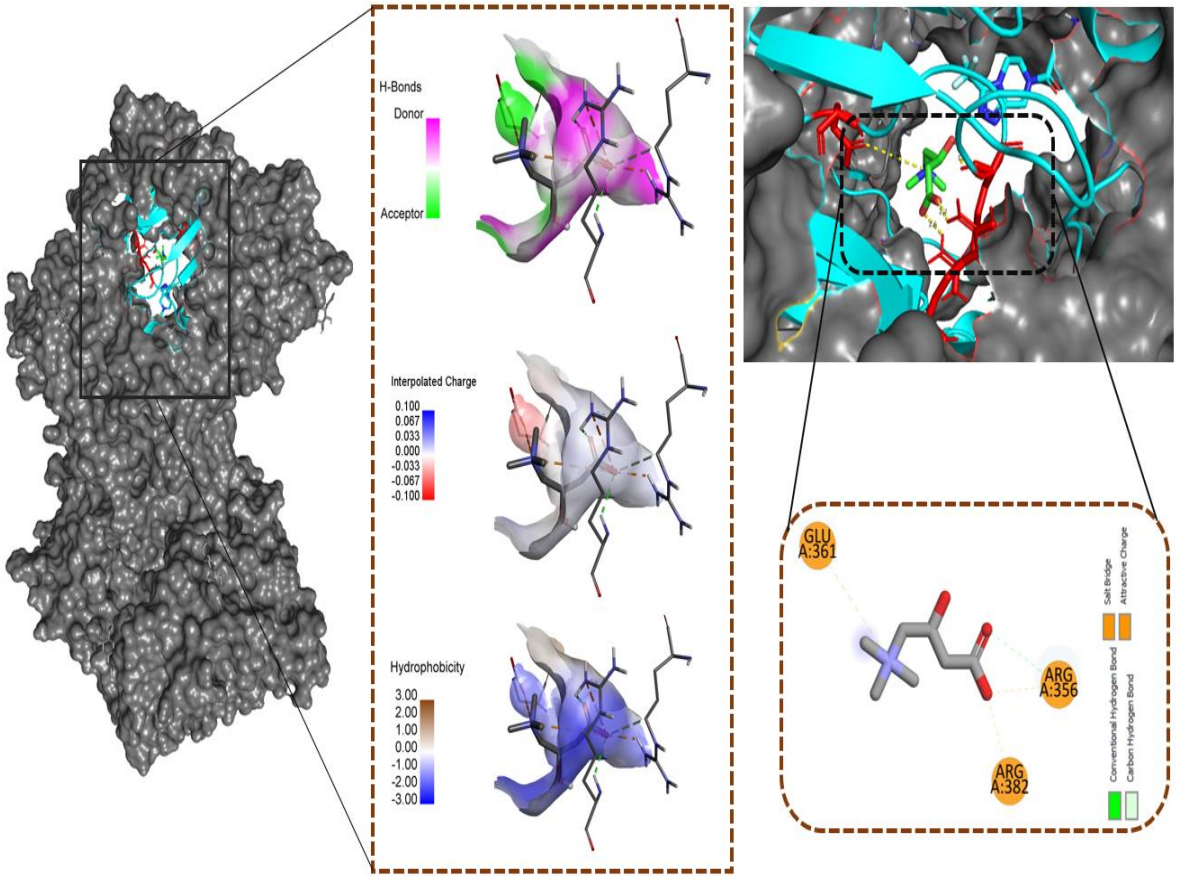


Figure 2. Molecular docking results of L-carnitine with the DPP-4 enzyme

The 2D interaction analysis showed that L-carnitine interacted with GLU A:361, ARG A:356, and ARG A:382 amino acid residues within the active site of DPP-4. In particular, salt bridge and attractive charge electrostatic interactions were observed with GLU A:361 and ARG A:382 residues. In addition, conventional hydrogen bond and carbon hydrogen bond interactions were formed with ARG A:356. These interactions may contribute to the relatively stable conformation of L-carnitine within the active site of the enzyme. DPP-4 plays an important role in the rapid degradation of incretin hormones such as GLP-1 and GIP. Therefore, inhibition of this enzyme may prolong the biological activity of GLP-1, support glucose-dependent insulin secretion, and contribute to the reduction of blood glucose levels. From this point of view, the

binding of L-carnitine with DPP-4 can be considered as additional molecular evidence supporting its possible involvement in the antidiabetic mechanism through the incretin system.

Ammonium glycyrrhizinate

Molecular docking analysis was performed between ammonium glycyrrhizinate and the alpha-glucosidase target protein. During the docking procedure, the active site coordinates of the enzyme were set as center_x = −21.417000, center_y = 7.904000, and center_z = −31.219399. According to the obtained results, ammonium glycyrrhizinate showed a binding energy of −10.2 kcal/mol with alpha-glucosidase. The binding energy value of −10.2 kcal/mol indicates that this ligand has a high binding affinity toward the active site of alpha-glucosidase. This value was considerably stronger than that obtained for L-carnitine, suggesting that ammonium glycyrrhizinate may have a higher potential to inhibit alpha-glucosidase enzyme activity.

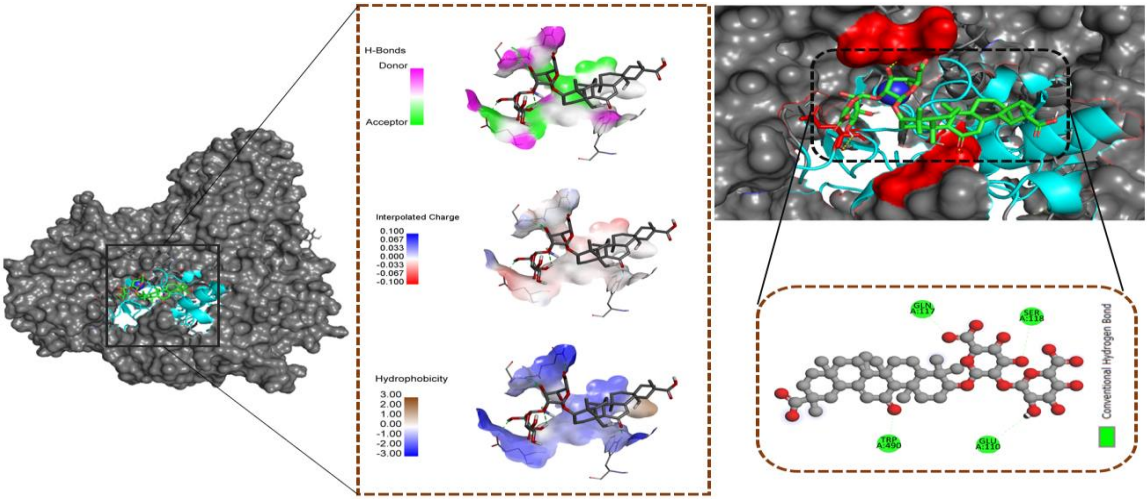


Figure 3. Molecular docking results of ammonium glycyrrhizinate with alpha-glucosidase

The 2D interaction analysis showed that the ligand interacted with several important amino acid residues within the active site of alpha-glucosidase. In particular, conventional hydrogen bond interactions were formed with GLN A:117, SER A:118, TRP A:490, and GLU A:110 residues. The presence of hydrogen bonds may contribute to the stabilization of the ligand–protein complex and ensure a stable positioning of the ligand within the active site.

Since ammonium glycyrrhizinate contains several hydroxyl and carboxyl groups, it has the ability to form multiple hydrogen bonds with amino acid residues in the active site of alpha-glucosidase. This may explain its stronger binding with the enzyme and suggests a possible ability to reduce enzymatic activity. Alpha-glucosidase is an important enzyme involved in the breakdown of carbohydrates into glucose in the intestine. Inhibition of this enzyme may slow the conversion of carbohydrates into glucose, reduce glucose absorption into the bloodstream, and help decrease postprandial hyperglycemia. From this point of view, the strong binding of ammonium glycyrrhizinate with alpha-glucosidase may play an important role in its antidiabetic mechanism.

Molecular docking analysis was also performed between ammonium glycyrrhizinate and the DPP-4 target protein. During the docking procedure, the active site coordinates of the DPP-4 enzyme were set as center_x = 51.046000, center_y = 56.003000, and center_z = 44.224154. According to the calculation results, ammonium glycyrrhizinate showed a binding energy of −13.2 kcal/mol with DPP-4. The highly negative binding energy indicates that the complex between the ligand and DPP-4 is energetically very stable. The value of −13.2 kcal/mol demonstrates that

ammonium glycyrrhizinate has a strong binding affinity toward the active site of DPP-4. This result suggests that this compound may have a high potential to inhibit DPP-4 enzyme activity.

The 2D interaction analysis showed that the ligand interacted with several amino acid residues within the active site of DPP-4. In particular, conventional hydrogen bond interactions were observed with SER A:212, TRP A:305, and ALA A:306 residues. In addition, a carbon hydrogen bond interaction was formed with THR A:304. These interactions may contribute to the stable positioning of the ligand within the active site of the enzyme and support the stabilization of the ligand–protein complex. At the same time, an unfavorable acceptor–acceptor interaction was observed with PHE A:364. However, the overall binding energy of −13.2 kcal/mol indicates that this unfavorable interaction did not significantly reduce the general stability of the ligand binding. On the contrary, the presence of multiple hydrogen bonds and other stabilizing interactions may have allowed the ligand to remain strongly bound within the active site of DPP-4.

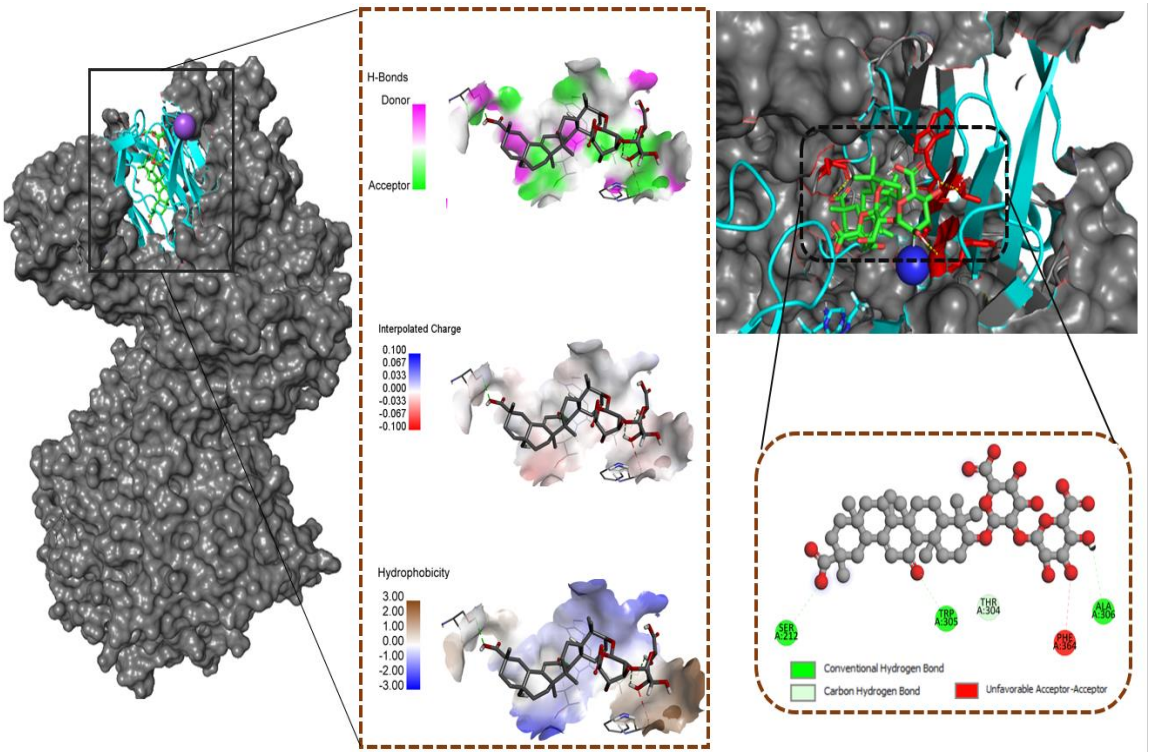


Figure 4. Molecular docking results of ammonium glycyrrhizinate with the DPP-4 enzyme

Quercetin

Evaluation of the interaction between quercetin and alpha-glucosidase showed that this compound had a high binding tendency toward the active site of the enzyme. Docking was performed using the coordinates center_x = −21.417000, center_y = 7.904000, and center_z = −31.219399. The calculated binding energy for quercetin was −8.4 kcal/mol, indicating that the ligand was positioned in a stable conformation within the active region of alpha-glucosidase. The polyphenolic nature of quercetin played an important role in its interaction with the enzyme. The hydroxyl groups present in the molecular structure enabled the formation of several hydrogen bonds with amino acid residues located in the active site of the enzyme. In particular, conventional hydrogen bond interactions were observed with GLU A:510, LYS A:776, GOL A:3002, and LEU A:286 residues. These interactions may play an important role in maintaining quercetin within the active site and stabilizing the ligand–protein complex.

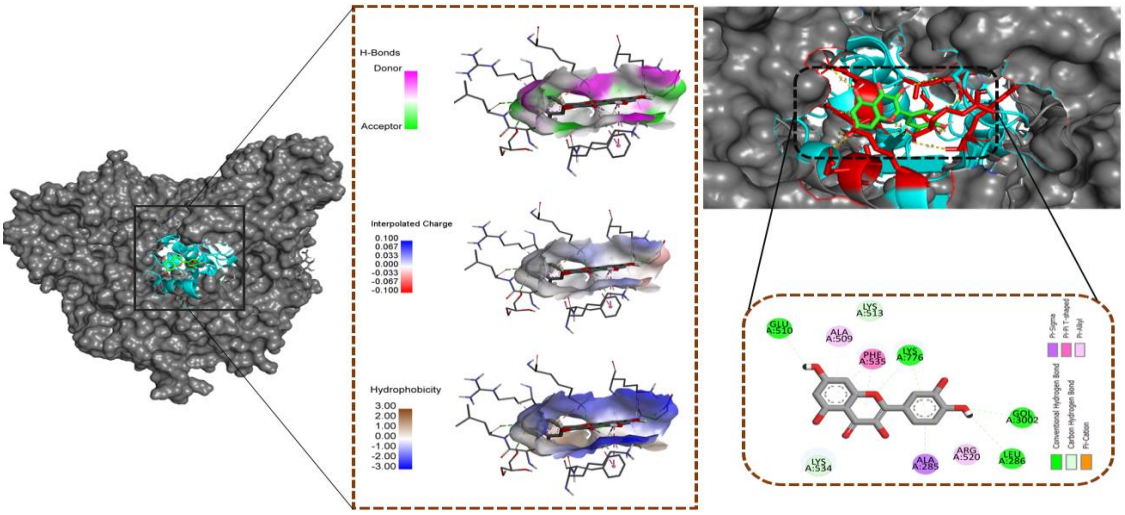


Figure 5. Molecular docking results of quercetin with alpha-glucosidase

At the same time, the aromatic rings present in the quercetin molecule contributed to the formation of additional π-type interactions within the active site of the enzyme. In particular, π-sigma interaction was observed with ALA A:285, π–π T-shaped interaction with PHE A:535, and π-alkyl interactions with ALA A:509 and ARG A:520 residues. The π-cation interaction recorded with LYS A:776 may further contribute to the stronger stabilization of the ligand within the enzyme pocket. In addition, carbon hydrogen bond interactions were also detected with LYS A:513 and LYS A:534 residues. The obtained results indicate that quercetin binds to the active site of alpha-glucosidase through several types of interactions rather than through a single interaction mode. The combined participation of hydrogen bonds, π-interactions, and hydrophobic contacts may enhance the stability of the ligand–protein complex. Therefore, the binding energy of −8.4 kcal/mol was considered an important molecular indicator of the potential ability of quercetin to inhibit the alpha-glucosidase enzyme. The molecular docking results of quercetin with the DPP-4 enzyme made it possible to evaluate the possible involvement of this compound in antidiabetic mechanisms related to the incretin system. The docking calculation was performed using the active site coordinates of DPP-4: center_x = 51.046000, center_y = 56.003000, and center_z = 44.224154. As a result, a binding energy of −7.6 kcal/mol was recorded for quercetin. This value indicates that quercetin has a noticeable binding tendency toward the active site of DPP-4. The binding energy of −7.6 kcal/mol suggests the possible formation of a stable complex between the ligand and the enzyme. This result indicates that quercetin may reduce the degradation of incretin hormones such as GLP-1 and GIP by suppressing DPP-4 enzyme activity.

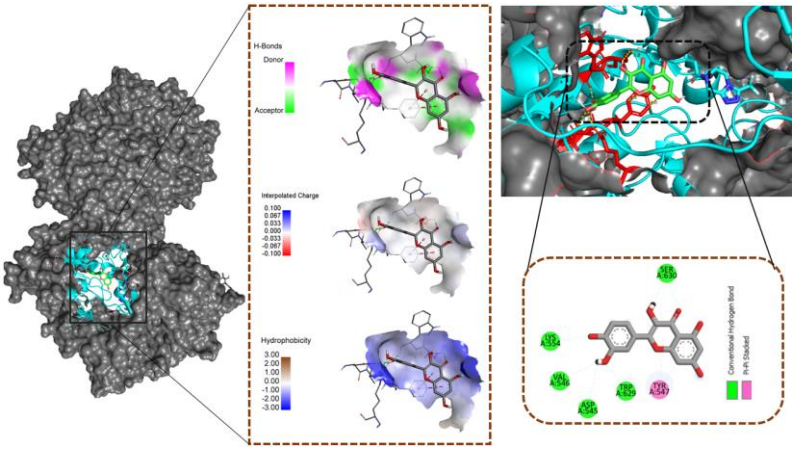


Figure 6. Molecular docking results of quercetin with the DPP-4 enzyme

In the 2D docking map, quercetin was shown to interact with several important amino acid residues within the active site of DPP-4. In particular, conventional hydrogen bond interactions were observed with LYS A:554, VAL A:546, ASP A:545, TRP A:629, and SER A:630 residues. These hydrogen bonds may be important for the specific orientation of quercetin within the active region of the enzyme and for maintaining the stability of the ligand–protein complex. In addition, the aromatic rings of quercetin formed a π–π stacked interaction with the TYR A:547 residue. This type of interaction is especially important for polyphenolic compounds, as it may contribute to the formation of stronger contacts with the hydrophobic regions of the enzyme. Therefore, both hydrogen bonds and aromatic π-interactions were involved in the binding of quercetin to DPP-4.

Cysteine

The interaction of cysteine with the alpha-glucosidase enzyme was also evaluated using molecular docking analysis. Docking was performed based on the active site coordinates of alpha-glucosidase: center_x = −21.417000, center_y = 7.904000, and center_z = −31.219399. The calculated binding energy for cysteine was −4.0 kcal/mol. This result indicates that cysteine is able to interact with the active site of alpha-glucosidase; however, its binding strength was lower compared with quercetin and ammonium glycyrrhizinate. The binding energy value of −4.0 kcal/mol suggests that the ligand–protein complex can be formed, although the interaction appears to be relatively weak or moderate.

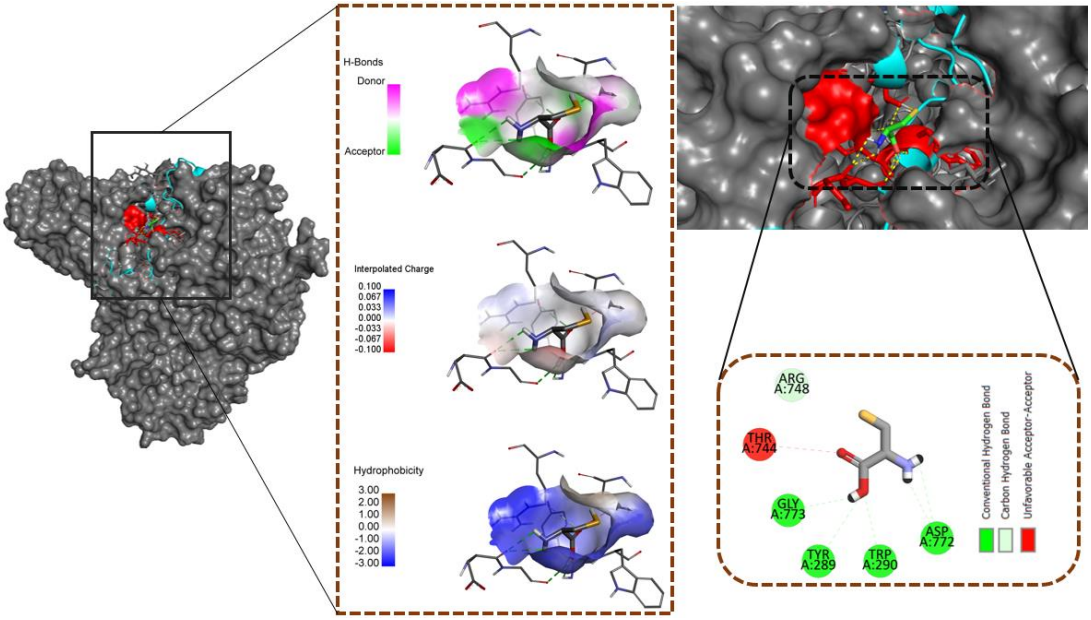


Figure 7. Molecular docking results of cysteine with alpha-glucosidase

The 2D interaction map showed that cysteine formed contacts with several amino acid residues within the active site of alpha-glucosidase. In particular, conventional hydrogen bond interactions were observed with ASP A:772, GLY A:773, TYR A:289, and TRP A:290 residues. In addition, a carbon hydrogen bond interaction was recorded with ARG A:748. These interactions may help cysteine to maintain a temporarily stable position within the active region of the enzyme. At the same time, an unfavorable acceptor–acceptor interaction was detected with THR A:744. This type of interaction may partially limit the overall stability of the ligand–enzyme complex. Therefore, the binding energy of −4.0 kcal/mol obtained for cysteine indicates that, although this compound is able to bind to alpha-glucosidase, its inhibitory potential is not strong. The interaction of cysteine with the DPP-4 enzyme was also evaluated based on the active region where quercetin was bound. The calculated binding energy for cysteine was −4.1 kcal/mol. This value indicates

that cysteine has the ability to interact with the active site of DPP-4; however, its binding strength is considerably lower than that of quercetin.

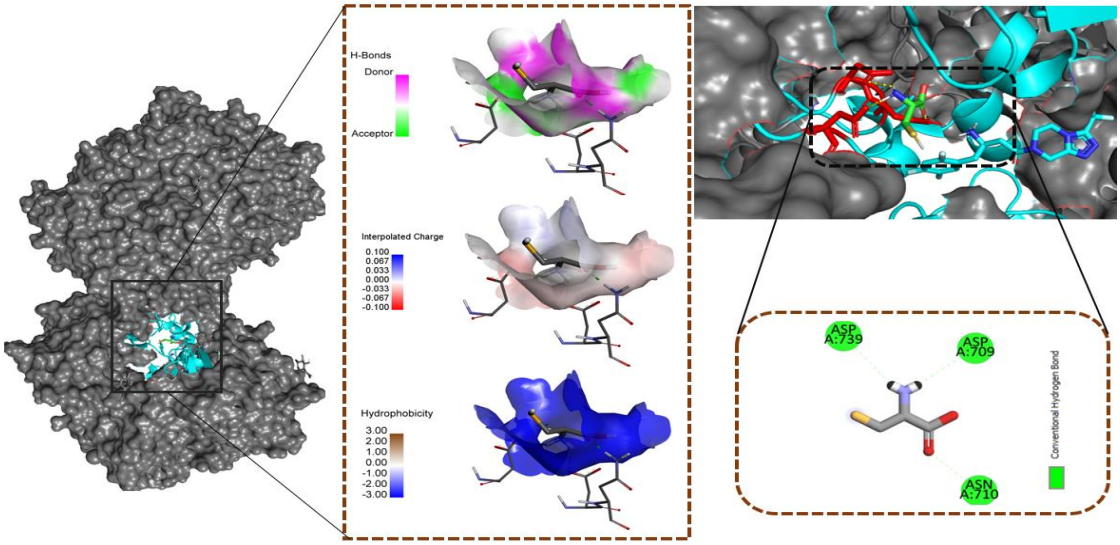


Figure 8. Molecular docking results of cysteine with the DPP-4 enzyme

According to the 2D docking analysis, cysteine interacted with the active region of DPP-4 mainly through hydrogen bonds. The ligand formed conventional hydrogen bond interactions with ASP A:739, ASP A:709, and ASN A:710 residues. These interactions may help cysteine to remain within the active region of DPP-4 to a certain extent. However, due to its small molecular structure, cysteine was unable to form a broad contact surface within the active site of DPP-4. While the aromatic rings and multiple hydroxyl groups of quercetin allowed the formation of several types of interactions with DPP-4, cysteine mainly showed limited hydrogen bond interactions. Therefore, the binding energy of −4.1 kcal/mol reflects a weak to moderate binding tendency of cysteine toward DPP-4. Since DPP-4 is involved in the degradation of incretin hormones such as GLP-1 and GIP, inhibition of this enzyme is important in the mechanism of antidiabetic activity. However, the docking result obtained for cysteine indicates that this compound is not the main strong inhibitor of DPP-4. Nevertheless, the formation of hydrogen bonds between cysteine and DPP-4 suggests that it may participate as an auxiliary molecular factor in the overall antidiabetic effect.

Discussion

The present in silico study was performed to support and explain the possible molecular mechanisms underlying the antidiabetic activity of the C-4 composition. Molecular docking analysis was carried out using two important antidiabetic target proteins: alpha-glucosidase and dipeptidyl peptidase-IV (DPP-4). These targets were selected because they are directly involved in two key mechanisms of blood glucose regulation. Alpha-glucosidase participates in the intestinal hydrolysis of carbohydrates into glucose, while DPP-4 is responsible for the rapid degradation of incretin hormones such as GLP-1 and GIP. Therefore, inhibition of these enzymes may contribute to the reduction of hyperglycemia through different but complementary pathways. The docking results demonstrated that the studied compounds interacted with both alpha-glucosidase and DPP-4 with different binding affinities. Among all investigated ligands, ammonium glycyrrhizinate showed the strongest binding toward both targets. Its binding energy with alpha-glucosidase was −10.2 kcal/mol, while its interaction with DPP-4 showed an even stronger binding energy of −13.2 kcal/mol. These values indicate a high molecular affinity of ammonium glycyrrhizinate toward the active sites of both enzymes. The

strong binding may be explained by the presence of several hydroxyl and carboxyl groups in its structure, which allow the formation of multiple hydrogen bonds and stabilizing interactions with amino acid residues of the target proteins. This suggests that ammonium glycyrrhizinate may be one of the main components responsible for the antidiabetic potential of the C-4 composition. Quercetin also demonstrated notable binding activity against both antidiabetic targets. The binding energy of quercetin with alpha-glucosidase was −8.4 kcal/mol, while its binding energy with DPP-4 was −7.6 kcal/mol. These results suggest that quercetin may contribute to the antidiabetic effect through dual interaction with carbohydrate-digesting and incretin-regulating enzymes. The interaction profile of quercetin was characterized by hydrogen bonds, π-interactions, and hydrophobic contacts. Such interactions are consistent with the polyphenolic nature of quercetin and may support the stable positioning of the ligand within the active sites of the enzymes. Therefore, quercetin can be considered an important active component that may support the hypoglycemic effect of the C-4 composition. In comparison, L-carnitine and cysteine showed lower binding energies with both target proteins. L-carnitine demonstrated binding energies of −4.7 kcal/mol with alpha-glucosidase and −4.8 kcal/mol with DPP-4. Cysteine showed binding energies of −4.0 kcal/mol and −4.1 kcal/mol with alpha-glucosidase and DPP-4, respectively. Although these values indicate that both compounds are able to interact with the selected targets, their binding strength was weaker than that of ammonium glycyrrhizinate and quercetin. This suggests that L-carnitine and cysteine may not act as the main enzyme-inhibiting components of the composition. However, their presence may still be biologically relevant, since they may contribute to the overall antidiabetic effect through additional metabolic, antioxidant, or supportive mechanisms. The stronger binding of ammonium glycyrrhizinate and quercetin to alpha-glucosidase suggests a possible mechanism related to the inhibition of intestinal carbohydrate hydrolysis. Suppression of alpha-glucosidase activity can slow the conversion of complex carbohydrates into glucose, reduce glucose absorption into the bloodstream, and decrease postprandial hyperglycemia. This mechanism is especially important in diabetes mellitus, where control of postprandial glucose elevation plays a significant role in maintaining glucose homeostasis.

The interaction of the studied compounds with DPP-4 provides another possible mechanism for their antidiabetic activity. DPP-4 inhibition may prolong the biological activity of incretin hormones, particularly GLP-1 and GIP. As a result, glucose-dependent insulin secretion may be enhanced, glucagon release may be reduced, and blood glucose levels may decrease. The high binding affinity of ammonium glycyrrhizinate and the moderate-to-strong binding of quercetin with DPP-4 suggest that these compounds may support incretin-mediated glucose regulation.

Overall, the molecular docking results indicate that the antidiabetic potential of the C-4 composition may be associated with multiple molecular mechanisms. The most important contribution appears to be related to ammonium glycyrrhizinate and quercetin, which showed the strongest interactions with both alpha-glucosidase and DPP-4. L-carnitine and cysteine showed weaker direct binding to the selected targets, but they may act as auxiliary components that support the general biological activity of the composition.

These findings provide additional molecular evidence for the hypoglycemic effect observed in the alloxan-induced experimental diabetes model. The in silico results suggest that the C-4 composition may exert its antidiabetic activity not through a single pathway, but through a combination of mechanisms, including reduced intestinal glucose absorption and

support of incretin-mediated insulin secretion. However, molecular docking is a predictive computational method, and the obtained results should be interpreted as supportive evidence. Further experimental studies, including enzyme inhibition assays and additional pharmacological investigations, are required to confirm the direct inhibitory effects of these compounds on alpha-glucosidase and DPP-4.

Conclusion

The molecular docking results showed that the studied compounds had different degrees of binding ability with alpha-glucosidase and DPP-4 target proteins. The negative binding energy values observed for both targets confirm that ligand–protein complexes were formed in an energetically favorable manner. At the same time, the differences in binding energies indicated that the molecular affinities of the compounds toward these enzymes were not the same.

According to the docking results with alpha-glucosidase, the strongest binding was observed for ammonium glycyrrhizinate. This compound bound to the active site of alpha-glucosidase with a binding energy of −10.2 kcal/mol, suggesting its high potential to inhibit the enzyme. Quercetin also demonstrated relatively strong binding to this target, with a binding energy of −8.4 kcal/mol. In contrast, L-carnitine and cysteine showed binding energies of −4.7 and −4.0 kcal/mol, respectively, indicating that although they are able to interact with alpha-glucosidase, their inhibitory potential may be lower.The results obtained for the DPP-4 target also showed the highest binding ability for ammonium glycyrrhizinate. This compound bound to the active site of DPP-4 with a binding energy of −13.2 kcal/mol, indicating a strong molecular affinity toward this enzyme. Quercetin showed a binding energy of −7.6 kcal/mol with DPP-4, suggesting its possible involvement in antidiabetic mechanisms related to the incretin system. L-carnitine and cysteine demonstrated binding energies of −4.8 and −4.1 kcal/mol, respectively, indicating that these compounds can interact with DPP-4, although their binding strength is relatively lower.

In the overall comparison, ammonium glycyrrhizinate demonstrated the strongest binding energies with both target proteins, alpha-glucosidase and DPP-4. This finding indicates that this compound may be an important component in the antidiabetic mechanism of action. Quercetin was evaluated as the second most active ligand, as it formed stable interactions with both enzymes. In contrast, L-carnitine and cysteine showed relatively lower binding energies, suggesting that their effects may be associated more with additional metabolic, antioxidant, or supportive biological mechanisms rather than with a primary inhibitory mechanism.

Based on the molecular docking results, ammonium glycyrrhizinate and quercetin were identified as the main components with higher potential to inhibit alpha-glucosidase and DPP-4 among the studied compounds. Inhibition of alpha-glucosidase may slow the intestinal breakdown of carbohydrates into glucose and reduce postprandial hyperglycemia. Inhibition of DPP-4 may prolong the activity of incretin hormones such as GLP-1 and GIP, thereby supporting glucose-dependent insulin secretion. From this perspective, the in silico results provide a molecular basis for the hypoglycemic effect observed under experimental conditions.

Thus, molecular docking analysis showed that the antidiabetic activity of the components of the C-4 composition may be mediated through several mechanisms. In particular, the strong binding of ammonium glycyrrhizinate and quercetin with alpha-glucosidase and DPP-4 suggests that these compounds may play an important molecular role

in reducing blood glucose levels. L-carnitine and cysteine, on the other hand, may be considered auxiliary components that support the overall antidiabetic effect.

REFERENCES

1. Ferreira LG, Dos Santos RN, Oliva G, Andricopulo AD. Molecular docking and structure-based drug design strategies. Molecules. 2015 Jul 22;20(7):13384-421. doi: 10.3390/molecules 200713384.
2. Kaur B, Singh P. Inflammation: Biochemistry, cellular targets, anti-inflammatory agents and challenges with special emphasis on cyclooxygenase-2. Bioorg Chem. 2022 Apr;121:105663. doi: 10.1016/j.bioorg.2022.105663.
3. Liu L, Jiao Y, Yang M, Wu L, Long G, Hu W. Network Pharmacology, Molecular Docking and Molecular Dynamics to Explore the Potential Immunomodulatory Mechanisms of Deer Antler. Int J Mol Sci. 2023 Jun 20;24(12):10370. doi: 10.3390/ijms241210370.
4. Dos Santos Maia M, Soares Rodrigues GC, Silva Cavalcanti AB, Scotti L, Scotti MT. Consensus Analyses in Molecular Docking Studies Applied to Medicinal Chemistry. Mini Rev Med Chem. 2020;20(14):1322-1340. doi: 10.2174/1389557520666200204121129. PMID: 32013847.
5. Preto J, Gentile F. Assessing and improving the performance of consensus docking strategies using the DockBox package. J Comput Aided Mol Des. 2019 Sep;33(9):817-829. doi: 10.1007/s10822-019-00227-7. Epub 2019 Oct 1. PMID: 31578656.
6. Dias MFR, Oliveira FLL, Pontes VS, Silva ML. Application of PolyPRep tools on HIV protease polyproteins using molecular docking. Braz J Biol. 2021 Dec 20;84:e245592. doi: 10.1590/1519-6984.245592.
7. Zi D, Shimadate Y, Wang JZ, Kato A, Li YX, Jia YM, Fleet GWJ, Yu CY. Design, synthesis and glycosidase inhibition of DAB derivatives with C-4 peptide and dipeptide branches. Org Biomol Chem. 2023 Mar 29;21(13):2729-2741. doi: 10.1039/d3ob00097d.
8. Yadav H, Bakshi A, Anamika, Singh V, Paul P, Murugan NA, Maurya SK. Co-localization and co-expression of Olfml3 with Iba1 in brain of mice. J Neuroimmunol. 2024 Sep 15;394:578411. doi: 10.1016/j.jneuroim.2024.578411. Epub 2024 Jul 25.
9. Saad HE, El-Reash GMA, Gaber M, Hashem MA, El-Reash YGA, Elamin NY, Elamin MR, El-Sayed YS. A novel isatin Schiff based cerium complex: synthesis, characterization, antimicrobial activity and molecular docking studies. BMC Genomics. 2024 Feb 8;25(1):162. doi: 10.1186/s12864-024-10037-3.
10. Xu S, Cui W, Zhang X, Song W, Wang Y, Zhao Y. Exploring the mechanisms of Guizhifuling pills in the treatment of coronary spastic angina based on network pharmacology combined with molecular docking. Medicine (Baltimore). 2024 Jul 19;103(29):e39014. doi: 10.1097/MD.0000000000039014. PMID: 39029023; PMCID: PMC11398759.
11. Kumar S, Chaudhary B, Singhal B. Phylum-level studies of bacterial cutinases for unravelling enzymatic specificity toward PET degradation: an in silico approach. Braz J Microbiol. 2024 Sep;55(3):2385-2400. doi: 10.1007/s42770-024-01362-6. Epub 2024 May 15.
12. Suresh PK, Divya N, Nidhi S, Rajasekaran R. Phenytoin-Bovine Serum Albumin interactions - modeling plasma protein - drug binding: A multi-spectroscopy and in silico-based correlation. Spectrochim Acta A Mol Biomol Spectrosc. 2018 Mar 15;193:523-527. doi: 10.1016/j.saa.2017.12.069. Epub 2017 Dec 27.

Contents

03.00.00 BIOLOGICAL SCIENCES

A. Abdurashidov, F. Kholiyorova, N. Tosheva, R. Sayidova, E. Yusupova
ENDOPHYTIC FUNGI FROM *PERSICARIA HYDROPIPER* PRODUCE METABOLITES WITH SELECTIVE ANTIBACTERIAL AND CELL-PROLIFERATIVE ACTIVITIES 4

Z.X. Qutlimurodova, S.A. Abdusamatov, Z. Eshbekova, J.U. Boyxonov
ENZYMATIC CHARACTERISTICS OF BACTERIA ASSOCIATED WITH THE POTATO TUBER MOTH (*PHTHORIMAEA OPERCULELLA*) 12

F.I. Turdiyev
BIOLOGICAL DEVELOPMENT OF MEDICINAL LEMON BALM (MELISSA OFFICINALIS L.) AND PATTERNS OF VEGETATIVE ORGAN FORMATION 20

Sh. Shamsiddinova
EFFECTIVE METHODS OF IN VITRO PROPAGATION OF ZINGIBER OFFICINALE ROSC: LITERATURE ANALYSIS AND PROSPECTIVE RESEARCH DIRECTIONS 27

06.00.00 AGRICULTURAL SCIENCES

U.K. Abdurakhimov, D.A. Rakhimbayeva
CHEMICAL COMPOSITION, OIL CONTENT, AND AMINO ACID CONTENT OF CASTOR BEAN (RICINUS COMMUNIS L.) SEEDS CULTIVATED IN THE KHOREZM REGION 34

N.M. Djumabekova
DIGITAL MONITORING OF IRRIGATED AGRICULTURAL LANDS USING REMOTE SENSING TECHNOLOGIES: RESULTS AND ANALYSIS FROM AMUDARYA DISTRICT, KARAKALPAKSTAN 46

Kh.K. Nazarov, T.Kh. Farmanov, K.K. Azizov
ECONOMIC EFFICIENCY OF NEW EARLY-MATURING, HIGH-YIELDING MAIZE VARIETIES AND THEIR PRIMARY SEED PRODUCTION 56

14.00.00 MEDICAL SCIENCES

Sh.Yu. Abdullaev, A.V. Zhdanov, M.G. Khatypova, F.A. Dzhumaev, A.A. Hodjimetov
ELEVATOR-SUCTION AS A NEW HYBRID INSTRUMENT IN THE CONTEMPORARY PRACTICE OF SURGICAL DENTISTRY 68

T.F. Abduraimov
RATIONAL ANTIMICROBIAL USE IN OBSTETRIC CARE AS A STRATEGY FOR MATERNAL SEPSIS PREVENTION: RESULTS OF A POINT PREVALENCE SURVEY 73

M.R. Ruzibakieva, J.J. Ramziddinov, A.J. Jangavarov, F.T. Ryskulov, K.E. Grigoryants
MICRORNAS AS LIQUID BIOMARKERS OF CANCER: A REVIEW OF CURRENT APPROACHES TO CIRCULATING MICRORNAS IN ONCOLOGICAL DIAGNOSTICS 86

A.A. Mamajonov
PRODUCTIVITY TRAITS IN F1 HYBRIDS DERIVED FROM COTTON CULTIVARS, A WILD SPECIES, AND INTROGRESSIVE FORMS 96

D. Rahmatullayeva
OPTIMIZATION OF POSTOPERATIVE REHABILITATION AFTER HYSTERECTOMY IN WOMEN WITH BENIGN UTERINE TUMORS: A COMPARATIVE ANALYSIS OF LAPAROSCOPIC AND OPEN SURGICAL APPROACHES 103

B.I. Urinov, N.M. Djuraeva
NON-ALCOHOLIC FATTY LIVER DISEASE: A REVIEW OF EPIDEMIOLOGY, PATHOPHYSIOLOGY, CLINICAL COURSE AND DIAGNOSIS METHODS 108

M.A. Zikrillayev
MODERN APPROACHES TO THE EARLY DIAGNOSIS OF MYOCARDIAL INFARCTION AND THEIR CLINICAL SIGNIFICANCE 116

15.00.00 PHARMACEUTICAL SCIENCES

L.U. Makhmudov, R.A. Yakubova, N.A. Tagayalieva
IN SILICO EVALUATION OF THE ANTIDIABETIC ACTIVITY OF THE C-4 COMPOSITION 123

International Scientific Journal
Science and Innovation Series D
Volume 5 Issue 6

ISSN: 2181-3337

Published: 30.06.2026. Font: "Times New Roman".

LLC "Science and innovation"
License Mass Media №:1597 27.04.2022
License Publisher №:455168 21.11.2024
Address: 100121, Uzbekistan, Tashkent city, Yakkasaroy district,
Shota Rustaveli Street 150, Vega Business Center, 6th floor, Room 2.
www.scientists.uz, info@scientists.uz, +998901259654